



The University
Of Sheffield.
Energy
Institute.



PhD Mechanical Engineering Thesis

EFFECT OF PARTICLE SIZE DISTRIBUTION ON KINETICS AND OVERALL DEGRADATION IN ANAEROBIC DIGESTION OF WASTE BIOMASS

By:

Scholastica Ebaye Bejor

Thesis submitted to the Department of Mechanical
Engineering, University of Sheffield in partial
fulfilment of the requirements for the degree of PhD

Submission date: 29thMarch 2020

THE UNIVERSITY OF SHEFFIELD RESEARCH AND INNOVATION SERVICES

The undersigned certify that they have examined and had advocated the research innovation services for the thesis acceptance entitled “Effect of Particle size distribution on Kinetics and Overall Degradation on Anaerobic Digestion of Waste Biomass” submitted by Ebaye Scholastica Bejor for the degree of “Doctorate of” Philosophy”.

Supervisor, Professor Bill Nimmo, Mechanical Engineering

Supervisor, Professor Pourkashanian, Mechanical Engineering

Supervisor, Professor Lin Ma, Mechanical Engineering

Date -

Acknowledgements

This project work is dedicated first and foremost to God, in whom I live and have my being; to Jesus, the saviour and Lord of my life; to the Holy Spirit, my comforter, helper, and guide; and in evergreen memory of my grandmother Abung Maria Mbeh, my late fathers Bassey Emeng Okoro and Mr Ebaye Charles Bejor Nsed (1962 -2003). My love goes to my God given daughter Miracle Amarachukwu James-Okoli. To my wonderful mother, Mrs Esther Ogar Ojong, for her prayers and prophesy over my life, and to Evangelist Sharon Emmanuel for her support, as well as to my ever-loving brothers, Master Bassey Prince Bassey and Emmanuel Takon Bassey and family, for their challenge that has driven me to this height. Finally, aside from God, this project is dedicated to Mr. and Mrs. Ekenna Nnamdi, without whose love, understanding, and patience my educational pursuit would have ended. May God bless you all as you continue to change people's lives across the world, but without a rare gem like you, our society would have been the devil's workshop. My heartfelt gratitude goes to my supervisor, Professor Bill Nimmo, a man with a golden heart, and Dr Mark Walker for their encouragement and assistance in completing my thesis and instilling confidence in me. My achievement can be attributed to their efforts to keep me focused on this research. Finally, I am thankful to all of Apostles, Prophets and Prophetesses, Oluwaseyi Ogungbe and Nana Elaine Rutty for their prayers, encouragement, and support, as well as to all my well-wishers.

Abstract

Particle size distribution (PSD), or the distribution of particles over distinct size ranges, in pre-treated organic substrate is relatively unknown, even though it is generally recognised that particle size reduction affects the efficacy of microbial fermentation. When the size of the particles is reduced, biological responses have access to a greater specific surface area. A shorter retention period reduced capital and operational expenses could also result from smaller particle size distribution, which would be beneficial to remote, rural, and urban regions alike. As a result, the cost of the substrate biomass that must be disposed of is reduced, and a greater percentage of biogas is produced. The study consisted of laboratory tests to reduce particle sizes and analyse the result PSD profile. These techniques were used, like as collected, manual chopping, shredding, grinding, and mincing. Shredders were shown to be less effective at reducing particle sizes for pre-treatment level one when compared to manual chopping and non-treated waste. The fine particle size distribution (PSD) ranges of the non-treated tomato waste were noticeably higher (41%) than those of the other three substrates, such as grass waste 10% < 2.9, banana peel waste 14% < 2mm, and paper waste 25% < 3mm. The trials showed that, combine effect of mincer, grinder and extending processing time by 5 minutes resulted in a greater methane output at higher pre-treatment levels with more surface area. The study found that of the four substrate biomass pre-treatment levels, banana peel waste substrate biomass (BPWSB) produced the most methane, at a rate of about $332 \pm 36 \text{ Nml/gVS}$ and a volatile solids reduction (VSR) of 67% for batch tests, while GWSB of semi-continuous tests produced $253 \pm 29 \text{ Nml/gVS}$. The simulation results and experimental data for different levels of degradability revealed that while large particles decay slowly, a smaller fraction degrades more rapidly. This supports the findings of other studies in terms of specific surface area, smaller particles had a greater influence on biodegradation than the larger particles.

Key Words: Anaerobic, methane, particle size, biomass, banana peel grass, paper, tomato substrate, biochemical methane potential, batch and semi continuous

Abbreviations and acronyms

A	Surface Area Is Available for Hydrolysis [m ²].
AD	Anaerobic Digestion
BMP	Biochemical Methane Potential
BPW	Banana Peel Waste
BPWSB	Banana Peel Waste Substrate Biomass
BR	Batch Reactor
C/N	Carbon to Nitrogen Ratio
CSTR	Continuous Stirred Tank Reactor
Dm	Dried matter
GW	Grass Waste
GWSB	Grass Waste Substrate Biomass
HRT	Hydraulic Retention Time
IA	Intermediate Alkalinity
K _{sbk}	Surface-Based Hydrolysis Constant (Kg/M ² day).
M	Mass of The Substrate (Kg)
OLR	Organic Loading Rate
PA	Partial Alkalinity
PS	Particle size
PSD	Particle size Distribution
PSR	Particle Size Reduction
PT	Pre-treatment
PTLs	Pre-treatment levels
PW	Paper Waste
PWSB	Paper Waste Substrate Biomass
Ro	Initial Organic Solid Particle Radius [L],
Rt	Average Particle Radius at Time T (m);
SMP	Specific Methane (CH ₄) Production
T	Time (Days)
TA	Total Alkalinity
TS	Total Solid
TW	Tomato Waste
TWSB	Tomato waste substrate biomass
VFA	Volatile Fatty Acids
VS	Volatile Solid
VSR	Volatile solid reduction
P	Density of The Substrate (Kg/m ³),

CONTENTS

Contents	vi
1 Introduction	1-1
1.1. Background of the Study.....	1-1
1.1 The energy situation in Nigeria.....	1-4
1.2 Research motivation	1-6
1.3 Scope of study.....	1-6
1.4 Project Aim and Objectives.....	1-7
1.4.1 Aim	1-7
1.4.2 Objectives of the study	1-7
1.5 Structure of the thesis	1-8
2 Literature Review.....	2-9
2.1 The Biogas Technology	2-9
2.2 Phases of the anaerobic digestion process.....	2-11
2.2.1 Hydrolysis.....	2-11
2.2.2 Acidogenesis	2-14
2.2.3 Acetogenesis	2-15
2.2.4 Methanogenesis.....	2-15
2.2.5 History of the anaerobic digestion	2-19
2.2.6 Future of the anaerobic digestion in Nigeria	2-20
2.2.7 Achievable merit of the anaerobic digestion in Nigeria	2-21
2.3 The end-products of the anaerobic complex particulate matter	2-24
2.3.1 Biogas	2-24
2.3.2 Digestate	2-25
2.3.3 Available feedstock.....	2-26
2.4 Factors affecting the digestion of the anaerobic substrate biomass. ..	2-26
2.4.1 Operating temperature of the reactor	2-27
2.4.2 Retention time	2-28
2.4.3 Mixing.....	2-30
2.4.4 The Organic loading rate of an anaerobic digestion system	2-30
2.4.5 pH.....	2-32
2.5 The C/N ratio.....	2-33

2.6	Inhibition of the anaerobic digestion degradation	2-34
2.6.1	Inhibition by ammonia	2-35
2.6.2	Organics inhibition	2-36
2.6.3	The effects of light and heavy metal ions	2-36
2.6.4	Volatile Fatty Acids inhibition	2-37
2.7	Biogas technology for the pre-treatment of solid waste	2-38
2.7.1	Single-phase mixed mesophilic wet digesters	2-40
2.7.2	Single-phase continuous feed, dry thermophilic digesters	2-42
2.7.3	Anaerobic digestion performance in a single- and two-phase system.	2-44
2.7.4	Multiphase and two-phase systems	2-45
2.8	Anaerobic degradation system overview and enhancements	2-48
2.9	Physical pre-treatment	2-48
2.9.1	Mechanical pre-treatment.....	2-50
2.10	Review of various mechanical particle size reduction techniques	2-52
2.10.1	Hammer mills	2-52
2.10.2	Shear shredders	2-53
2.10.3	Wet pulverisation.....	2-54
2.10.4	Chippers:	2-55
2.10.5	Grinders:	2-55
2.10.6	Roll or screw mill.....	2-55
2.10.7	Ball mill.....	2-56
2.10.8	Cutting mills	2-57
2.11	Reasons for size reduction in anaerobic digestion processes	2-58
2.12	The effects of various mechanical comminution equipment on feedstock characteristics and particle size distribution.....	2-59
2.13	Biological pre-treatment.....	2-63
2.14	Chemical Pre-treatment.....	2-64
2.15	Previous studies on particle size	2-65
2.15.1	Summary of the previous work.....	2-71
2.16	Review on foaming and causes.....	2-72
2.17	Wide use process modelled of the anaerobic digestion	2-74
2.18	Review of the particle size base degradation process model	2-78

2.19 Evaluation of the BMP Test.....	2-79
2.20 Findings from Literature Review.....	2-81
2.21 Knowledge gaps and possible ideas for improving biogas production of the anaerobic digesters and improving the system’s performance.....	2-81
2.22 Conclusion of a review of the literature	2-82
3 Materials and Methods.....	3-84
3.1 Feedstock and Inoculum	3-84
3.2 Feedstock preparation and mixing	3-84
3.2.1 Feedstock particle size communiton	3-84
3.3 Analytical parameters measured in this study for substrate digestion and digestate	3-87
3.4 Preparation of the reagents and indicator	3-87
3.4.1 pH.....	3-88
3.4.2 Preparation, determination of total solid TS and volatile solid VS.....	3-88
3.4.3 The alkalinity of the biomass sample.....	3-89
3.5 Estimation of theoretical maximum methane production.....	3-91
3.6 Composition of elements (CHNS)	3-91
3.7 Experimental procedure	3-92
3.7.1 Sample preparation and anaerobic condition employed for BMP testing and methane production.	3-92
3.7.2 Leak test	3-93
3.8 Batch testing set-up and monitoring	3-94
3.9 Semi-continuous testing	3-96
3.9.1 Gas volumes for BMP assay and semi continuous testing	3-98
3.10 Overview of Experimental set-up	3-99
3.11 Particle size distribution determination	3-99
3.12 Conclusion.....	3-100
4 Results and Discussion	4-101
4.1 Organic Particle Size Distribution Characterisation	4-101
4.1.1 Choice of Substrate and Equipment	4-101
4.2 Substrate Biomass Characterisation	4-102
4.3 Banana Waste Particle Size Distribution.....	4-103

4.4	Grass Waste Particle Size Distribution	4-107
4.5	Paper Waste Particle Size Distribution	4-110
4.6	Tomato Waste Particle Size Distribution	4-113
4.7	Comparison of various particle size reduction methods and equipment	4-116
4.8	Results Summary.....	4-118
5	Batch Testing.....	5-120
5.1	BMP Assay for Banana Peel Waste Substrate Biomass (BPWSB)	5-120
5.1.1	Calculation of BPWSB theoretical calorific value of biomass potential	5-125
5.1.2	Banana peel waste substrate biomass BMP Kinetics	5-127
5.1.3	Statistical Analysis of Variance for the Four Selected Substrate Biomass.	5-130
5.1.4	ANOVA of Banana Peel Waste Substrate Biomass	5-131
5.2	BMP Assay for Grass Waste Substrate Biomass (GWSB).....	5-133
5.2.2	Grass waste substrate biomass BMP Kinetics	5-139
5.2.3	ANOVA of Grass Waste Substrate Biomass	5-141
5.3	BMP Assay for Paper Waste Substrate Biomass (PWSB).....	5-144
5.3.2	Paper waste substrate biomass BMP Kinetics	5-150
5.3.3	ANOVA of Paper Waste Substrate Biomass.....	5-152
5.4	BMP Assay for Tomato Waste Substrate Biomass (TWSB).....	5-154
5.4.1	Calculation of TWSB theoretical calorific value of biomass potential	5-158
5.4.2	Tomato waste substrate biomass BMP Kinetics.....	5-159
5.4.3	ANOVA of Tomato Waste Substrate Biomass.....	5-162
5.5	The effects of various mechanical devices on methane yield in biogas	5-164
5.5.1	Comparing the responses of the chosen substrates to various treatments in terms of methane yield and volatile solid reduction	5-165
5.6	Expected outcome of the batch test	5-167
5.6.1	The following conclusions can be made considering the results:	5-168
5.7	Conclusion.....	5-168
5.8	Semi-Continuous Testing; The effect of mechanical pre-treatment on degradation of complex organic matter	5-169
5.8.1	Feedstock Characterisation	5-169
5.9	Grass Waste Substrate Biomass	5-173
5.9.1	Biogas output methane production of the GWSB	5-173

5.9.2 The specific production rate of methane (CH ₄) in semi-continuous testing of GWSB	5-175
5.10 Banana Peeled Waste Substrate Biomass	5-178
5.10.1 Percentage and Average Methane Production Rate of BPWSB	5-178
5.10.2 The specific production rate of methane (CH ₄) in semi-continuous testing of BPWSB	5-180
5.11 Paper Waste Substrate Biomass	5-183
5.11.1 Percentage and average production rate of paper waste substrate biomass	5-183
5.11.2 The specific production rate of the methane (CH ₄) in semi-continuous testing of PWSB	5-184
5.12 Performance of reactor R1 to R6	5-187
5.13 Conclusions	5-188
5.14 Stability operations of a semi-continuous test	5-189
5.15 Comparison of experimental and theoretical methane and energy yield	5-192
5.16 Comparison of batch and semi-continuous tests	5-195
5.17 Comparison of reactors performances for semi continuous testing..	5-197
5.17.1 Performance of the three substrates in terms of methane production	5-198
5.17.2 Results of the analysis of variance: Average specific methane potential of the GWSB.	5-199
5.17.3 Results of the analysis of variance: Average specific methane potential of the BPWSB.	5-203
5.17.4 Results of the analysis of variance: Average specific methane potential of the PWSB.	5-205
5.18 A comparison of the specific methane yields of four substrate pre-treatment levels used in the batch test.	5-208
5.19 Expected outcome of the semi-continuous test.	5-210
5.20 Based on the findings, it is possible to draw the following conclusions:	5-211
6 Process Modelling	6-212
6.1 Model Description	6-212
6.1.1 The purpose of the particle size distribution-based degradation model	6-214
6.1.2 Kinetic Model of Anaerobic Digestion	6-218
6.1.3 Purpose of this Model	6-218

6.1.4	Model parameter definition	6-218
6.2	Limitation of the particle size distribution-based model	6-219
6.3	Modelling Results.....	6-219
6.3.1	Selection and processing of experimental data from the literature	6-219
6.3.2	Modelling the effect of particle size distribution at a different percentage of biodegradability factor	6-225
6.3.3	Modelling the effect of particle size distribution with a constant biodegradability factor and variation in K_{sbk}	6-227
6.3.4	Cumulative model output of particle size distribution of total surface area contribution of digested slurry.....	6-230
6.4	Physical Interpretation of Model Results	6-231
6.4.1	All Particle sizes have different degradability and shape.	6-232
7	Conclusions and recommendations.....	7-234
8	Further Works	8-237
9	References	9-238
10	Appendices.....	10-260

List of Tables

Table 2. 1 Summaries of the stages of anaerobic digestion	2-18
Table 2. 2 Population of microbial organisms in anaerobic digestion system	2-18
Table 2. 3 Environmental benefits of the anaerobic degradation of complex organic matter	2-23
Table 2. 4 Methane production component from the complex particulate matter of substrate waste biomass	2-25
Table 2. 5 Inhibitor concentration in anaerobic digestion	2-34
Table 2. 6 Compares mesophilic and thermophilic process operations.....	2-38
Table 2. 7 Benefit and drawback of wet phase digesters	2-41
Table 2. 8 Benefit and drawback of dry -phase digesters.....	2-43
Table 2. 9 A comparison of single-stage and two-stage processes.	2-45
Table 2. 10 Benefit and drawback of two-phase digesters	2-47
Table 2. 11 Waste fraction characteristics in the scenario of shredding	2-52
Table 2. 12 The benefits and drawbacks mechanical size reduction equipment.....	2-57
Table 2. 13 Foam classification	2-74
Table 2. 14 The physical effects of foaming in anaerobic digestion fermentation	2-74
Table 3. 1 Nomenclature of the pre-treatment of each biomass.....	3-86
Table 3. 2 Analysed experimental testing parameters	3-87
Table 3. 3 Alkalinity Definition	3-90
Table 3. 4 Summary of the experimental methodology of the continuous stirred tank reactor (CSTR)	3-92
Table 3. 5 Batch testing employed condition.	3-93
Table 4. 1. Substrate biomass characterization.....	4-102

Table 4. 2 Summary of the particle size distribution of the banana waste substrate biomass according to the pre-treatment levels used during experimental testing of batch and semi-continuous testing.	4-107
Table 4. 3 Summary of the particle size distribution of the grass waste substrate biomass according to their pre-treatment level used during experimental testing of batch and continuous testing.	4-110
Table 4. 4 Summary of the Particle size distribution of the paper waste substrate biomass according to their pre-treatment level used during experimental testing of batch and continuous testing.	4-113
Table 4. 5: Summary of the Particle size distribution of the tomato waste substrate biomass according to their pre-treatment level used during experimental testing of batch and semi continuous testing.....	4-116
Table 4. 6 A summary of the size reduction of four selected substrates utilising various mechanical methods and techniques, as well as their effectiveness in relation to their PTL1-4.....	4-118
Table 5. 1 Maximum biochemical methane (CH ₄) achieved from BPWSB.	5-124
Table 5. 2 Calculation of the volatile solids from the biomass of banana peel waste.	5-125
Table 5. 3 Measured and predicted maximum specific methane production with respective % volatile solids reduction.	5-126
Table 5. 4 First order kinetic parameters value from BMP modelling.....	5-129
Table 5. 5 Modified Gompertz model kinetic parameters value from BMP modelling. .	5-130
Table 5. 6 One-way analysis of variance of the grass waste substrate biomass.....	5-131
Table 5. 7 Maximum biochemical methane (CH ₄) achieved from grass waste	5-137
Table 5. 8 Calculation of the grass waste substrate biomass volatile solids reduction	5-137
Table 5.9 Measured and predicted Maximum specific methane production with respective % volatile solids reduction.	5-139
Table 5. 10 First order kinetic parameters value from BMP modelling.....	5-141
Table 5. 11 Modified Gompertz model kinetic parameters value from BMP modelling.	5-141
Table 5. 12 One-way analysis of variance of the grass waste substrate biomass.....	5-142

Table 5. 13 Maximum biochemical methane (CH ₄) achieved from the paper waste substrate biomass.	5-148
Table 5.14 Calculation of the volatile solid reduction of paper waste substrate biomass ultimate degradation.	5-148
Table 5. 15 Measured and predicted Maximum specific methane production with respective % volatile solids reduction.	5-149
Table 5. 16 First order kinetic parameters value from BMP modelling.....	5-151
Table 5. 17 Modified Gompertz model kinetic parameters value from BMP modelling.	5-151
Table 5. 18 One-way analysis of variance of the grass waste substrate biomass.....	5-153
Table 5. 19 Maximum Biochemical Methane (CH ₄) Achieved From TWSB	5-157
Table 5. 20 Calculation of volatile solid reduction of tomato waste substrate biomass ultimate degradation.	5-157
Table 5. 21 Measured and predicted Maximum specific methane production with respective % volatile solids reduction.	5-159
Table 5. 22 First order kinetic parameters value from BMP modelling.....	5-161
Table 5. 23 Modified Gompertz model kinetic parameters value from BMP modelling.	5-161
Table 5. 24 One-way analysis of variance of the grass waste substrate biomass.....	5-162
Table 5. 25 Comparison of the methane yield of the four-substrate biomass in Nml/gVS.	5-166
Table 5. 26: Calculated organic loading rate (OLR) of banana peel waste substrate biomass.	5-170
Table 5. 27: Calculated organic loading rate (OLR) of grass peel waste substrate biomass.....	5-171
Table 5. 28: Calculated organic loading rate (OLR) of paper waste substrate biomass.	5-171
Table 5. 29: Parameters measured during semi-continuous testing.	5-172
Table 5. 30: Duplicate reactor used for semi-continuous testing of three substrate biomass degradation.	5-173
Table 5. 31 Average% biogas methane content for reactor R1 to R6 PTLs	5-188
Table 5. 32: An overview of digester performance	5-193

Table 5. 33 Average specific methane output from batch and semi-continuous tests of GWSB, BPWSB and PWSB across the duration of the study.	5-196
Table 5. 34 Specific Methane yield differences in reactors R1 and R2.....	5-197
Table 5. 35 Specific Methane yield differences in reactors R3 and R4.....	5-197
Table 5. 36 Specific Methane yield differences in reactors R5 and R6.....	5-198
Table 5. 37 An independent samples t test of the three-substrate used for semi-continuous test	5-199
Table 5. 38 Results of the analysis of variance: Average specific methane potential of the GWSB.	5-201
Table 5. 39. Results of the analysis of variance: Average specific methane potential of the BPWSB.	5-203
Table 5. 40 Results of the analysis of variance: Average specific methane potential of the PWSB.....	5-206
Table 5. 41 Results of the analysis of variance between the four substrates used in the batch test for a period of 25 days.....	5-209
Table 6. 1 Calculation example of the mass concentration (C_i).....	6-220
Table 6. 2 Calculation example of the weighted average particle size range of each of the 10 fractions	6-221
Table 6. 3 Assume degradability factor (exp.+ model), for digested output with 0.28 kinetic constants K_{sbk}	6-225
Table 6. 4 Experimental digester slurry and model output of digested slurry at 100% degradability.	6-230

List of Figures

Figure 1.1 Installed Nigeria distribution capacity.	1-3
Figure 2.1 Four main pathway of anaerobic particulate	2-9
Figure 2.2 Main steps in enzymatic hydrolysis	2-13
Figure 2.3 Glycerol and triglycerides	2-13
Figure 2.4 Protein chain and amino acids linked by amide group.....	2-13
Figure 2.5 Acidogenesis products from C6 monosaccharide fermentation	2-14
Figure 2.6 depicts the various methanogenic pathways: Hydrogenotrophic (red), methylotrophic (blue), and acetolactic (green) pathways.	2-17
Figure 2.7 Pathogens' modes of infection in humans through solid waste.....	2-22
Figure 2.8 Effect of temperature on the anaerobic digestion process.....	2-28
Figure 2.9 Simple scheme of high organic loading rate (OLR)reactor, methanogenic microbial population activities, hydrolysis constant and the degradation of complex particulate matter	2-32
Figure 2.10: The influence of pH on the degree of anaerobic solubilization	2-33
Figure 2.11 Anaerobic fermentation process options based on the classification of 'wet' or 'dry.'	2-39
Figure 2.12 A typical one-phase 'wet' mesophilic digester.	2-41
Figure 2.13 Different digester used in 'dry' anaerobic systems. A: Dranco design, B; Kompostogas and BRV designs, and C: Valorga design.	2-43
Figure 2.14 Multistage reactor system	2-47
Figure 2.15 Role of pre-treatment in the transformation of substrate biomass into biogas	2-49
Figure 2.16: Three main types of mechanical comminution equipment extensively used in municipal waste processing.	2-50
Figure 2.17 Components of the size comminution equipment.....	2-51
Figure 2.18 Diagram of a hammer mill	2-53
Figure 2.19 Schematic of a shredder's operating mechanism.....	2-54
Figure 2.20 A diagram of a roller mill	2-56

Figure 2.21 A diagram of a Ball Mill	2-56
Figure 2.22 Diagram of a cutting mill.....	2-57
Figure 2.23 Particle size analysis on size reduced OFMSW using a shear shredder, rotary cutter, and wet macerator.....	2-60
Figure 2.24 Cumulative particle size distribution using various shredding equipment types.....	2-61
Figure 2.25 Cumulative particle size distribution of the organic kitchen and garden waste fraction using various types of shredding devices.	2-62
Figure 2.26 Paper/cardboard grain size distribution when employing various shredder components.	2-63
Figure 2.27 Effect of particle size on the yield of methane production of sisal fibre	2-68
Figure 2.28 Enhancement of biogas production through batch degradation process as a result of particle size reduction and corresponding degrees of degradation level of the raw substrate (a; Mixture of apples, carrots, and potatoes; meat; c: Sunflower seeds; d: Haye: leaves).....	2-69
Figure 2.29 depicts the arithmetic mean of re-analysed data for three grass digestions. .	2-71
Figure 2.30 Foam images (Abb1) from a biogas digester (Abb2) from a microscope	2-73
Figure 2.31 Conversion processes of the physiochemical and biochemical in an anaerobic digestion digester	2-75
Figure 2.32 Biochemical (vertical) and biochemical processes(horizontal) in an anaerobic digester	2-77
Figure 3.1 Schematic of the sample preparation methodology	3-85
Figure 3.2 Leak testing of batch reactor	3-94
Figure 3.3 Experimental setups for BMP testing, stirred incubation unit in a water bath with NaOH as a scrubber and a volumetric gas flow meter multi-channel and software user interface.....	3-96
Figure 3.4 Experimental setups for semi continuous testing	3-98
Figure 3.5 Overview methodology of batch and semi- continuous testing.	3-99
Figure 3.6 Process flow for characterising particle size distribution.....	3-100

Figure 4.1 Particle size distribution of banana waste substrate biomass pre-treatment one.	4-105
Figure 4.2 Particle distribution of banana peel waste substrate biomass pre-treatment two.	4-105
Figure 4.3 Particle size distribution of banana peel waste substrate biomass pre-treatment three.	4-106
Figure 4.4 Particle size distribution of banana peel waste substrate biomass pre-treatment four.	4-106
Figure 4.5 Particle size distribution of grass waste substrate biomass.....	4-108
Figure 4.6 Particle size distribution of grass waste substrate biomass pre-treatment level two.....	4-108
Figure 4.7 Particle size distribution of grass waste substrate biomass pre-treatment level three.	4-109
Figure 4.8 Particle size distribution of grass waste substrate biomass pre-treatment level four.	4-109
Figure 4.9 : Particle size distribution of paper waste substrate biomass pre-treatment one.	4-111
Figure 4.10 Particle size distribution of paper waste substrate biomass Pre-treatment two.	4-111
Figure 4.11 Particle size distribution of paper waste substrate biomass pre-treatment level three.	4-112
Figure 4.12 Particle size distribution of paper waste substrate biomass pre-treatment level four.	4-112
Figure 4.13 Particle size distribution of tomato waste substrate biomass pre-treatment level one.....	4-114
Figure 4.14 Particle size distribution of tomato waste substrate biomass pre-treatment level two.....	4-114
Figure 4.15 Particle size distribution of tomato waste substrate biomass pre-treatment level three.	4-115

Figure 4.16 Particle size distribution of tomato waste substrate biomass pre-treatment level four.	4-115
Figure 5.1a & b Cumulative methane (CH ₄) production for a triplicate sample of the blank, contains only 400ml inoculum and for control (cellulose and inoculum) digested during BPWSB.	5-123
Figure 5.2 Specific methane (CH ₄) production for BPWSB with average control from triplicates (CH ₄ subtracted from the inoculum and data expressed in terms of grams of volatile solid (gVS) added).....	5-123
Figure 5.3 Cumulative flow rate and accumulated % volume of the methane production for BPWSB degradation after the subtraction of the inoculum CH ₄ production.	5-124
Figure 5.4 Compares the BMP of the BPWSB with the theoretical methane yield at STP based on the experimentally determined volatile solids reduction (PTL1-4) and carbon feed material.	5-126
Figure 5.5 Experimental results for BPWSB and the kinetics of specific CH ₄ production for first order (model 1) and modified Gompertz (model 2).....	5-129
Figure 5.6 Means boxplot of the variation of the methane yield of BPWSB four pre-treatment levels.....	5-132
Figure 5.7 Fisher LSD means comparisons plot for banana peel waste methane yield of four pre-treatment levels.	5-133
Figure 5.8a&b: Cumulative methane (CH ₄) production for a triplicate sample of the blank, contains only 400ml inoculum and for control (cellulose and inoculum) digested during GWSB.	5-135
Figure 5.9 Specific methane (CH ₄) production for grass waste substrate biomass (GWSB) with average control from triplicates (CH ₄) subtracted from the inoculum and data expressed in terms of grams of volatile solid (gVS) added).	5-136
Figure 5.10 Cumulative flow rate and accumulated % volume of the methane production for GPWSB degradation after the subtraction of the inoculum CH ₄ production.....	5-137

Figure 5.11 Compares the BMP of the GWSB with the theoretical methane yield at STP based on the experimentally determined volatile solids reduction (PTL1-4) and carbon feed material.	5-139
Figure 5.12 Experimental results for GWSB and the kinetics of specific CH ₄ production for first order (model 1) and modified Gompertz (model 2).....	5-140
Figure 5.13 Means boxplot of the variation of the methane yield of GWSB four pre-treatment levels.....	5-143
Figure 5.14 Fisher LSD means comparison plot for grass waste methane yield of four pre-treatment levels.	5-143
Figure 5.15a &b Cumulative methane (CH ₄) production for a triplicate sample of the blank, contains only 400ml inoculum and for control (cellulose and inoculum) digested during PWSB.....	5-146
Figure 5.16 Specific methane (CH ₄) production for paper waste substrate biomass (PWSB) with average control from triplicates (CH ₄ subtracted from the inoculum and data expressed in terms of grams of volatile solid (gVS) added).	5-147
Figure 5.17 Cumulative flow rate and accumulated volume of the methane production for PWSB degradation after the subtraction of the inoculum CH ₄ production.....	5-148
Figure 5.18 Compares the BMP of the PWSB with the theoretical methane yield at STP based on the experimentally determined volatile solids reduction (PTL1-4) and carbon feed material.	5-150
Figure 5.19 Experimental results for PWSB and the kinetics of specific CH ₄ production for first order (model 1) and modified Gompertz (model 2).....	5-151
Figure 5.20 Means boxplot of the variation of the methane yield of GWSB four pre-treatment levels.....	5-153
Figure 5.21 Fisher LSD means comparisons plot for grass waste methane yield of four pre-treatment levels.	5-154
Figure 5.22a&b: Cumulative methane (CH ₄) production for a triplicate sample of the blank , contains only 400ml inoculum and for control (cellulose and inoculum).	5-155

Figure 5.23 Specific methane (CH ₄) production for paper waste substrate biomass (TWSB) with average control from triplicates (CH ₄) subtracted from the inoculum and data expressed in terms of grams of volatile solid (gVS) added).	5-156
Figure 5.24: Cumulative flow rate and accumulated volume of the methane production for TWSB degradation after the subtraction of the inoculum CH ₄ production.....	5-157
Figure 5.25 Compares the BMP of the TWSB with the theoretical methane yield at STP based on the experimentally determined volatile solids reduction (PTL1-4) and carbon feed material.	5-159
Figure 5.26 Experimental results for TWSB and the kinetics of specific CH ₄ production for first order (model 1) and modified Gompertz (model 2).....	5-160
Figure 5.27 Means boxplot of the variation of the methane yield of GWSB four pre-treatment levels.....	5-163
Figure 5.28 Tukey Test Means Comparisons plot for grass waste methane yield of four pre-treatment levels.	5-163
Figure 5.29: Percentage biogas methane CH ₄ content produced from the degradation of GWSB (R1 and R2).....	5-175
Figure 5.30: Semi-continuous testing showing specific CH ₄ production of GWSB (R1 and R2).	5-177
Figure 5.31: Semi-continuous testing showing average specific CH ₄ production from GWSB in a bioreactor (R1 and R2).	5-178
Figure 5.32: Methane (CH ₄) content of biogas production of the degradation of BPWSB (R3 and R6).....	5-180
Figure 5.33: Specific methane (CH ₄) production of the degradation of BPWSB (R3 And R4).	5-182
Figure 5.34: Semi-continuous testing showing average specific CH ₄ production of BPWSB degradation.	5-182
Figure 5.35: Percentage biogas methane CH ₄ production of the degradation of PWSB (R5 and R6).....	5-184
Figure 5.36: Semi-continuous testing showing specific CH ₄ production of the PWSB.....	5-186

Figure 5.37: Semi-continuous testing showing average specific CH ₄ production of PWSB.5-	
186	
Figure 5.38: The average % of biogas methane content for GWSB, BPWSB, and PWSB duplicate reactors R1 to R6.....	5-188
Figure 5.39: shows the pH, total and IA:PA alkalinity, for the GWSB digester during the semi-continuous test.	5-190
Figure 5.40 shows the pH, total and IA:PA alkalinity, for the GWSB digester during the semi-continuous test.	5-191
Figure 5.41: shows the pH, total and IA:PA alkalinity, for the GWSB digester during the semi-continuous test.	5-191
Figure 5.42: Means bar chart of the GWSB average specific methane yield's variation. ..	5-202
Figure 5.43: Means Comparison plot using fisher LSD.	5-202
Figure 5.44: Means plot SD as error for the BPWSB average specific methane yield's variation.	5-204
Figure 5.45: Means Comparison plot using fisher LSD.	5-205
Figure 5.46: Means boxplot of the PWSB average specific methane yield's variation.	5-207
Figure 5.47: Means Comparison plot using fisher LSD.	5-207
Figure 5.48: Means bar plot of the average specific methane yields of four substrate from batch test	5-210
Figure 6.1 Demonstrates the feedstock radius frequency as a function of time	6-213
Figure 6.2 displays the feedstock PSD over time.	6-215
Figure 6.3 Experimental data for PSD used for extraction	6-222
Figure 6.4: Converted experimental data of PSD digested slurry and model output digested slurry.....	6-223
Figure 6.5: Experimental digester slurry and model output of digested slurry at 100% degradability.	6-224
Figure 6.6: Particle size distribution (PSD) result, Experimental digested and model output for digested slurry.	6-226
Figure 6.7: Variation of hydrolysis constant (K_{sbk}) at 50% degradability constant.	6-229
Figure 6.8: Variation of hydrolysis constant (K_{sbk}) at 70% degradability constant.	6-229

Figure 6.9: Cumulative model output of particle size distribution of total surface area
contribution of digested slurry. 6-231

1 Introduction

1.1. Background of the Study

Energy is very critical for economic development. No country can achieve sustainable development when its energy sector is not well developed. The production of energy is indeed through various means, but having an energy mix that will help mitigate, or not compound, the problem of global warming remains a challenge, especially in a developing nation like Nigeria. Most of the people in rural and remote areas of developing countries depend on firewood to meet basic energy needs. This practice is known to have caused air pollution and significant health problems for individuals. On the other hand, the continued over-reliance on fossil fuels such as coal, oil and natural gas presents risks like, land degradation and environmental pollution of air, water, leading to global warming and, climatic change, thus resulting in multiple problems for humans and animals in the future. Nigeria as the seventh-largest country in the African continent and like other developing nations has a growing potential for increased demand for energy. The population is more than 170 million with a GDP growth rate of about 7%. The current population made up of females is about 49.4% and male about 50.6%. Also, population growth has resulted in an increase in uncontrolled waste across the country, thereby creating environmental hazards through skin contact, inhalation and ingestion, economic and social problems that need urgent attention by the nation. About 95 million Nigerians and 55% of the population have no access to clean energy (electricity) while those linked to the nation's national grid are faced with the challenge of lengthy power interruptions. Systemic problems influence all the stages of the power value chain, such as production, transmission, distribution, and gas supply. This has driven most of the people to rely mainly on self-generation of energy in the residential, commercial, and industrial sectors with diesel generators at a higher cost (NGN 62-94 kWh) compared to the national grid-based (NGN 26-38 kWh)

power. This self-generated energy has resulted in an environmental hazard that using clean energy could reduce this impact. These have been the existing historic gap between the demands for power across the nation that needs renewable energy technology. Also, it causes the price of the commodity to increase. This affects the consumers because of recurrent expenditure by business owners because of the self-generation of energy (electricity). In Nigeria, energy (electricity) has contributed to the total gross domestic product (TGDP), yet the nation is affected by many problems because of the inadequate power supply. Also, the country's energy sub sector cannot meet the electricity demand and is currently causing enormous economic challenges across the nation. Historically, a lower investment level of power generation in the country creates a massive barrier for most of the private investment companies in Nigeria. The World Bank reported that 41% of business owners in Nigeria produce their power supply as this will enable them to augment the supply from the country's national grid supply at about 126 kWh per capita. In comparison, the Ghana per capita consumption of energy is about 361kWh which is 2.9 times higher compared to Nigeria and South Africans per capita consumption (3926 kWh) which is 31 times greater with growth in the population of about 52 million as compared to the size of Nigeria. From literature data, as the population of a country increases, the demand and supply for energy equally increase. Surprisingly, Nigeria as an oil producer could only generate about 7,411 MW of electricity and with a lower operational capacity of about 3879MW. Figure 1 shows Nigeria has a transmission capacity of 3,600MW and 3,100 MW distributed [1]. However, the main drawback to the nation's energy generation capacity includes:

- ❖ Vandalism
- ❖ Demand and supply imbalance because of higher interest recurrence
- ❖ Infrastructure tools transmission insufficiency (line requirement)
- ❖ Poor management of natural water resource

However, Nigeria has an installed electricity generation capacity for supply to the natural grid of 12,522 MW, but at the end of January 2016, the demand for electricity in Nigeria was estimated to be 12,800 MW, yet less than 26% of Nigeria installed

capacity could reach the end-user [1]. Also, access to electricity is about 10%, for the rural communities, 51% for the urban region of the nation, and the energy consumption per capita is 8.1 MWhr while the total power consumption is 1259 TWhr per annum. According to [2] energy prevents deprivation and poverty resulting from economic degradation while at the same time, supports production in manufacturing, agriculture, commerce, and mining. Also, poverty is significant in Nigeria as about 61% of the nation live below the poverty line. Energy plays a significant role in education, transport, and communication. Nigeria is faced with a massive economic challenge and a lack of access to clean energy. However, the energy situation in most developing countries, especially rural communities, can be improved [1], [3].

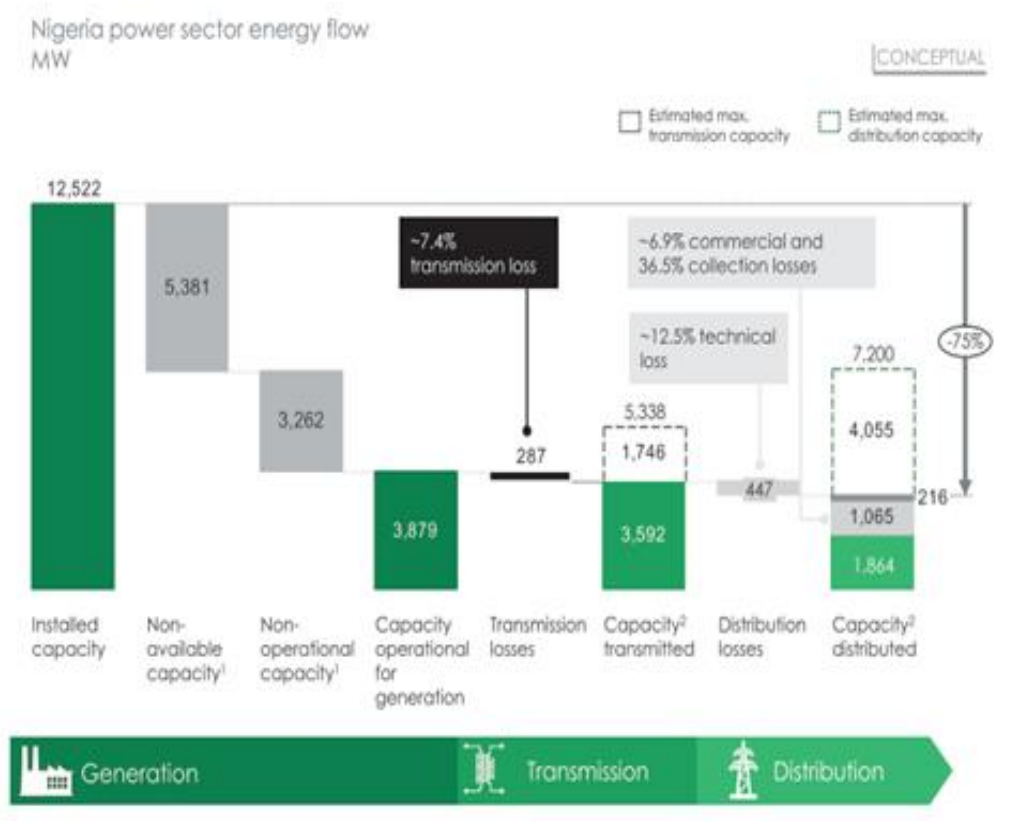


Figure 1.1 Installed Nigeria distribution capacity.

Source : [1]

The biogas technology undoubtedly can assist developing nations in enhancing their ability to access clean energy. The process generates methane, which is a useful energy resource. A valuable horticultural soil conditioner and fertilizer-like materials are also produced by the AD process [4]. The AD process, when adequately developed, can contribute significantly to solving the energy problems of developing countries. The AD system runs on a small scale and requires little capital. It allows for decentralisation of the system, which is very advantageous. These imply that the AD system can be installed in remote, rural, and urban locations across the nation. This technology will clearly be used to help Nigerians with their energy issues because it will contribute to their solution. Therefore, it is expedient to improve our understanding of the operation and optimisation of the AD process concerning the mechanical pre-treatment and particle size distribution of biodegradable fractions of some selected waste biomass. This thesis focuses on the effect of particle size distribution on system kinetics and overall degradation on the anaerobic digestion of waste biomass by exploring various mechanical equipment and four selected feedstocks (Banana, grass, paper, and tomatoes respectively).

1.1 The energy situation in Nigeria

The following are some aspects of the energy crisis in Nigeria:

- ❖ Nigeria, which is richly endowed with a variety of energy resources, is the most populated country in all of Africa.
- ❖ Over 60% of Africa's oil resources are in Nigeria and Angola.
- ❖ Nigeria has enormous resources of lignite and bitumen in addition to ranking second to Algeria in terms of natural gas reserves [5].
- ❖ The Nigerian economy's growth is mostly dependent on energy.
- ❖ Additionally, energy is used as a raw material in the nation's transportation, healthcare, and education sectors as well as an instrument of security, politics, and diplomacy [6].
- ❖ Nigeria's crude oil reserves, which make up well over seventy percent (70%) of the country's GDP, are the source of all the country's energy income.

- ❖ Resources for primary energy are plentiful in Nigeria. With a barrel capacity of around 36.2 billion, the country is home to the tenth-largest reserve of unrefined petroleum in the entire globe.
- ❖ Nigeria is regarded more as a normal gas base than an oil one, with an estimated reserve of 166 trillion standard cubic feet. Nigeria is among the top ten countries with the largest gas reserves in the world based on this amount, which includes linked and unrelated reserves.
- ❖ Despite having ample biomass resources to cover both traditional and modern energy needs, Nigeria [7] lacks both advanced technologies and a tight supply-demand balance.
- ❖ The Nigerian federal government continues to encourage increased alienation and isolation because most communities are not adequately represented in national planning. Given the profound effects it has on the economy, society and environmental well-being of every person affected, the gravity of this issue cannot be overstated.

However, most oil and gas reservoirs can be found in the Niger Delta region, the Gulf of Guinea, and the Bight of Bonny. Residents in remote and rural villages suffer in Nigeria, like they do in other developing countries, when problems with infrastructure, logistics, inhospitable terrain, and vandalism affect energy generation, transmission, and distribution. To reduce the energy deficit, it is advantageous to use the waste from these communities to produce clean fuel in the form of biogas. This is because almost all these rural villages' major sector is agriculture, which generates large quantities of agricultural waste and municipal (biodegradable) waste. Additionally, because the energy generated would be transmitted inside the same region, the federal government would save money in that area. There would be further benefits as well, like better public health (since trash is not disposed of), a stronger local economy through the creation of jobs, and valuable fuels as this would also help to save the country from the current severe economic crisis.

1.2 Research motivation

From the summaries of Nigerian energy situations, it can be concluded that alternative renewable energy technology plays an increasingly significant role in the economic development of any country, including anaerobic digestion and my motivation is the exploitation of agricultural resources described earlier in 1.1.1, for the purpose of bio-energy generation.

1.3 Scope of study

The initial part of my research work focuses mainly on three mechanical types of machinery, specifically:

- ❖ **Inox No.8 Stainless Steel Electric Mincer 220/50:** It minces the feed material using a sharp knife and is made entirely of stainless steel. It consisted mainly of a mincer knife, two nozzles, and two stainless steel plates (6mm and 16mm). When the knife is taken out of the mincer and the plate is inserted, it works by inserting one of the nozzles through the front screw. A casing should be spread out over the nozzle, leaving an inch hanging over the end before the material is filled and fed through the mincer. One of this machine's main benefits is how easily it can be unbolted, which makes it simple to clean and maintain.
- ❖ **Magimix 5200XL Premium Blender Mix Food Processor:** It operates on the principle of impact and can quickly and easily slice, chop, grind, and knead feed material. The powerful motor adapts to the task at hand because of its straightforward and simple operation, which only requires 3 buttons to access all functions. The convenient storage box that is provided keeps all the blades and discs securely. The size of the plate's hole determines how much grinding is done.
- ❖ **Paper Shredder PS1840 Product-SKU: SHRED102001):** Shredders consist of two parallel, counter-rotating shafts with a series of discs. The core of the

counter-rotating shafts is where the shredder waste is directed. Shearing and tearing serve as its governing principles.

This mechanical equipment that is selected is of different types because it will be used to assess the performance of different size fractions of municipal solid waste (MSW). They were also selected because they could emulate the type of common mechanical pre-treatment equipment for AD plants. e.g., shredders, macerators etc. This mechanical machinery for the biomass size reduction of feedstocks such as paper, grasses, banana peeling, and laboratory analysis of their particle sizes. The scope of this research work will include the utilisation of both a batch reactor and a semi-continuous stirred tank reactor. Investigating the effect of particle size (PS) distribution on the anaerobic digestion (AD) process, the effects of the PS distribution on the operation and optimisation of the AD process about the maximum OLR and other relevant process parameters. Evaluation of the impact of mechanical pre-treatments applied to the AD system.

1.4 Project Aim and Objectives

The project aims to use experimental and modelling methods to study the effect of mechanical size reduction on the performance of anaerobic digestion processes. The experiment using Automatic Methane Potential Test System (AMPTS II) and Bioreactor Simulator (BRS) bioprocess for batch testing and semi-continuous testing was performed in the AD lab at the University of Sheffield.

1.4.1 Aim

The study's aim is to investigate the effects of various mechanical pre-treatment methods on the size reduction of different organic materials and their potential to degrade under anaerobic conditions in terms of particle size distribution and other process parameters.

1.4.2 Objectives of the study

- ❖ To evaluate the effect of mechanical reduction methods on the PS distribution of the biomass constituents of MSW.

- ❖ To investigate the effect of PS distribution on the biogas potential and biogas production kinetics.
- ❖ To study the effect of the particle size distribution (PSD) on the operation and optimization of the AD process on the maximum OLR and other relevant process parameters.
- ❖ To develop and validate a particle size distribution (PSD) based degradation model to incorporate the effects of PS distribution and its effects on kinetics.
- ❖ To investigate the difference in methane production at the different physical pre-treatment levels.

1.5 Structure of the thesis

The thesis comprises seven (7) chapters which include about 70% laboratory work and 30% simulation in terms of effort. The results obtained from the experiment are adapted for simulation using MATLAB/Simulink code and integrated into an anaerobic digestion model no. 1 for the complex organic matter to predict the overall biogas production [8]. This research work follows the regular thesis structure; introduction to energy, review of relevant literature data, description of the experimental material and methods used, presentation of the results and discussion of the laboratory experimental investigations obtained, summary, conclusion, and recommendations for further work. Generally, the thesis has been presented following the order that the investigation was carried out from the start on the background of energy, previous work, and relevant literature review, experimental material and methods, results, and discussion. This is followed by the investigation which progresses in increasing complexity after baseline study to establish fundamentals.

2 Literature Review

2.1 The Biogas Technology

The term anaerobic digestion (AD) is a known process by which a consortium of microbial cultures attacks a complex organic material in the absence of free oxygen. The AD process results in the generation of biogas together with solid and liquid residues due to the natural decay of organic matter that is fed into a digester [7] the principal constituents of biogas are methane (CH₄) and carbon dioxide (CO₂). Other components, such as hydrogen (H₂), hydrogen sulphide (H₂S), ammonia (NH₃), nitrogen, carbon monoxide, oxygen, and siloxanes, are sometimes found in biogas, but in small amounts [9]. In contrast to aerobic systems where the rate of reaction occurs when oxygen is present. The general equation for anaerobic digestion action is given by [10] as follows: Organic matter + Combined Oxygen + Anaerobic microbes' → CH₄ + CO₂+Other end-products **(1.1)**

As indicated in figure 2.1, the four dynamic biological stages of AD processes are hydrolysis, acidogenesis acetogenesis, and methanogenesis which provides a brief summary of their core methodologies [11].

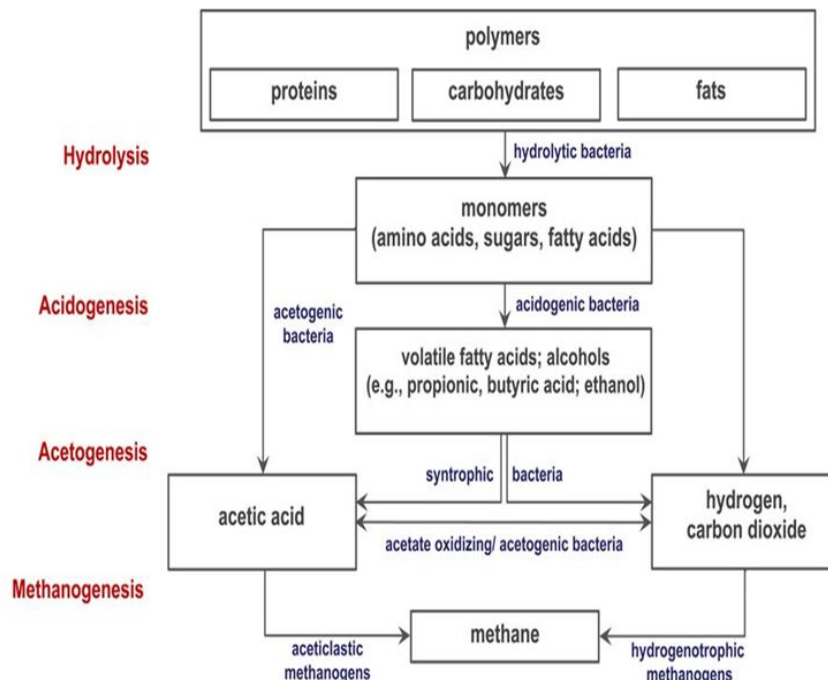


Figure 2.1 Four main pathway of anaerobic particulate

Source [11]

From figure 2.3, the AD process is the product of several metabolic activities among various groups of microorganisms comprising the hydrolytic and fermentative bacteria, acetogenic bacteria, and the methanogenic archaeobacteria. Bacterial relationships have a role in the AD process. This demonstrates that the microbes in the first and second groups (hydrolysis and acidogenesis), as well as the third and fourth groups (acetogenesis and methanogenesis), are closely related. As a result, the AD process can be separated into two major categories [12], [13]. The syntrophic interaction between archaea that use hydrogen, like methanogens, and organisms that produce hydrogen through fermentation is known as interspecies hydrogen transfer. Methanogens archaea need fermenters/acetogens to provide them with the hydrogen, carbonate, and acetic acid they need as substrates, while acetogens depends on methanogens to release hydrogen because their catalysts are just endothermic at very low hydrogen levels [14]. Additionally, these bacteria work together to utilize the substrate in the AD system. As a result, solids cannot build up and obstruct the gas pipeline. The biomass in the bioreactor will therefore be adequately agitated, minimizing an excessive accumulation of VFA, ammonia, pH, and foaming that could lead to the failure of the AD system. However, for complete degradation to take place, many microbes need to be present in the reactor to speed up the digestion process of the substrate [15]. Also, the techniques of anaerobic digestion systems are very superior to the aerobic system due to low energy input and the production of biogas as a valuable product. According to Angelidaki and Sanders [16], greater contact between enzymes and substrate is essential for hydrolysis. This is because the microorganism emits hydrolytic enzymes and equally benefits from the digestion of the first-order surface area of particulate materials. Also, the reduction of substrate particle size through pre-treatment can increase the surface area that becomes available for microbial activity, and this can cause the generation of more biogas. Many scientific researchers have explored diverse pre-treatment techniques such as physical, chemical, biological, and even a combination of techniques to enhance the microbial degradation of complex waste [17]–[20]. Pre-treatment of lignocellulosic materials was found to cause profound alterations

in the structure of the complex materials at the level of polymerisation, therefore breaking the molecular bonds between lignin and carbohydrate and expanding the shallow area of particulate matters [21], [22]. Thus, to enhance microbial activity and methane production, it is advantageous to give mechanical pre-treatment before anaerobic digestion [20]. Therefore, it is expedient to check some mechanical devices that are employed in the combination of feedstock and to study the different particle sizes and shapes of the feedstock shredded and fed into the anaerobic digester system to have an enhanced understanding of the particle size and shape of the feedstock and how they affect the performance of the AD process.

2.2 Phases of the anaerobic digestion process

2.2.1 Hydrolysis

A process whereby complex organic matter is converted into much simpler soluble molecules is known as hydrolysis. This process is catalysed by enzymes, which is produced by the activity of the anaerobic bacteria feeding on the substrate [23]. It includes carbohydrates, proteins, lipids, or composite compounds such as sludge or yeast. The core products are long-chain fatty (LCFA), amino acids and monosaccharides, respectively. According to Esposito et al [24] there are three fundamental pathways of enzymatic hydrolysis:

- ❖ The anaerobic bacteria release catalysts into the mass fluid where it adsorbs onto a molecule or responds with a dissolvable substrate.
- ❖ The anaerobic bacteria attach to the particle and produce enzymes near the particle. After the enzymatic reaction, the microorganism benefits from the soluble products that are discharged.
- ❖ The anaerobic organisms have an attached catalyst, which may double up a vehicle receptor to the inner part of the cell. This technique requires the bacteria to adsorb onto the surface of the molecules [25]–[27].

According to the study of Vavilin et al [26], the hydrolysis of complex particulate substrates is a two-phase reaction propelled by extracellular enzymes during hydrolytic reactions secreted by bacteria that obligate the facultative anaerobes. The first phase is bacterial colonization, a point where the hydrolytic bacteria cover the surface of particulate matter, and the reaction rate strongly relies on the available contact area. Bacteria that are on the surface, or close to the surface, secrete enzymes and produce the monomers that are used by the hydrolytic bacteria. In the second phase, the hydrolytic enzymes degrade the complex particulate matter on the available surface at a constant depth per unit of time. Also, the extent of the reaction rate of hydrolytic enzymes relies on the substrate physical and chemical composition, solid concentration and the digester hydraulics, which significantly affect the rate at which hydrolysis takes place [28]–[30]. The steps involved in the enzymatic hydrolysis process are as follows:

- ❖ Production of catalysts can decrease when there is excessive soluble substrate available [31].
- ❖ The producing microbe transfers enzymes to the bulk.
- ❖ Enzymes diffuse from the bulk to the feedstock particle.
- ❖ The Adsorption processes are limited to the substrate particle (surface area).
- ❖ The reaction rate is limited by the enzyme concentration and the substrate surface area.
- ❖ Diffusion of product from the particle to the bulk.
- ❖ Deactivation of the catalyst can become excessive when there is a shift from optimal pH and temperature [25].

However, there has been a wide range of different complex hydrolysis kinetic models that include all these steps (Figure 2.2) [30], but the validation of this complex model has been difficult. The first-order kinetic rate model proposed by

Eastman and Ferguson [32] is the simplest and the most commonly used in practice to describe the hydrolysis process.

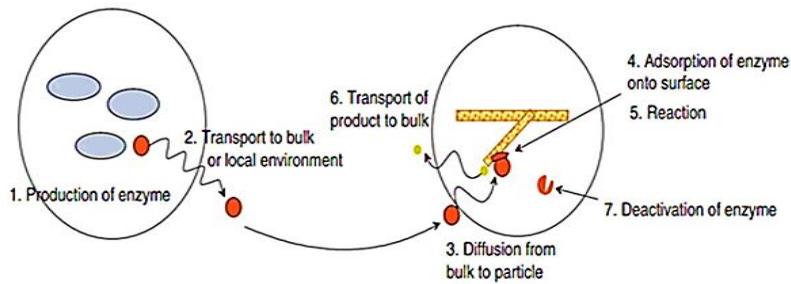


Figure 2.2 Main steps in enzymatic hydrolysis

Source: [30]

Also, the first-order kinetic model has been presented by Eastman and Ferguson [32], as an empirical expression that represents the cumulative effects of all the microbial action occurring in the AD process. During the hydrolysis process, the particulate substrate met the hydrolytic microbial cells and realised a catalyst for long-chain fatty acid ester (LCFA) known as hydrolases and lapses. Lapses break down the bonds in the polymeric, and this results in shorter chain molecules [15], [26], [30], [33]. The reaction of the hydrolysis of lipids and protein is indicated in figure 2.3 and 2.4 respectively.



Figure 2.3 Glycerol and triglycerides

Source: [30]

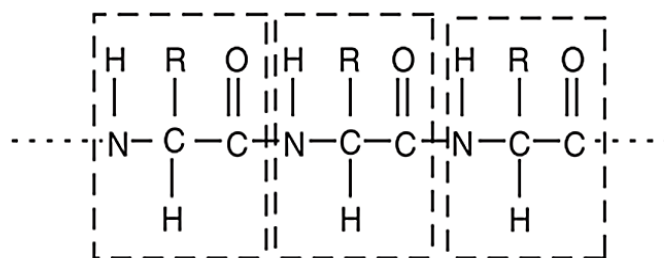


Figure 2.4 Protein chain and amino acids linked by amide group.

Source: [30]

Hydrolysis is affected by substrate biodegradability of complex organic matter structures (lignocellulosic biomass) such as part of food waste and manure [34], [35]. The cellulose degradation rate is affected by the hydrolysis enzymatic activity, as well as it also depends on the cellulose polymers, physical, chemical conditions, and high-temperature pre-treatment [36].

2.2.2 Acidogenesis

In acidogenesis, the products of hydrolysis are broken down into further simpler and easily degradable fractions. It is the second stage of the AD process, and the fastest step as well [15], [34], [37]. This stage yields VFA alongside ammonia, CO₂, H₂, and other by-products through the action of acidogenic bacteria. The most essential of the organic acids is acetate since it can be used directly as a substrate by the methanogenic organisms. The common products of acidogenesis from C₆ monosaccharide are shown in figure 2.5 in which the anaerobic microbial organisms generate acetate and butyrate (VFA) from glucose.

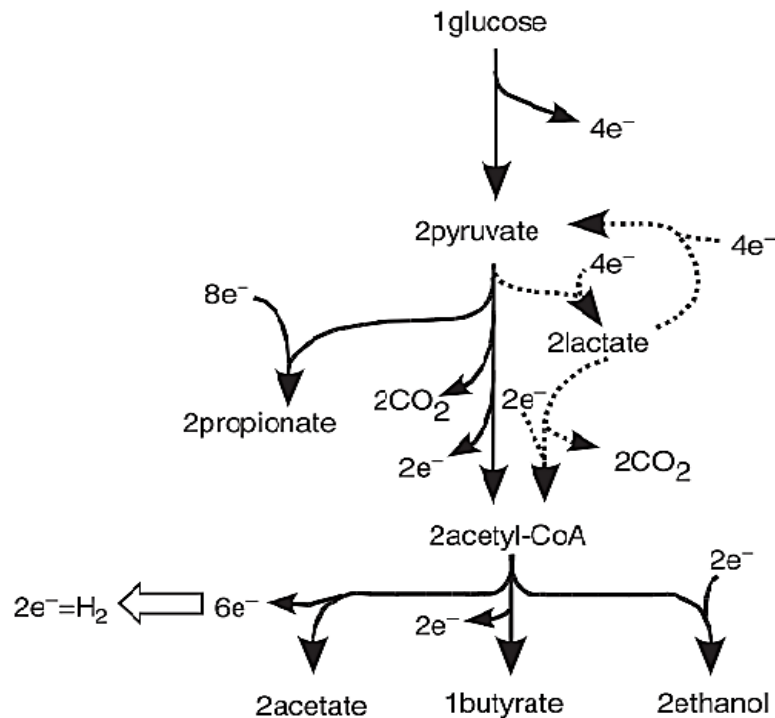


Figure 2.5 Acidogenesis products from C₆ monosaccharide fermentation

Source [30].

2.2.3 Acetogenesis

This is the third stage of the AD process. During this stage, the hydrogen-producing acetogens consume VFAs and LCFAs, which are produced during the hydrolysis of lipids into acetic acid, hydrogen, and CO₂. These bacteria work in synergy with methanogenic bacteria, which is known as the interspecies transfer of hydrogen, while the homoacetogenic bacteria break down the CO₂ and H₂ to acetic acid. Acetogenic bacteria are known to be very sensitive to both physical and chemical conditions such as temperature, and hydrogen ion concentration.

2.2.4 Methanogenesis

Methanogenesis is the final stage of the anaerobic digestion where methane is synthesized by methanogens archaeobacteria. This synthesis is achieved by breaking down acid molecules to form carbon dioxide and methane. It would also be achieved through the reduction of carbon dioxide (CO₂) with hydrogen [38]. Anaerobic bacteria and acetogenins provide methanogens archaea with their needed substrate such as hydrogen, carbonate, and acetic acid whereas the acetogens depend on the methanogens at a very low concentration of dissolved hydrogen and making the degradation of organic matter thermodynamically favourable [15]. This involves two groups of bacteria that depend on the substrate they can use in the AD system known as the acetoclastic methanogen and hydrogenotrophic methanogens. Methanogen archaea can produce methane, a potential fuel energy. Enzymes have been used to activate the acetate in the *Mathosarcina* and *Methanosaeta* genera of methanogens archaea. They can both produce acetoclastic methanogenesis. On the other hand, *Methanosaeta* struggles to adapt to acetate habitats and outperforms *Mathosarcina* in waste environments. Additionally, the *Methanosaeta* genus only eats acetate [30], [39]. Members of this genus can also use CO₂, hydrogen, and methylated C₁ compounds. The *Methanosaeta* dominates the acetate below 10⁻³ M while the *Mathosarcina* dominates the acetate above 10⁻³ M. *Methanosaeta* is more sensitive to pH, and ammonia and is found in high-rate systems and while the *Mathosarcina* is often found present in a solid digester with the high effluent of organic acids [30]. Figure 2.6 shows the different paths of methanogenesis. The

Methanogenic archaea in an anaerobic system are the most sensitive anaerobes that can function better at very low dissolved oxygen concentrations. But it also requires a redox potential of less than -300mV for growth and in an anaerobic system, and it requires physical conditions such as temperature and pH to be a monitor for efficient production of methane. Methanogen archaea live in a natural habitat such as sediment and a digester system which is known to be a more suitable condition for the organisms [15]. Retention of methanogenic bacteria in the digester is paramount to maintain the reactor performance since the methanogenic organism grows very slowly in the AD system [40]. The development rate of the methanogenic archaea is slow; this makes the methanogenesis phase become a rate-limiting phase because the rate of growth of the methanogenic organisms is prone to wash out. In the methanogenesis phase, methane production is often produced in two potential ways, as shown in equation (2.2a and b).



However, equation (2.2a and b) represents the most important one that most of the anaerobic organisms depend on. Also, if the methanogen phase is unable to keep pace with the generation of VFA, the accumulation could prompt inhibition of the methanogenic process and possibly failure of the digester system. The methanogenesis process can be inhibited with excessive accumulation of toxic compounds such as sulphide, ammonia, or hydrogen. Table 2.1 below gives the summaries of the stages of anaerobic digestion. Besides, the degradation of complex particulate substrate biomass is incomplete until the substrate has passed through all the four-phase digestion. The microbial organisms found in the anaerobic system are developed from a customary or facultative form of culture at the concentration shown in Table 2.2. This microbial organism is very sensitive to environmental conditions like pH, temperature, and the organic complex matter (substrate) that is fed into the system.

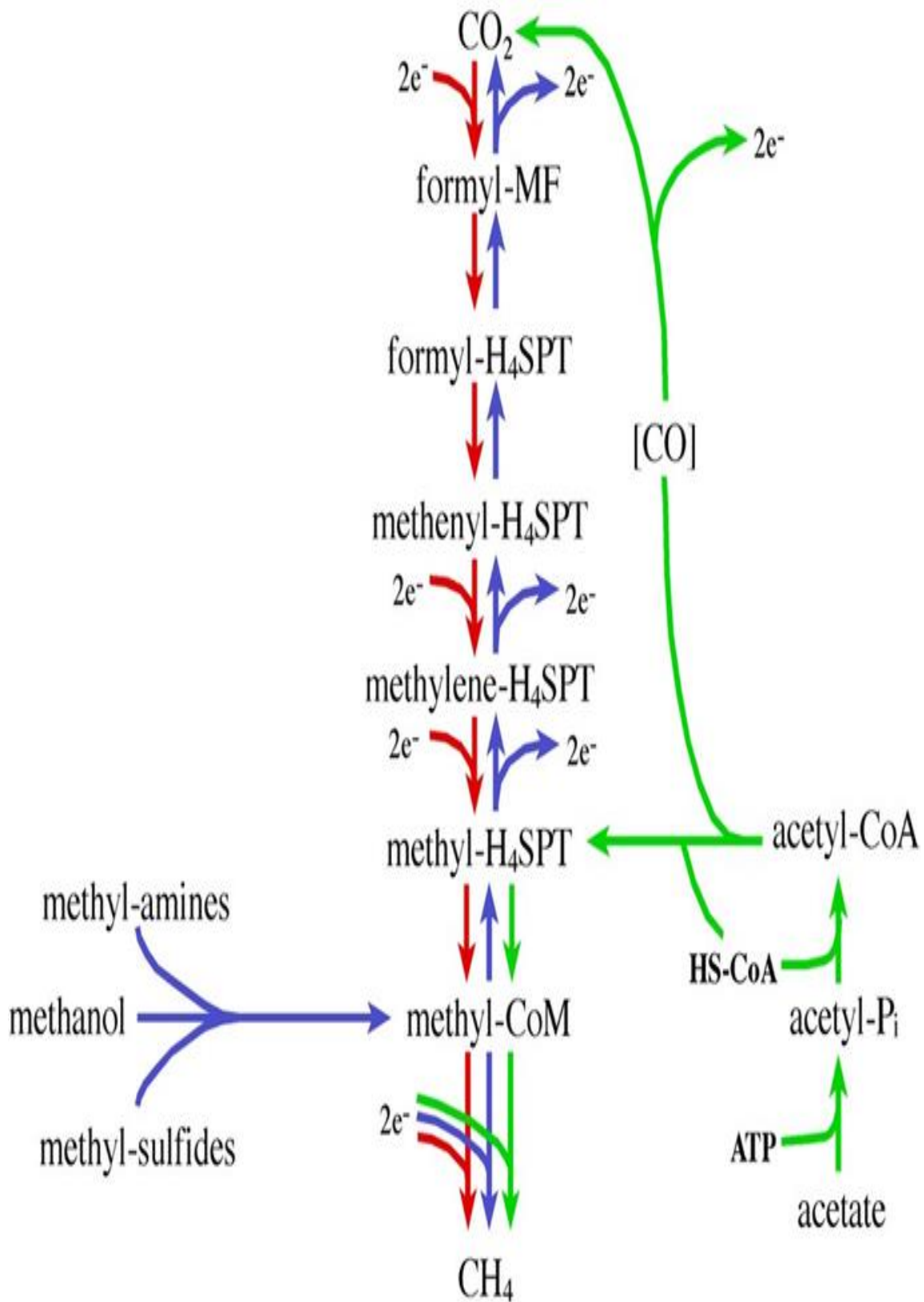


Figure 2.6 depicts the various methanogenic pathways: Hydrogenotrophic (red), methylotrophic (blue), and acetolactate (green) pathways.

Source: [11]

Table 2. 1 Summaries of the stages of anaerobic digestion

Stages	Description	bacteria	potential drawbacks	Two-phase categories
Hydrolysis	Solubilization of complex organic matter into simpler soluble molecules	Hydrolytic or fermentative bacteria	Hydrolysis of lignocellulosic materials	Acid phase
Acidogenesis	Excessive accumulation of VFA alongside ammonia, CO ₂ , H ₂ , and other by-products	Acidogenic bacteria	Accumulation of acid	
Acetogenesis	The hydrogen-producing acetogens consume VFA and long-chain fatty acids, resulting from the hydrolysis of lipids into acetic acid, hydrogen, and CO ₂ .	Acetogenic bacteria	Competition with sulfate reducers, low production of acetate	Methane phase
Methanogenesis	Acetate is cleaved to methane (CH ₄) and carbon dioxide (CO ₂), and it involved two groups of bacteria known as the acetolactic methanogen and hydrogenotrophic methanogens	Methanogenic bacteria	Slow development rates, wash-out, inhibition due to excessive accumulation of toxic compound like sulfide, ammonia, or hydrogen	

Table 2. 2 Population of microbial organisms in anaerobic digestion system
Source [41]

Anaerobic Microbial Bacteria Group	Cell/mL
Hydrolytic microbial bacteria	10 ⁸ -10 ⁹
Proteolytic	10 ⁷
Cellulolytic	10 ⁵
Hemicellulolytic	10 ⁶ -10 ⁷
Acetogenic microbial organisms (Hydrogen –producing)	10 ⁸ -10 ⁹
Homoacetogenic microbial bacteria	10 ³
Methanogens	10 ³ -10 ⁶
Sulphate reducers	10 ⁴

2.2.5 History of the anaerobic digestion

Anaerobic digestion technology is a well-established technology that has existed for centuries, and lots of studies and discoveries concerning the AD process have been carried out. Jan Baptista Van Helmont discovered in the 17th Century that organic matter gave out flammable gasses; and in 1776, Count Alessandro Volta discovered a clear correlation between the number of biological materials decaying and the amount of combustible gas produced. Sir Humphry Davy discovered methane in the fumes released by cow manure in 1808 [40], [42]. The first digestion plant was actually created in 1859 at a leper colony in Bombay, India [42]. AD came into England for the first time in 1895 through Exeter, where biogas from a "well built" sewage treatment plant was recovered and used to light streetlamps [43]. In 1881, anaerobic digestion was used to treat sewage in a septic tank; since then, it has been used on far larger scales. Buswell and other researchers carried out investigations in the 1930s to identify anaerobic bacteria and the environmental factors that stimulate methane production [43]. The most prevalent AD technology facilities are probably those that are based on farms. With different degrees of success, six to eight million family-sized, low-tech digesters are utilised to produce biogas for cooking and lighting purposes. The use of larger, more intricate electricity-generating systems is becoming more popular in China and India. Additionally, these technologies offer better process control. In general, AD plants in Europe have had success treating a variety of acceptable farm, industrial, and municipal wastes. The approach was widely used during and after World War II when energy sources were scarce. There are AD facilities that have been operational for more than 20 years across Europe. More than 600 farm-based digesters are in use in Europe, and their easy design is the key element of the profitable facilities. Around 250 of these systems were put into use in the past five years, just in Germany [42]. The country with the most experience utilizing large-scale digesting facilities is Denmark, that is currently operating 18 enormous, centralised plants. These facilities commonly co-digest manure, municipal solid waste, and clean organic industrial wastes (MSW). The energy strategy for Denmark, which calls for a quadruple of biogas production

by 2005 and a doubling by 2000, has increased its support for AD. One of the main government strategies used to promote the use of cutting-edge technology is "green pricing," or allowing producers of fuel produced from biogas to sell their product at a profit [44]. It's intriguing to observe how providing co-generated hot water to advanced district heating plants is transforming into a more significant revenue source for developers. Over the past ten years, there has been a huge increase in the use of the Biogas technology for the treatment of industrial wastewaters. There are currently more than 1,000 supplier systems in use or being built throughout the globe. According to estimates, 44% of the installed base is made up of European plants. Only 14% of the plants are in North America. Most of the plants are found in South America, predominantly in Brazil, and are utilised to the vinasse by-products of ethanol production from sugar cane. The first biogas plants for using MSW as a substrate was built in the United States from 1939 to 1974, there is recently a resurgence of interest in this technology [42], [45]. The commercial exploitation of MSW production plants has been in operation for more than 15 years has advanced greatly in recent years. There are various kinds of developed technologies, and each of them has a significant advantage. The only biological treatment for promoting recycling and nutrients from MSW's organic content is through processes like as AD and composting.

2.2.6 Future of the anaerobic digestion in Nigeria

Biogas technology is a thriving technology that has not been used in Nigeria due to the abundance of other natural resources such as solar and fossil fuels. Although Nigeria is also blessed with different waste streams (biomass) that are readily biodegradable. The country is also known to operate at an ambient temperature of 30 to 40°C with a high climatic condition of 5.538kwh/m²/day permitted [46].It means that Nigeria can operate a mesophilic digester at full scale to meet some of the energy needs of the nation, which is faced with a severe energy shortage. However, biogas production is a current technology which could be used to treat various waste streams, and in the process, generate methane which is a useful energy resource. The AD process can contribute significantly to solving the energy

problems of developing countries like Nigeria because it is also operated on a small scale. This means that the AD system can decentralize among rural, urban, and remote areas, which is a huge advantage to the country. According to the review of [47], Nigeria biogas technology started in 1982 in the state of Nsukka, Sokoto and among other tertiary research institutions that are involved in the research of renewable energy, but this technology has not been utilised. It reported that less than 20 pilot-scale projects might exist in the country. However, because Nigeria is a producer, the recent fall in the prices of oil and natural gas may drive the current economy towards alternative renewable energy sources. The AD process and its by-products offer a variety of advantages to Nigeria. The generated biogas could power lights, generators, gas stoves, etc., while the end products, called the digestate, can serve as a source of fertiliser to farmers across the country. It is also fascinating to know that all the materials (raw sewage, agricultural and food waste) fed into the anaerobic digester are most of the time, considered unwanted but can cost little or nothing in most developing nations which can be a benefit to the society for its responsible treatment and disposal method.

2.2.7 Achievable merit of the anaerobic digestion in Nigeria

There is an agreement by the United Nations Development Programme (UNDP) that the anaerobic digestion (AD) system is the most valuable decentralised energy source (UNDP 1997). According to [48] the AD process is useful for the supply of cooking gas to homes, whereas farm-based digesters provide cheap and low-cost energy regarding electricity and cooking. MSW is one of these waste streams that is often recklessly deposited on the ground, shops, markets, supermarkets, drainage, putting the environment and the health of the locals at risk. Also, in urban area, MSW are often deposited in open dumps and unregulated landfills in most locations with extremely poor waste collection facilities. Open dumping of waste is not an eco-friendly approach of waste disposal. There are a variety of dangers connected to open dumping, such as the health threat to scavengers at the dump site, contamination of the groundwater aquifers, the transmission of infectious diseases

such as air, water, and foodborne diseases (E-coli, molds, salmonella etc), as well as an unpleasant odour from decomposing waste. Diseases such as, typhoid fever, malaria, and cholera, poor respiratory infection, tuberculosis are primarily brought on by ingestion, inhalation, and dermal absorptions [49]. Additionally, Nigeria experiences its yearly flooding rituals because of anthropogenic activity obstructing drains. The routes by which pathogens and diseases from solid waste spread to people are shown in figure 2.7 [40], [50].

Pathogens and Diseases Associated with Disposal of Solid Waste

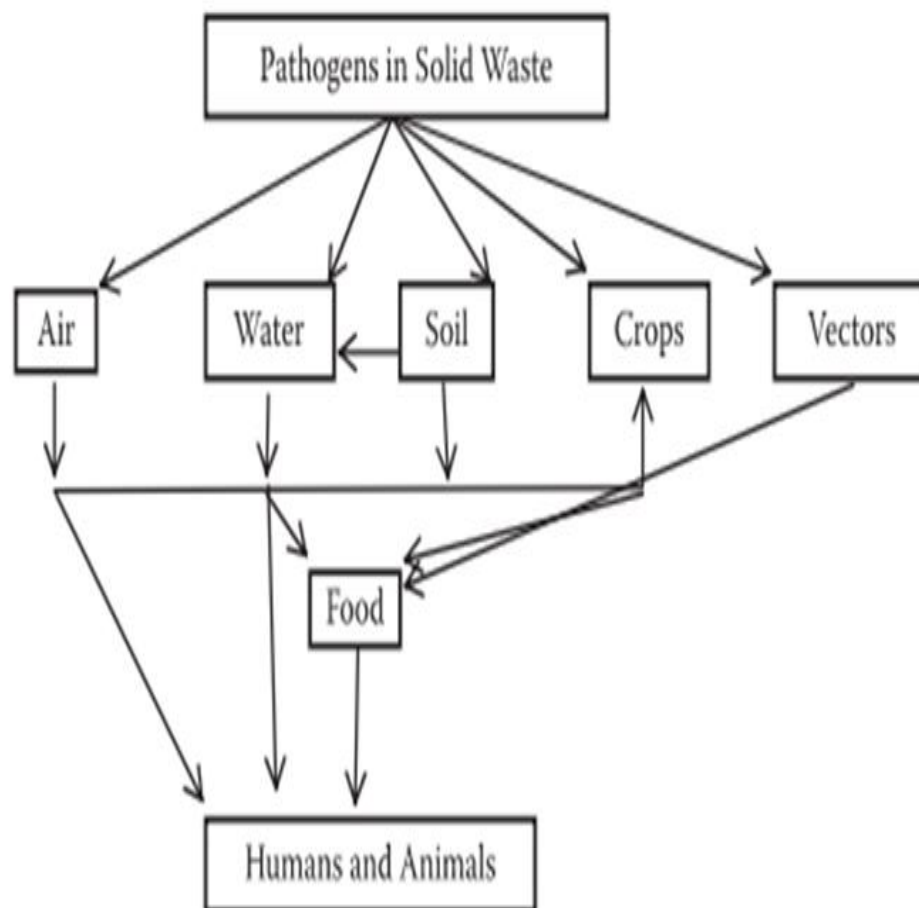


Figure 2.7 Pathogens' modes of infection in humans through solid waste

Source [49]

Some of the many advantages that anaerobic digestion can bring to Nigeria include:

- ❖ Conversion of waste materials to chemical fertilisers for farmers
- ❖ Reduction of nuisance from foul odours from the waste
- ❖ Provides low-cost cooking fuel and reduces particulates and greenhouse gas emissions.
- ❖ Reduces the agricultural waste pathogens such as *Escherichia coli*, salmonella etc that cause health problems, especially in the rural regions of Nigeria.
- ❖ Provides affordable and reliable energy for economic development, especially in rural communities.
- ❖ Creates job opportunities for Nigerians.
- ❖ Consumptions of fossil fuel will be reduced.

[51] Reported some global energy needs and various environmental merits of biogas table 2.3. It means the cost of the waste is significantly reduced with relatively low feedstock cost in developed countries and might cost little or nothing in developing nations such as Nigeria when compared to diesel and petrol prices that are estimated to be \$ 0.77 and \$0.75 respectively [52].

Table 2. 3 Environmental benefits of the anaerobic degradation of complex organic matter

Aspects	Obtained Benefits	References
Water (H₂O) treatment benefits	Reduce leachate concentrations	[53]
	Reduce the volume to be disposal waste and the weight to be landfill	
	The natural process of waste treatment	
Economic benefits	Low-cost production as compared to other processes of treatment	[53]
Production of energy benefits	Production of high-quality renewable energy e.g., Heat, trigeneration, vehicle fuel, Electricity	[51], [53]
	Producing process of net energy	
	Biogas to methane proven application to various end-use	
Environmental protection benefit	Generation of organic sanitised compost and nutrient use for soil conditioning (Fertilizer)	[51],[53],
	Elimination of odours and pathogenic microbial bacteria	
	Effective reduction of emission from greenhouse gas production by the substitution of conventional energy sources	
	Reduction of air and water (H ₂ ⁰) pollution	

2.3 The end-products of the anaerobic complex particulate matter

2.3.1 Biogas

Biogas is produced in the AD system by the degradation of the organic materials caused by the four anaerobic bacteria (hydrolytic, acidogenic, acetogen and methanogens bacteria in an AD system. The vital primary constituents of biogas determine the energy values of the gas known as methane (CH₄) and carbon dioxide (CO₂). Other components, such as ammonia (NH₃), hydrogen (H₂), nitrogen,

hydrogen sulphide (H₂S) oxygen, and volatile siloxanes, are sometimes present in the biogas in inconsiderable amounts. However, for biogas to be used as fuel, it required scrubbing or upgrading to biomethane. The presence of sulphide (H₂S) in biogas makes it toxic. Therefore, it is important to remove sulphide (H₂S) from biogas whereas another inhibitive element is the siloxanes which come from the AD of wastewater and household waste [54].

Table 2. 4 Methane production component from the complex particulate matter of substrate waste biomass

Source : [50], [55], [56].

Components	Symbol	Concentration (Vol-%)
Methane	CH ₄	55-70
Carbon dioxide	CO ₂	35-40
Water	H ₂ O	2 (20°C)-7 (40°C)
Hydrogen sulphide	H ₂ S	20-20000 ppm (2%)
Nitrogen	N ₂	<2
Oxygen	O ₂	<2
Hydrogen	H ₂	<1
Ammonia	NH ₃	<0.05

2.3.2 Digestate

Digestate is known as the processed influent of the biogas generated from feedstock materials after converting to biogas through the AD system. It can be used as produced or refined through various treatments and technology. The digestate is collected from different anaerobic reactors, and they are in solid-liquid form. In an AD process, the initial step is to separate the liquid from the solid digestate into a low dry matter, and solid dry matter materials, for instance fibre sludge. However, the inhibition level in the digestate relies mainly on the source and nature of the

substrate that is fed into an AD system. At the point when there are high ammonia contents in the digestate, ammonia will decrease into nitrates and thereby increase the level of nutrients in the fertiliser; subsequently, the digestate turns into a good fertilizers [54].

2.3.3 Available feedstock

Any material or substrate that can be easily biodegradable by anaerobic microorganisms is known as a feedstock. A fundamental requirement for feedstock is that it contains substantial amounts of degradable organic matter which can be converted into methane (CH₄) and carbon dioxide (CO₂) in the final stage of the AD process [57]. Some commonly found wastes used in AD reactors include livestock manure, food processing wastes, industrial wastes, slaughterhouse wastes, sewage sludge, garden wastes, agricultural wastes, among others. Also, in Nigeria, feedstock sources come from the wastes of sheep, goats, cattle, pigs, poultry, and abattoirs. Other sources may be cropped wastes, human excreta, and municipal solid waste (MSW) [58]. However, the skills in converting these feedstocks to biogas vary. Depending on their physical and chemical characteristics (cellulose and lignin content), biodegradability, toxicity, and moisture content [36], [59]–[61] [36]. This means that substrate containing larger amounts of cellulose and lignin is harder to process in the AD reactors because of the bond holding the molecules, which is the basic reason for the difficulty in degradation [62].

2.4 Factors affecting the digestion of the anaerobic substrate biomass.

Several factors influence the stability of the AD kinetics, both at the reactor input and output. These include the most important operational measures and pre-treatment methods of feedstocks and post-treatment of the end-product in anaerobic food chain production. However, the factors affecting reactor inputs include pH, temperature, organic loading rate (OLR), mixing, retention time, physical, chemical, and biological treatments, etc. Whereas those influencing the reactor output include by-products such as biogas and digestate [51], [59] – [61].

2.4.1 Operating temperature of the reactor

Anaerobic digestion can occur under a wide range of temperatures, including psychrophilic (10 to 25°C), mesophilic (30 to 40°C) and thermophilic (50-60°C). The temperature in the AD system represents an important parameter of interest of most researchers, used when biogas is generated. The major effects are that temperature affects the microbial activity of bacteria, bacteria community structure, process stability, and hydrolysis kinetic operations [30], [63]–[65]. Most bacteria depend strongly on temperature for their microbial activities and when the bacteria activities become suppressed, result in volatile fatty acids (VFAs) accumulation till the bacteria recover from the shock that has taken place because of the change that has occurred by temperature. Bacteria in the mesophilic reactor grow between 5°C and 40°C whereas thermophilic bacteria grow best at 45°C and 70°C. These temperatures are the two most significant ranges known for high methanogenic bacteria action [15], [54], [55], [59]. Most digesters are operated either at mesophilic temperatures with an optimum temperature of 35 °C or thermophilic temperature with an optimum of 55 °C as shown in Figure (2.8) [55], [66]. Figure 2.8 shows the graphic connection between temperature and the rate of anaerobic digestion. At thermophilic temperatures, the retention time reduces. Thermophilic anaerobic digestion has the potentially promote microbial growth, enhanced biogas production and digestion efficacy since thermophilic bacteria have a faster specific growth rate than mesophilic bacteria [67]. Thermophilic conditions outperform mesophilic ones in terms of production because of a more loaded reactor and a slight increase in methane production. Additionally, yields are boosted, and more methane is produced at thermophilic temperatures. In thermophilic conditions, it is also possible to accelerate the degradation of organic acids and the eradication of pathogens. Additionally, thermophilic anaerobic digestion can provide high-quality residue that can be used as fertiliser or soil conditioner instead of being dumped in landfills. [30], [37], [46], [53]. According to [66], the mesophilic condition is considered as the fastest operation rate, with a higher load-bearing limit, whereas the thermophilic systems achieve more efficient sterilization and higher methane

production [68], [69]. This means that a thermophilic system also assists in increasing the destruction of pathogenic organisms, solid reduction as well as enhancing dewatering in the AD system [37].

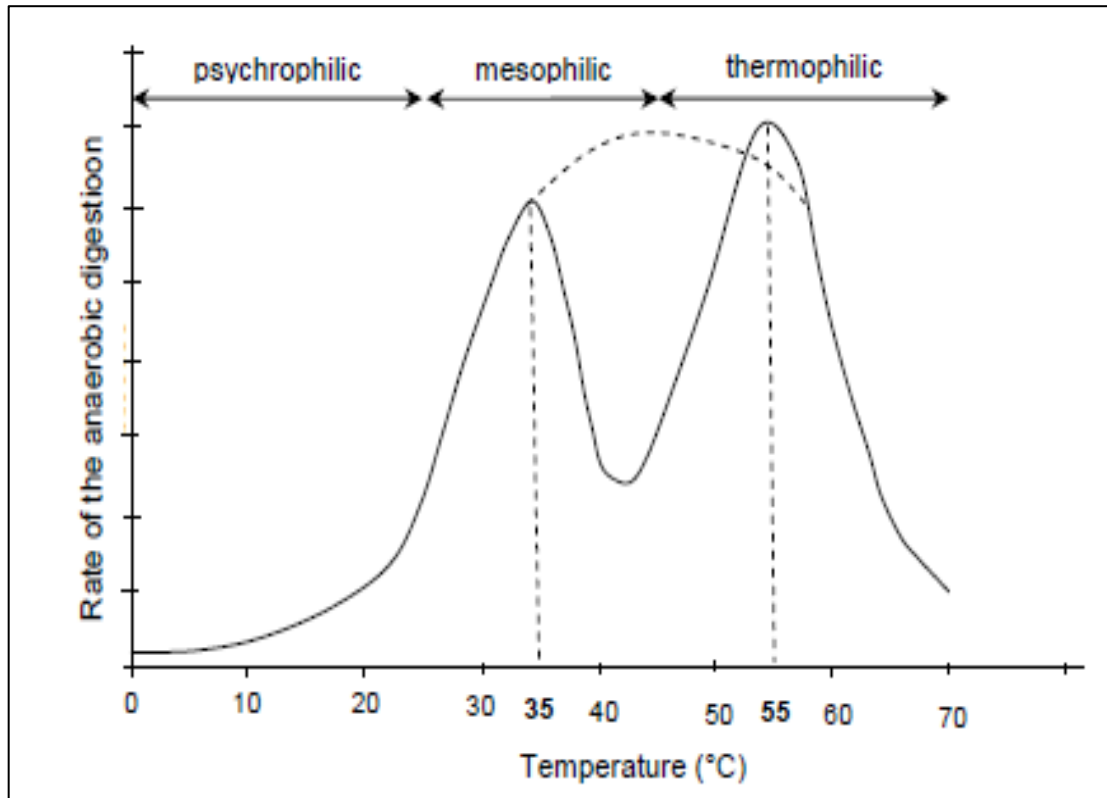


Figure 22.8 Effect of temperature on the anaerobic digestion process

Adapted From:[55], [66].

Among the problems associated with thermophilic digesters is that fermentation may occur, thereby hindering the production of biogas. Also, the system is very susceptible to environmental conditions, while low-quality influents can result in poor methanogens and greater energy input [51], it has a more expensive technology and requires a high operational degree and monitoring. According to [37], [70]–[72], temperature significantly affects the anaerobic digestion processes, including methanogenic bacteria actions, pH, VFAs, and biogas generation.

2.4.2 Retention time

Retention times come in two main types such as:

- ❖ Hydraulic retention time (HRT)

❖ solid retention time (SRT)

Hydraulic retention time (HRT) is the mean duration that the input slurry spends inside the digester [48], [69]. This may be explicit as follows:

$$HRT = \frac{V}{Q} \quad (2.3)$$

Where;

V is the biological digester volume and.

Q is the influent stream rate in time.

Whereas, solid retention time (SRT), which is the average time that microorganisms (solids) spend in the digester. Anaerobic processes (hydrolysis, fermentation, and methanogenesis) and reactors volume are closely related to these factors [73]. A longer retention time incurs more cost as it requires digesters with large volumes while short retention times may bring about washout of the active bacterial population. Achieving a good HRT often relies upon the substrate, organic loading rate and the composition of the substrate, temperature, and other environmental conditions. The anaerobic digestion (AD) system is sensitive to HRT. VFA accumulation often occurs when the HRT is reduced, whereas improper digester component utilization occurs when the HRT is prolonged [51]. While studying the effects of temperature and HRT on the anaerobic digestion (AD) of food waste (FW), Kim et al.[74] , reported that a hydraulic retention time (HRT) of 10 days produced a higher yield of methane from food wastes compared to the HRT of 8 days where the anaerobic digestion stability decreased. Similarly, HRT below 10 days also results in a decrease in the production of methane yield of algal biomass. This implies that to achieve maximum production of methane, long HRT, and low organic loading rate is required [74]. Although increasing SRT means an increase in HRT. It should be achieved by utilising greater digester volume by reducing the influent flow to prevent biomass from washing out of the AD process digester such as sludge reused, or biomass immobilisation becomes the opinion [66]. However, [37] concluded that SRT is an important parameter when designing the operation of an AD system.

2.4.3 Mixing

Mixing is one of the important parameters in AD and could have a profound effect on the behaviour of anaerobic microorganisms. This means mixing is essential for the growth of anaerobic organisms to ensure each of the anaerobic bacteria obtained their nutrients as rapidly as possible. Additionally, mixing prevents the build-up of scum and the emergence of temperature gradients inside the digester. Anaerobic digesters can perform poorly if there is excessive mixing in the anaerobic reactors, which can disturb the anaerobic microorganisms. In the AD of primary sludge (PS) or a mixture of PS and the fruit and vegetable fraction of municipal solid wastes, a low mixing ratio (80 rpm) lead to a high specific production rate methane of 0.5 and 0.61 L g⁻¹ VS, respectively, whereas the lack of stirring resulted in a decline in specific biogas production (0.3 and 0.5 L g⁻¹ VS) because the substrate and bacteria had less interaction [72], [75] . A slow mix is preferred. This is because mixing is necessary to prevent dead zone scum formation. It plays a vital role in enhancing the contact between substrates and microorganisms in the reactor [68], [69]. Whereas vigorous mixing can affect the operation of anaerobic digesters, reducing the speed and degrees of methane production, slowing the oxidation of fatty acids, and causing instabilities in the bioreactors. However, minimal mixing can allow the anaerobic digester remain constant and perform much better [76].

2.4.4 The Organic loading rate of an anaerobic digestion system

The organic loading rate (OLR) is the mass of VS fed into an anaerobic digester per unit volume per unit time. It represents an important parameter in an AD process because if it gets too high, potential methane production could be washed out of the system. The process can be impeded by an accumulation of ammonia and VFA. However, if the loading rate is too low, reduced organic materials will be degraded and low methane will be produced. It can be expressed as:

$$OLR = \left(\frac{KgVS}{m^3} / d \right) \text{-----} (2.4)$$

Additionally, larger, less productive digesters will need more heat. These factors mean that the optimal loading rate should maintain between having the maximum

production of methane and having adequate economic system [77]. As a result, the substrates, and operational conditions of the digester both affect the OLR. A typical range of organic loading for the low-rate digester is 0.64-1.64 and for high-rate digesters are 2.40 to 6.4 [78]. The daily addition of a significant amount of substrate can cause the AD to become unstable because of the accumulation of VFA, and a pH drop (figure 2.9). The process can inhibit microbial action during the early phase of the anaerobic fermentation process and can quickly prompt higher hydrolysis and acidogenesis microbial action than methanogenic bacteria activity in the AD system and thus increase the VFA production that can be uncontrollable. After that, there is a drop in pH in the digester, and the hydrolysis process becomes very inhibiting, meaning that the methanogenic bacteria cannot transform a large quantity of VFA into biogas [51]. According to Demirer and Chen [79], short retention times may have caused acidifiers to wash out, resulting in high OLR of 20 to 30 kgVS m⁻³ day⁻¹ in the AD of cattle manure that resulted in a decrease in specific methane production (0.066 m³ kg⁻¹ VS added day⁻¹) and pH value (pH 6). In a study of different PSD on AD of organic MSW under a semi-continuous condition, the wet digester was loaded at an OLR of 6 kg VS/m³/day. There was a shift in the PSD that changed the biogas yield, whereas in a dry reactor; the finer particle size shows a drop in pH and VFA. This leads the process to collapse at the highest organic loading rate (OLR) while with wet digestion the finer particle size results in severe foaming at OLR of 4- 5 kg VS m⁻³day. It means that an AD should be loaded fairly and monitored to avoid process failure [20]. Additionally, Borja et al. [80] found that the volume of biogas produced daily increased with increased OLR over the range tested when slaughterhouse wastewater was anaerobically treated in a fluidized-bed reactor, but the methane content decreased.

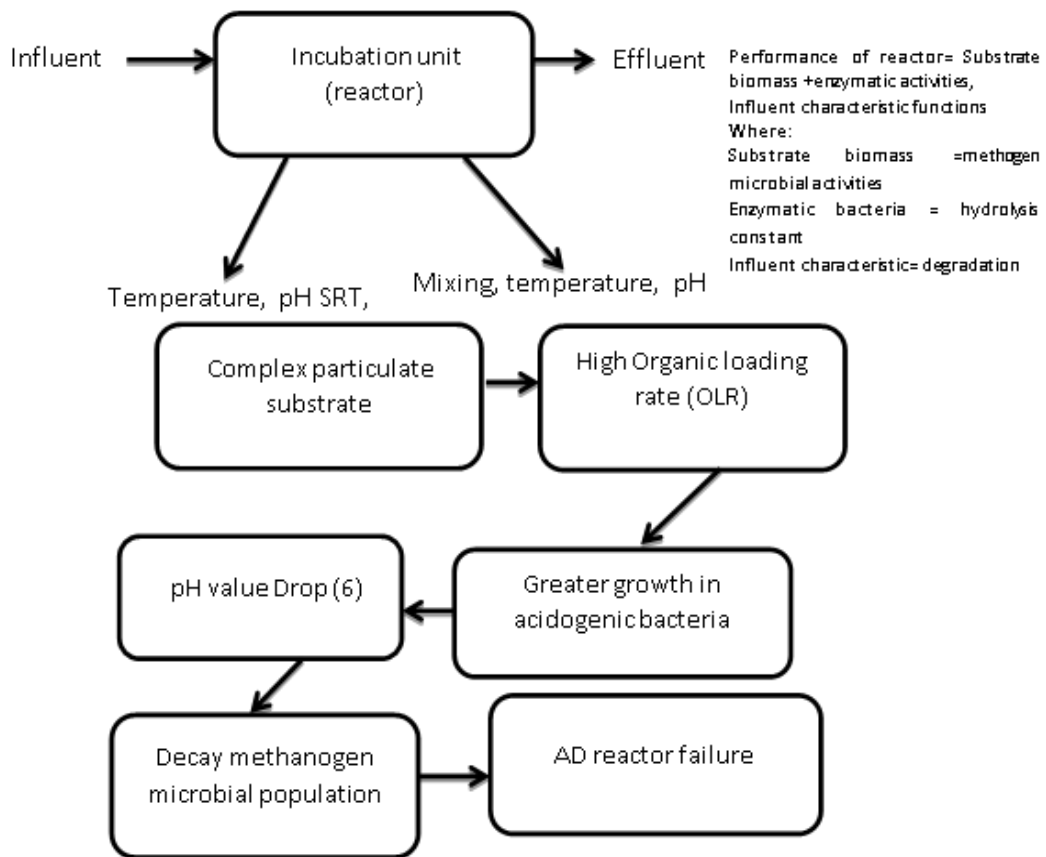


Figure 2.9 Simple scheme of high organic loading rate (OLR) reactor, methanogenic microbial population activities, hydrolysis constant and the degradation of complex particulate matter

2.4.5 pH

pH is an essential factor known for the development of microbes in anaerobic digestion processes. The optimal requirement for pH varies in the AD system, which depends on the microorganisms: hydrolytic (pH 6-7). According to research, controlling the pH in a hydrolytic bacteria reactor can boost microbial degradation about twice compared to an uncontrolled operation [81]. Figure 2.10a demonstrates how pH control over the range of 5 (no control) to 11 changed the degree of solubilization of kitchen waste. At different pH levels, rumen organisms degrade cellulose, as shown in figure 2.10b [82]. For optimal hydrolysis, many studies use hydrolytic reactors with pH control [83]. The optimum for acidogenic (5.5-6.5), acetogen pH 5-7 and methanogenic bacteria 6-7.6 in the AD process. To maintain a good environmental condition for methanogenic microbial organisms, it is necessary to keep the pH of the AD system between the pH of 7- 7.5 and this could be

obtainable if the pH of the AD system is a balance between the methanogenic microbial organisms and the acetogenic bacteria. However, the best operational pH range for methanogenic archaeobacteria is at pH 6.7-7.6 that methane produced [84]–[86]. At pH values lower than 6.6, methanogens archaea-bacteria grow more slowly as their action is reduced [15], [87], [88]. [84]. Low pH can result from an unbalanced condition in the AD bioreactor where the bacteria that produce acid dominate those that consume it [84]. Avoiding the preponderance of acid-forming microbes and minimize the accumulation of VFA, pH is normally kept under methanogenic limits [89], [90]. According to Veeken et al. [91] the concentration of volatile fatty acids (VFA) can cause a pH to rise or fall depending on the composition of the feedstock or waste and controls the overall rate of hydrolysis of solid organic matter. For example, protein digestion can increase buffer ability by producing ammonia, that could increase pH. Additionally, according to reports from [91], [92], the hydrolysis rate constant is pH-dependent.

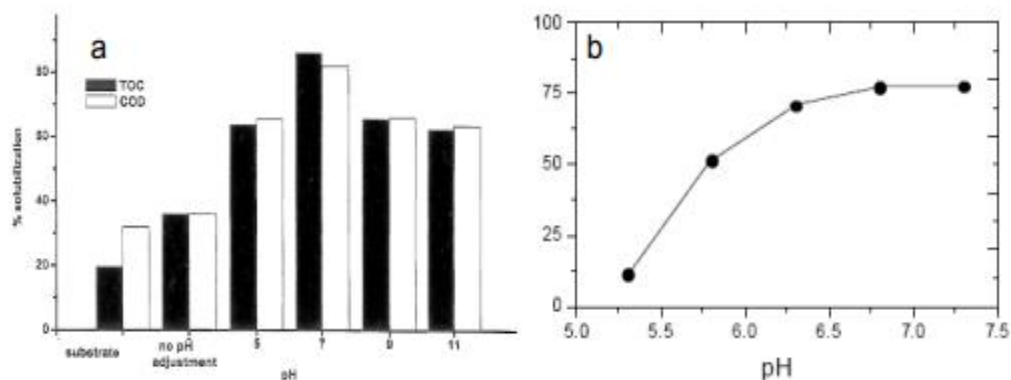


Figure 2.10: The influence of pH on the degree of anaerobic solubilization

Sources :[15], [82], [93]

2.5 The C/N ratio

The carbon/nitrogen (C/N) ratio of the feedstock is essential for the stability of an AD process. A very high C/N ratio could result in failure due to nitrogen deficiency for biomass synthesis, whereas a very low C/N ratio could result in inhibition due to

an excess of nitrogen. According to studies by [94], [95], the ideal C/N ratio for anaerobic digestion is thought to be between 20/1 and 30/1.

2.6 Inhibition of the anaerobic digestion degradation

Inhibition occurs when the biochemical reaction rate of bacterial growth decreases. In an anaerobic digestion system, many materials are reported to be inhibitory to microbial action. This process may result in the build-up of VFA and low methane output [8], [37]. More often, inhibition occurs in the thermophilic condition than the mesophilic condition of an AD system. There are four common inhibitors found present in an anaerobic reactor which have been believed to cause anaerobic digestion disturbance or failure. These inhibitors include ammonia, light metal ions, heavy metals, and various organics, although inhibitory concentration varies substantially in an anaerobic digester due to the origin of the feedstock and the difference in the anaerobic bacteria, waste composition, experimental methods as well as a condition [82]. The concentration of inhibitors used in anaerobic digestion is shown in Table 2.5.

Table 2. 5 Inhibitor concentration in anaerobic digestion

Inhibitor	Concentration (mg/L)
Volatile acids	>2,000 (as acetic acids) ^a
Ammonia nitrogen	1,500-3,000 (at pH>7.6)
Sulfide (soluble) ^b	>200; >300 (toxic)
Calcium	2,500-4,500; 8,000 strongly inhibitory
Magnesium	1,000-1,500; 3,000 strongly inhibitory
Potassium	2,500-4,500; 12,000 strongly inhibitory
Sodium	3,500-5,500; 8,000 strongly inhibitory
Copper	0.5 (soluble metal)
Cadmium	150 ^c
Iron	1,710 ^c
Cr ⁺⁶	3
Cr ⁺³	500
Nickel	2 ^d

Source: Polprasert, 1996

^a within the pH range 6.6-7.4, and with adequate buffering capacity, volatile acids concentration of 6,000-8,000 mg/L may be tolerated

^b off gas concentration of 6 % is toxic

^c Millimol of metal per kg of dry solids

^d Nickel promotes methane formation at low concentration. It is required by methanogens

Source:[41], [96]

2.6.1 Inhibition by ammonia

Ammonia inhibition is known to be a potential barrier of anaerobic digestion, especially when dealing with complex substrates, like organic fraction of municipal solid waste (OFMSW) or manure. Ammonia is produced through the biological degradation of nitrogenous compounds. It is accepted to be the end-product of the anaerobic digestion food chain and known to be a problem in the AD system. This is particularly the case when the anaerobic substrate contains high nitrogen content, for example, poultry manure and slaughterhouse waste [15], [93]. According to Chen et al. [97] ammonia has a complex mechanism of inhibition, which includes a change in the intracellular pH, the increase of maintenance, energy requirement, and inhibition of the specific enzyme reaction [83]. Ammonia inhibitions include free ammonia (NH_3) (non-ionic) and ammonium (NH_4^+). Free ammonia is the most poisonous compound which causes inhibition since it passes through the membrane of cells, while being hydrophobic causes potassium insufficiency and proton imbalance [37], [97]–[99]. Ammonia concentrations below 200 mg/l are beneficial to AD systems because nitrogen is a nutrient that is essential for the growth of microorganisms [37]. Waste containing a high concentration of total ammonium nitrogen, the bacteria and composition are affected by pH [37]. The actual toxic compound is said to be free ammonia in the AD process, thereby, a step up in the pH would result in a process where toxicity will be increased. Also, the anaerobic reactor becomes acclimated to a higher concentration of ammonia when there is a shift in the internal mechanisms of methanogens bacteria as well as a change in the bacteria that dominate other bacteria species in the anaerobic digester. As a result, free ammonia shifts the ionized (NH_4^+)/ ammonia ratio at a higher pH. However, the instability of the process occurs due to the excessive amount of VFAs in the digester which could lead to a reduction in pH and a lower concentration of free ammonia in the AD system. Also, the free ammonia (FA), VFAs, and pH interaction can achieve an inhibition steady state when the anaerobic digestion process is becoming stable with a lower synthesis of methane[97].

2.6.2 Organics inhibition

Long-chain fatty acids (LCFA), halogenated aliphatic, and lignin's/lignin-related compounds are just a few examples of the wide range of organic substances that can inhibit anaerobic processes [100], [101]. Organic substances like alkyl benzenes and halogenated hydrocarbons are toxic to anaerobic processes, according to reports [102], [103]. These compounds' concentration fluctuates for some particulate toxicants, and the parameters are impacted by toxicants such as exposure time, temperature, cell age, feeding pattern, toxicant concentration, and biomass concentration[97]. However, the biodegradation of a lower concentration range of toxicants prevents the occurrence of inhibition in the AD processes, whereas a higher level of some toxicants displays more prominent inhibition to the AD operations [74]. At the highest concentration of biomass, the anaerobic digester displays more prominent process stability in the presence of toxic shocks. [86] Reported that, at an equivalent concentration, younger cultures turn out to be more reliable and resistant to toxicants than older cultures. Also, in the bacterial membrane, the accumulation of hydrophobic pollutants causes the layer to swell and leak and thereby disrupting ion gradients and causing cell lysis [104], [105].

2.6.3 The effects of light and heavy metal ions

Light metal ions are present at the influent of an anaerobic reactor. These ions, which include Na, K, Mg, Ca, and Al, are added to the substrate as chemical adjustments. They can also be found present due to the microbial action in the breaking down of biomass [106]. However, these light metal ions are needed for the growth of bacteria in an AD system; but consequently, affect the specific development rate like any other nutrients [106]. At moderate concentration, light metal ions improve the development of the microbes while excessive addition of a significant amount of light metal ions can slow down the growth, and a higher concentration of light ions becomes very toxic [97]. Also, heavy metals stand out from many other toxic substances because they cannot degrade naturally and can build up to potentially toxic concentrations[106], [107]. Failure of anaerobic digesters has been majorly attributed to the toxicity of heavy metals or upsets,

resulting from the disruption of enzyme functions and structure by binding of the metals with other groups of protein molecules [97].

2.6.4 Volatile Fatty Acids inhibition

The accumulation of VFAs and the drop in pH are said to be the biggest problems associated with anaerobic digestion. The antagonistic impact of VFA on the methanogenic microorganism, especially acetate degraders, is particularly problematic as VFA is an intermediate in the process. It has been accepted in the literature that there is no possibility of separation of VFA and pH inhibition in the AD process, whereas few studies have also revealed that VFA causes inhibition of hydrolysis of the organic matter [108]. Hydrolysis is the important first stage in the AD process. However, the main issue with inhibition of microbial activity resulting from volatile fatty acid (VFA) is that when there is an increase in volatile fatty acid (VFA) concentration, there is also a drop in the pH value. Therefore, there is still unclear evidence about volatile fatty acid (VFA) or pH inhibiting the hydrolysis of organic matter in the AD process, i.e., Volatile fatty acid inhibition may also occur due to a drop in pH [15], [109]. In a study on the elucidation of growth inhibition and acetic acid generation by *Clostridium thermoaceticum*, inhibition for the undissociated acetic acid was found to be more than the ionized acetate ion. This implies a total growth of inhibition of the hydrolytic bacteria when the undissociated acetic acid concentration was within the range of 0.04 and 0.05 M at a lower pH drop, whereas the dissociated acetate ion played a significant role in pH value higher than 7. Mawson et al. [110], study the degradation of propionic and acetic acids during the fermentation of methane. The two acids, acetic and propionic acids, added to a concentration of 2000 and 1500 mg^l⁻¹. The authors found out that the deterioration of propionic acid added at 500 mg^l⁻¹ significantly inhibited at an increased concentration ranging from 1000 to 2000 mg^l⁻¹. The increase in the concentration of either acid from a low level implies that the rate of utilisation of microorganisms is reduced. In a similar study of the effect of undissociated acids on the activity of acetogenic bacteria at a concentration of 2300, 650, and 120 mg/L at pH 5, 6, and 7, respectively, [111] Babel et al. observed that at 5 low pH values, the

undissociated acids are more inhibitory. This implies that a decrease in the pH value of the acetogenic bacteria leads to an increase in VFA. Also, the authors showed that the reduction of the total volatile solids (VS) of the pineapple sample was 42–48% and 51–57% volume reduction of VFA at a pH 6.5–7. Meaning that there was no impact of VFA on the hydrolytic bacteria, which means that as the pH drops, the hydrolytic bacteria become less sensitive to the increase in volatile fatty acid (VFA).

2.7 Biogas technology for the pre-treatment of solid waste

Rapid innovation in reactor design has been made to address the challenges of anaerobic digestion treatment of BMW. This has produced many proprietary systems that are challenging to categorise. Nevertheless, based on how much solids are in the feedstock or in the slurry in the digester, the process has now been categorized as either "wet" or "dry" [112]. Less than 10% of total solids (TS) are present in low solids systems (LS), 15%–20% are present in medium solids systems (MS), and 22%–40% are present in high solids systems (HS) [113]. They can be single-phase where all reactions occur in a single digester or two-phase where the reactors are linked in series [112], [114]–[116]. The feed material can be fed into the reactor in batches or continuously. When using batch reactors, feedstock is added at the start of the reaction, and products are released at the end of a cycle. The other type of reactor frequently utilised for low solids slurries is a continuous flow reactor, in which the feedstock is continuously loaded and discharged. A static (unmixed) hydraulic system, a plug flow system, or both can be used in anaerobic digester [112]. The fermentation process takes place at ambient temperature range describe in session 2.4.1. Table 2-6 depicts how mesophilic and thermophilic process's function. Also, there are a few configurations that are more prevalent than others, and some of the other options might not be feasible in real life or might not have yet been developed for commercial use. Figure 2-11 depicts the operating possibilities for the 'wet' or 'dry' category.

Table 2. 6 Compares mesophilic and thermophilic process operations.

Source: [117]

<i>Process Operation</i>	<i>Mesophilic (35 °C)</i>	<i>Thermophilic (55 °C)</i>
Process stability	higher	lower
Temperature sensitivity	low	high
Energy demand	low	high
Degradation rate	decreased	increased
Detention time	longer or the same	shorter or the same
Sanitation	no	possible

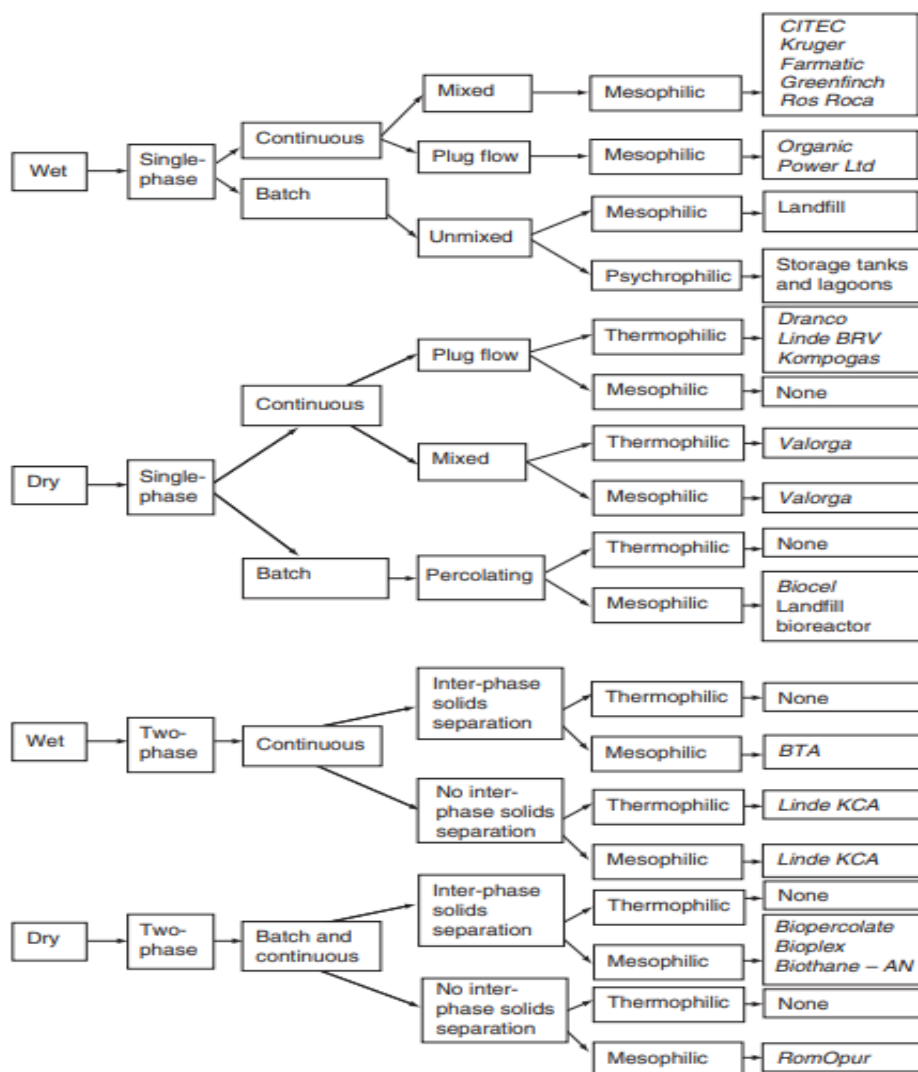


Figure 2.11 Anaerobic fermentation process options based on the classification of 'wet' or 'dry.'

Source : [112]

2.7.1 Single-phase mixed mesophilic wet digesters

These are also referred to as wet single-pass digesters or continuous stirred tank reactors (CSTRs) due to the mixing method. At a feed solids concentration of around 15%, they are fed continuously or semi-continuously. Figure 2-12 depicts a typical one-phase "wet" mesophilic digester [114]. They are the most common kind of digester and are used to break down sewage sludge, cattle slurries, and industrial sludge. As a result, there is indeed a wealth of design and performance data at our disposal [112]. The majority of CSTRs are mechanically heated and blended, resulting in a relatively homogenous condition in the digester[112]. The processing of waste into a viable slurry is a difficult process, and several pre-treatment methods have been developed to tackle concerns. For the operation of this digester type with high solids materials like MSW, the physicochemical composition of the material should be altered to that of a slurry by pulping with dilute water or return liquor[112]. This serves a dual purpose in MBT facilities that use wet pre-processing by removing contaminants. Because the CSTR is a one-pass completely mixed reactor, it needs a minimum hydraulic retention time (HRT) of 15 to 30 days in the mesophilic temperature range to maintain active microbe concentrations at optimal levels for methanogenic archaeobacteria [112]. The necessity to dilute the feedstock is probably the most major drawback of a CSTR methodology for solid waste digestion. To reduce the total solids content (TS) of biomass from 50% to 10-15%, 3-5 m³ of liquid must be added per tonne of organic material. Despite widespread use of heat conservation, there will be an additional fuel need to boost the temperature of the feedstock and maintain reactor temperature, as well as a demand for solids/liquid separation of the digestate to provide a liquor return for mixing [112].The advantages and drawbacks of the one phase wet digester is shown in table 2-7.

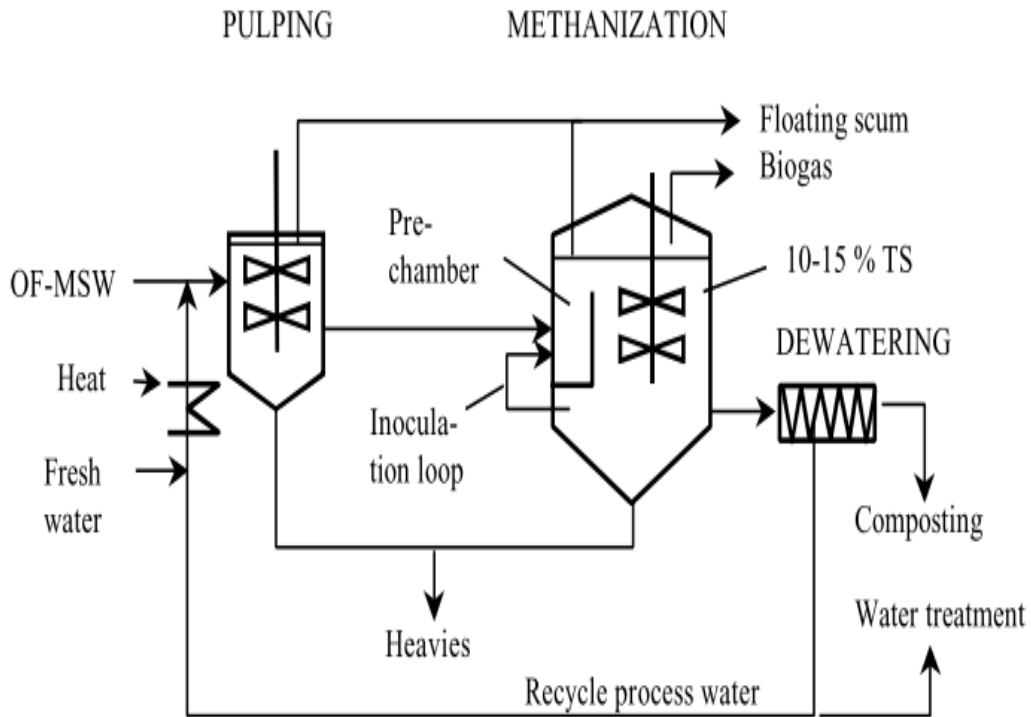


Figure 2.12 A typical one-phase 'wet' mesophilic digester.

Source: [114]

Table 2. 7 Benefit and drawback of wet phase digesters

Source: [114]

Criteria	Advantages	Disadvantages
- <u>Technical</u> :	- Inspired from known process	- Short-circuiting - Sink and float phases - Abrasion with sand - Complicated pre-treatment
- <u>Biological</u> :	- Dilution of inhibitors with fresh water	- Particularly sensitive to shock loads as inhibitors spread immediately in reactor - VS lost with inerts and plastics
- <u>Economical & Environmental</u> :	- Equipment to handle slurries is cheaper (compensated by additional pre-treatment steps and large reactor volume)	- High consumption of water - Higher energy consumption for heating large volume

2.7.2 Single-phase continuous feed, dry thermophilic digesters

These systems are also known as dry anaerobic fermenters or high solids digesters. They have a total solids concentration of more than 15% in the digester feed, though most operate at much higher levels. When the feedstock has a moisture content of less than 60-70%, dry fermentation eliminates the need to add water. As a result, the cost of post-digester treatment is decreased, the reactor volume is reduced, and higher organic loading rates at longer retention times are feasible. Furthermore, because of the high loading rates that can be achieved, dry digestion systems can produce a substantial amount of biogas per volume of reactor per day. They are resistant due barrier formation and accumulation of inert particle that don't really occur at the same degree compared to more diluted stirred systems [112]. High solids systems are more tolerant to variable densities of matter in the feed stream because both 'heavy' and 'light' fractions are trapped within the matrix and cannot raise as scum or sink as waste. This is Because high solids digesters do not strive for 100% material mixing, the most easily obtainable systems are either 'plug' flow or dispersion flow with certain internal mixing [112]. Additionally, because incoming biomass may not encounter the digester's 'active' microbes if the reactor is not entirely mixed, steps could be required to ensure that an inoculum is maintained within each 'plug' of biomass when balanced digestion is to proceed. The energy required for process heating is reduced since no dilution liquid is necessary, and the rates of reactions in the unit would liberate substantial metabolic heat to hold or raise the temperature. Thus, both characteristics lead to lower energy needs to operate the reactor at mesophilic temperatures and provide a realistic option of working at thermophilic temperatures while keeping a positive metabolic rate [112]. The difficulty with high solids digestion reactors is not related to microbes, instead to solid stream control, pumping, and mixing. High solids techniques are increasingly widespread, with more than 50% of plants treating organic municipal solid waste [112]. The dranco, kompogas, and BRV designs, as well as the valorga design, are depicted in figure 2-13. These are typical designs for anaerobic digesters used in 'dry'

systems [114]. The advantages and drawbacks of the one phase dry digester is shown in table 2-8.

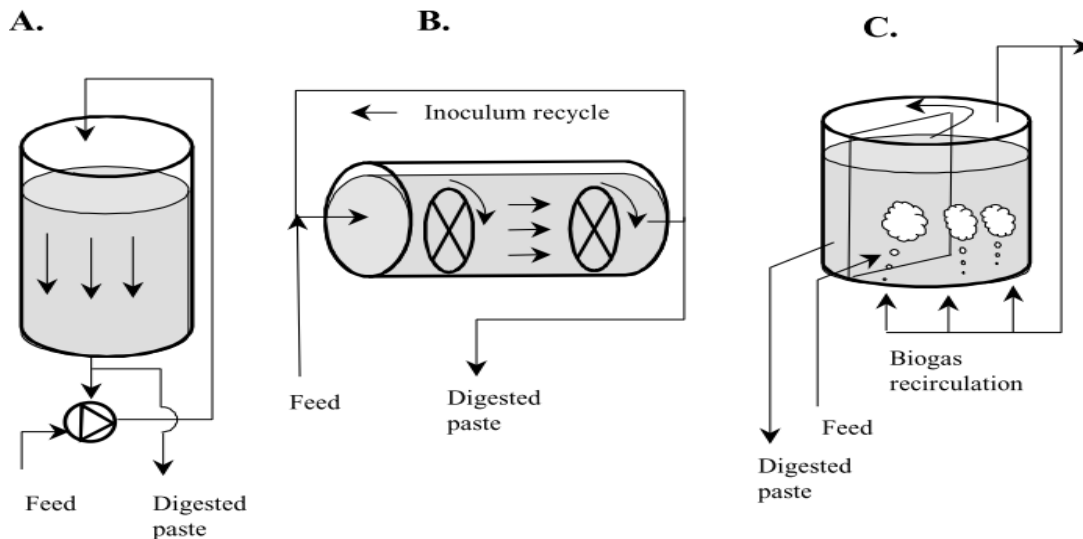


Figure 2.13 Different digester used in 'dry' anaerobic systems. A: Dranco design, B; Kompogas and BRV designs, and C: Valorga design.
Source: [114]

Table 2. 8 Benefit and drawback of dry -phase digesters

Source: [114]

Criteria	Advantages	Disadvantages
- <u>Technical</u> :	<ul style="list-style-type: none"> - No moving parts inside reactor - Robust (inerts and plastics need not be removed) - No short-circuiting 	<ul style="list-style-type: none"> - Wet wastes (< 20 % TS) cannot be treated alone
- <u>Biological</u> :	<ul style="list-style-type: none"> - Less VS loss in pre- treatment - Larger OLR (high biomass) - Limited dispersion of transient peak concentrations of inhibitors 	<ul style="list-style-type: none"> - Little possibility to dilute inhibitors with fresh water
- <u>Economical & Environmental</u> :	<ul style="list-style-type: none"> - Cheaper pre-treatment and smaller reactors - Complete hygienization - Very small water usage - Smaller heat requirement 	<ul style="list-style-type: none"> - More robust and expensive waste handling equipment (compensated by smaller and simpler reactor)

2.7.3 Anaerobic digestion performance in a single- and two-phase system.

A single-stage anaerobic digestion in continuously stirred tank reactors (CSTR) is a widely used technology for high-moisture waste fractions. (e.g., food waste, silage, manure, sewage sludge, waste activated sludge among others [118]–[121]). The four stages of anaerobic digestion are carried out in a single reactor. It may be difficult to achieve the best reaction conditions for the entire process due to the variations in the environmental requirements of each stage, which would cause a slower rate of degradation and the need for a longer retention time [122]–[124]. On the other hand, the biological performance of this system can be enhanced if the reactor design and operational conditions are carefully planned and chosen [116], [124]. According to Gunaseelan [121], two digesters with various retention times are essentially used in two-stage AD, with the first digester being optimised for acidification and the second for methanogenesis. Thus, compared to a single-stage digester, the digestion process may be completed more quickly. The two-phase AD of wastewater sludges increased methane yields and solid destructions, according to [125]. Additionally, [126] performed research on two-stage anaerobic digestion (AD) to enhance the AD process. The outcomes demonstrated that two-stage AD of sewage sludge could substantially increase sludge treatment efficiency, improve the transformation of organic molecules during the acidification phase, avoid potential inhibitors, and guarantee uniformity of feedstock for the methanogens. Various studies have shown that two-phase AD performs better in terms of digestion than single-phase AD [127]–[131]. Due to the two-phase system's complicated operation and control requirements and potential for higher capital costs, it is rarely used at full capacity [123], [132]–[135]. A single-stage system is ideal for many materials it has several benefits, such as less complexity, reduced capital costs, and efficient degradation of biological materials at typical retention times. Single stage systems are typically easier to operate and control, and less expensive to build [124], [134], [136]–[140]. According to Wan et al. [140], a single-stage digester efficiently co-digested a 2:1:1 mixture of wastepaper, food waste, and non-biodegradable plastics,

yielding approximately 0.592 and 0.370 m³ kg⁻¹ VS of high methane. Table 2.9 compares single-stage and two-stage anaerobic digestion processes.

Table 2. 9 A comparison of single-stage and two-stage processes.

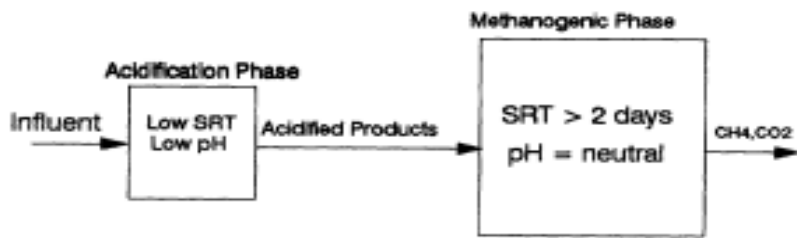
Source: [117]

<i>Process Operation</i>	<i>One-Stage</i>	<i>Two-Stage</i>
Operational reliability	in the same range	
Technical equipment	relatively simple	very complex
Process control	compromise solution	optimal
Risk of process instability	high	minimal
Retention time	long	short
Degradation rate	reduced	increased

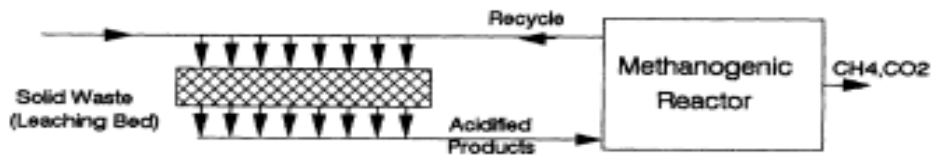
2.7.4 Multiphase and two-phase systems

Fermentation and methanogenesis are the two key process stages in anaerobic digestion. The basic drawback of single-phase digester systems (either high or low solids) is that these processes must occur under the same operational conditions, irrespective diversity of microbial growth rates and optimum pH. The basic principle behind two-phase digestion is to make it easier to optimise conditions by using alternative reactors for every stage. The first reactor's conditions are tweaked to promote the growth of bacteria competent of degrading biopolymers and releasing short-chain fatty acids. Because it triggers liquefaction and acidogenesis, is thus referred to as the hydrolysis/acidification process. The resulting volatile fatty acid solution is then transported to a second reactor, which can be any of several types

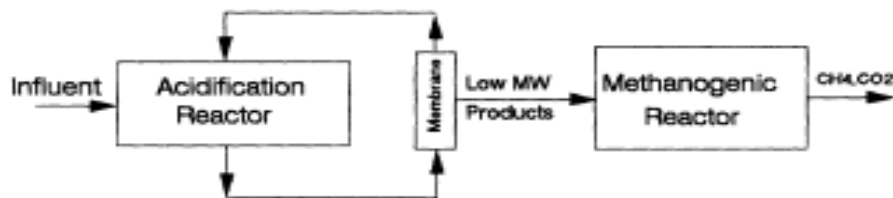
of methanogenesis-producing high-rate systems [112]. For phase separation, kinetic control of each digestion stage by operational adjustment of the dilution rate and recycling ratio is vital. Most two-phase digestion research has worked to preserve the acidogenic stage at pH 6 to maintain ideal conditions for substrate-to-acids conversion. Acidogenesis is promoted and methanogen growth is inhibited by a low pH and a short HRT. The first-phase reactor is a basic tank into which the liquor is poured before entering the methanogenic reactor. Because the key products of the first stage are volatile acids, a pH correction (at pH 7) could be required in the second stage if the buffer capacity exceeds [112]. The stability of the process of the multistage reactor can be improved when compared to one-stage systems, specifically, when digesting feedstocks that are readily hydrolysable [63], [123]. The instability of the multi-stage reactor could result from excessive inhibition of hydrogen accumulation or waste heterogeneity and fluctuations of organic loading rate (OLR) during anaerobic bacteria action in the system. In the hydrolysis phase, the multistage reactor gives some protection against fluctuating organic loading rates as more of the methanogenic bacteria are buffered [112]. The substrate passing through the hydrolysis stage to the acidogenesis stage is homogenised, and therefore, stability is achieved by the process [55]. Also, Multistage is capital intensive to construct and maintain but has a higher performance than one stage reactors. However, the multistage reactor is grouped into three as shown in (Figure 2.14). According to Walker et al. [15], the simplest form of the multistage reactor is based on the hydrolysis (Kinetic) phase separation, which is a combination of the continuously stirred tank reactor (CSTR), plug flow and other reactors that are similar. Furthermore, rather than higher yields, the key benefit of the two-phase digester, according [116], would be greater metabolic reliability for waste materials that cause unstable performance (Table 2.10). Even though two-phase digesters are typically preferred in laboratory studies because each phase is easier to control, [114], [132] stated that their potential benefits are still uncertain. In contrast, a one-phase digester has been shown to achieve a high rate of digestion.



Kinetic Phase Separation



Leaching Beds



Membrane/Dialysis Phase Separation

Figure 2.14 Multistage reactor system

Source: [15], [141].

Table 2. 10 Benefit and drawback of two-phase digesters

Source [114]

Criteria	Advantages	Disadvantages
- <u>Technical</u> :	- Design flexibility	- Complex
- <u>Biological</u> :	- More reliable for cellulose-poor kitchen waste - Only reliable design (with biomass retention) for C/N < 20	- Smaller biogas yield (when solids not methanogenized)
- <u>Economical & Environmental</u> :	- Less heavy metal in compost (when solids not methanogenized)	- Larger investment

2.8 Anaerobic degradation system overview and enhancements

The process of anaerobic degradation of substrate biomass includes the following.

- Materials sourcing
- Source separation of contaminating material
- Organic loading rate (OLR)
- Pre-treatment of the substrate due to digester size
- Digestion/degradation of the sample
- Methane, CO₂, digestate production
- Treatment of the degradation residue

However, Pre-treatment is said to be a vital tool for the conversion processes of practical cellulose and is used to break down the structure of cellulosic biomass into different sizes. However, the plant fibres of cellulose are exposed to make cellulose readily available for bacterial action for the conversion of waste biomass to methane. Also, cost-effective pre-treatment techniques are required to avoid the formation of toxic by-products, loss, or degradation of carbohydrates. Pre-treatment is necessary to prevent the waste biomass-related problem that could affect the availability of cellulose to enzymatic hydrolysis. The reduction of the crystallinity of cellulose and degree of polymerisation, create a new surface area that is made available for anaerobic bacteria, thereby making the cellulose readily accessible for enzymatic hydrolysis which, allow conversion of the substrate biomass and result in an ultimate maximum production of biogas from anaerobic digestion compared with ethanol production where there is a loss of hemicellulose. Also, pre-treatment equally has the potential to enhance efficiency as well as to lower costs through research and development [142]. Pre-treatment methods are divided into three broad categories including physical, chemical, and biological processes.

2.9 Physical pre-treatment

The role of size reduction is significant in the anaerobic reactor, reducing the formation of floating layers that can cause problems such as blockage of outlets and

the viscosity of the digester. Mechanical and thermal pre-treatment are both considered to be physical pre-treatment [22]. Additionally, the feedstock must be sliced, shred, or grind to increase the surface area for enzymatic hydrolysis activity. At the industrial and scientific levels, other technologies are being implemented. These include microwaves, ultrasound devices, and high-pressure machines. Thus, pre-treatment has reportedly been widely used around wastewater treatment plant (WWTP) residues and activated waste sludge (AWS), followed by lignocellulosic materials [143]. Pre-treatment is known to be the fundamental step, which operates on characteristics of feedstock to enhance the production of biogas in an AD system [22]. Also, the anaerobic bacteria transform sugar, such as glucose into methane. Starch and cellulose are chains of glucose, but starch is utilized by the plant as an energy store and is easy to break down. Cellulose is hard to break down because of the bond between the cellulose chains (cellulose, hemicelluloses, and lignin) and this is where efficiency improvement can be made by pre-treatment. The cellulose has an interwoven structure that is more resistant to hydrolytic bacteria activity. Therefore, the conversion of this lignocellulose complex sugar becomes the key to biogas production [39]. Pre-treatment has been grouped into three main categories: mechanical, chemical, and biological. The main aim of pre-treatment is to disrupt lignin-cellulose, hemicellulose (figure 2.15).

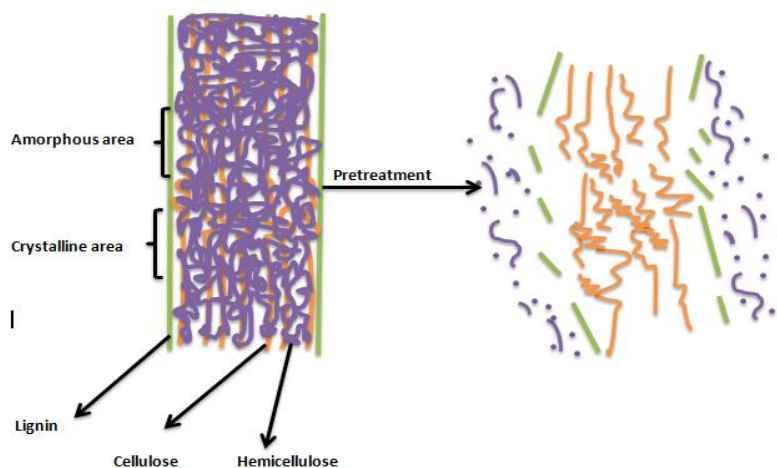


Figure 2.15 Role of pre-treatment in the transformation of substrate biomass into biogas

2.9.1 Mechanical pre-treatment

Mechanical pre-treatment is a simple form of pre-treatment that is used to disintegrate feedstock into different particle sizes to create a large specific surface area of the feedstock that is made available for microbial action. Thus, the AD process can be enhanced when the specific surface area is increased, and there is better contact between the anaerobic bacteria and the digestible material. The reduction process for larger solid into small size is known as grinding and when mechanical equipment is utilized, the process is referred to as milling. Besides, there are several size reduction equipment in the literature that have been tested both at industrial and laboratory scales, such as rotating drum, knife milling, hammer mills, choppers, and grinder shear shredders, wet pulverization, and extrusion. Also, high shear effective machines, shredders, vibro energy milling, disc milling, two roll milling, and colloid mills [144]–[148]. This equipment is often developed empirically to handle some specific feedstock materials (Feedstock) and well as other situations. Knowing the characteristics of the feedstock to be digested is essential. Probably because the most important factor governing particle size reduction is the hardness of the molecules' bonds, where additional energy is required to hold the feed particles together [149]. Despite the use of various methods, figure 2.16 depicts three types of size reduction equipment used in municipal waste processing. Generally, there are three main parts of particle size reduction equipment, such as the milling chambers hopper, discharge chute, and receiver as shown in Figure (2.17).

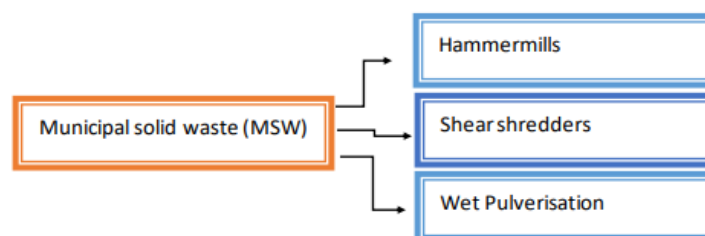


Figure 2.16: Three main types of mechanical comminution equipment extensively used in municipal waste processing.

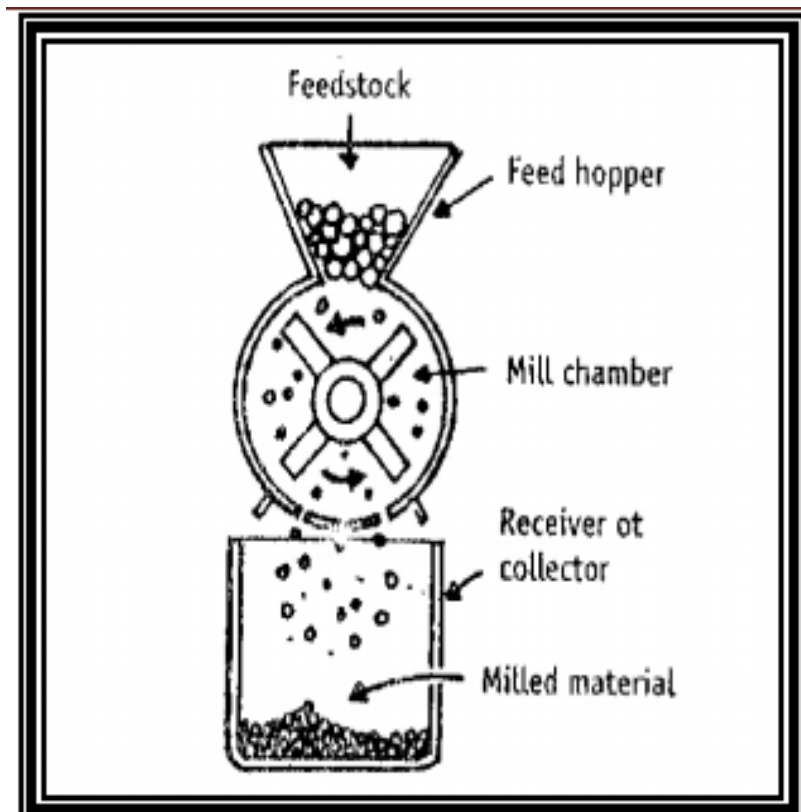


Figure 2.17 Components of the size comminution equipment

Adapted from [149].

Additionally, mechanical pre-treatment is an expensive process in the transformation of waste biomass into energy, though it helps to increase the specific surface area as well as methane production, the electrical power demand is quite high. Kratky and Jirou [147], stated that for efficient hydrolysis 1-2mm of particle size is recommended. Furthermore, to attain an optimal particle size, the size reduction requirements for the mechanical phase must be recognised, which comprise.

- ❖ The input organic feedstock size distribution, and;
- ❖ The effect of the type of mechanical comminution device on particle size distribution for various waste fractions. As waste is heterogeneous by nature, each fraction varies during comminution. The key characteristics of the various waste fractions used in the optimal size reduction processes are hardness, toughness, abrasiveness, stickiness, soften temperature, material compositions, moisture content, purity need for wear mechanisms during grinding, feed-to-

product ratio, bulky density, and physiological effect. Table 2-11 depicts the key characteristics affecting size reduction in the case of waste shredding. However, for this piece of work, three mechanical types of equipment are utilised, such as the shredders, manual chopping, and macerators/grinding.

Table 2. 11 Waste fraction characteristics in the scenario of shredding

Source [150]

Material property	Example for single waste fractions	Operational demands			
		Compression	Percussion	Cut	Shearing strain
Tough	Glass, ceramics, metals, sand, stone	OO	-	-	-
Medium tough	Salt, curable plastics	OO	OO	-	-
Soft	Organics, thermoplastic, textiles, paper, paperboard, wood	O	O	OO	OO
Brittle	Glass, ceramics	OO	OO	-	-
Elastic/flexible	Thermoplastics, rubber, metals	-	O	OO	O
Viscous/malleable	Plastics, organics	-	OO	OO	OO
Fibrous	Paper, paperboard, textiles, plastic fibre	-	-	OO	O
Sticking together	Plastics, organics	-	-	OO	O

OO: Highly applicable O: Moderately applicable -: Not applicable

2.10 Review of various mechanical particle size reduction techniques

2.10.1 Hammer mills

Hammer mills (Figure 2.18): In size reduction operations, the hammers in the hammer mills smash the waste materials as they enter and eventually force the shredder materials through a discharge unit. They are widely used to reduce waste size in large-scale processes. It is a high-speed rotating impact device having hammer parts that force into an inner disc. Efficient heat causes waste to disintegrate and tear, reducing waste size. It is also an integral part of particle size reduction technology in MBT plants. They are also the most utilised equipment for regulating waste composition and size reduction. Breaking, slashing, cutting, and crushing are

their major modes of operation. They can handle all types of municipal waste as well as a diverse variety of other waste streams.

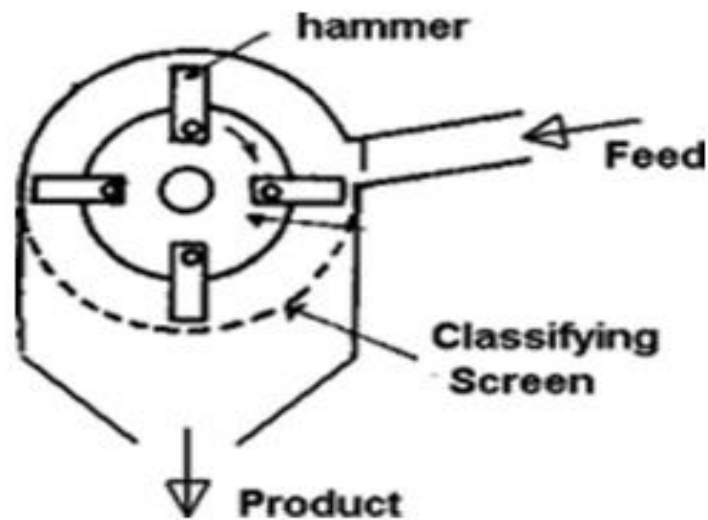


Figure 2.18 Diagram of a hammer mill

Source : [151]

2.10.2 Shear shredders

Shredders are mostly used to reduce the size of municipal solid waste (MSW). It is made up of two parallel counter rotating shafts with a succession of discs. The shredder waste is directed to the core of the counter rotating shafts. Also, it is used for pre-treatment of compacted hard to handle feedstock such as food waste (bones), paper waste, and grasses. Shredders' key modes of action are shearing and tearing, and they can handle all types of municipal solid waste. Hammer, knife and screw shredders or their mixes are the most commonly used equipment for lignocellulosic disintegration [147], [150]. The operation mechanism of a shredder is schematically depicted in figure 2.19.

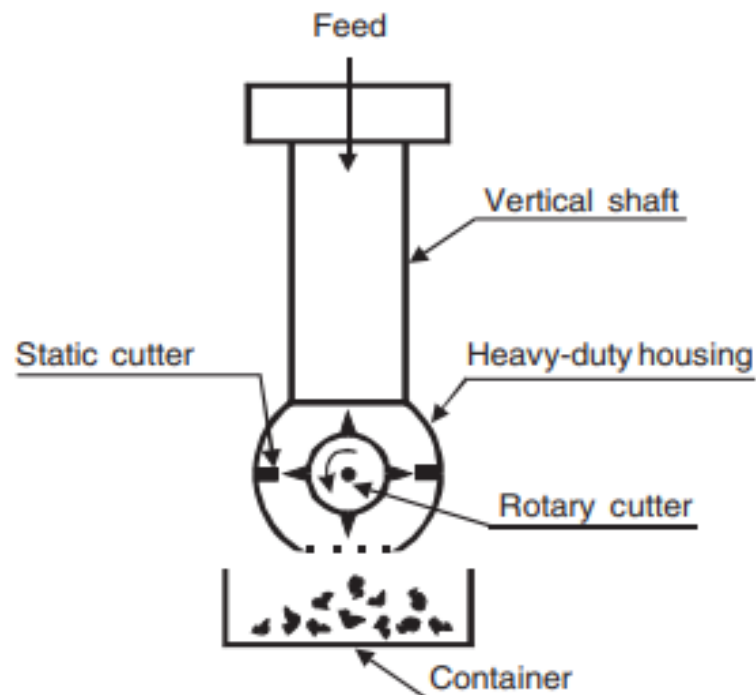


Figure 2.19 Schematic of a shredder's operating mechanism.

Source: [152]

Generally, the shredders are known as:

- ❖ Machines that break apart particles.
- ❖ A machine with one or more rotary shafts and low velocity, high torque shear shredders with a collection of closely packed cutting discs or knives on each shaft that is located somewhere towards the bottom of a feed hopper; particles are driven downward by the rotating propeller cutters through the small gaps between the discs/knives and the chamber's walls. This is widely utilised in the recycling industry.
- ❖ Machine that produces shearing action by compressing particles in offset planes.
- ❖ A machine where developing particles have a slender shape.

2.10.3 Wet pulverisation

When MSW is "wet pulverised," it is mixed with water or other wet materials, including sewage sludge, and tumbled around a rotating cylinder. Material is propelled up the sidewalls of the rotating drum where it falls naturally using internal flights or vanes similar to those found in trommel screens. The method may be used

as a bioreactor because degradation typically begins rapidly inside the drums. The final particle size of pulverisation is intended to be in the range of nm, producing fine and ultrafine particles [144]. However, mechanical comminution equipment has a variety of types in the market. During this research, it became evident that there are no industry-wide categories or standardised criteria for various size-reducing devices. According to [153], size reduction devices are classified as chippers, grinders, and shredders (Session 2.10.2)

2.10.4 Chippers:

- ❖ a collection of knives positioned on a rotating disc or plate that impart a slicing action and slices the material up into small fragments.
- ❖ Commonly used to cut wood into various sizes of chips.
- ❖ Emerging fragments: smooth, uniformly formed granules or chip.
- ❖ Generally, their mode of operations is cutting and slicing and can be apply to yard waste, plastics, paper, carboard, timbers and tree trimmings.

2.10.5 Grinders:

- ❖ The pounding device is mostly a hammer mill (tub or horizontal feed grinders)
- ❖ New fragments: ragged, fractured, and smashed.
- ❖ Particles are decreased in size by repeatedly smashing them into smaller fragments using a mix of tensile, shear, and compressive forces.

2.10.6 Roll or screw mill.

Roll mill works by drawing waste into the mill and forcing it to a lower rotating roller through the action of two high-level screws. The of the cutter and the distance between roller and cutter determine particle size. Because of its simple shape, they are commonly used to grind flour. A diagram of a roller mill is shown in the figure 2.20.

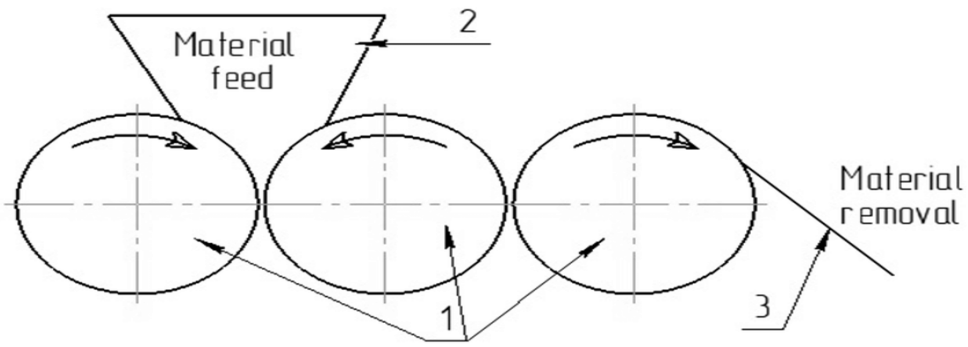


Figure 2.20 A diagram of a roller mill

Source: [150]

2.10.7 Ball mill

The ball mill, also known as the Cascade mill, is a rotatory drum with a heavy-ball-filled drum that is used to shred or pulverise waste. They are built of a slow-moving rotary drum with a maximum diameter between 4 to 7 metres that is packed with steel balls that account for around 17% of the available capacity. The relative movement of the balls and waste particles causes intense grinding and milling, which results in crushing/shredding action. The crushed waste is filtered through an appropriate particle size mesh filter [150]. A diagram of a Ball mill is shown in the figure 2-21.

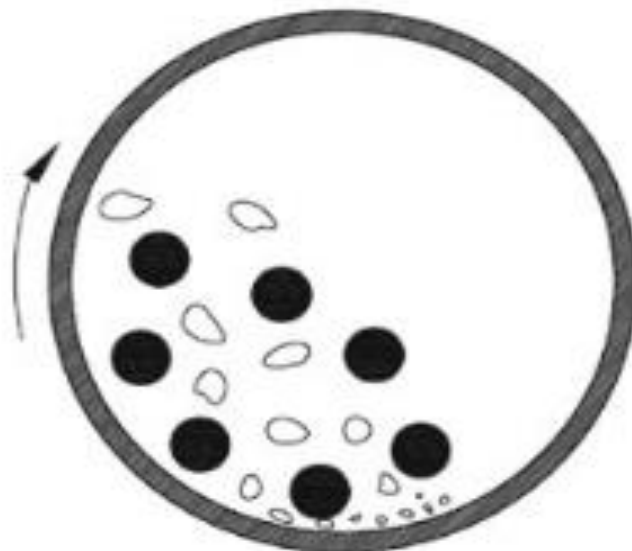


Figure 2.21 A diagram of a Ball Mill

Source: [154]

2.10.8 Cutting mills

Cutting mills are typically slow-moving shredders with a variety of cutting processes. Cutting mills can grind product mixes that are soft, medium-hard, elastic, fibrous, or heterogeneous. Because size reduction by cutting and shearing is done carefully and fast, making the mills are suited for temperature-sensitive samples. The diagram of a cutting mill depicted in figure 2.22. The benefits and drawbacks of some mechanical size reduction equipment commonly found in MBT plants are shown in Table 2.12.

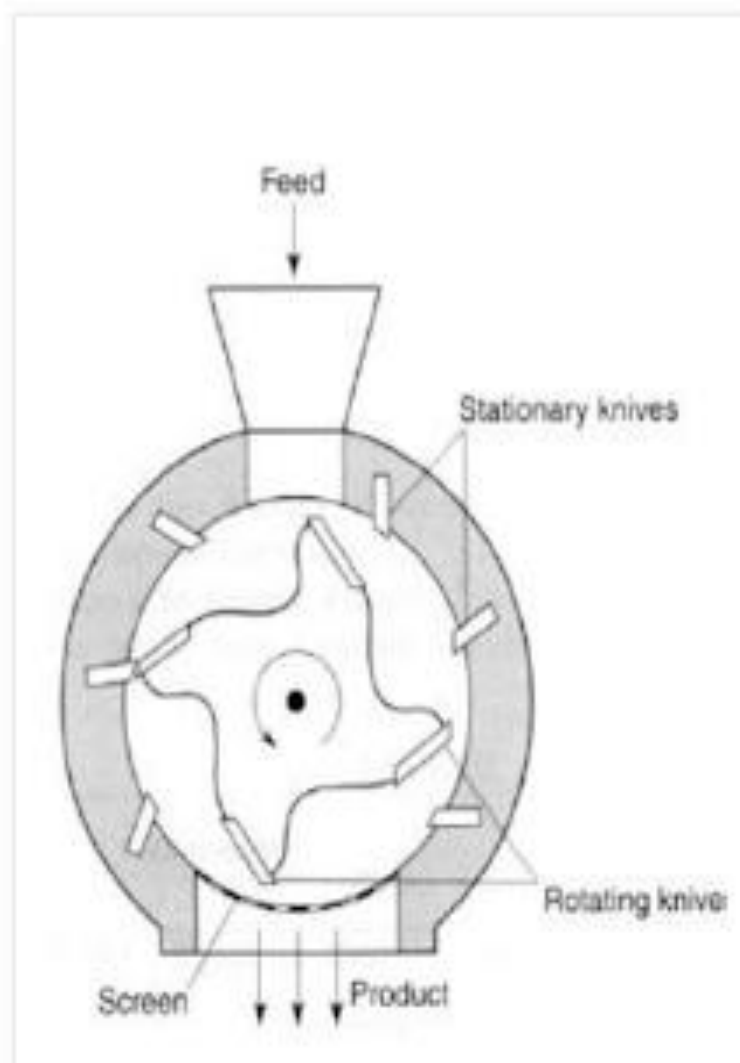


Figure 2.22 Diagram of a cutting mill

Source: [149]

Table 2. 12 The benefits and drawbacks mechanical size reduction equipment

Modified from [155].

Processes	Merit	Drawback	Suited for	reference
Hammer mills	<ul style="list-style-type: none"> ❖ High size reduction ratio and can promote the cubic structure of the particles. ❖ High rates of processing. ❖ There are affordable and simple to use ❖ Regularly increases the fluidity of the digester. ❖ A high level of shredding is attained. ❖ Increase the surface area of organic complex waste to accelerate degradation. 	<ul style="list-style-type: none"> ❖ Severe wear and tear ❖ High maintenance costs, sensitivity to stones, etc. ❖ The screen can become clogged at some point. ❖ Production of noise ❖ Increased moisture content and final smaller particle sizes both of which influence energy, leading to a increase in demand. ❖ Production of dust ❖ The mill may clog and incur damage if the feed rate is not regulated. 	<ul style="list-style-type: none"> ❖ Brittle waste with a high density that is easily broken or split 	[144], [145], [147], [150], [155], [156]
Mixing drums	<ul style="list-style-type: none"> ❖ Low demand for energy ❖ Low levels of dust emissions ❖ Performs various function. ❖ Controllable moisture content 	<ul style="list-style-type: none"> ❖ The ability to crush large particle sizes is limited. ❖ It can lead in an overabundance of smaller particles. 	<ul style="list-style-type: none"> ❖ Mostly suited for smaller size of particles 	
Cutting mill	<ul style="list-style-type: none"> ❖ Shredding at a high level is achieved. 	<ul style="list-style-type: none"> ❖ Reduced production rates 	<ul style="list-style-type: none"> ❖ Obtaining a specific distribution of particle sizes. 	
Ball mill	<ul style="list-style-type: none"> ❖ Requires little space. ❖ Shredding to a high degree is attained. ❖ Integration of many processes (crushing/sieving) in a single phase of production. ❖ Reduced dust emissions. 	<ul style="list-style-type: none"> ❖ High energy usage ❖ Reduced throughput rates. ❖ Long-time of operations 	<ul style="list-style-type: none"> ❖ Waste with various degrees of brittleness, density, and physical durability 	
Roller or screw mill	<ul style="list-style-type: none"> ❖ Low production of noise ❖ Low production of dust ❖ low wear and tear ❖ low energy demand 	<ul style="list-style-type: none"> ❖ Reduced throughput rates. ❖ Labour and maintenance costs 	<ul style="list-style-type: none"> ❖ Waste with various degrees of brittleness, density, and physical durability 	

2.11 Reasons for size reduction in anaerobic digestion processes

Mechanical pre-treatment of organic solid waste involves size reduction, both in the laboratory and on a large scale, for the following reasons:

- ❖ Large and bulky materials must be reduced in size before being digested by the anaerobic digestion unit or digester.
- ❖ Particle size reduction increases the overall specific surface area of waste particles while decreasing particle size distribution.
- ❖ Package (e.g., closed bags) must be accessible.
- ❖ Digester stability.

2.12 The effects of various mechanical comminution equipment on feedstock characteristics and particle size distribution.

Mechanical biological treatment (MBT) is a bioprocessing technique used in Europe to biologically stabilise the organic fraction of municipal solid waste (MSW). There have been over 30 MBT facilities in operation or under construction in the United Kingdom alone in 2017 [157]. The most common method used in the treatment of mechanical—biological waste is shredding [157]–[159], but other processes, such as milling, are also used [144], [160]. It has been discovered that the particle size distribution of the solid waste fed into the hammermill and its residence time in the machinery are dependent on the particle size distribution of the output (PSD). Hammer milling has been discovered to be more suitable for materials with low moisture, such as straws, despite clogging issues having been reported for biomass with moisture levels of higher than 10 to 15% [147], [160]. Shredders use less energy, are more reliable, and cause less damage than mills. Typically, shredding reduces particle size to a few centimetres or less. Although the impact varies for different types of organic complex materials due to their physiochemical characteristics, mostly those with higher lignin and moisture contents, such as paper or woody components, can affect the shape and size distribution of the substrate [136], many researchers have found that shredding has a positive overall effect on MSW bioprocessing [158], [159], [161], [162]. However, little is known about the actual particle size distribution (PSD) that results from substrate size reduction, specifically the PSD in the organic-complex fraction that would be exposed to biological treatment. This shows that they are driven on by the presence of a wide range of particle sizes in pre-treated MSW for bioprocessing. It is usual practise to report the highest or mean particle size of particle size reduction material, which is insufficient data. Pre-treatment of waste does not produce uniform, equal-sized particles; instead, it produces a diversity of particles of varied sizes. On fermentation processes and results, PSD is thought to have a direct influence. A shear shredder, rotary cutter, and wet macerator were used by [20] to separate the organic fraction of municipal solid waste into streams with various particle size distributions (Figure 2-23). Similar to shear shredder material, single and double pass material has

particles that seem larger than the shredder's jaw opening. This is because the material was not uniformly sized throughout. For instance, after sieve analysis, some paper was split into strands that flattened against the sieve mesh.

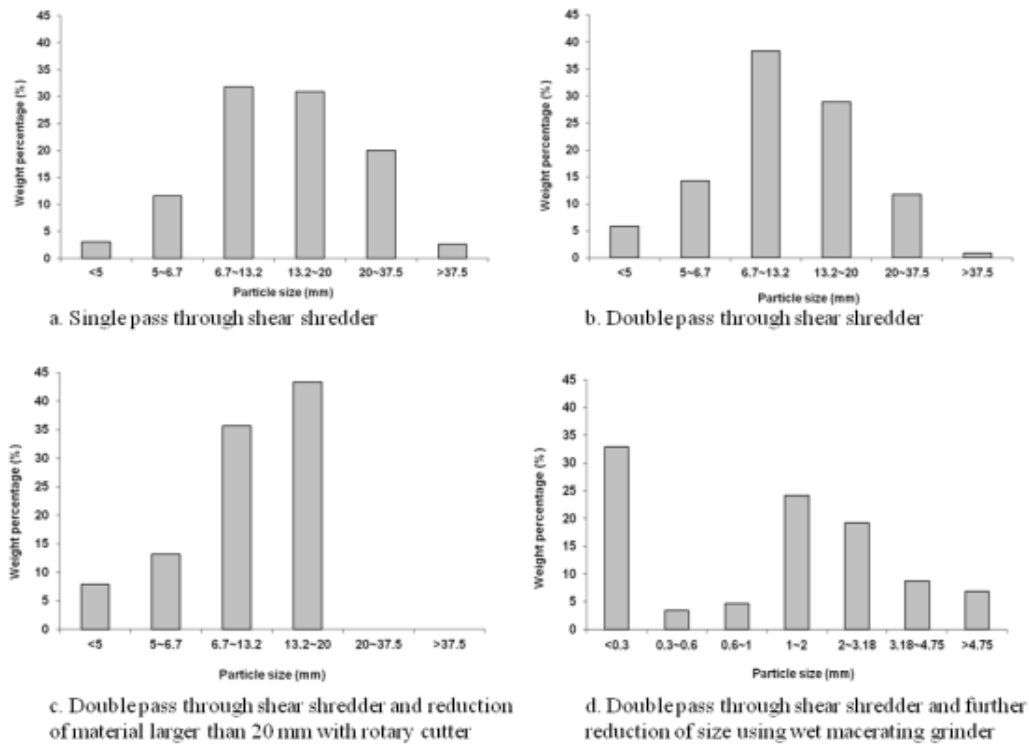


Figure 2.23 Particle size analysis on size reduced OFMSW using a shear shredder, rotary cutter, and wet macerator.

Source: [163]

Many of the particulates were found naturally in the waste instead of being mechanically altered by the action of the cutting discs. It was also observed that the initial material with a fraction larger than 20 mm before being fed into the shredder was substantially reduced in size after shredding. Particle sizes were reduced when double processing was used, with most particles ranging from 6.7-13.2 mm compared to a high fraction in the ranges of 13.2-20 mm and 20-37.5 mm when a single pass was used. Using a rotary cutter to further reduce the size >20 mm, the fraction in the 13.2-20 mm range increased, making this the largest fraction after treatment. The wet macerated material's mean particle size was around 2 mm, with a significant percentage (33%) of 0.3 mm. Each fraction's VS content was calculated,

and the fraction with the smallest particle sizes had the lowest VS content (75% of TS, compared to those with particle sizes larger than 2 mm). Paper and cardboard fibres dominated the fraction larger than 2 mm even though they did not easily move around the surface of the sieve. However, several researchers have calculated a mean value with standard deviations for residual waste shredding with hammer mills. The particle size distributions of solid waste processed with various shredding equipment were compared to non-shredded waste (Figure 2-24) [164]

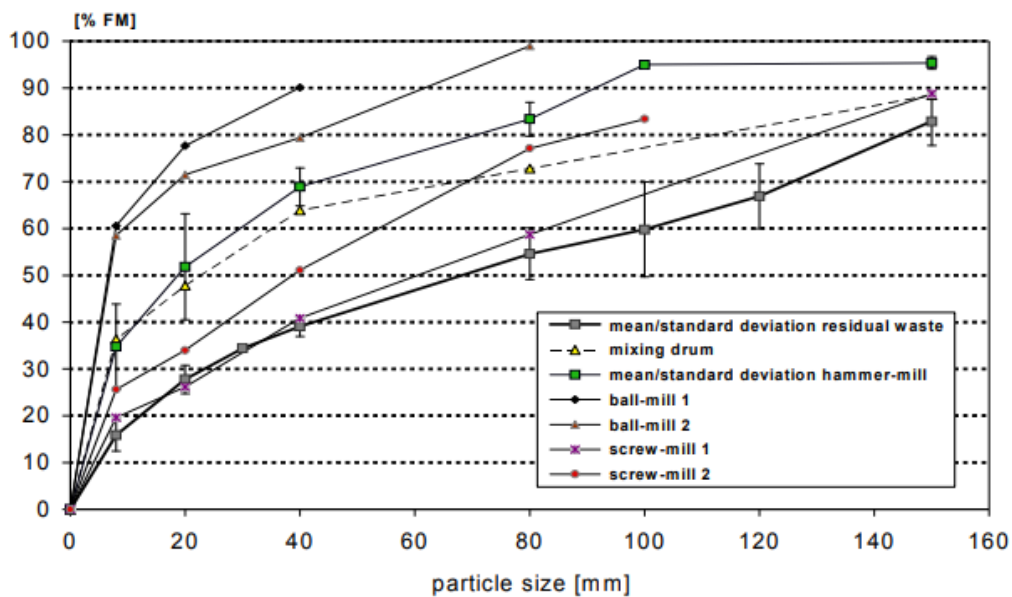


Figure 2.24 Cumulative particle size distribution using various shredding equipment types.
Source: [150], [164]

The researcher discovers that differences in manufacturer, operational configuration, and shredder wear and tear all have a significant effect on productivity but are difficult to determine because there are no clear and precise results available to assess the performance variation for both new and used shredder cutting equipment. When compared to Screw mill 1, Screw mill 2 (Diepholz plant) achieved a substantial reduction in particle diameter (Quarzbichl plant). It is noteworthy that the fine fraction, regardless of crushing method, contains 40 to 90% of the waste. The mixing drum treatment works similarly to the hammer mill. The ball mill allows for extensive shredding and crushing. After crushing, the 20 mm fraction contains nearly 80% of the material and the 40 mm fraction contains 90%

of the material. Also , organic kitchen and garden waste was discovered to contain smaller particle size fractions prior to shredding (figure 2-25); according to [164], roughly 80% of waste can be classified in the 80 mm fraction. After shredding, more than 80% of the organic wastes are in the 40 mm fraction (except for screw mill 1). The fraction of organic wastes in the 40mm fraction is higher (90%) in the mixing drum study results than in the hammer mill study results (80%). After shredding/crushing with a hammer mill and composting drum, less than 10% of the organics had particle sizes larger than 80 mm. The 80 mm container was filled with shredded organic kitchen and garden waste.

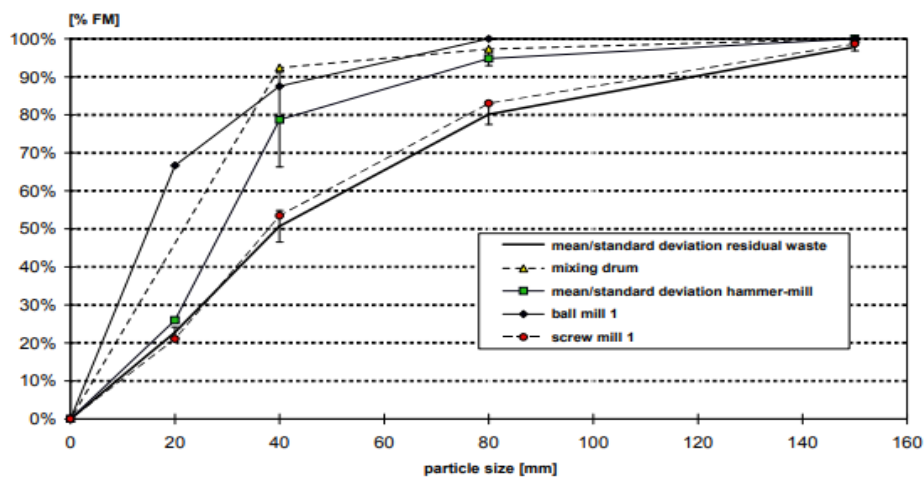


Figure 2.25 Cumulative particle size distribution of the organic kitchen and garden waste fraction using various types of shredding devices.

Source: [150], [164]

Additionally, according to [164] studies, the paper/cardboard proportion is discovered in oversize > 150 mm, or roughly 20 to 30% (figure 2 26) . The study found that between 60 and 70 mm in size made up about 80% of the oversize fraction. The hammer and ball mill shred the paper or cardboard to a vast degree. The entire fraction is crushed in a ball mill to produce the fraction 80 mm because the grain fraction 40 mm accounts for over 80% of the fraction. The hammer mill was made with a heavy crushing motion in mind. Before the decaying drum, the fraction of the paper/cardboard fraction that was larger than 150 mm was segregated. Nearly all the paper in grain classes >40 mm is destroyed after the decaying drum. Due to the fraying effect of the drum operation and the quick mixing in the composting drum, the bulk of the paper/cardboard fraction has shifted to

the non-sortable waste < 8 mm. The cardboard/paper fraction of the cardboard composite package are also segregated, and they are fed to the grain fraction with a diameter of <40 or < 8 mm.

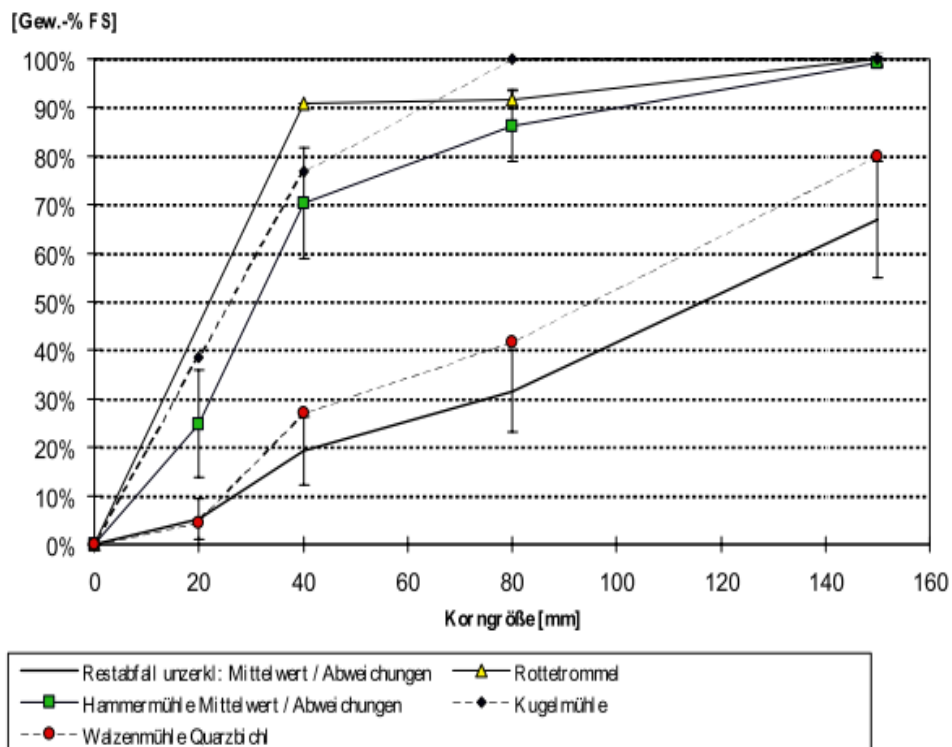


Figure 2.26 Paper/cardboard grain size distribution when employing various shredder components.

2.13 Biological pre-treatment

Biological pre-treatment involves the use of high-capacity microorganisms in degrading a substrate with the addition of enzymes that give support responses inside the anaerobic digester. Biological pre-treatment has a positive impact on the degradation rate of the substrate, and the hydrolysis step could be enhanced through the increase in the microbial action per unit surface area. The effect can be achieved by feedstock inoculation (i.e., the introduction of bacteria to the substrate) and using enzymes. Hemicellulose, cellulose, and starch degrading enzymes operate best at the temperature of 30-50°C and pH level between 4 and 6. The pre-acidification step in biological pre-treatment uses the acidogenic stage of the anaerobic process by optimizing the growth of acidogenic bacteria in the AD system. When the acidogenic bacteria restrict the growth of methanogenic bacteria, it

increases the anaerobic degradation rate. This is because acidogenic organisms are much harder and build up faster than methanogenic bacteria. This process is achieved by the addition of a high supplement loading rate to the digester, particularly for starch degradation [22]. The effect of mature compost addition, as a biological pre-treatment for two industrial organic fractions of municipal solid waste (OFMSW) at 15 days solid retention time. The study demonstrated that the productivity of anaerobic digestion of industrial OFMSW in terms of the removal of dissolved organic carbon and volatile solids was increased by 61.2% and 35.3% respectively as against the control without pre-treatment. This is because the hydrolysis step should have improved through the increase in the microbial action per unit surface area. Therefore, the methane and biogas generation, expressed as (L/L reactor), is increased up to 73.3% and 60.0% over the control [165]. Also, the authors stated that the specific methane generation is enhanced up to 35.48%, whereas the cumulative methane and biogas productions is enhanced 141.6% and 190.0% respectively [165]. In conclusion, only a few studies have been performed on biological pre-treatment as seen in the literature [22], [165]. The key merits of this process are that it uses a specific species of microorganisms that can result in lower capital cost and less energy input, without any addition of chemicals. This could encourage rural communities across the world, and the major drawback is the lower hydrolysis rate compared with other methods, such as physical and chemical processes.

2.14 Chemical Pre-treatment

Chemical pre-treatment is the kind of treatment that includes oxidative reactions and the addition of acids or alkalis that are used for the destruction of organic matter. This treatment process has been applied to all classes of a substrate obtained from a different waste stream such as agricultural, industrial, and municipal waste streams. Chemical pre-treatment could be performed in a combination of increased temperature known as a thermo-chemical method [143], [166]. This can lead to significant solubilisation. Few researchers have combined both thermal treatment and chemical addition to a substrate such as waste

activated sludge, or fibrous biomass. This allows for significant solubilisation with alkaline treatment and enhanced biodegradability performance [167]. Substrates containing higher amounts of starch are not appropriate for chemical treatment due to their faster degradation and later excessive accumulation of volatile fatty acid (VFA). This causes problems with the methanogenesis phase of the AD process, leading to failure [168] whereas a substrate that is rich in lignin can be processed and can improve the biodegradability performance and safeguard the methanogenesis step without collapse of the AD system. Also, anaerobic digestion requires pH adjustment by the increase in alkalinity; it can be concluded that alkaline pre-treatment is the most preferred chemical pre-treatment method to be used during anaerobic digestion [169]. The hydrolysis phase and biogas production can also be enhanced when oxidative and acidic pre-treatment, such as ozonation, are utilised. The method and type of substrate characteristic determine the chemical treatment to be used [170]. In another study on barley waste for methane production, the researchers found that both co-digestion and alkaline hydrolysis pre-treatment with kitchen waste were valuable to improve the production of biogas from grain waste. Although the best result in TS and VS reduction was observed in the assay with the alkaline hydrolysis, the researchers also noticed that the pH correction at the industrial process can be costly when treating high amounts of waste. This means that, in full-scale production, alkaline pre-treatment may not be suitable [171].

2.15 Previous studies on particle size

Hydrolytic bacteria are surface-attached bacteria that mediate cellulose solubilization in anaerobic digestion systems [15], [172]. The particle size of the substrate has been found to have a significant effect on biodegradation in studies, and cellulose has been identified as the rate-limiting stage in the anaerobic degradation of the organic fraction of municipal solid waste OFMSW [172]. Furthermore, mechanical pre-treatment can be effective in reducing the impact of this rate-limiting step by breaking down the properties of the feedstock. Biological hydrolysis can thus be optimised [70]. In the past, Hills and Nakano [173].

investigated how particle size affects the anaerobic digestion (AD) of tomato wastes. In doing this, the authors used laboratory digesters with operating volumes of 4 litres to ascertain the impact of the particle size (PS) on methane gas production. Chopped tomato solid waste of the particle, sizes 1.3, 2.4, 3.2, 12.7 and 20mm, were used as the substrates, and fed to the mesophilic digesters at 3g volatile solids per litre, with a retention period of 18 days. The 1.3mm PS gave 3 times more biogas than the 20mm PS. The 1.3mm PS produced 0.81 volumes of methane per volume of digester per day with a VS reduction of 60.3% as against 21% VS reduction by the 20mm particle size (PS). The authors concluded that, for tomato solid waste, it does appear that methane gas production varies inversely with the product of particle diameter and sphericity. Similarly, a study by Sharma et al [36] on the impacts of particle size (PS) using agricultural waste and forest residues yielded similar results. The results showed that the highest quantity of biogas was generated by the particle sizes in the range 0.088mm to 0.40mm, out of the five particle sizes (i.e., 0.088, 0.40, 1.0, 6.0, and 30.0mm). The digester runs on PS 0.088mm and shows 16.9 to 50.2% more biogas than when the digester runs on the largest PS, while there is less than a 3% change in the biogas production between PS 0.088 and 0.4mm, thus implying that grinding particles below about 0.4mm is apparently of little benefit and possibly uneconomical. These studies were carried out in batch digesters at a temperature of 37°C [36]. The relationship for carbohydrate particles was corroborated by Sanders[174], with much smaller characteristic sizes. A decrease of particle radius was then described as a linear function of time. showings 16.9 to 50.2% more biogas than when the digester runs on the largest PS, while.

$$r_t - r_o = -\frac{-K_{sbk}}{\rho} t \quad (2.5)$$

Where: r_t is the average particle radius at time t (m).

r_o = initial organic solid particle radius [L],

ρ is the density of the substrate (kg/m³)

K_{sbk} is a surface-based hydrolysis constant (kg/m² day).

is time (days),

This was reformulated by [24], [175] among others, which characterized the disintegration process surface area that was also explored by [176]. Kim et al [177] studied the impacts of particle size (PS) on the AD of food waste (FW) at thermophilic temperature 45°C. The maximum substrate utilization rate coefficient k was obtained as 0.24/hr, while the half-saturation coefficient K_S was 700mg/l, at a non-inhibiting organic loading. 1000 mg/L gave the substrate inhibition factor for inhibiting organic loading range, and the inhibitory effect was observed until 5 g/L sodium ion was added to the serum bottle reactor. The volume of methane gas was then gradually reduced to concentrations of greater than 5 g/L of sodium ion (Na^+) applied. However, the sizes of all food waste particles were kept constant, and the substrate usage rate constant was inversely related to the particle size. This implies that the substrate usage rate coefficient doubled as the average particle size decreases from 2.14mm to 1.02mm, thus indicating that particle size reduction is a vital factor in anaerobic food waste degradation and ultimate methane production. Also, pre-treatment to reduce particle size has been shown to enhance the surface area available for hydrolysis enzymes. The research on particle size reduction as a pre-treatment technique for the gain in the potential of biogas from Tanzanian sisal fibre waste corroborated this assertion. These treated sisal fibres were then tested in anaerobic batch experiments to determine the influence of pre-treatment. The researchers utilized sediment from a stabilization pond as seed at a sisal production plant. The results showed that fibre degradation increased from 31% to 70% for the 2 μm PS, compared to the untreated sisal fibres. There was also a 23% methane yield increase and 0.22m³ CH₄/kg volatile solids for the 2 μm fibres as compared to 0.18m³ CH₄/kg volatile solids for untreated sisal fibres. The result also confirmed that methane production was inversely proportional to particle size compared to untreated sisal fibres. The effect of pre-treatment of particle size reduction of sisal fibre waste on anaerobic biodegradability is shown in figure 2.27 [178].

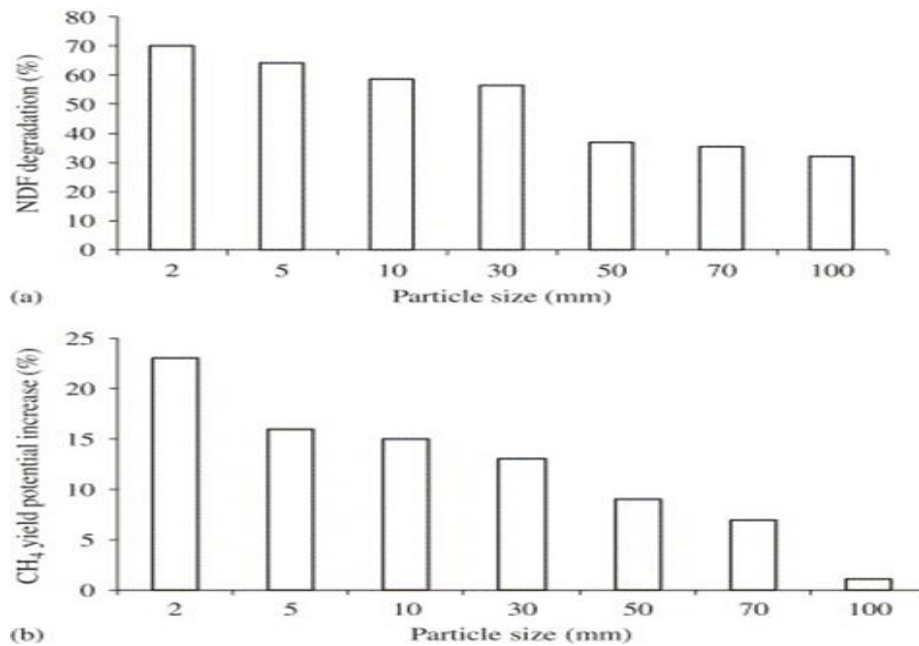


Figure 2.27 Effect of particle size on the yield of methane production of sisal fibre

(Adapted from [178])

A similar result was obtained by [179], [180]. A study carried out on the effects of the particle size (PS) reduction on anaerobic biodegradation of many organic materials, it was discovered that reducing the particle size of the substrate by a mechanical treatment can improve gas production by up to 18% with a reduced degradation level of about 59% (Figure 2.28). The authors reported that the effects of the particle size reduction on reactor biogas production are not significant with organic materials, including the mixture of carrots, potatoes, apples, and meat. It implies that these materials account for an excellent biodegradability of up to 95% and 88%, respectively, the authors also noted that for substrates with very good biodegradability resulting from material composition and structure, and low cellulose and lignin content, mechanical pre-treatment does not enhance biodegradation and biogas yield. This is because the substrates can be degraded by microorganisms sufficiently so that comminution does not yield any further improvement. They further reported that for substrates with high fibre content, degradability could reach 50% without mechanical pre-treatment, and could increase up to 20% by comminution depending on the state of the ground sample. For the high fibre substrates, the authors were of the opinion that comminution

releases usable cell compounds in a more easy and quick form by making them available, for microorganisms and enzymes, areas which ordinarily would have been difficult to reach for bacterial and enzymatic actions [179].

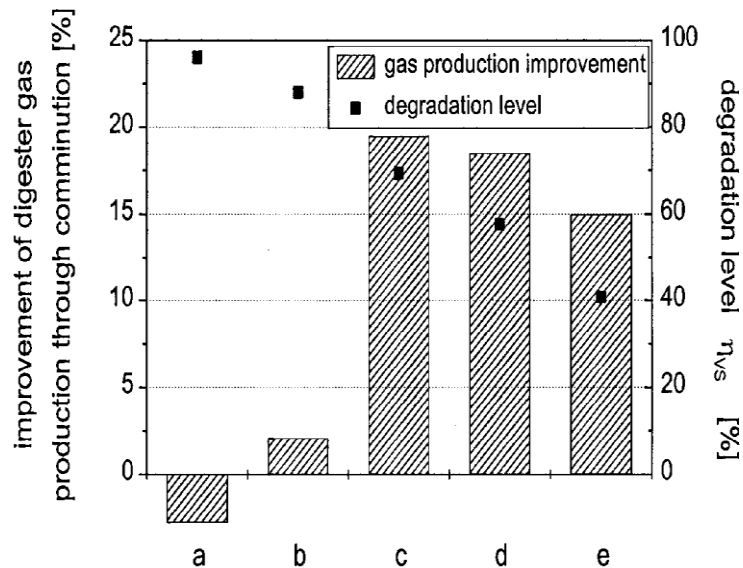


Figure 2.28 Enhancement of biogas production through batch degradation process as a result of particle size reduction and corresponding degrees of degradation level of the raw substrate (a; Mixture of apples, carrots, and potatoes; meat; c: Sunflower seeds; d: Haye: leaves).

Source: [179].

Similarly, Angelidaki and Ahring [180], reported an increase in the methane yield of 16% for macerated manure bio fibres with particle sizes between 1 and 2 mm and a 20% increase in fibre size of 0.35 mm. There was no significant difference found with fibre sizes of 5–20 mm. The findings clearly illustrate that particle size reduction increases substrate utilization, and hence gives enhanced biogas production. Also, Hajji and Rhachi [181], studied the effects of particle size (PS) on the process of an AD system of municipal solid waste (MSW). The authors operated the reactor at a temperature of 40°C under mesophilic conditions, keeping the PS in a diameter range from 10mm to 100mm. The results obtained indicated an increased relationship involving the PS and biogas production, with an optimal production rate recorded for the 10mm particle size which was 20% higher compared to the 100mm PS. A similar study was also carried out by [182]. The authors studied the effect of

PS reduction on whole crop maize silage and grains, which enhanced the production of methane from both biomass substrates operating in a batch mode. The results obtained suggested less than a 10% increase in methane generation of the biomass. Few studies have dealt with the effect of particle size distribution on anaerobic digestion (e.g. [183]). Marcato et al [183], reported particle size and metal distributions in anaerobically digested pig slurry. The authors found that particle size distributions in both raw and digested slurries (RS and DS) show a shift in smaller particle size distribution towards larger sizes which were of greater resistance to anaerobic biodegradation. However, there has been a consensus that the capital cost alongside the operating costs of the AD plant could be achieved by reducing waste into different particle sizes, which would consequently allow faster reaction rates through the increased exposure of the particles to microbial attacks during the decomposition process of waste materials in the AD system. It means to prevent the likely congestion of the digester by large-sized particulate matter and to boost the digester performance by increasing the biogas production [36], [173], [174], [184]–[186]. Contrary to this assertion, other researchers have stated that particle size (PS) reduction has little or no effects on the rate of combination or ultimate biodegradability of the complex organic fraction of municipal solid waste (OFMSW) [57], [121], [185]. At particle size range of 2-20mm, Nopharatana et al [185], found no significant digestion benefits from an extensive particle size reduction of biodegradation soluble and insoluble fraction of municipal solid waste (MSW) sample and the digestion rate alongside the biogas yield. It could be from the shape of the particle as well as the quantity of OFMSW where size reduction does not eventually cause exposure of the surface area of the feedstock. Particles with different shapes have different biodegradability since biodegradability also depends on the shape of the particle. However, differences in particle shape could result from the milling process where some particles that pass the screen are most probably smaller or even dissolved, whereas others may have been larger having passed through longitudinally. Also, the differences in the particle shape could result from the particles not being uniform in all dimensions, or that some particles are naturally

present in finer particles rather than being physically changed due to the action of the machine. [20]. Furthermore, one of the key factors that have an impact of anaerobic degradation processes is the particle size of the substrate. A larger surface area exposed to enzymatic attack results in smaller particle size, that could optimise fuel availability and hydrolysis of the processed material. Nevertheless, Re-analysing data from [36] on three grasses (wheat straw (*Triticum aestivum*), rice straw (*Oryza sativa*), and dhub grass) (*Cynodon dactylon*) (figure 2-29). The particle size paradox was discovered by [187].The study found that the relative rate of biogas production per unit surface area decreased rapidly as particle size decreased, suggesting that factors other than mean size particle play a significant effect.

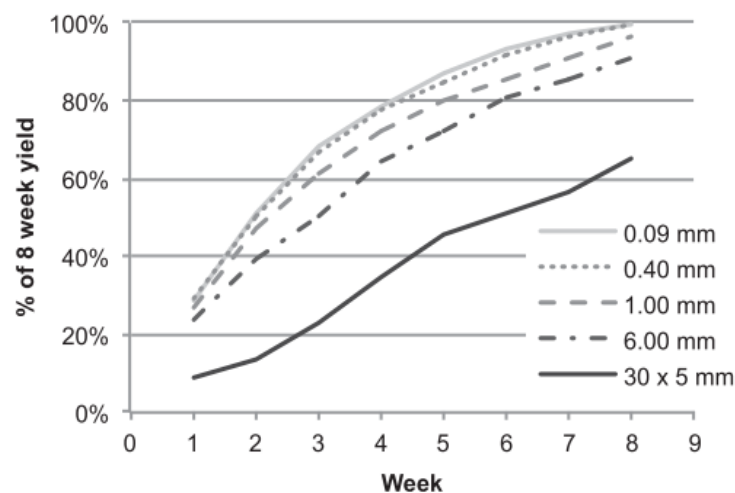


Figure 2.29 depicts the arithmetic mean of re-analysed data for three grass digestions.
Source [187]

2.15.1 Summary of the previous work

It has been shown by past researchers that the maximum quantity of biogas can be produced by smaller particle sizes than when the digester runs on the largest PS range, thus indicating that particle size (PS) is a vital factor in the anaerobic biodegradation of waste biomass and ultimate methane production (Oh et al., 2000; Sharma et al., 1988). The researchers have also shown that pre-treatment to reduce particle size can improve the surface area available for hydrolysis enzymes. on the contrary, after re-analysing data from previous studies,[187] Mason and Stuckey

[12] discovered the particle size paradox. According to the study, as particle size decreases rapidly, so does the relative rate of biogas production per unit surface area, indicating that other characteristics other than mean particle size play a key role. A review of the literature by Hernandez-Beltran et al. [188] revealed that there is no one universal, optimum particle size that is best suited for bioprocessing technologies [157]. Additionally, it has been discovered that biodegradability is affected by particle shape. This can result from particles not being uniform in all dimensions or where some of the particles are naturally present in finer particles rather than being physically changed due to the machine action. In contrast to this, some researchers also highlighted the biggest problems associated with particle size reduction. Particle size effects could speed up the first two processes of AD processes known as hydrolysis and acidogenesis. It can result in the production of soluble organic materials, such as VFAs, leading to excessive-high organic loading in the anaerobic reactor. When such overloading occurs, the unbalance in the output and uptake of volatile fatty acids (VFAs) lead to the build-up of (VFAs) and a drop in pH, thereby inhibiting the biogas production rate and possibly causes the anaerobic digestion (AD) system to collapse.

2.16 Review on foaming and causes.

In bioprocessing, foaming is a common problem, particularly in agitated and aerated bioreactors. The foam on the sludge surface is defined as a collection of gas bubbles surrounded by a liquid film [189]. Table 2-12 depicts classification of foam. Also, foam can occur in many anaerobic digestion digesters, which can have significant effects on the process and result in significant economic costs. Figure 2-31 depicts foam through a microscope and in a biogas, digester indicating severe problem of form in a big digester plant.

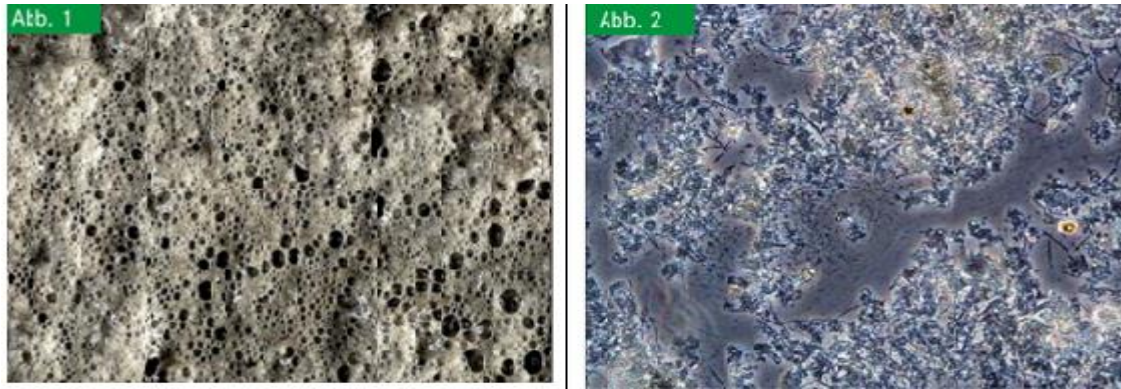


Figure 2.30 Foam images (Abb1) from a biogas digester (Abb2) from a microscope. Foaming causes various problems, such as a reduction in biomethane production and a reduction in organic matter degradation [190]. Table 2-13 details the problems caused by foaming in anaerobic fermentation. Low foam concentrations can create a condition that promotes cell damage, potentially leading to more damage. Foaming seems to be triggered by a variety of factors, including:

- ❖ Hydrophobic substances, poor mixing, or acetic acid accumulation [191].
- ❖ Excess filamentous bacteria such as *Gordonia* and *Microthrix* [192].
- ❖ Feed sludge composition and inconsistency of digester feed [193].
- ❖ Substrates rich in protein and easily degradable [194].
- ❖ Excess surface-active agents example oils and grease [192], [195].
- ❖ Unstable conditions caused by shock load or overloading [84], [194].
- ❖ Temperature fluctuation [196];
- ❖ Air entrainment and solids concentration [192].

Because the excess feedstock is not completely degraded by microorganisms in the digester, a high OLR can cause foaming, resulting in the accumulation of hydrophobic or surface-active by-products [189]. Many operational digesters have observed foam formation difficulties during start-up or when there is a low OLR followed by a rapid increase in OLR [197]. Table 2.14 depicts the severe effects of foaming in the anaerobic digestion process [198]. It has also been reported that enhanced mixing intensity, balanced distribution of nutrients and the addition of lime in the reactor can provide a solution to the problem of anaerobic reactor instability and the application

of antifoam products can mitigate the cause of foaming by hydrophobic discharge. This study does not focus on foam formation.

Table 2. 13 Foam classification

Source [198]

Type	Characteristics
True	Predominantly gaseous dispersion
Fluid	Predominantly liquid dispersion with enhanced holdup of gas in a large portion of the liquid
Unstable	Equilibrium state is continuously approached
Metastable	Progress to the equilibrium state is arrested
Transient	Lifetime of seconds
Persistent	Lifetime of hours or days if undisturbed

Table 2. 14 The physical effects of foaming in anaerobic digestion fermentation

Source: [198]

Physical Effects	<ul style="list-style-type: none"> • Increased heterogeneity of broth • Enhancement of gas-liquid oxygen transfer • Increased effective reactor volume • Reduction in the working volume • Enhanced gas holdup • Changes in air bubble size and composition • Decreased power dissipation • Changed pattern of dissolved gases due to heterogeneous dispersion • Reduction in apparent viscosity • Lower mass and heat transfer rates • Invalid process data due to interference at the electrodes • Decreased circulation rate • Incorrect monitoring and control • Reduction in aeration and mixing • Blockage of inlet and exit gas filters
Biological Effects	<ul style="list-style-type: none"> • Enrichment of cells in the stagnant liquid film around the air bubbles • Deposition of cells on upper parts of the bioreactor • Loss of culture fluid from exit lines causing product and biocatalyst loss • Microbial lysis • Changes in microbial metabolism due to nutrient limitations • Froth flotation and foam separation causing preferential removal of surface active agents • Protein denaturation in the foam layer • Problems in sterile operation • Risk of environmental contamination due to aerosol formation

2.17 Wide use process modelled of the anaerobic digestion

Anaerobic digestion model.No.1 (ADM1) is a mathematical model that simulates the behaviour of complex organic matter into simpler soluble molecules within the anaerobic digestion (AD) reactor. This model involved three dimensions such as:

❖ Processes

- ❖ Components and,
- ❖ Time.

Substrate input into the model is believed to be the composite particulate matter broken down into different feedstock components through the anaerobic digestion processes taking place within the reactor Figure (2.14). The reaction within the AD system is complex with some parallel steps and sequential steps. Therefore, mass conservation is applied to the model. The conversion processes that occur in an anaerobic digestion system are categorized into two main processes known as biochemical and physical-chemical processes Figure (2.14) [8], [40].

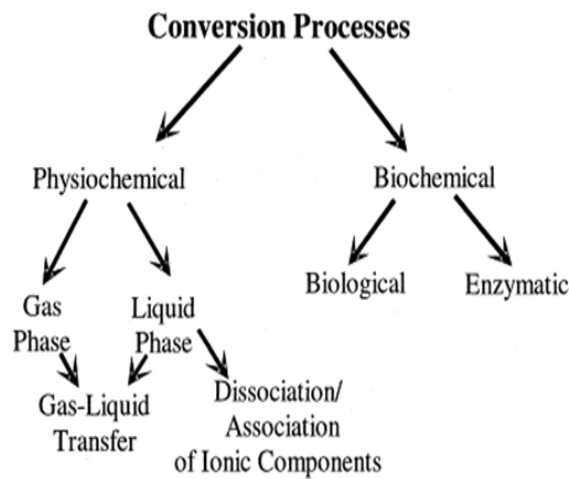


Figure 2.31 Conversion processes of the physiochemical and biochemical in an anaerobic digestion digester

Source:[199]

The Biochemical reactions involved the four steps of the anaerobic digestion (AD) process when the biodegradable fraction disintegrates into carbohydrates, proteins, and lipids, which becomes hydrolysed resulting in biomass growth and subsequent decay. The first-order kinetic equation representing hydrolysis describes the disintegration, hydrolysis, and the rate of decay of bacteria. The Physico-chemical reactions are not biologically mediated by organisms but occur in the water system spontaneously Figure (2.15). Some of the physicochemical reaction that takes place in anaerobic reactors includes:

- ❖ Liquid-liquid reactions (i.e., ion association/dissociation of weak acids and bases such as carbon dioxide, ammonia organic acids occurring rapidly)
- ❖ Gas-liquid exchanges (i.e. Gas transfer of carbon dioxide, methane, hydrogen sulfide and hydrogen occurring from rapid to medium process).
- ❖ Metal-ion precipitation (i.e., to form solid precipitates occurring from medium to slow process). The physicochemical processes are very significant in the modelling of an AD system because:
 - ❖ The pH control setpoint is calculated from the physicochemical state rather than the addition of chemical treatments such as strong acids or base which can result in a higher cost to real practice.
 - ❖ The correct estimation of the physicochemical transformations enhanced the key performance variables like the gas flow and carbonate alkalinity.
 - ❖ Different biological inhibitions may be expressed as free acids, bases and pH and dissolved gas concentrations [30]. In this thesis, the ADM1 model is intended to assess the performance of particle size distribution and its effects on the kinetics and biogas production rate.

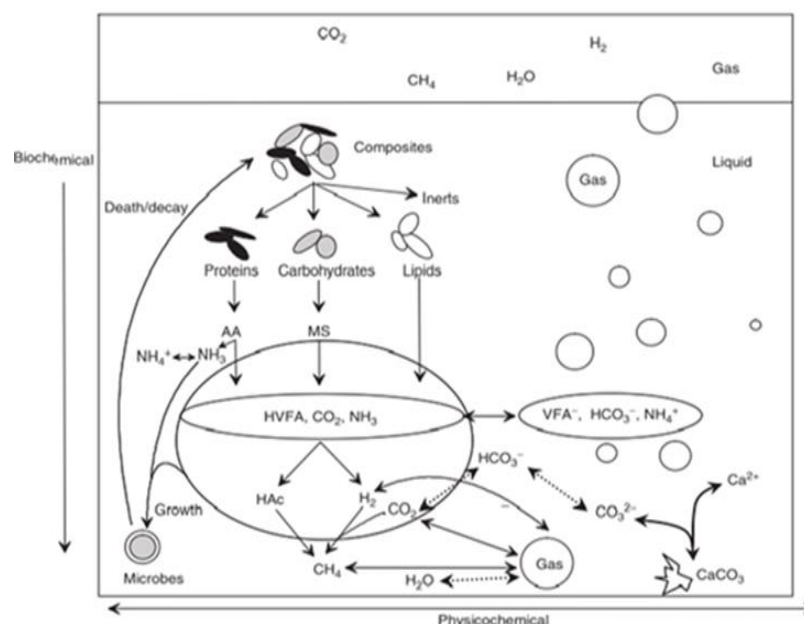


Figure 2.32 Biochemical (vertical) and biochemical processes(horizontal) in an anaerobic digester

Source: [30]

VFA- dissociated organic acids
HAc, acetic acid
AA, amino acids.
HVFA, associated organic acids
Ac-, acetate
MS, monosaccharides

In anaerobic digesters the biochemical and physicochemical reaction systems are strongly connected through the following mechanisms:

- a. Biochemical reactions produce weak acids and bases, including long-chain fatty acids (LCFAs), ammonia NH_3 , organic acids and carbon dioxide. Gasses are produced by biochemical reactions.
- b. Gasses produced by biochemical reactions.
- c. Biological activity is restrained through a disturbance of homeostasis and denaturing of enzymes when the pH value is low, though with some specialized organisms that can still work in extreme conditions, e.g., methanogenesis bacteria.
- d. The Formation of many weak acids and bases such as organic acids, ammonia, and hydrogen sulphide, is inhibitory to organisms [8], [30]. This means that both parent compounds such as sulphides, inorganic nitrogen, etc. and the pH effect in determining the concentration of the inhibited form like hydrogen sulphide and ammonia.
- e. Both weak acids and bases buffer around their characteristic acidity coefficient; this implies that bicarbonate, specifically, opposes pH changes around 6.3, since that is its peak.

However, the anaerobic digestion model No.1. (ADM1) has been widely used by many researchers to simulate different AD systems. A task group developed as the model was adopted for the International Water Association (IWA Task Group) for mathematical modelling of anaerobic digestion processes, and it was published in the year 2002 [[8]. Many researchers have focused on updates and modifications of the model since then.

2.18 Review of the particle size base degradation process model

A mathematical model was used to predict how PS would affect the anaerobic digestion (AD) of a complex organic substrate [174], [176], [200], [201]. The kinetics constant of the surface-based disintegration process was estimated using the model [174], which was replicated by [24], [200]. Many authors have described the hydrolysis stage using first order kinetics and biodegradable substrate at constant temperature and pH [174], [202]. First order kinetics occurs when the substrate is soluble, as described in ADM1 by [8]. Eastman and Ferguson [32] proposed equation 3.1, which depicts an empirical relationship in which different KH can be determined by changes in the PSD of the biomass substrate even when other reactor conditions and substrate type are held constant [173], [203]. Many studies (e.g., Vavilin et al, Esposito et al; Hobson [26], [174], [204] have explored the hydrolysis process to develop a deterministic model for anaerobic hydrolysis. Bacteria completely cover the substrate particles during the hydrolysis stage and secrete hydrolytic exoenzymes. Because the model assumes an abundance of hydrolytic enzymes, the hydrolysis rate per unit area of substrate readily accessible for hydrolysis becomes constant. Unlike the empirical model, which can determine different hydrolysis constants based on changes in the PS of the substrate, the hydrolysis constant in this model is unaffected by the PS of the substrate. As a result, Sanders et al. [174] refer to the model as the Surface-Based Kinetics (SBK).

$$\frac{dM}{dt} = -K_{sbk} \cdot A \quad (2.6)$$

Where;

M = mass of substrate (kg)

T = time (days)

K_{sbk} = surface-based hydrolysis constant (kg/m² day)

A = surface area available for hydrolysis [m²]

Additionally, the proposed mathematical model is based on the differential mass balance equations for the substrate. In the study, a PSD-based degradation model is presented that uses a surface-based kinetics model for spherical particles in batch and semi-continuous digestion to explain changes in PSD of substrates over time.

The calculation of the PSD model is based on the mass fraction of a pig slurry from literature data. The proposed model is explained in chapter six using completely mixed state variables that account for both degradation and methane production.

2.19 Evaluation of the BMP Test

A substrate's ability to degrade under anaerobic conditions is determined by the biochemical Methane Potential (BMP) assay, which measures cumulative methane production during the test [205], [206]. The fundamental concept involves using a seed sludge (anaerobic bacteria) inoculum to degrade an organic concentration. Anaerobic digestibility and potential biogas (methane) production from biomass substrates, among other pertinent data, can be determined by this measurement, which is helpful for assessing, planning, and optimising the anaerobic digestion (AD) process [207]. BMP test can be used to measure not only how much organic material is converted to methane (CH₄) as well as how much of the remaining organic substance is still susceptible to anaerobic treatment, how much of it is non-biodegradable after test, and how effective anaerobic digestion may be for a given substrate [86]. Standards for the methods and measurement units used in BMP tests were created by [208]. The substrate and its characteristics, substrate particle size, inoculum and its activity, nutrients/micronutrients/vitamins, and mixing are crucial factors to consider when conducting a BMP test. A typical basic medium used in the test is also described in these guidelines. The BMP produced methane yields of 0.20 m³ kg⁻¹ VS for MSW and 0.21 m³ kg⁻¹ VS for yard waste, while paper waste ranged between 0.08 and 0.37 m³ kg⁻¹ VS for different classes of paper, according to [209], who tested the BMP for MSW and some of its components. However, this thesis utilised the bioprocess reactor due to its advantages over the conventional BMP Trial (BPC 2009) [210]. These reactors were chosen based on the following criteria:

- ❖ It has low and simple maintenance.
- ❖ The computerized explanatory technique, thus reducing the workload.
- ❖ It is a real-time, temperature and pressure compensation for biogas flow and volume measurement.

- ❖ It has a constant time for logging data of accumulated flow rate and biogas volume.
- ❖ It can assist the scientific analyst to understand that the generated biogas content will be periodically measured,
- ❖ thus, making it possible to acquire satisfactory data to completely understand degradation dynamics.
- ❖ It enables the researcher to have a high level of data for extracting the kinetics information.
- ❖ The period of incubation is long, and this will significantly reduce the time and labour demand for performing the analysis.

On the other hand, is effective to achieve the experimental accuracy of methane production. An automatic methane potential test system used in this study measure the produced biogas in real time. This is done by feeding easily biodegradable organic complex waste (feedstock) into the AD reactor, where it is converted to methane during the process. This system is made of three main components known as:

- ❖ The incubation unit (reactor)
- ❖ Scrubbers
- ❖ The gas flow meter and the PC

The AMPTS II system has been configured to simultaneously conduct 15 analyses. The incubation unit is a 15*0.5 litre Each of the reactors incubation unit is stirred by a moulder with mechanical stirring to ensure efficient and gentle mixing of the substrate biomass and inoculum fed into the reactor The reactor is completely sealed by a gas line, biogas is continually produced and the biogas produced in the reactor passes through tubing into a corresponding scrubbing reactor .The scrubbers are where the biogas from the reactor flows into and where CO₂ is removed during anaerobic digestion (AD) allowing the biogas drained goes into the gas flow meters. The gas flow meter is where the methane that is drained from the scrubbers goes into and where the gas volume is measured, the gas flow meter is made up of 15 cells, each connected to each channel of the flow meter, one to each reactor

connected by tubing whereas the PC is used to monitor real-time data logging of accumulated methane volume and flow rate. The data were recorded by the data acquisition system.

2.20 Findings from Literature Review

The following study findings are listed as being among the most intriguing and under-explored areas: A case study could provide a significant contribution to the body of knowledge.

- ❖ Pre-treatment in the form of size reduction of anaerobic feedstock particles affects the biogas production of AD systems.
- ❖ Particle size distribution affects the performance of the AD system.
- ❖ There are other characteristics other than mean size particle that play a key role. In methane production
- ❖ The change in the generation of biogas from various particle size distributions (PSD) may not be significant across most substrates.
- ❖ A balance of particle size distribution (PSD) and organic loading is critical to avoid system failure from acidification.
- ❖ Several operational factors could influence the observed increase or changes in the biogas yield resulting from substrate pre-treatment in the form of particle size reduction.

2.21 Knowledge gaps and possible ideas for improving biogas production of the anaerobic digesters and improving the system's performance.

Even though there is interest in the advancement of this technology, there hasn't been much discussion in the following area: Therefore, by exploring these limitations, a study in this field could contribute in a useful way to the body of knowledge.

- ❖ There is a limited study on the effects of various mechanical size reduction methods on the performance of AD systems.
- ❖ There is a limited study on the effects of various PS reduction methods on biogas production of AD systems.
- ❖ There is a limited knowledge of the effects of mechanical size-reduction equipment on particle size and PSD.
- ❖ There is a limited study on the effect of the optimal particle size of substrates that would give the best biogas production.
- ❖ A study of the effect of the co-digestion of various mechanical pre-treated substrates on the AD system kinetics is necessary.

2.22 Conclusion of a review of the literature

In earlier chapter (one), we have discussed that energy exists in many forms including electromagnetic, nuclear, chemical, thermal, mechanical. Bulk of the world's energy consumption comes from fossil fuels. Risks related to resource depletion and the greenhouse gas effect come with an overreliance on fossil fuels mostly from developing countries. Majority of people in developing countries do not have access to electricity, thus depend on firewood to meet basic energy needs [211]. Cooking with firewood causes air pollution problem, rapid depletion of forest, and health problems. The biogas technology undoubtedly can assist developing nations in enhancing their ability to access clean energy. Therefore, this research work came into 3 underlying assumptions:

- 1) Fossil fuel technology represents risk such as depletion of resources and greenhouse gas effect, but it is also true the biogas technology is a feasible option.
- 2) Biogas technology have the potential opportunities to promote social, economic, and human growth and easy to operate on a very small scale, simple designs, and low cost of capital and suitable for remotes, urban and rural areas.
- 3) A scientific approach: provide a theoretical based experimental methodology to study this potential under qualitative and quantitative method.

An analysis of the literature, however, concentrated on anaerobic digestion and particle size (PS), which is thought to optimise the anaerobic digestion process. In Chapter 2, the current understanding of the relationship between AD particle size and mechanical treatment processes and mechanical reduction systems is reviewed. Emphasis was made on knowledge gaps to highlight limitations and potential research areas. Only a few studies have been done in relation to different mechanical size reduction techniques on the performance of AD systems and how different particle (PS) reduction methods affect biogas output. There has also been little research on how substrate particle size affects the production of biogas. A significant portion of the current body of knowledge can be discovered in the studies is from [20], [24], [88], [121], [159]–[162], [164], [173]–[175], [178], [179], [181], [183], [200], [212]–[217]. Additionally, it has been shown that mechanical pre-treatment accelerated the rate of microbial metabolism of complex waste. The production of methane can then be increased by mechanical pre-treatment after anaerobic digestion [20]. Particle size distribution (PSD), or the distribution of particles over distinct size ranges, in pre-treated organic substrate is relatively unknown, even though it is generally recognised that particle size reduction affects the efficacy of anaerobic digestion. Thus, the outcome of the operation can be determined by how well the particle size reduction equipment is matched to the kind of bioreactor. Therefore, it is vital to explore the various mechanical equipment that are used in the reduction of feedstock and to look at various particle sizes distribution of the substrate fed into the digester to have a better understanding of the particle size of the feedstock and how they affect the efficacy of the AD process.

3 Materials and Methods

3.1 Feedstock and Inoculum

Four waste biomasses are used in this investigation, namely (i) paper waste was collected from the University of Sheffield Energy Group Offices. (ii) Banana peel is collected from households (iii) grasses are obtained from the University of Sheffield and tomato waste obtained from the moor market in Sheffield. The feedstock is source-separated from three selected routes. After a sufficient sample has been collected (20kg), the raw waste is screened to remove any contaminants (if any), and then homogenised for characterisation and further size reduction. Also, anaerobic fresh active digestate was also collected from the existing mesophilic AD energy plant at Blackburn Meadows (BbM) wastewater treatment works (WwTW). Before using fresh active digestate from mesophilic digesters, the active digestate was filtered with a 1mm mesh sieve to remove solid materials for batch or semi-continuous testing.

3.2 Feedstock preparation and mixing

3.2.1 Feedstock particle size comminution

Using an analytical weighing balance, a quantity of the respective waste feedstock was measured and divided into three (4) equal parts. Each biomass type is subject to four particle size methods which begin with a coarse chopping/shredding operation (PTL1), a finer chopping operation (PTL2) and a maceration/mincing operation (PTL3) as per the process is shown in figure 3.1 and table 3.1 which depicts the nomenclature for each biomass size reduction, with differences in pre-treatment Levels, include processing time, and reduction mechanisms. However, pre-treatment 2 (PTL2) involved passing 3/4 of the waste through a Mincer Ring RAUT 12 16#, For 2 minutes, pre-treatment level 3 (PLT 3) involved passing the 2/3 parts of the waste through a food processor with a cut 5200 (Grinder for 3 minutes). Pre-treatment level 4 (PTL4) involved passing the third part of the feedstock through

a Mincer Ring # 12 6mm and then through a Grinder (5200) for 5 minutes, respectively. The feedstock was stored at 5°C before the experiment. Each fraction is characterised by its particle size distribution by the most relevant method. However, the generation of biogas yield depends upon the type of feedstock utilized.

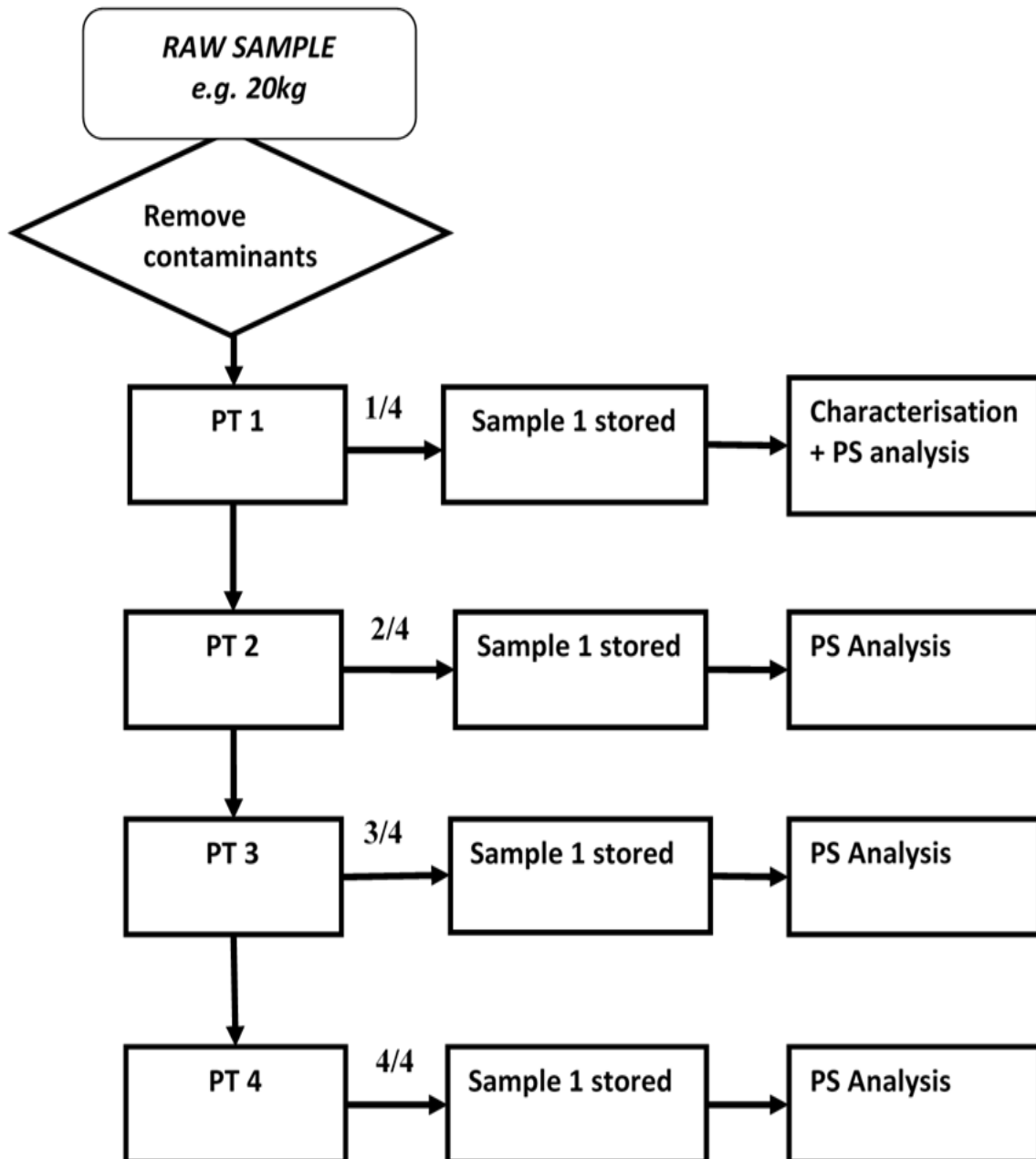


Figure 3.1 Schematic of the sample preparation methodology

Table 3. 1 Nomenclature of the pre-treatment of each biomass

Biomass Type	Units	Quantity	Water (H ₂ O) addition (g)	Pre-treatment (PT) level					
				1	2		3		4
Paper waste	kg	5	3	Shredded	PW1-3 passed through a mincer for 2mins	Divided into three equal parts	Part 2 -3 PW2 slurried with water and 3min in food processor	Divided into two equal parts	Part 3 PW3 slurried with water and 5min in food processor and in mincer
Banana peel	kg	8	-	Manual chopping	BPW1-3 passed through a mincer for 2mins	Divided into three equal parts	Part 2 -3 BPW3 in food processor 3minutes	Divided into two equal parts	Part 3 BPW3 slurried with water and 5min in food processor and in mincer
Grass waste	kg	6	-	As collected	GW1-3 passed through a mincer for 2mins	Divided into three equal parts	Part 2 -3 GW2 slurred with water and 3 min in food processor	Divided into two equal parts	Part 3 GW3 slurried with water and 5min in food processor and in mincer
Tomato waste	kg	6	-	As collected	TW1-3 passed through a mincer for 2mins	Divided into three equal parts	Part 2 -3 TW2 slurred with water and 3 min in food processor	Divided into two equal parts	Part 3 TW3 slurried with water and 5min in food processor and in mincer

3.3 Analytical parameters measured in this study for substrate digestion and digestate

Table 3.2 shows the parameters examined in this study for feedstock physicochemical and biological composition, such as total solids (TS) and volatile solids (VS), pH, alkalinity, and elementary analysis, biogas composition, and volume. The total solid (TS) and volatile solid (VS) contents of the digester's liquid digestate were determined. pH and alkalinity analysis were used to determine the digestate's stability. Methane and CO₂ levels in biogas were measured. The study's reagents were purchased from the fisher Scientific" (Loughborough United Kingdom). The chemical is graded on a laboratory scale, unless otherwise specified.

Table 3. 2 Analysed experimental testing parameters

Parameter	Substrate	Methane	Digestate
PS	○	-	-
TS/VS	○	-	○
CHNS	○	-	-
BMP	○	-	-
pH	-	-	○
Alkalinity (PA, IA, TA)	-	-	○
Biogas composition	-	○	-
Methane volume	-	○	-
○ measure - Not measure			

3.4 Preparation of the reagents and indicator

CO₂- fixation: 3 mol of NaOH solution was prepared by dissolving 240g of the substance in 1.5 litres of distilled water and making the solution to 2 litres using distilled water. The experiment was performed in a fume cupboard due to the heat generated. 10ml of 0.4% Thymolphthalein-pH indicator was mixed with 2 litres of the 3 mol NaOH solutions. 80ml of the mixture containing NaOH solution

and Thymolphthalein pH indicator was transferred to each of fifteen 100ml glass bottles.

3.4.1 pH

The pH of the sample's biomass is measured using a pH probe meter Omega PHH-37 with Omega PHE 1335 probe. Before the use of the pH meter, Buffer solutions used for calibration were (pH 4.01, 7.00 and 10.1). Deionised water (H₂O) was poured into two beakers of about 200ml each and this was used to rinse the pH probe. Equally the beakers were emptied and refilled for a rinse of the probe meter. This was done during the time of measurements and at the end of the measurement. The measurement of the pH was taken immediately the biomass samples are taken out of the reactor to avoid the samples volatiles being evaporated or the evolution of dissolved carbon dioxide (CO₂), thereby, keeping the reading accurate without alteration. During the P^H measurement substrate, biomass samples were well stirred to ensure the samples are properly homogenized before the pH measurement. The pH meter accuracy was ± 0.03 and a resolution of 0.01, but according to the standard method of water and wastewater 4500-H⁺ [218] on the normal basis, the accuracy of the PH meter is ± 0.1 pH.

3.4.2 Preparation, determination of total solid TS and volatile solid VS

After the sample had been properly homogenised, the anaerobic fresh active digestate and substrate were determined for total solid (TS) and volatile solids (VS) measurements. While the fresh active digestate is poured into the crucible, a portion of the well-mixed biomass sample is transferred to the weighted empty crucibles with a spatula, and the weight of the wet samples plus the empty crucible weight is weighed again and data is recorded. The biomass sample is then dried in an oven at 105^oC for 24 hours. After cooling for about an hour in a desiccator, the biomass sample is weighed to the nearest sensitivity of 0.1mg. The biomass samples are then transferred with a stainless-steel tong into the box furnace (Elite thermal BSF12/10A box furnace with temperature control of 3216i)

heated at 550^oC for two hours. However, the tongs are used to transfer the washing sample to a desiccator, which is then allowed to cool to room temperature before weighing it again to the nearest sensitivity of 0.1mg using the same weight balance and recording the results. The measurement was done using standard methods 2540G [218]. The unit measurement was (g). However, after each set of the analysed sample of the fresh active digestate and substrate, detergent [virkon solution (1%)] is used to wash the crucible, and the crucible is then rinsed with deionised water. The crucible is then placed in an oven for further analysis by laboratory users. Total solids (TS) and volatile solids (VS) were determined using equations 3.1-3.3

$$\% \text{ Total solid (TS)} = \frac{w_3 - w_1}{w_2 - w_1} \quad (3.1)$$

$$\% \text{ Volatile solids (VS)} = \frac{w_3 - w_4}{w_2 - w_1} \quad (3.2)$$

$$\% \text{ (VS based on total solids)} = \frac{w_3 - w_4}{w_3 - w_1} \quad (3.3)$$

Where:

W₁ is the empty weight of the crucible measured in (g)

W₂ is the measured weight of the crucible with a fresh active digestate, or substrate measured in (g)

W₃ is the substrate or digestate sample weight after drying in an oven at 105^oC measured in (g)

W₄ is the measured weight of the crucible and a wet sample weight after the heating at 550^oC measured in (g)

3.4.3 The alkalinity of the biomass sample

Standard method 2320 B was used to determine the alkalinity of liquid digestate samples [218]. Prior to analysis, the digestate sample was sieved to ensure homogeneity. 5ml of the liquid digestate was mixed into 50ml of deionized water. The pH of the digestate sample was determined using a 0.25N sulphuric acid solution. Magnetic stirring was used to ensure no fouling was observed while using the pH probe. To avoid cross-contamination of the samples, the pH probe

was calibrated at the start of the titration with a buffer solution, and deionised water was used to rinse the pH probe between measurement intervals. The three alkalinity ratio measures considered by [219] (PA, IA, and TA) were used for the analysis, which is given in table 3.3 based on the initial pH and pH endpoints. The liquid digestate sample was titrated as mg CaCO₃l⁻¹ using an automatic digital S1 analytics titroline 5000 titrator.

Table 3. 3 Alkalinity Definition

Source: [15]

Type of Alkalinity	Definition	Initial pH	Endpoint pH
PA	buffer of bicarbonate	pH of sample	5.7
IA	buffer of Volatile fatty acid (VFA)	5.7	4.3
TA		pH of sample	4

Alkalinity was calculated according to mg CaCO₃l⁻¹ =

$$\text{Partial Alkalinity (PA)} = \frac{A_{5.7} \times N \times 50000}{V_{\text{substrate}}} \quad (3.4)$$

$$\text{Total Alkalinity (TA)} = \frac{(V_{4.0} \times V_{4.3} \times V_{5.7}) \times N \times 50000}{V_{\text{substrate}}} \quad (3.5)$$

$$\text{Intermediate Alkalinity (IA)} = \frac{B_{5.7} \times N \times 50000}{V_{\text{substrate}}} \quad (3.6)$$

Where:

A represent the volume of H₂SO₄ added in mL to attain the end point

Intermediate endpoint pH 5.7.

B represent the volume of H₂SO₄ added in mL to attain the ultimate endpoint pH 4.3

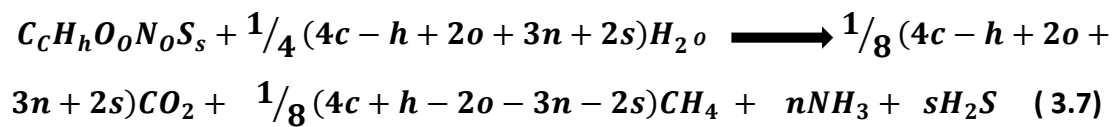
N is the titrant's normality, H₂SO₄.

V represents the sample volume in ml.

From equation 3.4 to 3.6, it indicates the titrant volume used to the endpoint point of analysis is 4.0.4.3 and 5.7 ml, respectively.

3.5 Estimation of theoretical maximum methane production

The basic substrate biomass that can be digested are carbohydrates, proteins, and lipids. The composition of the feedstock has an impact on the relative amounts of methane and carbon dioxide in biogas, which has an impact on energy production [220]. Maximum methane production requires a 25:1 ratio of carbon to nitrogen. When a known mass of volatile solid (VS) is broken down by anaerobic digestion, the amount of water used and the amount of methane and carbon dioxide produced can be calculated using the Buswell equation [221],



Several methods can be used to calculate the calorific value (CV) of biomass or solid waste. The basis for this should be their physical composition, proximate analysis, or ultimate analysis/elemental content (C, N, H, S, O) [222]–[225]. Additionally, it has been noted by various studies that calculating calorific Value (CV) of biomass by using the elemental composition or ultimate analysis gave the highest validity and was overall more precise than other methods. [225], [226]. Therefore, in this study, the theoretical calorific value (CV) of four substrate biomass samples—BPWSB, GWSB, PWSB, and TWSB—was determined using Dulong equation 3.8 and 3.9. Using this value, the potential energy content from AD of four biomass can then be calculated.

$$HHV = (337C + 1419(H - 1419O/8) + 93S + 23.26N) \quad (3.8)$$

$$TCV = (34.1C + 102H + 6.3N + 19.1S - 9.85O)/100 \quad (3.9)$$

3.6 Composition of elements (CHNS)

A sample that had been weighed (1.8–2.2 mg) and crushed to remove air inclusions was sealed in tin foil. The Vario Micro Cube's CHNS analysis mode was used for this. The results were corrected for blanks. A daily factor correction is provided by running sulfanilamide standards (x3) every 12 samples. The measures followed are in accordance with the manufacturer's instructions.

3.7 Experimental procedure

3.7.1 Sample preparation and anaerobic condition employed for BMP testing and methane production.

The samples were kept in a freezer at 4°C. Prior to starting the BMP tests, the fully automated methane potential test system (AMPTS II) and software were configured as described in the bioprocess manual. Table 3.4 provides a description of the digesters that were used for the semi-continuous test. A 3M NaOH solution was prepared in the fume cupboard. The chemical mixtures (3M NaOH and pH indicator thymolphthalein) were carried out in accordance with the manufacturer's instructions, taking all necessary precautions. Table 3.5 shows the batch test conditions used in this study is to promote degradation/ultimate rate of methane (CH₄) production and characteristic kinetics during anaerobic material preparation.

Table 3. 4 Summary of the experimental methodology of the continuous stirred tank reactor (CSTR)

	SET1(R1+2)	SET1(R3+4)	SET1(R5+6)
PT Levels	PT4	PT4	PT4
Substrate	GWSB	BPWSB	PWSB
	SET2(R1+2)	SET2(R3+4)	SET2(R5+6)
PT Levels	PT3	PT3	PT3
Substrate	GWSB	BPWSB	PWSB
	SET2(R1+2)	SET2(R3+4)	SET2(R5+6)
PT Levels	PT2	PT2	PT2
Substrate	GWSB	BPWSB	PWSB
Reactors numbers	6 (2 duplicates)		
Feed	Wet Substrate waste biomass (WSWB)		
Organic loading rate (OLR)	3gVS wet/day		
Reactor size and size	2000ml CSTR		
Allowed headspace	300ml		
HRT	20 each PT level		
Fed per day	1 time daily		
Interval of feed	24hh:mm		
Mixing	Mechanical stirring		
Inoculum	Fresh active digestate		
Reactor temperature	38°C		
Operation of feed	Semi -continuous (Manual)		

Table 3. 5 Batch testing employed condition.

Conditions employ BMP testing	Freshly active digestate (Inoculum)	To maintain active anaerobic bacteria and promote CH ₄ production rate
	Mesophilic Conditions 38°C	For high methanogenic microbial activity
	Short hydraulic retention time	Average of 15 to 30days is required to treat waste
	Mechanical stirring	To ensure a very good mixture of the inoculum and biomass substrate
	Large inoculum to substrate ratio 3:1 (VS basis)	To enhance the methane (CH ₄) production rate
	Automated incubation unit 15 x0.5 with the headspace of 100ml	15 incubation units are analysed the same time

3.7.2 Leak test

A leak test was performed for each of the reactors by creating some overpressure (Figure 3.3). This was done by blocking one of the metal tubing ports and the air was injected through the remaining port and the reactor was immersed in water and monitored if any air bubbles would escape from the reactors. The Thermostatic water bath was switched on and set at 38°C. The gas volume measuring device was flushed with methane calibration gas at 5l/min for 60 seconds to create the anaerobic condition. Connections to the computer software were completed following the AMPTS II manual.



Figure 3.2 Leak testing of batch reactor

3.8 Batch testing set-up and monitoring

This experiment relates to Objectives 1 and 2 of Chapter 1. The obtained results allow for an assessment of the impact of particle size distribution on the AD process kinetics and the overall biodegradability/ultimate methane potential of the system, allowing recommendations on the optimal pre-treatment level. The experiment entails performing BMP tests on each of the biomass samples that have been characterised for particle size distribution as described in chapter 4. The methodology for the test is as follows: The four substrates described in section 3.2 were tested for biomethane potential (BMP) using BMP equipment (Bioprocess Control, AMPTS II, Sweden, 2009). Up to 10 L of anaerobic digestate inoculum was obtained from a mesophilic digestion plant at the start of the BMP test (section 3.6). After collection, the inoculum was immediately filtered to ensure homogeneity. It was immediately measure to 15 test bottles. Each bottle received the correct amount of feed and inoculum. First, the inoculum's weight

was measured, and data was recorded. Second, the substrate was weighed and put in a glass bottle containing the weighted inoculum. 400g of inoculum and substrate were added to a 500ml reactor bottle at a VS inoculum to substrate ratio of 3:1 by weight. This was done to avoid anaerobic digester failure and foaming, as well as to optimise methane during the test. For biogas collection, a headspace of 100 mL was allowed in each reactor. The BMP test was run in triplicate for statistical purposes (variation in the results). The substrate's % VS was also determined (section 3.4.3). Simultaneously, using a known biogas potential, blank samples containing only inoculum and control samples containing only cellulose and inoculum were set up. The bottle lid properly and quickly placed in an incubation unit and connected to a jar in the carbon-dioxide absorption unit via Tygon gas tubing, which was then connected to the biogas flow cell array via Tygon gas tubing. The incubation unit was set to 38°C. Water was used to keep the reactors and contents at the desired temperature. For each substrate and pre-treatment level (PTL), The headspace was deoxygenated by flushing it with synthetic biogas containing approximately 35% carbon-dioxide and 65% methane. For each fed bottle, the programme data logging software for methane production was started. The magnetic stirrer was turned on to complete the test settings, and the methane yield were recorded on the software. While the CO₂ binding capacity of the NaOH was monitored by a change in the colour of the Thymolphthalein pH indicator from blue to colourless. When the NaOH's binding capacity was reached, the old indicator bottle was replaced with a fresh NaOH solution. The pH was kept constant (between 7 - 7.3). After digestion, the volume of accumulated methane (CH₄) potential was calculated. The biochemical methane potential was computed using equation 4.

$$BMP = \frac{V_{substrate + Inoculum} - V_{inoculum}}{Substrate \text{ gram VS added}} \quad (3.6)$$

Where;

BMP = Biochemical methane potential is the normalized volume produced per gram VS of substrate added (Nml/gVS).

$V_{substrate} + Inoculum$: The accumulated volume produced from the reactor samples with both mixture of inoculum and substrate.

Vinoculum: The mean value of the accumulated volume produced by the blanks. The accumulated volume of methane (CH₄) produced is calculated per gVS of the substrate biomass fed into the reactors because the substrate added to the reactors has a gVS attribute. Each triplicate test produces a characteristic methane production curve over time, allowing assessment of (a) the ultimate biogas potential of the biomass substrate and (b) the characteristic kinetics. The experimental data is fitted to a standard first-order kinetics equation proposed by [31], which can be expressed as $\frac{dC}{dt} = kH \cdot C$ — — equation 5, yielding a first-order constant (K) that is then used to evaluate the effects of the pre-treatment. The experimental setups for BMP testing are depicted in Figure 3.3.

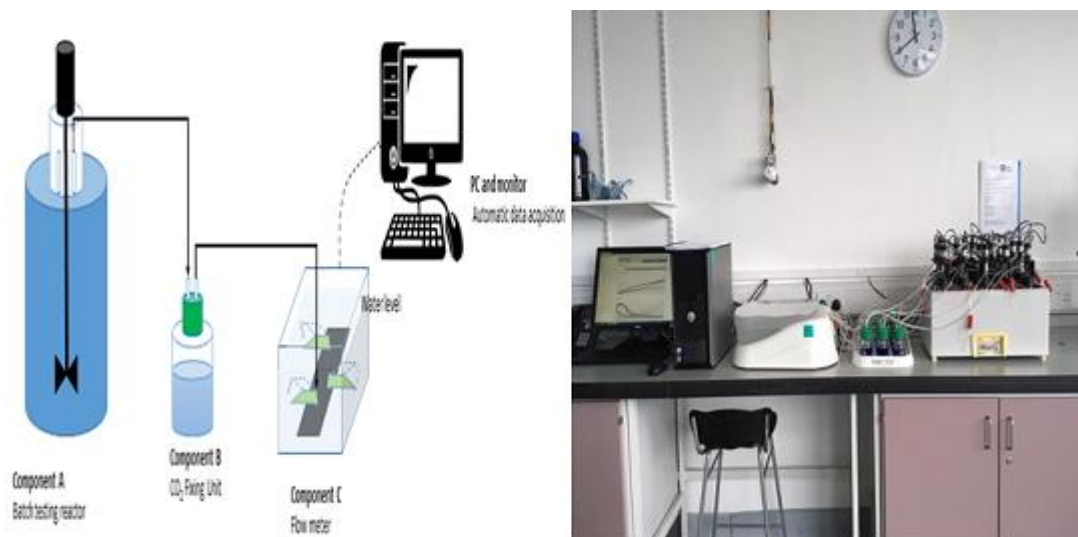


Figure 3.3 Experimental setups for BMP testing, stirred incubation unit in a water bath with NaOH as a scrubber and a volumetric gas flow meter multi-channel and software user interface.

3.9 Semi-continuous testing

This experiment relates to Chapter 1 objectives 3 and 4. The experiment determines the maximum biogas production rate of the system using various pre-treatment methods, as well as whether pre-treatment has any effect on stability,

production kinetics, and other factors. Different levels of pre-treatment of banana peel, grass waste, and paper waste are digested. R1-R6 digesters are seeded with fresh active digestate. The substrate was weighed and poured into a digester containing the seeded digestate in a 2000ml bottle with a head space of about 300ml. During the incubation period, alkalinity and pH are measured, and mixing is achieved with a mechanical stirrer. Prior to the start of the semi-continuous laboratory test, each reactor was subjected to a leak test by applying some overpressure. For statistical purposes, the test was carried out in duplicated for all substrates. The reactor has three major ports.

- ❖ A port used for the discharge of the digested sludge.
- ❖ A port used for feeding of the substrate (anaerobic feedstock).
- ❖ A port for the measurement of pH and temperature.

The inlet and outlet funnels are sealed off with a tubing clamp and two-way valves to create an anaerobic environment. The third port is closed with a screw connector without a hole because it is not used for pH measurement during the anaerobic degradation process. The system continuously produces and records biogas using the bioreactor software (BRS). The volume of released gas is measured using a multi-flow arrangement device. On a fifteen-minute rotatory timer, the desired time is set. Before the flow direction changes, time will pass. Each day, before feeding the substrate, anaerobic digestate and samples for analysis are removed. The digestate removed reduces the reactor's working volume from 2000mL to around 1700mL. It is done to reduce the risk of foam clogging the gas tubes during the degradation of the substrate biomass. Also, to reduce the risk of air entering the anaerobic reactor headspace, the substrate biomass was fed through a hydraulically sealed inlet. This was done to avoid increasing the percentage flow rate of methane (CH₄) production during each fed period by limiting the CO₂ concentration in the reactor. The experimental setup is shown in Figure 3.4.

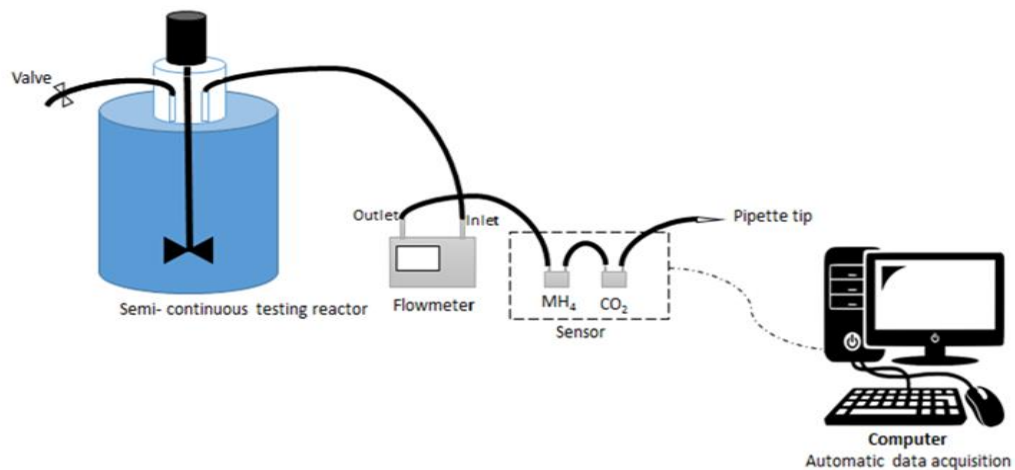


Figure 3.4 Experimental setups for semi continuous testing

3.9.1 Gas volumes for BMP assay and semi continuous testing

The volume of the gas was gauged using an ultra-low flow gas flowmeter (Flow, Bioprocess Control, Sweden). The flowmeter's precision was 1%, and its resolution was $10 \text{ mL} \pm 1 \text{ mL}$. The processing unit of the flowmeter used the flowmeter cell volume calibration value. The flowmeter adjusted the gas measurements automatically to $0 \text{ }^\circ\text{C}$ and 1 atm (STP).

3.10 Overview of Experimental set-up

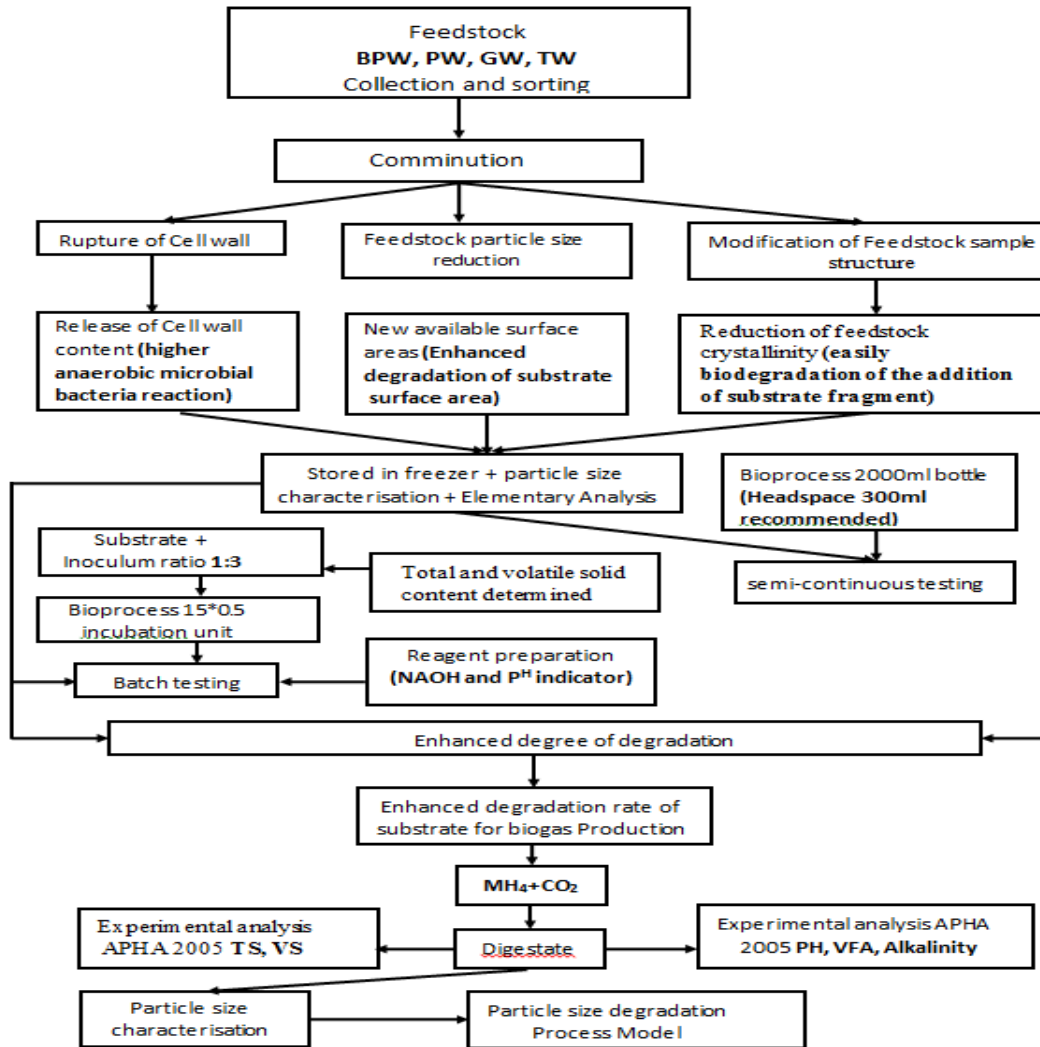


Figure 3.5 Overview methodology of batch and semi- continuous testing.

3.11 Particle size distribution determination

A representative of well-mixed substrate biomass sample (SBS) was dried, and many image was taken using the camera according to their individual substrate PTLs (1-4). ImageJ particle size analyser was used to analyses the image of individual sample PTLs. The tests were marked according to the contained samples and their degree of pre-treatment (1-4). About 4g per sample (1-4) was analysed in each sample pre-treatment level. A background colour was selected during processing to contrast with the particle(s)' colour. This has been done to

get a better contrast. ImageJ device calibration to separate the ImageJ output from both the inputs and the user platforms to determine the scale factor. This allows the representation of pixels to be transformed into a physical unit for measuring particle size (mm) [227], [228]. Initially, the original image colour became a grey (8 bit) image and then was binarily used to get the particle size reported by the ImageJ plugin known as the particle size analyser. In this research, the analytical procedure for the characterization of the particle size distribution using the ImageJ software is shown in figure 3.7. However, Origin-pro software 2022 was used in plotting the graph of the size distributions.

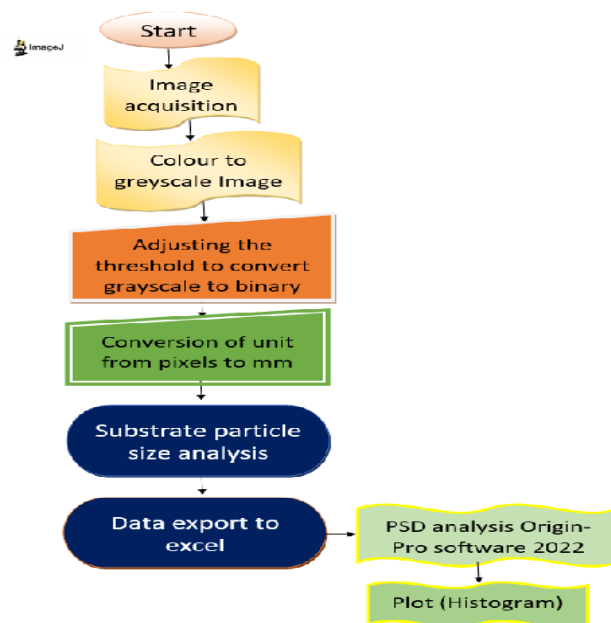


Figure 3.6 Process flow for characterising particle size distribution.

3.12 Conclusion

As part of the study, laboratory-scale experimental research was done using qualitative and quantitative methodology to explore the existing problems and achieve the goals outlined in session 1.4 to 1.4.2. The investigation includes batch and semi-continuous tests to determine the efficiency of four substrate biomass pre-treatment levels using various type of mechanical equipment to boost methane outputs.

Organic Particle Size Distribution Characterisation

4 Results and Discussion

This chapter presents the discoveries and results of the characterisation of the sample organic particle size distribution, used for batch testing and semi-continuous testing.

4.1 Organic Particle Size Distribution Characterisation

4.1.1 Choice of Substrate and Equipment

Four different feedstock wastes were chosen as the experimental feedstock because they are suitable for both rural and urban areas and are very much accessible. Because there has been little research on these four selected substrate feedstocks in the literature, the results of this experiment would add to the existing body of knowledge. This waste also includes agricultural and food waste (banana peel and tomato waste), garden waste (grass waste), and office waste (paper waste), which are low-cost and readily available waste feedstocks that are underutilised as potential methane production sources in both developed and developing countries. Few researchers [36], [173] have used this feedstock in previous studies, and it has the advantage of increasing biogas production after mechanical reductions. Because of the increased surface area available to extracellular enzymatic activity, the positive impact of reduction in particle size for feedstocks is most likely to occur from a faster hydrolysis process. Furthermore, three types of mechanical equipment were chosen:

- ❖ Inox Stainless Steel Electric Mincer
- ❖ Magimix 5200XL Premium Blender Mix Food Processor
- ❖ Paper Shredder PS1840 Product-SKU: SHRED102001

They were also chosen because they could emulate the type of common mechanical pre-treatment equipment used in AD plants, such as shredders and

macerators. This is because each waste fraction necessitates a different type of mechanical particle comminution equipment based on the following criteria:

- ❖ Waste physicochemical properties such as: inputs size distribution, moisture content of biomass, composition, durability, and ease of disintegration) (e.g., degree of shredding, maximum particle density).
- ❖ Required output specifications (e.g., degree of shredding, maximum particle density)
- ❖ operational characteristics such as energy needs, the necessity of continual well-equipped maintenance, ease of operation stability, noise production, and air and water pollution requirements.
- ❖ Problems of safety and safety systems (University Laboratory scale)
- ❖ Required speed.

4.2 Substrate Biomass Characterisation

As described in section 3.2.1 (Table 3.1), the material was prepared in large batches for each feedstock, enough to feed both the batch and semi-continuous test runs for the duration of the test. While a lot of effort was taken to preserve a consistent composition between each batch, certain variations are inevitable due to the addition of water to substrate biomass like paper, waste biomass during the mechanical breakdown. The results of the physicochemical analysis used to characterise four different substrate biomass are in shown in Table 4.1. This was carried out in duplicate for each of the substrate biomass. The analysis was carried out as described in sections 3.4.2 in Chapter 3.

Table 4. 1. Substrate biomass characterization

Biomass	Total solid (TS)%	Volatile solid (VS)%	Measured Inoculum		I/S ratio
The initial parameter of the measured at the start of experimental batch testing					
BPWSB	10.96 ±0.05	9.09±0.07	384		3:1
GWSB	23.38 ±0.01	18.34±0.01	384		
PWSB	23.2±0.2	20.33±0.11	380		
TWSB	10.34±0.06	7.18 ±2.78	381		
The final parameter of the Measured remaining at the end of batching testing.					
BPWSB	8.22±0.18	7.853±0.09			
GWSB	11.16±0.15	9.133±0.57			
PWSB	11.29±0.12	10.465±0.29			
TWSB	5.46±0.26	4.980±0.13			
	BPWSB	GWSB	PWSB	TWSB	
Inoculum VS	2.03	1.92	1.58	1.33	
Feedstock elemental composition					
	GWSB	PWSB	BPWSB	TWSB	
C	39.19	38.19	40.01	39.55	
H	5.8	5.57	5.82	5.65	
N	3.08	None - detected	1.43	2.04	
S	None – detected	None - detected	None-detected	None-detected	
C/N ratio	12.72	Carbon	28.04	19.39	

Table 4.4 also displays the C/N ratio for the four biomass that were chosen. The results of this study are consistent with the elemental composition values reported by [229] for the BPWSB. The optimum C/N ratio for the BPWSB is found to be 28.04% weight, which falls within the 20–30/1 range that is typically considered to be ideal for anaerobic digestion (AD) [95]. In contrast, tomatoes have a weight of 19.39%, which is slightly lower than values that have been reported in the literature) [95]. PWSB, on the other hand, has a carbon content of 38.19% weight and no nitrogen content was found.

4.3 Banana Waste Particle Size Distribution

The PSD results for Banana Peel Waste Substrate Biomass (BPWSB) which was subdivided into four pre-treatment levels are shown in Figures 4.1, 4.2, 4.3 and 4.4 respectively. The results are presented in the form of histograms with a curve of normal distribution and are reported together with the mean value and SD

shown in table 4.2. The photograph of each pre-treatment level is shown in appendix A1. The difference in the processing time of each pre-treatment level as well as the mechanical equipment employed, and their ring sizes (opening) used for each pre-treatment level as described in section 3.3 gave the difference in the size of the particles. PTL 1 is in the range of 0 to 14.5mm, followed by PTL 2 (0 to 8.5mm), PTL 3 (0 to 5.25) and PTL 4 (0 to 2.1mm) respectively. According to [230], the predominance of particles of less than 2 mm facilitates metabolic processes in AD, and when the proportion of these particles decreases, biodegradation slows down and blockage of pipes of reactor become imminent, as the larger particles from thick slurries. Considering the particle sizes of the BPWSB, in PTL 1, 40% of the particles ranged from 6 to 8mm, 25% are particles between 3 to 6 mm, those between 8 to 10mm are 16%, those <2mm were 14%, while the particles of 10 to 15mm diameter are <5%. In PTL 2, 60% of the particles are <3mm, as others ranging from 3 to 8.5mm 40%. Like PTL 2, smaller particles of size 0.5 to 2.5 mm were about 72% in PTL 3. In the last PTL for BPWSB, particles of 0.1 to 0.6mm were 87% while the other 13% were between 0.65 to 2.1mm in the biomass. From the results, it is observed that particles of PTL 2 and 3 and 4 were more biodegradable than those of PTL1. This is due to the predominance of smaller particles less than 3mm in them. This result agrees with postulations by other researchers that biodegradability and rates of methane production is a function of particle size. Pre-treatment of waste substrate biomass into smaller particles (not excessively fine particles) increases the surface areas of the feedstock and hence favours the AD process. The wet materials were folded, twisted, clumped, thin, and sticky together, and had an irregular shape. This makes size distribution classification for soft or easily biodegradable feedstock more difficult. Because the feedstock structure changes during mechanical breakdown, an observed highly irregular sample can become a bottleneck since separation attempts can easily alter the size distribution of the sample and can be time consuming. As a result, the mean particle size and distribution profile had shifted, as shown in table 4.2 and Figure 4.2 and 4.3, respectively.

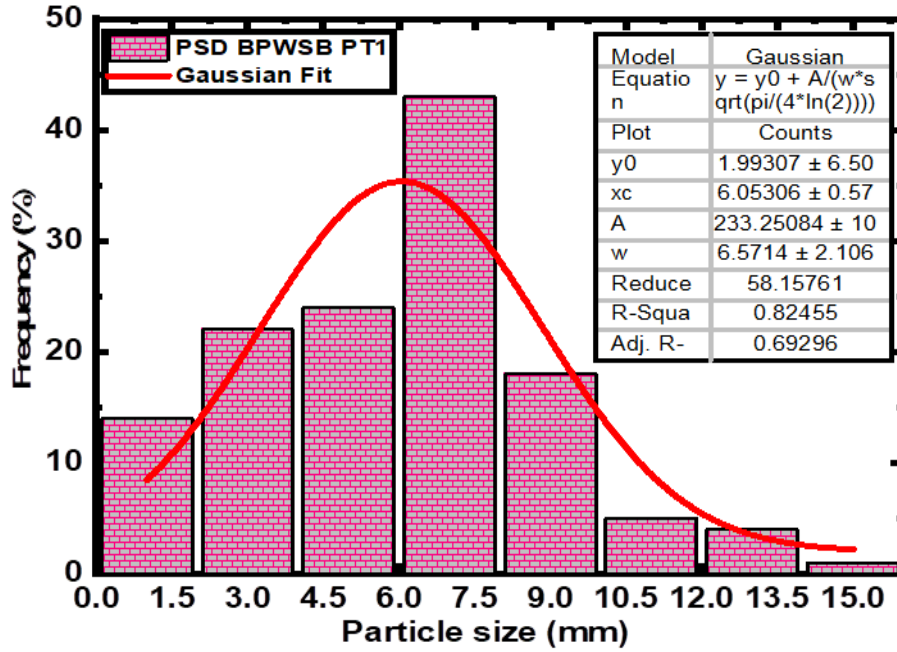


Figure 4.1 Particle size distribution of banana waste substrate biomass pre-treatment one.

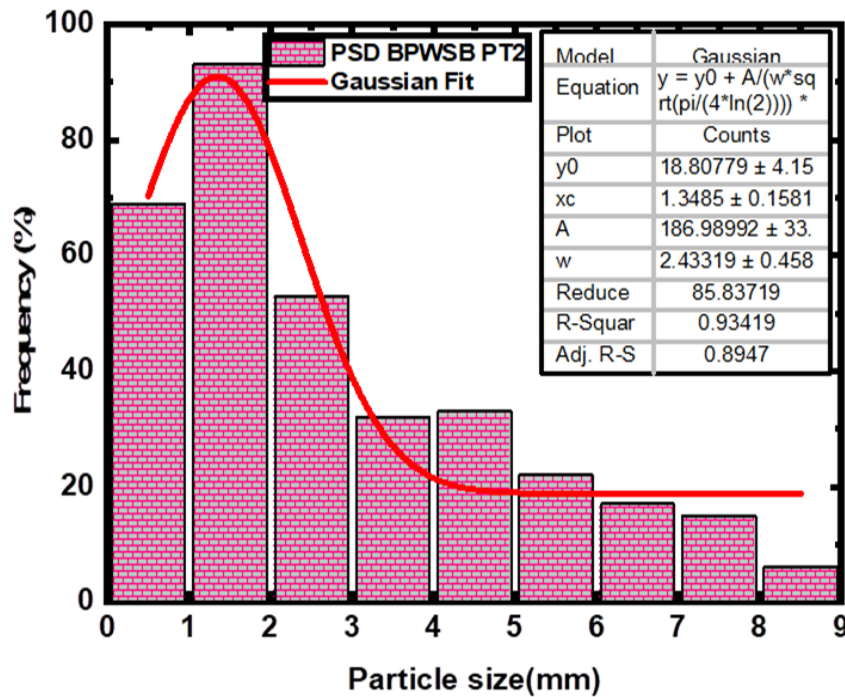


Figure 4.2 Particle distribution of banana peel waste substrate biomass pre-treatment two.

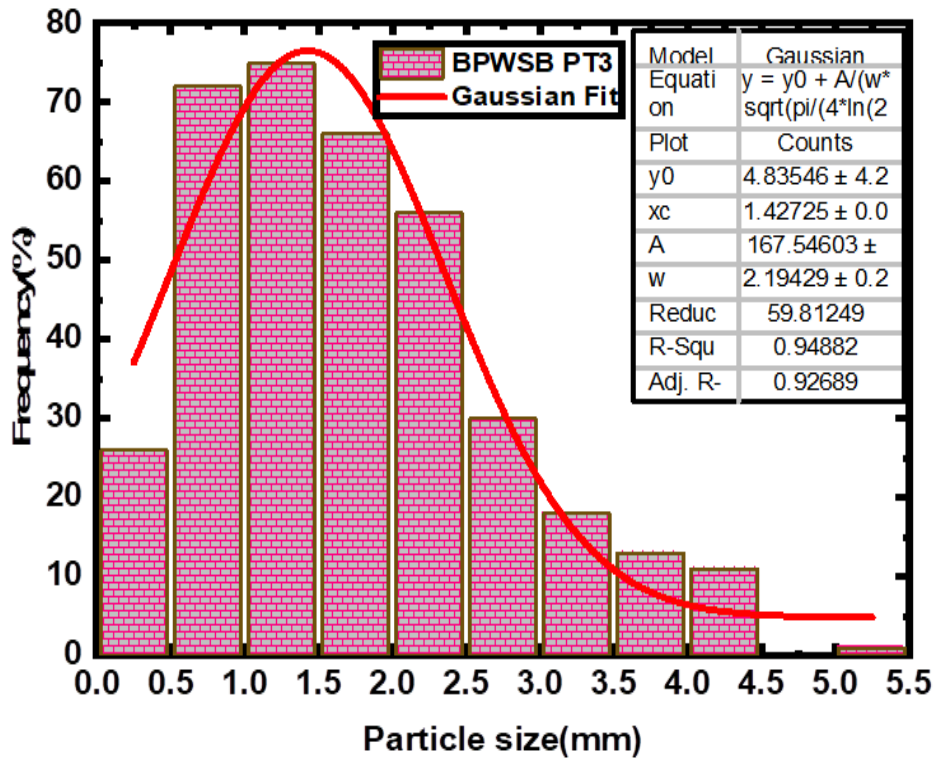


Figure 4.3 Particle size distribution of banana peel waste substrate biomass pre-treatment three.

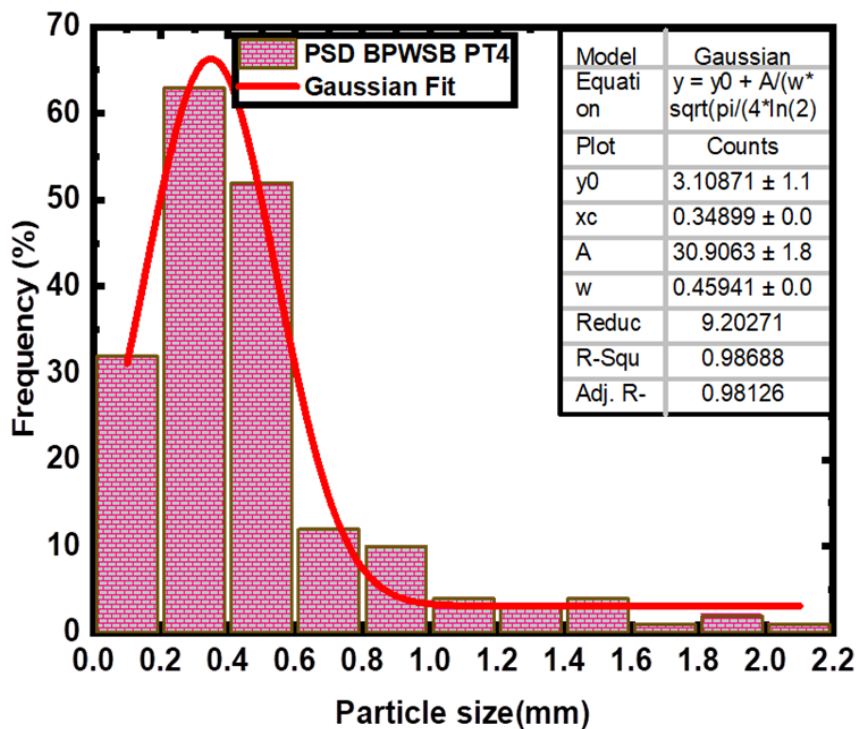


Figure 4.4 Particle size distribution of banana peel waste substrate biomass pre-treatment four.

Table 4. 2 Summary of the particle size distribution of the banana waste substrate biomass according to the pre-treatment levels used during experimental testing of batch and semi-continuous testing.

Substrate identity, pre-treatment level and size distribution				
Substrate biomass and Pre-treatment level	PSD (mm)	Mean PSD (mm)	PSD	Av. PS with error
Banana peel waste substrate biomass				
BPWSB PT1	1-15	6.05	$(\sigma) = w/2=3.29$	$XC \pm \sigma = 6.05 \pm 3.29$
BPWSB PT2	0.5-8.5	1.35	$(\sigma) = w/2=1.22$	$XC \pm \sigma = 1.35 \pm 1.22$
BPWSB PT3	0.25-5.25	1.43	$(\sigma) = w/2=1.095$	$XC \pm \sigma = 1.43 \pm 1.095$
BPWSB PT4	0.1-2.1	0.35	$(\sigma) = w/2=0.23$	$XC \pm \sigma = 0.35 \pm 0.23$

4.4 Grass Waste Particle Size Distribution

For the GWSB, the PSD results for its four PTLs are presented as histograms with a curve of the normal distribution as shown in Figs. 4.5 to 4.9. Its mean value and SD are also detailed in Table 4.3. The photograph of the GWSB is shown in Appendix A2. The four pre-treatment levels of different particle sizes of the GWSB are also a result of the grinding processes as detailed in section 3.3. PTL 1 ranged from 3 to 17mm, PTL 2 (0.5 to 9.5mm), PTL 3 (0.5 to 7.5) and PTL 4 (0.25 to 4mm). In terms of predomination, PTL 1 has 90% of particles > 3mm, PTL 2 has 56% of particles <3mm, PTL 3 contains 62% of particles < 3mm while PTL 4 contains 90% of particles < 3 mm in sizes. As could be observed among the four PTLs of GWSB, PTL 1 has a very high content of larger particles of the GWSB and a paltry of finer particles while the finer particles < 3mm predominate in the other three PTLs. Based on the above, GWSB is inferred to favour the metabolic process due to the dominance of finer particles in three out of its four PTLs. Also, the GWSB has no severe effects on the bioreactor since there are fewer of coarse materials". In fact, grass digesters often experience significant problems with particle floating and matting. The density of each feed particle, along with any associated gas-filled spaces and bound water, is represented by their initial functional specific gravity of less than 1.0. while GWSB floats for more than a day [231]–[233]

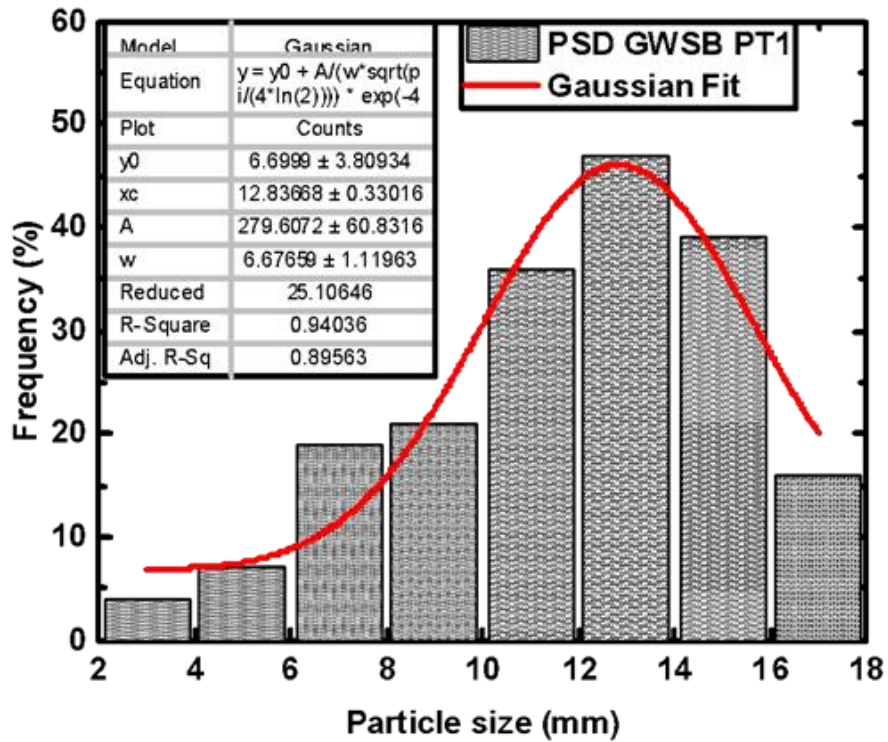


Figure 4.5 Particle size distribution of grass waste substrate biomass pre-treatment level one.

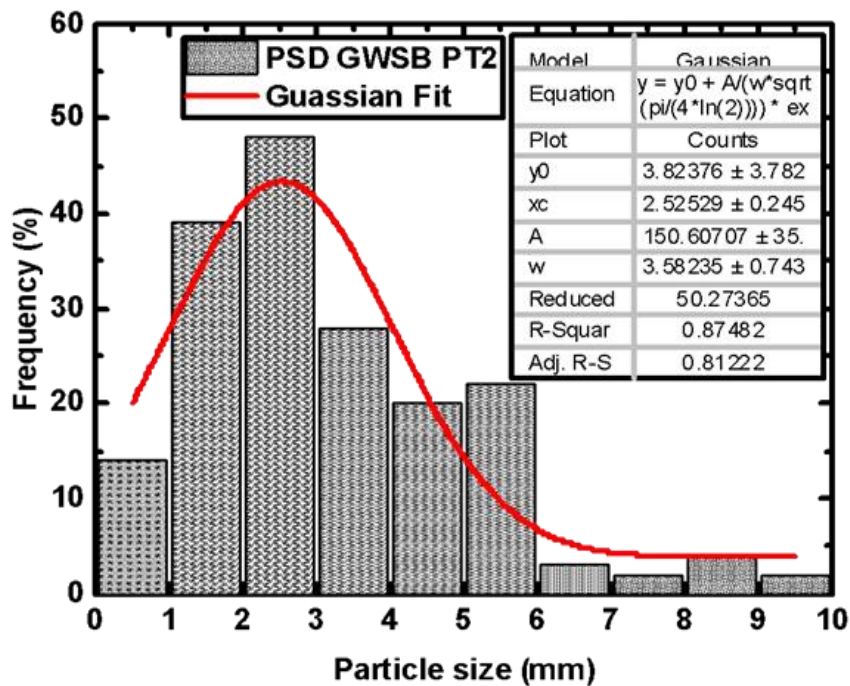


Figure 4.6 Particle size distribution of grass waste substrate biomass pre-treatment level two.

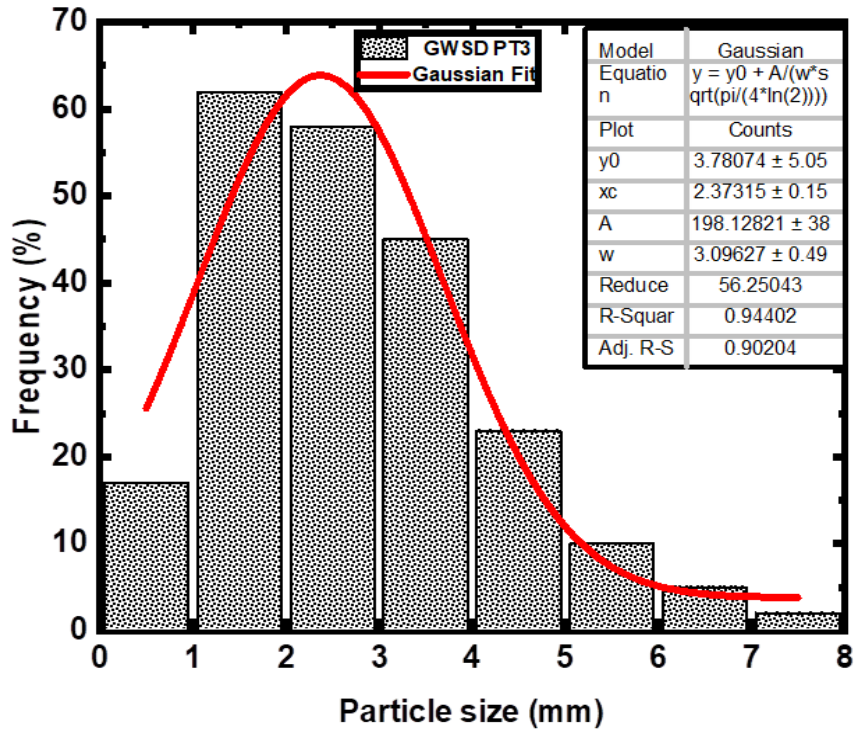


Figure 4.7 Particle size distribution of grass waste substrate biomass pre-treatment level three.

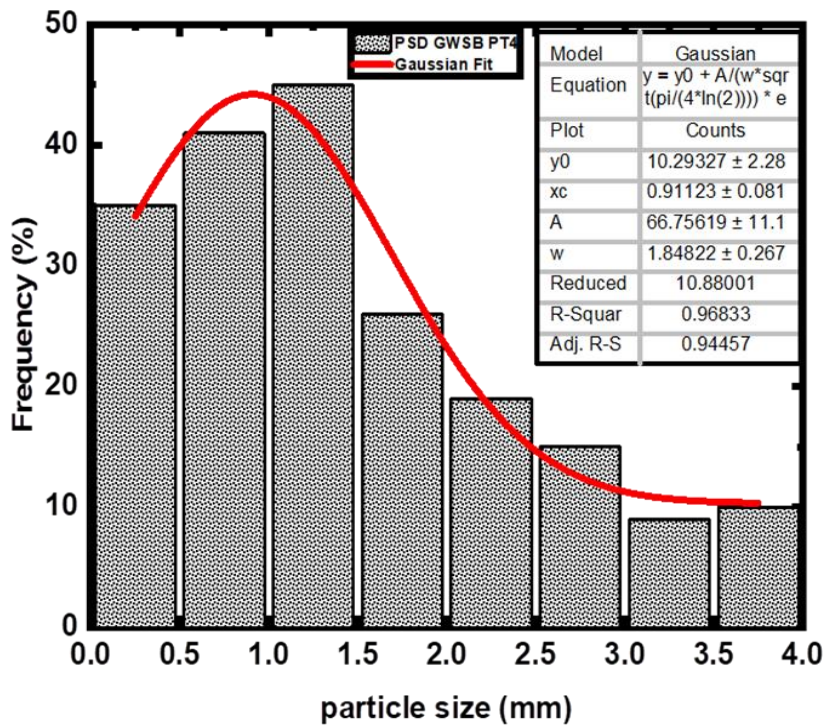


Figure 4.8 Particle size distribution of grass waste substrate biomass pre-treatment level four.

Table 4. 3 Summary of the particle size distribution of the grass waste substrate biomass according to their pre-treatment level used during experimental testing of batch and continuous testing.

Substrate identity, pre-treatment level and size distribution				
Substrate biomass and Pre-treatment level	PSD (mm)	Mean PSD (mm)	SD	Av. PS with error
Paper waste substrate biomass				
GWSB PT1	1-17	12.84	(σ) = w/2=3.34	XC \pm σ = 12.84 \pm 3.34
GWSB PT2	0.5-9.5	2.53	(σ) = w/2=1.79	XC \pm σ = 2.53 \pm 1.79
GWSB PT3	0.5-10.5	2.37	(σ) = w/2=1.55	XC \pm σ = 2.37 \pm 1.55
GWSB PT4	0.1-2.1	0.91	(σ) = w/2=0.92	XC \pm σ = 0.91 \pm 0.92

4.5 Paper Waste Particle Size Distribution

The PSD results for Paper Waste Substrate Biomass (PWSB) which was shredded and subdivided into four pre-treatment levels are shown in Figs 4.9 to 4.12 respectively. With PT1 as shredded with a fair amount of the addition of water added during mechanical breakdown as described in session 3.3. The results are also presented in form of histograms with a curve of normal log distribution and are reported together with the mean value and SD shown in table 4.4. The photograph of each pre-treatment level is shown in appendix A3. After shredding and PT2, PT3 and PT4 passes through a grinding process as detailed in section 3.3, the four PTLs showed a range of 1-25, 0.5-14.5, 0.5-10.5, and 0.25-4.75, respectively. For PTL 1, only 25% of the particles are < 3mm. In PTL 2, approximately 39% fall between 0.5 and 3.5mm. In PTL 3 the smaller particles sizes (< 2.5mm) account for only 17.5% and in PTL 4, an appreciable 85% of smaller particles were recorded. This is further verified by the mean particle sizes as recorded in table 4.4. Unlike the previous biomass considered, PWSB comprised more of larger particles in pre-treatment levels 1-3, but a spike in the content of finer particles in PTL 4. This is also indicated in the mean PSD of the four PTLs of PWSB. The physicochemical properties (Lignin) of the PWSB are seen to have affected its PSD during the mechanical pre-treatment under the same conditions used for other materials. However, it agrees with fact that smaller particles are

more suitable for the AD processes. Paper digesters has long been faced with problem of foaming and clogging.

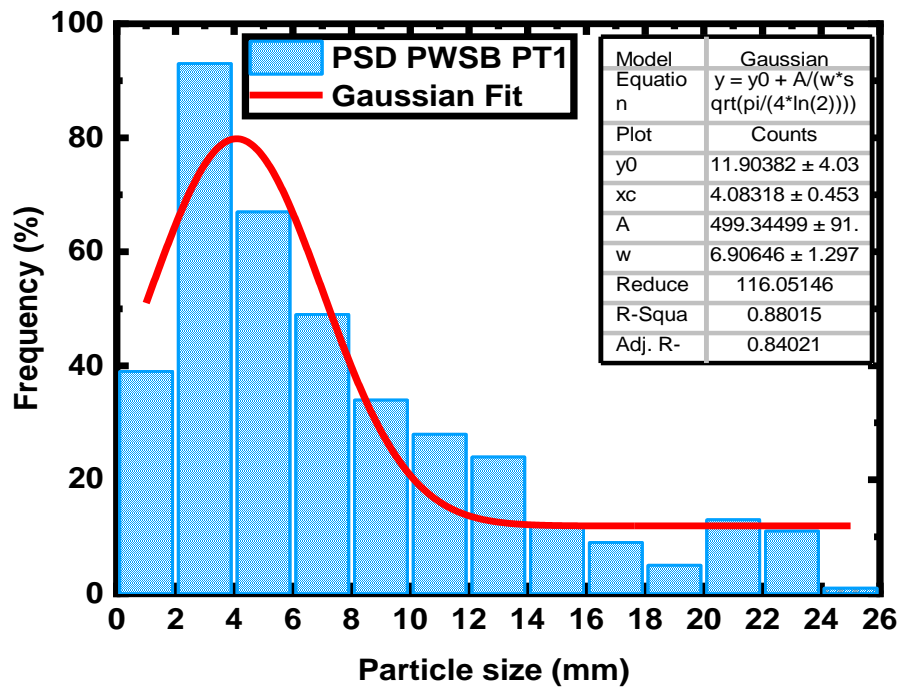


Figure 4.9 : Particle size distribution of paper waste substrate biomass pre-treatment one.

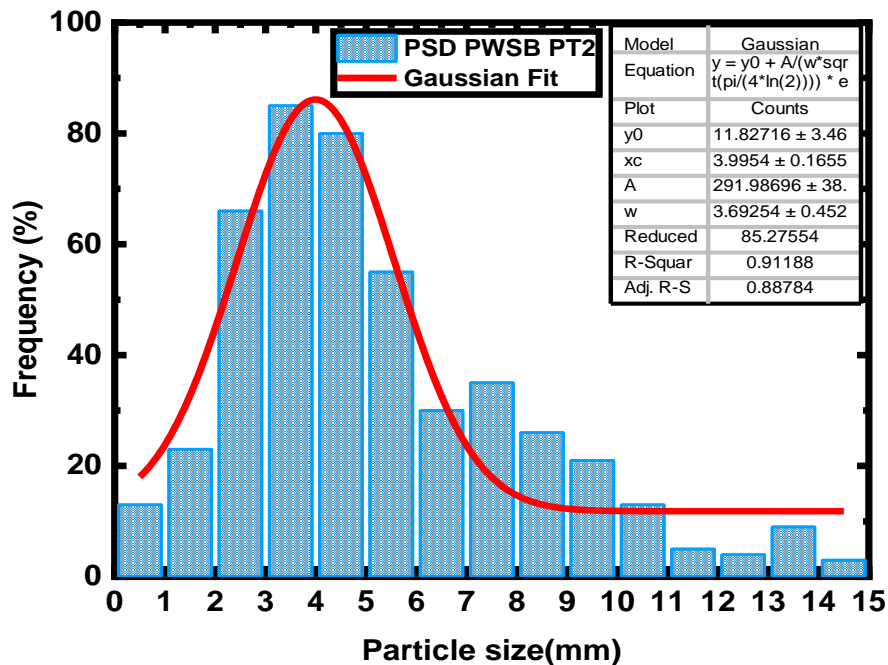


Figure 4.10 Particle size distribution of paper waste substrate biomass Pre-treatment two.

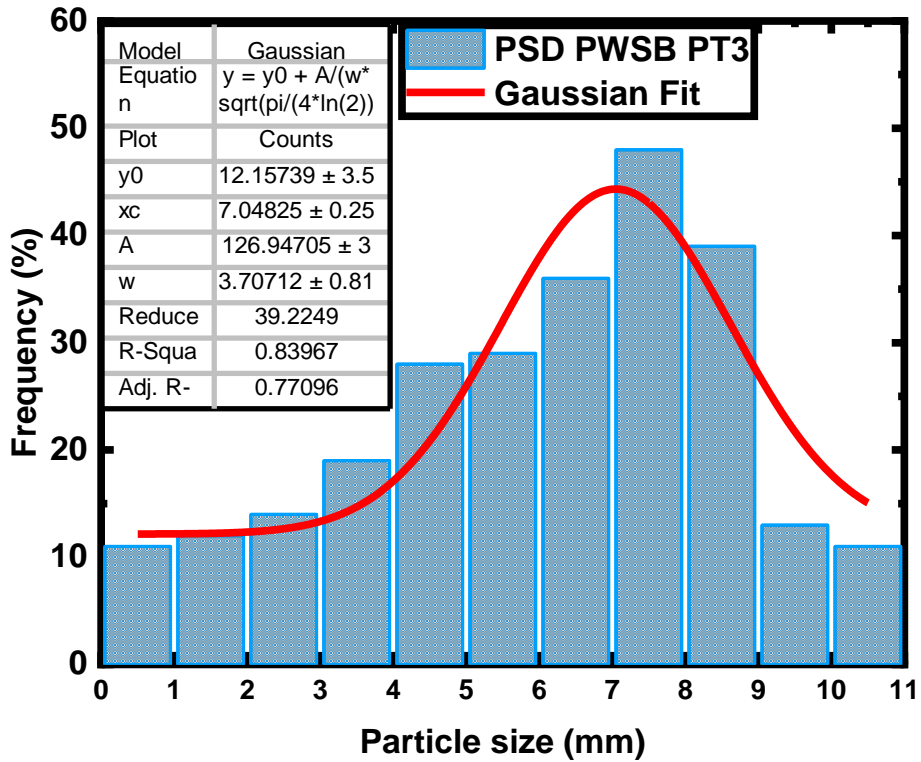


Figure 4.11 Particle size distribution of paper waste substrate biomass pre-treatment level three.

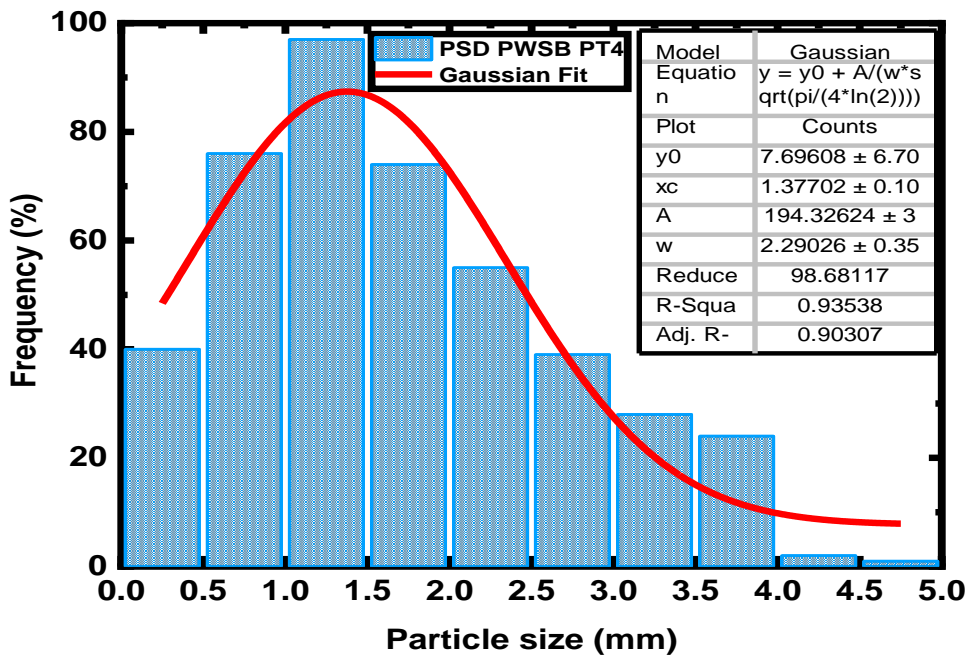


Figure 4.12 Particle size distribution of paper waste substrate biomass pre-treatment level four.

Table 4. 4 Summary of the Particle size distribution of the paper waste substrate biomass according to their pre-treatment level used during experimental testing of batch and continuous testing.

Substrate identity, pre-treatment level, size distribution				
Substrate biomass and pre-treatment level	PSD (mm)	Mean PSD (mm)	SD	Av. PS with error
paper waste substrate biomass				
PWSB PT1	1-25	4.08	(σ) = w/2=3.46	XC \pm σ = 4.08 \pm 3.46
PWSB PT2	0.5-14.5	3.99	(σ) = w/2=1.85	XC \pm σ = 3.99 \pm 1.85
PWSB PT3	0.5-10.5	7.05	(σ) = w/2=1.86	XC \pm σ = 7.05 \pm 1.85
PWSB PT4	0.25-4.75	1.38	(σ) = w/2=1.15	XC \pm σ = 1.38 \pm 1.15

4.6 Tomato Waste Particle Size Distribution

The last sample used is TWSB, and the PSD results for its four PTLs are presented as histograms with a curve of the normal distribution as successively shown in Figs. 4.13 to 4.16. Its mean PSD value and SD are also detailed in Table 4.5. The photograph of the TWSB is shown in appendix A4. The four pre-treatment levels of different particle sizes of the TWSB are also the result of the maceration/grinding process as detailed in section 3.3. PTL 1 ranged from 1 to 11mm, PTL 2 (0.75 to 7.25mm), PTL 3 (0.25 to 3.75) and PTL 4 (0.1 to 1.5mm). Considering PS abundance, PTL 1 has 41% of particles < 3mm, PTL 2 has 66% of particles < 2.9mm, PTL 3 contains 94% of particles < 3mm while PTL 4 entirely contains finer particles between 0.1 and 1.5mm. Amongst all the PTLs of TWSB, particles of PTL4 favoured the AD process better due to their sizes which were much smaller in diameter and agrees with general standards.

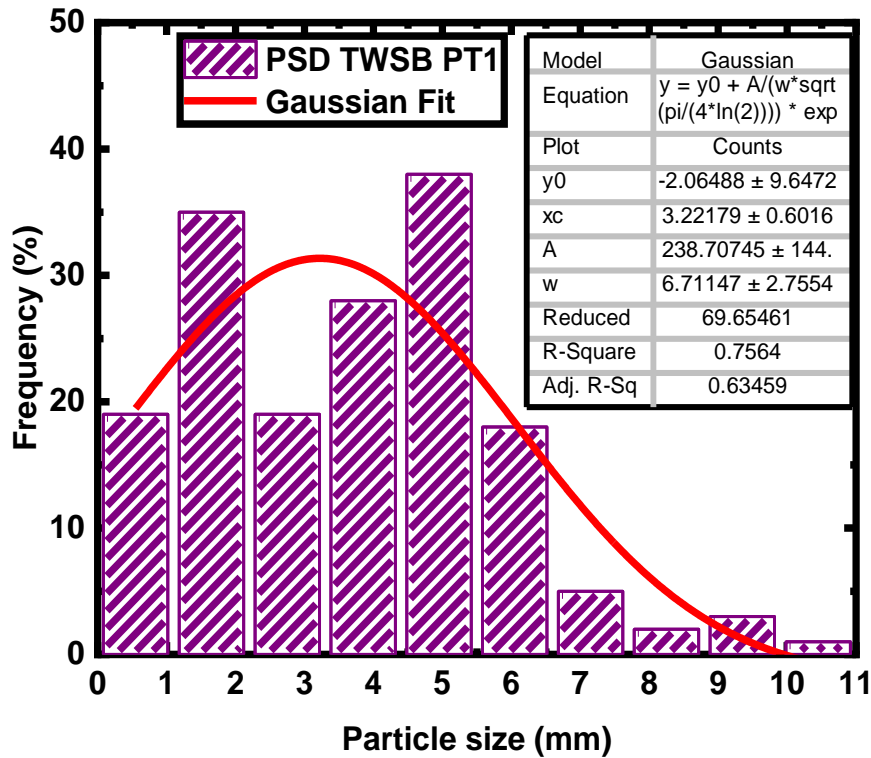


Figure 4.13 Particle size distribution of tomato waste substrate biomass pre-treatment level one.

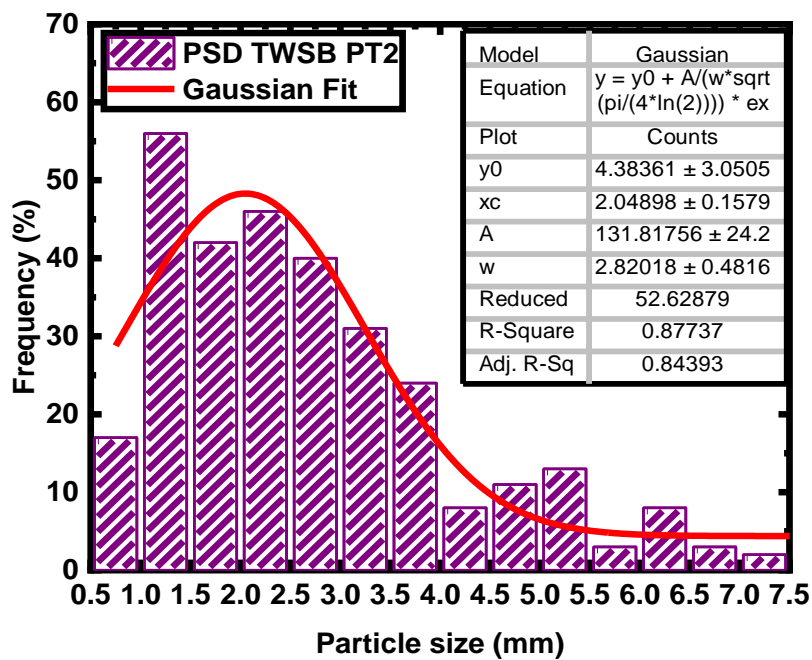


Figure 4.14 Particle size distribution of tomato waste substrate biomass pre-treatment level two.

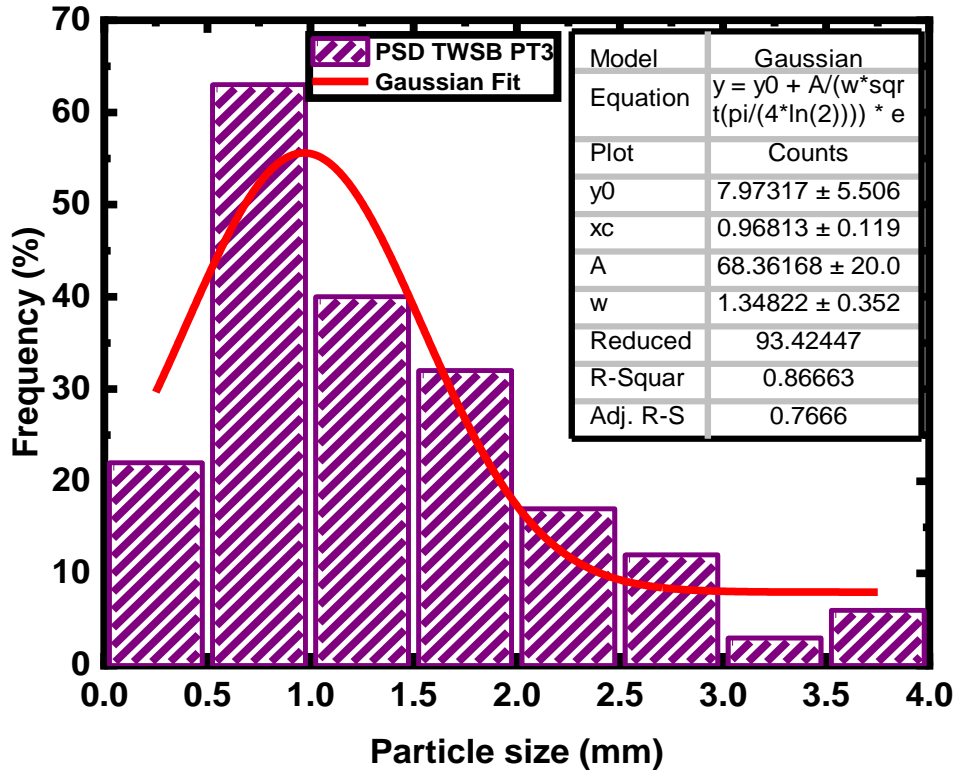


Figure 4.15 Particle size distribution of tomato waste substrate biomass pre-treatment level three.

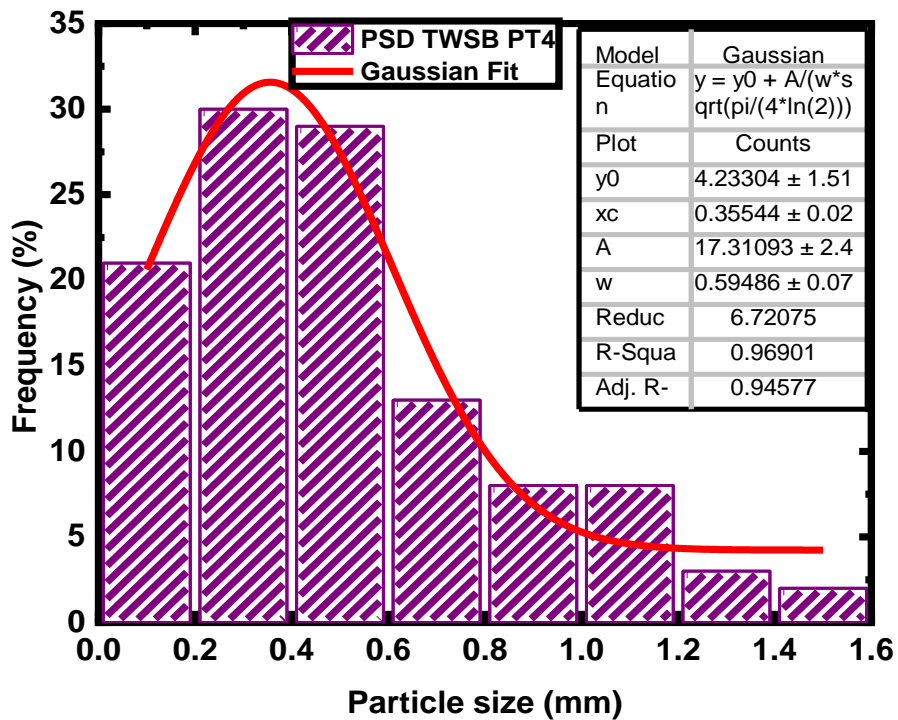


Figure 4.16 Particle size distribution of tomato waste substrate biomass pre-treatment level four.

Table 4. 5: Summary of the Particle size distribution of the tomato waste substrate biomass according to their pre-treatment level used during experimental testing of batch and semi continuous testing.

Substrate identity, pre-treatment level and size distribution				
Substrate biomass and Pre-treatment level	PSD (mm)	Mean PSD (mm)	SD	Av. PS with error
Tomato waste substrate biomass				
TWSB PT1	1-11	3.22	(σ) = w/2=3.36	XC \pm σ = 3.22 \pm 3.36
TWSB PT2	0.75-7.25	2.05	(σ) = w/2=1.41	XC \pm σ = 2.05 \pm 1.41
TWSB PT3	0.25-3.75	0.97	(σ) = w/2=0.68	XC \pm σ = 0.97 \pm 0.68
TWSB PT4	0.1-1.5	0.36	(σ) = w/2=0.30	XC \pm σ = 0.36 \pm 0.30

4.7 Comparison of various particle size reduction methods and equipment

Materials were bulk sampled (8 to 10kg of each substrate) as described in session 3.2.1, and PSD was computed for each sample using the steps provided in session 3.12. Other than the PTL1, which was discussed in session 3.2.1. When the PTLs of the four chosen substrates are compared. The tomato and grass waste were non-treated, fine particles was discovered to be naturally present in their size distribution rather than being mechanically altered, whereas PWSB particle size distributions are presented after processing with a shredder and BPWSB were manually chopped for PTL1. The results show that tomato waste (non-treated) had fine particle size distribution (PSD) ranges that were noticeably higher (41%) from the other three substrates, such as grass waste 10% < 2.9, banana peel waste 14% < 2mm, and paper waste 25% < 3mm, which are detailed in chapter four (4) for all feedstocks. Comparing the maceration/mincing (PTL2) method. The study found that although there was a change in size distribution, as shown in chapter 4, the fine PS range increased more in BPWSB (46%), and GWSB (46%) with PS < 3mm than in tomatoes (25%). Although only 19% of the PS in paper waste was between 0.5 and 3mm, the mincing time did not considerably increase the fine PS even though the PS fraction was significantly lower than it was in PTL1. The mincer's ring size (opening) may be the reason for the minimal boost in fine PS, and the physicochemical characteristics of paper waste may

also be a communiton-limiting factor. Since roughly 41% of the tomato waste was naturally present before treatment, the mincer is more effective at reducing the size of wastes like banana peels and grass than it is at reducing wastes like tomatoes and paper. When comparing the mechanical tool grinder's efficacy in the communiton of PTL3, it was discovered that fine PS increases with a reduced range of particle sizes. Except for the paper waste, which exhibits a very slight increase in fine PS (<2.5mm) of roughly 17.5%, all sample waste had an increase in fine PS with a 28% increase in fine PS for tomato waste, the grinder was more successful than it was for other substrates like BPWSB (13%) and grass waste (6%). Although the mechanical breakdown rate for tomato waste processed with a grinder is slightly higher than the mincer. PTL4 was processed into the desired size distribution for around five minutes using a mincer and grinder combined. When the mechanical breakdown of the substrate is compared, all other substrate, including tomato waste, showed a higher rise in their fine particles. Tomato waste makes up 100% of the fine PS (0.1 to 1.5 mm), banana peel waste makes up 87% (0.1 to 0.6 mm), paper waste (85%) and grass waste make up 90% of the PS <3 mm. This proves that using a mincer and grinder was more effective at size reduction than using a mincer (PTL2) or grinder (PTL3) alone. This provides a larger surface area for enzymatic hydrolysis. This work demonstrates that longer processing times have a significant effect on particles size, which is consistent with earlier studies in the literature [234], [235]. According to the study, medium-tough, viscous/malleable fibrous materials, such paper and other organics materials, can be effectively mechanically treated using a combination of mechanical size reduction equipment, such as a mincer and grinder. The particle size distributions of solid waste processed using various shredding tools and untreated waste were compared. The performance of the shredder was significantly influenced by manufacturing variances, operational conditions, and wear and tear, according to [150]. After crushing, the ball mill was discovered to enable extensive shredding, which accounts for around 80% of the material found in the fraction < 20 mm and 90% in the fraction < 40 mm. The various mechanical equipment and methods are

briefly compared in Table 4.6, along with their performance in relation to substrates PTL1-4.

Table 4. 6 A summary of the size reduction of four selected substrates utilising various mechanical methods and techniques, as well as their effectiveness in relation to their PTL1-4.

Substrate	PTL1		PTL2	PTL3	PTL4
	coarse		Maceration/mincing	Grinding	mincing/grinding
			g		g
Banana peel waste	Manual chopping	0	00	00	000
Grass waste	As collected	-	00	00	000
Paper waste	Shredded	-	-	0	000
Tomatoes waste	As collected	000	00	000	000
Time of processing			2 minutes	3minutes	5 minutes
OOO: Very effective		OO: Moderately effective		O: Effective -: Not effective	

4.8 Results Summary

At a laboratory scale, PSD was tested in the output of mechanical size reduction equipment for four distinct substrates: BPWSB, GWSB, PWSB, and TWSB. Although large PS were more predominant in the distribution of some substrates that were processed using the same mechanical method and for the same amount of time as others, the shift in PSD distributions profile is the most obvious difference. The following conclusions were drawn from this study, which involved mechanical pre-treatment of the substrate with a various size reduction equipment and operation modes:

- ❖ Tomato waste from Sheffield's moor market was found to include a significant number of small size particles without being mechanically changed or pre-treated in PTL1 as compared to grass waste from the University of Sheffield, PWSB was collected from the University of Sheffield Energy Group Offices which was shredded, and banana peel

collected from households was found to be presents after being manually chopped.

- ❖ The use of a mincer and a grinder for PTL4 was found to be far more effective in processing the organic fraction of the four substrates tested, including paper waste with a high lignin content.
- ❖ The grinder (macerator) produced particle size distributions (PSD) with mean PS of 1.43mm, 2.37mm, 7.05mm, and 0.97 for BPWSB, GWSB, PWSB, and TWSB for PTL3, respectively; however, such substantial particle size reduction might not be beneficial in future treatment.
- ❖ The ring size jaw opening of the mincer can alter the distribution of particle size and can affect the mid-range rather than the smaller sizes that pass through the mincer without change.
- ❖ The mincer can effectively decrease the size of feedstock particles bigger than the jaw opening, however, the output may comprise particulates that are highly irregular in shape - folded, twisted, clumped, thin, and so on.
- ❖ The mincer employed in this study for processing a wet waste fraction of PTL2 with a ring size jaw aperture RAUT 12 16# was unsuitable for handling the four-substrate biomass, especially PWSB and TWSB. This could be related to the physiochemical properties of organic materials, particularly in the case of PWSB.

There are differences in the actual PSD trends even though different particle size reduction methods have shown to be efficient in reducing the mean particle size. Many techniques profit from using diverse particle sizes at the same time. The method of biotechnological operations should be accounted for while choosing a pre-treatment method. The can promotes the optimal treatment outcome for organic materials. More research is required to understand how the characteristics of various waste components throughout the size reduction process and other factors affect the particle size distribution.

The impact of mechanical pre-treatment on degradation of complex organic matter

5 Batch Testing

This chapter presents the results from the batch testing and semi-continuous testing, and anaerobic degradation model describing changes in the PSD of substrates over time using the Surface-Based Kinetics model for spherical particles in a continuous anaerobic digestion system with literature and survey data. The results of biochemical methane potential (BMP) of the four-substrate biomass used in this study are presented below. BMP results obtained from experimental testing provides the assessment of biodegradability/ ultimate methane (CH₄) potential production rate per gram volatile solid (gVS) of biomass substrate and characteristic kinetics. Biochemical methane (CH₄) potential (BMP) performance of a given biomass substrate is used to assess the effectiveness of the biomass substrate due to variation of the feedstock across the globe. This is referring to the physicochemical properties of the anaerobic organic materials as well as their capacity for degradation. Therefore, this research work takes into consideration the importance of biochemical methane (CH₄) potential (BMP) testing of the four-biomass substrate used in this study.

5.1 BMP Assay for Banana Peel Waste Substrate Biomass (BPWSB)

The batch test results for the four pre-treatment levels of BPWSB are presented as graphs in figures 5.1A, 5.1B, 5.2 and 5.3. Figure 5.1A portrays the daily accumulated methane production for a triplicate sample of the blank (inoculum) and for control. Figure 5.2B shows the daily accumulated methane (CH₄) yield for a triplicate sample of the BPWSB according to their mechanical breakdown pre-treatment levels. Figure 5.2 is a record of specific methane (CH₄) production for BPWSB with average control from triplicates (CH₄ subtracted from the inoculum and data expressed in terms of grams of volatile solid (gVS), while fig. 5.3 is a

measure of daily flow rate in Nml/day and accumulated percentage of methane production for BPWSB degradation after the subtraction of the inoculum CH₄ production. Also, the summary of the maximum BMP achieved from the inoculum and four pre-treatment levels of BPWSB is presented in table 5.1 and the volatile solids reduction is shown in table 5.2. From fig. 5.1B, BPWSB of PTL4, with an average particle size of 0.35mm yielded the highest 332 Nml/gVS as shown in table 5.1, other PTLs with their respective mean PSD of 1.43mm, 1.35mm, and 6.5mm yielded less in descending order. The flow rate (measured in Nml/day) of the four substrate sizes followed a similar pattern as the particles in PTL4 showed more production rate than substrates of PTL3 and 2 and 1, in the same order, although all the substrates experienced a sharp decrease in flow rate after 3 days. Worthy of note is the fact that PTL4 reached its peak flow rate on the first day. This is further proven by the number of volatile solids (VS) of the substrate that degraded out of each PTL as shown in table 5.2. From the results obtained, the optimal production of methane is recorded for smaller particle sizes, throughout the 30 days retention time for the four separate PTLs. Also, the average pH at the end of the batch testing for the four pre-treatment levels are shown in Table 5.1. The pH was 7.33 for (PT1), 7.31 (PT2), 7.35 (PT3) and 7.33 (PT4) respectively. This falls within the pH range that is suggested to produce biogas [84]–[86], [94], [236]. This result showed that the microorganisms in the digester were intact and not affected by the pH of the slurry. A normal degradation curve was seen after 28 days of the BMP test. As can be seen, PTL4 degraded more quickly than the other three PTLs, but the production of methane over time was similar for all four PTLs, including the cellulose samples. After 28 days, the methane potential had not yet been reached, but the PTLs 1-4 exhibits a rapid initial rate of biogas production that continues over time. The biogas production curves have a slightly different shape, but not significantly. The curves show a normal degradation curve. In addition, the results of BPWSB's BMP testing shown in figure 5.2 showed that PTL4 produced SMP at rates of 35.5%, 22.5%, and 13.3% higher than PTL1, PTL2, and PTL3. PTL3 had specific methane yields that were at about 19.6% and 8.1% higher

than PTL1 and PTL2, and PTL2's maximum methane yield was at about 10.6% higher than PTL1. When PTL4 is compared to the others, it can be concluded that PTL4 has achieved the highest level of methane production of about 332 ± 36 Nml/gVS. Other than differences in particle size, the BPWSB samples (PTL1-4) were tested under similar conditions (using the same inoculum, with the same I/S ratio and at the same temperature). As a result, differences in microbial activity during the degradation process are likely to account for the variations in error between the four groups of biomass PTLs (1-4). Also, the differences in specific methane production and the methane production kinetics demonstrated that BMP assays of the various PTL1-4 are probably different as a result of the use of various equipment with different aperture, operation conditions, and more unit surface area. The value of the methane yields obtained as shown in table 5.6 is comparable to the BMP for BPWSB (PS) reported by [212], [237], [238] ranging from 223 to 336 Nml/gVS volatile solids (VS) operated in a 5L batch digester at 37°C. This shows that the batch test for BPWSB work correctly during degradation process. Similar to this, many studies have revealed that banana stalks have a BMP ranging from 188 to 334 Nml/gVS.

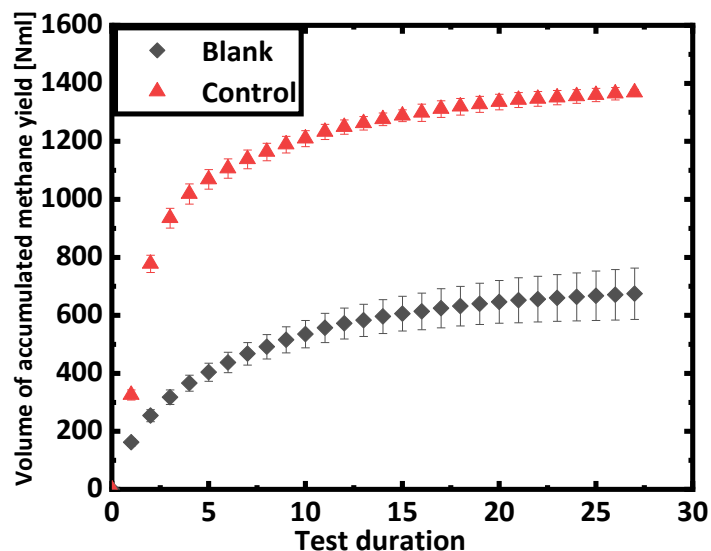


Figure 5.1a & b Cumulative methane (CH₄) production for a triplicate sample of the blank, contains only 400ml inoculum and for control (cellulose and inoculum) digested during BPWSB.

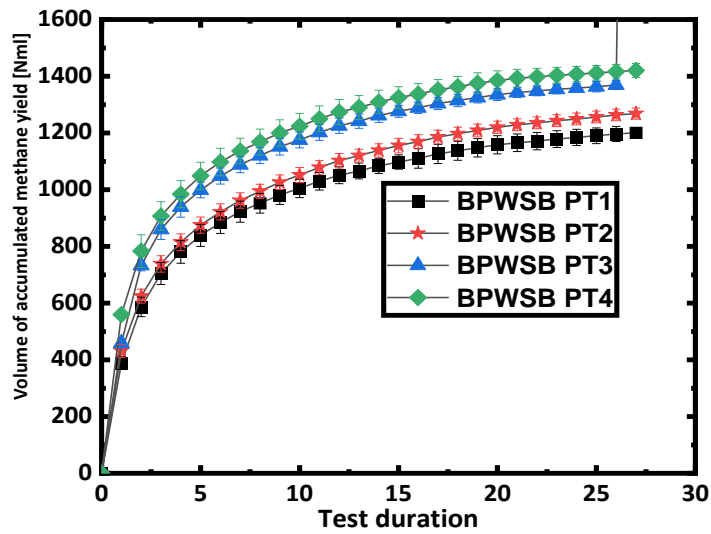


Figure 5.1b Cumulative methane (CH₄) production for a triplicate sample of the BPWSB according to their mechanical breakdown pre-treatment levels including calculated measured among of the freshly active inoculum in grams (g).

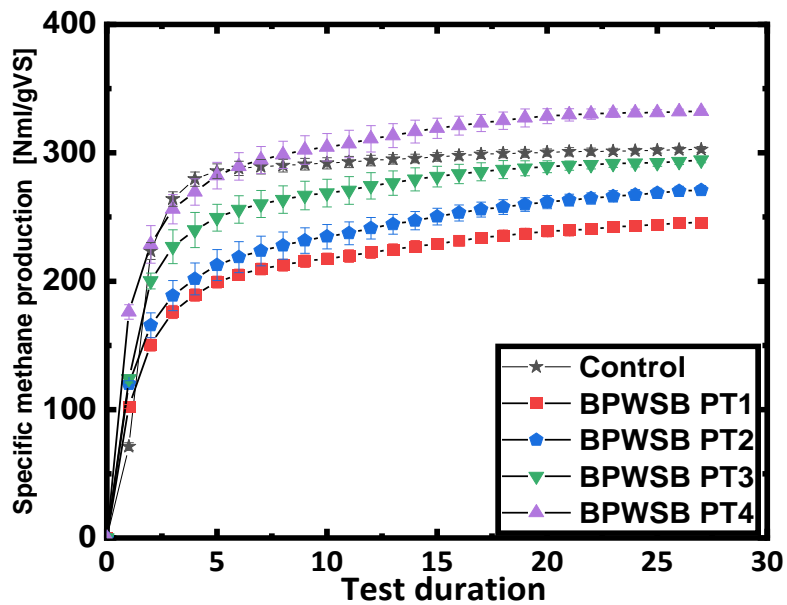


Figure 5.2 Specific methane (CH₄) production for BPWSB with average control from triplicates (CH₄ subtracted from the inoculum and data expressed in terms of grams of volatile solid (gVS) added.

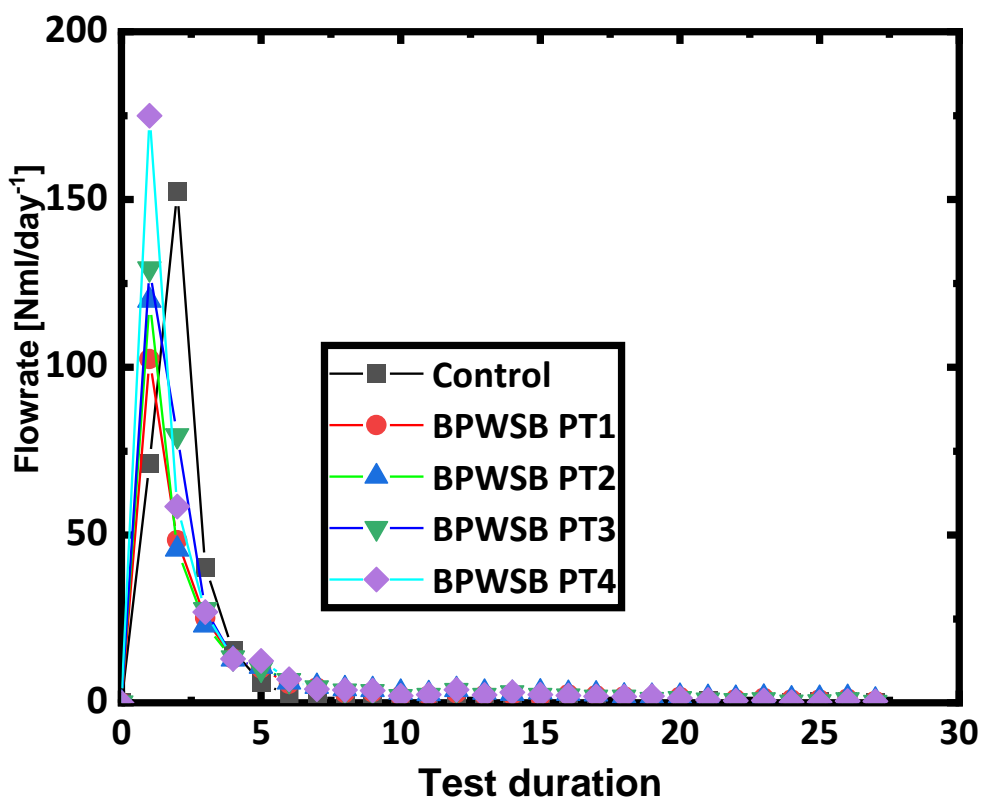


Figure 5.3 Cumulative flow rate and accumulated % volume of the methane production for BPWSB degradation after the subtraction of the inoculum CH₄ production.

Table 5. 1 Maximum biochemical methane (CH₄) achieved from BPWSB.

Substrate biomass	Pre-treatment level	Units	BMP result	measure Inoculum	pH after digestion
Control		Nml/gVS	302±19	380	-
BPWSB	PT level 1	Nml/gVS	245 ±32	388	7.32(0.01)
	PT level 2	Nml/gVS	271 ±35	376	7.31(0.04)
	PT level 3	Nml/gVS	293 ±36	379	7.32(0.01)
	PT level 4	Nml/gVS	332 ±36	376	7.33(0.04)

Table 5. 2 Calculation of the volatile solids from the biomass of banana peel waste.

BPWSB (PTLs)	VS			
	initial		Final	
PTL1	9.090	0.9090	7.965	0.7965
PTL2	9.090	0.9090	7.913	0.7913
PTL3	9.090	0.9090	7.825	0.7825
PTL4	9.090	0.9090	7.712	0.7712
AV	9.090	0.9090	7.853	0.7853
Batch anaerobic degradation: Calculated (%) Volatile solid reduction (VSR)				
$(\%) \text{ Volatile solid reduction (VSR)} = \frac{(VS_{Bin} - VS_{digestedout})}{(VS_{Bin} - (VS_{Bin} \times VS_{digestedout}))} \quad \text{where:}$				
VS_{Bin} percentage (%) of volatile solid (VS) of biomass in the inflow $VS_{digestedout}$ percentage (%) of volatile solids (VS) of digested in the outlet.				
$\frac{(0.9086 - 0.7965)}{(0.9086 - (0.9086 \times 0.7965))} = \frac{(0.1121)}{(0.9086 - (0.7236999))} = \frac{0.1121}{0.1849} = 60.4\%$				
The amount of substrate biomass Volatile solid (VS) degraded				
PTL1	60.4%			
PTL2	61.9%			
PTL3	63.5%			
PTL4	66.7%			
AV	63.4%			

5.1.1 Calculation of BPWSB theoretical calorific value of biomass potential

The practical results from the BMP tests and the theoretical value were compared to ascertain the ability of theoretical methods to predict the biogas composition of complex substrates. The percentage of volatile solids reduced by each PTLs was used to explore the Buswell equation with a combination of carbon feed material to estimate the maximum methane production. For each PTLs, the calculation of the BPWSB proportion of the CH₄, CO₂, and carbon balance is shown in appendix B1 to B4. Methane (CH₄), which accounts for 70.7%, and carbon dioxide (CO₂) account for the remaining portion (29.3%). Also figure 5.5 shows the specific methane yield comparison plot of the actual versus predicted values. Based on the theoretical biogas yield at STP values presented in appendix B1 to B4, it is evident that PTL4 produces more biogas (353Nml/gVS), followed by PTL3, PTL2, and PTL1 in that order indicating that smaller particle sizes result in more surface area exposed to enzymatic attack, which may enhance carbon accessibility and hydrolysis of the processed material [121], [160], [239], [240]. The results showed that the actual methane production is lower than theoretical value as seen in table

5.3. Methane production in the digesters can be measured theoretically versus experimentally to determine the proportion of volatile solid reduction (VSR). Methane yield will be higher with a higher % volatile solid reduction (VSR) than it will be with a lower VSR % (table 5.3). The percentage change difference in methane production between the measured and predicted methane yields is shown in Table 5.3. The average theoretical specific methane yield at STP for BPWSB is 353Nml/gVS, whereas the measured data is 285Nml/gVS.

Table 5. 3 Measured and predicted maximum specific methane production with respective % volatile solids reduction.

Parameter	BMP experimental	BMP theoretical	% VSR
PTL1	245	321	60.4
PTL2	271	327	61.9
PTL3	293	339	63.5
PTL4	332	353	66.7
AV	285.2	353	63.4

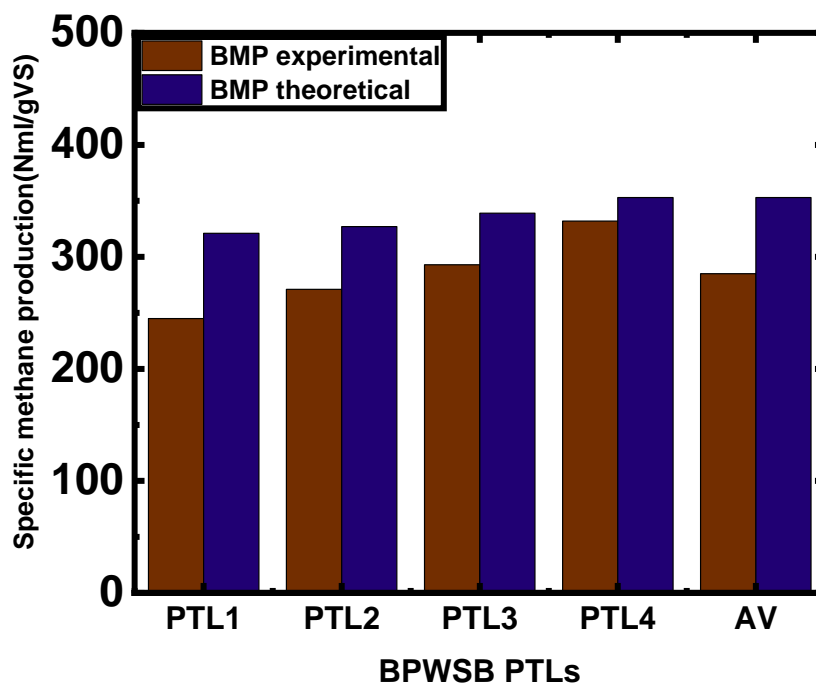


Figure 5.4 Compares the BMP of the BPWSB with the theoretical methane yield at STP based on the experimentally determined volatile solids reduction (PTL1-4) and carbon feed material.

5.1.2 Banana peel waste substrate biomass BMP Kinetics

The biodegradability of the BPWSB (PTL1-4) samples was tested using BMP kinetic data. Equations 5.1 and 5.2 show the two different kinetic models that were used to fit the experimental data. This was carried out to evaluate how effectively the AD process performed.

$$G(t) = g \cdot (1 - \exp(-k \cdot t)) \quad (5.1)$$

Where:

g is the cumulative methane yield at time t

k is the hydrolysis Kinetic constants

t = Duration of batch test

and a modified Gompertz model (equation (5.2))

$$G(t) = g \cdot \exp(-\exp(((R \cdot 2.7183)/g) \cdot (L - t) + 1)) \quad (5.2)$$

Parameters: g , R , L

Where:

$G(t)$ is the cumulative methane yield at time t

G is the maximum cumulative methane production

k is the hydrolysis Kinetic constants

Euler's number (2.71828)

R is the maximum methane production rate (NmL/gVS)

L is the lag (λ) phase time

The parameter values for g , R , and L were derived using the modified Gompertz model, whereas the parameter values for g and K were derived using first order kinetics. Both strategies made use of the statistical analysis software SPSS. The kinetic constants for equations 5.1 and 5.2 are provided in tables 5.4 and 5.5, and figure 5.5 shows the results of the BPWSB (BMP) Kinetic model. Pre-treatment levels 1-4 demonstrate that equation 5.1 for the first order BMP kinetics offers a better fit with R squared (R^2) values of 0.965, 0.944, 0.976, and 0.959 when compared to the Modified Gompertz model, which had R squared (R^2) values of 0.937, 0.915, 0.952, and 0.929. The Modified Gompertz model, with R squared

(R²) values of 0.965, provides a better fit for cellulose. All PTLs have similar k values, however PTL4 has a higher k value for first order kinetics (0.59), as would be expected. The availability of a large surface area makes this possible. This value represents the presence of microbial fermentation products that are easily assimilated by the methanogenesis population. In terms of k-value, PTL3 significantly trailed PTL4 behind. On the other hand, PTL1's K-value is higher than PTL2's. This demonstrates the difference in means and the shift in particle size distribution profiles. Table 5.5 shows that the four PTLs had a relatively short lag period before the microorganisms started to act on. The bacteria in the AD digester are active, and the substrates were easily biodegradable. This is because biogas was produced quick after inoculation. The inoculum employed in this test, which is discussed in session 3.4.2, contains bacteria that are already adapted to their habitats. These results agreed with those of [241], [242]. Results of the Gompertz model showed a negative temporal lag (λ). This has shown that either the favourable substrate conditions speed up the growth of methanogens in the early phases of the anaerobic digestion (AD) process or that the growth of methanogens began earlier during the lag phase than the Gompertz model predicted, which shorten the time it takes to reach the exponential phase. According to [243], a potential organic loading rate (OLR) must be estimated in a continuous or batch fed digester for a kinetic study because during a BMP test, the substrate degraded quickly, suggesting the need for a small reactor and a cost-effective digestion process [244]. The BMP test results suggest that BPWSB is a very viable feedstock for anaerobic digestion (AD).

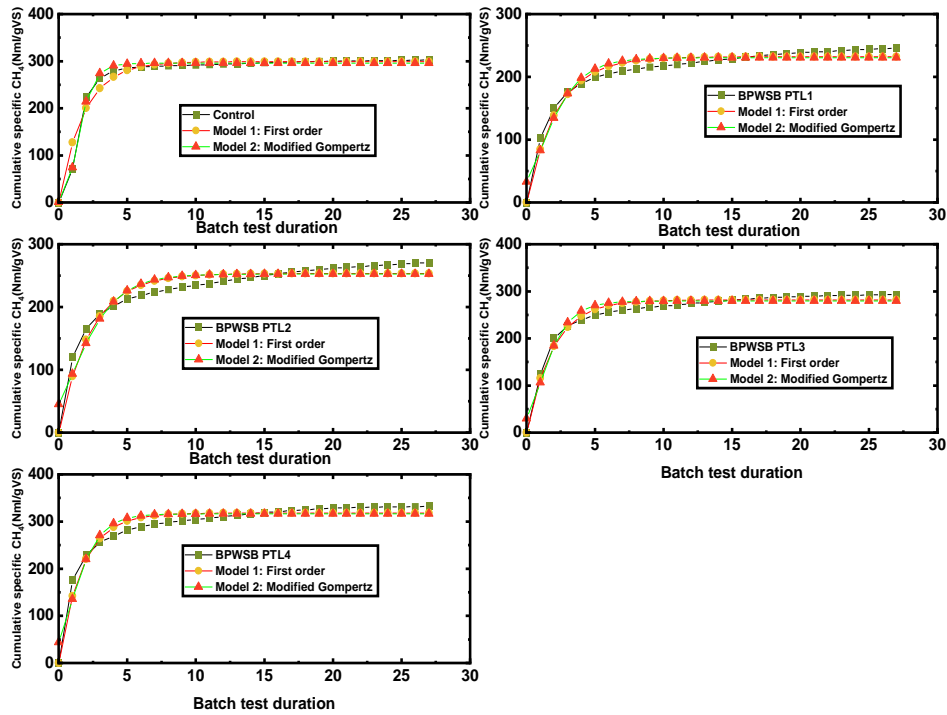


Figure 5.5 Experimental results for BPWSB and the kinetics of specific CH₄ production for first order (model 1) and modified Gompertz (model 2)

Table 5. 4 First order kinetic parameters value from BMP modelling

Parameter Estimates					
Parameters value	Estimate	Std. Error	95% Confidence Interval		
			Lower Bound	Upper Bound	
Control					
g	299.246	2.92	293.244	305.248	R ² 0.965
k	0.555	0.04	0.473	0.638	
BPWSB PTL1					
g	232.275	2.27	227.608	236.942	R ² 0.965
k	0.453	0.029	0.393	0.513	
BPWSB PTL2					
g	253.563	3.133	247.123	260.002	R ² 0.944
k	0.438	0.035	0.366	0.51	
BPWSB PTL3					
g	281.962	2.175	277.492	286.432	R ² 0.976
k	0.528	29	0.467	0.588	
BPWSB PTL4					
g	318.243	3.031	312.013	324.474	R ² 0.959
k	0.59	0.043	0.501	0.679	

Table 5. 5 Modified Gompertz model kinetic parameters value from BMP modelling.

Parameter Estimates					
Parameters value	Estimate	Std. Error	95% Confidence Interval		R Squared
			Lower Bound	Upper Bound	
Control					R ²
g	296	1.23	293.4	288.4	0.993
R	158	9.52	138.1	177.2	
L	0.53	0.06	0.407	0.652	
BPWSB PTL1					R ²
g	231	2.997	224.6	236.9	0.937
R	54.2	6.83	40.2	68.3	
L	-0.53	0.294	-1.137	0.076	
BPWSB PTL2					R ²
g	253	3.91	244.7	260.8	0.915
R	51.1	7.3	36.1	66.1	
L	-833	0.393	-1.642	-24	
BPWSB PTL3					R ²
g	280	2.997	273.5	286.432	0.952
R	86.8	10.2	65.7	0.588	
L	-299	0.208	-656	199	
BPWSB PTL4					R ²
g	317	3.99	312.013	324.474	0.929
R	98.7	13.92	0.501	0.679	
L	-376	0.248	-887	134	

5.1.3 Statistical Analysis of Variance for the Four Selected Substrate Biomass.

The means of the methane yield produced by the four substrate (GWSB, PWSB, TWSB and BPWSB) biomass are compared in this study using one-way ANOVA (analysis of variance). This was carried out in accordance with the pre-treatment levels (PTL1-4) for each substrate using the OriginPro-2021 software. comparing the cumulative output of specific methane (CH₄) from batch test. The population means of the methane output were compared to check if there were any statistically significant differences between the four PTLs. This enable a concise conclusion to be drawn based on the performance efficiency of substrate pre-treatment level and potentially what caused the performance differences between the groups. The samples were evaluated to verify the assumptions of the one-way ANOVA (Normally distributed populations, independent observations, and the homogeneity of variance). The yield of methane is independent of the particle size of the substrate biomass, which is grouped into four (PTL1-4) pre-

treatment levels. As a result, the four pre-treatment levels' methane yields had no effect on one another during anaerobic biodegradation. The Levene's test was used at an alpha level of 0.05 to test the assumption of variance homogeneity, with the null hypothesis that the means of the four pre-treatment levels are equal [245].

5.1.4 ANOVA of Banana Peel Waste Substrate Biomass

This study compared the average specific methane yields of the four PTLs 1-4 of BPWSB to determine if there were any significant variations. A higher specific methane yield was hypothesised to be more likely from BPWSB's PTL4. Using an ANOVA with a one-way between-subjects comparison, the data collected were analysed. Table 5.6 displays the findings. The studies found $F(3,108) = 10.3$, $P=4.97E-06$, that PTL4 significantly differs from other PTLs. The Fisher LSD was used to conduct the post hoc analysis. The studies showed that PTL4 had a significantly higher specific methane yield ($M=293.3$ $SD=67.6$) compared to PTL3 ($M =257.7$, $SD=61.9$), and PTL1 ($M=210$, $SD=52$), while PTL3 had a differs significantly from PTL1. However, the specific methane yield did not differ significantly between PTL3 and PTL1 and between PTL2 and PTL1. In comparison to other PTLs, the result revealed that PTL1 has the lowest mean methane yield and PTL4 has the highest specific methane yield due to its higher surface area and smaller PS. The statistically significant differences between the PTLs were displayed using box charts and fisher LSD plots (figures 5.6 and 5.7).

Table 5. 6 One-way analysis of variance of the grass waste substrate biomass.

Descriptive Statistics					
	N Analysis	N Missing	Mean	Standard Deviation	SE of Mean
BPWSB PT1	28	0	209.9801	51.99837	9.82677
BPWSB PT2	28	0	228.7962	56.72017	10.7191
BPWSB PT3	28	0	257.6911	61.89203	11.6965
BPWSB PT4	28	0	293.3233	67.63126	12.78111
One Way ANOVA					
	DF	Sum of Squares	Mean Square	F Value	Prob>F
Model	3	110913.6	36971.18	10.3231	4.97E-06
Error	108	386791.7	3581.405		
Total	111	497705.3			
Fit Statistics					
	R-Square	Coeff Var	Root MSE	Data Mean	
	0.22285	0.24185	59.84484	247.4477	

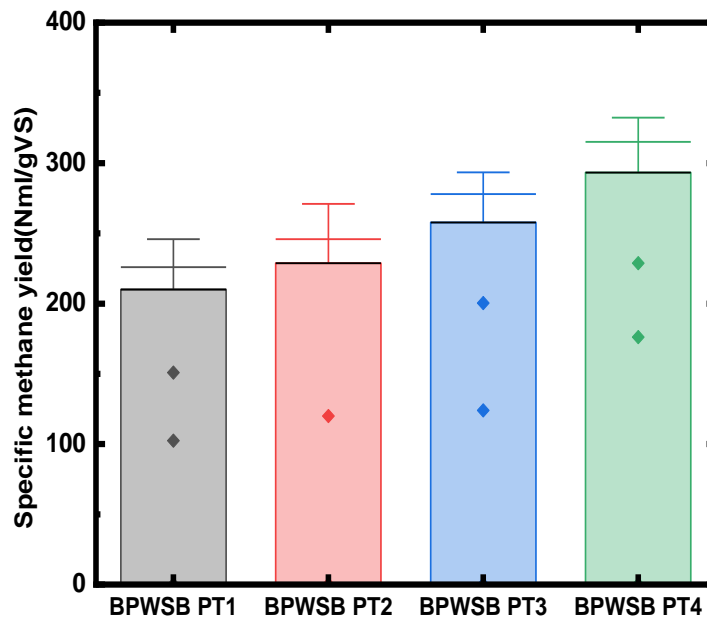


Figure 5.6 Means boxplot of the variation of the methane yield of BPWSB four pre-treatment levels.

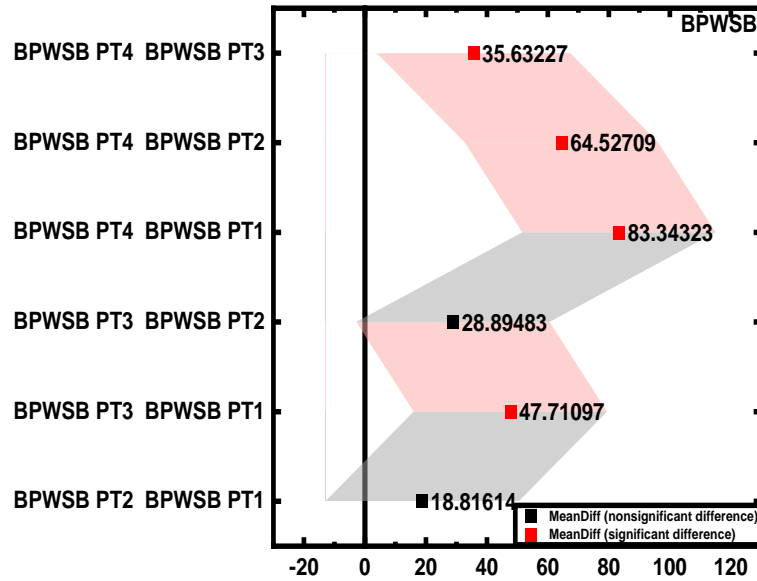


Figure 5.7 Fisher LSD means comparisons plot for banana peel waste methane yield of four pre-treatment levels.

5.2 BMP Assay for Grass Waste Substrate Biomass (GWSB)

The batch test results for the four pre-treatment levels of GWSB are presented as graphs in figures 5.8a, 5.8b, 5.9 and 5.10. The daily methane production for a triplicate sample of the blank (inoculum) and for control is displayed in Figure 5.8a. Figure 5.8b shows the daily accumulated methane (CH_4) yield for a triplicate sample of the GWSB according to their mechanical breakdown pre-treatment levels. Figure 5.10 is a record of specific methane (CH_4) production for GWSB with average control from triplicates (CH_4 subtracted from the inoculum and data expressed in terms of grams of volatile solid (gVS), while fig. 5.10 is a measure of daily flow rate and accumulated percentage of methane production for GWSB degradation after the subtraction of the inoculum CH_4 production. Also, the summary of the maximum BMP achieved from the four pre-treatment levels of GWSB is presented in table 5.7 and the volatile solids reduction is shown in table 5.8. Similar to the trend in BPWSB, it would be observed that the biomethane production, (specific methane production) and flow rate in Nml/d is related to the

degree of processing, although all the substrates experienced a decrease in flow rate after 3 days. With a mean PSD of 0.91 in PTL 4, a BMP of 270.3Nml/gVS, under the same temperature and inoculum conditions as shown in table 5.3. This maintains the standard that particle size influences methanation in AD processes, all other things being equal. Also, the residual VS at the end of batch testing of the GWSB decreased subsequently with its PTLs, showing that as particle sizes decreased, surface area increased, allowing the inoculum to act on the feedstock during the biodegradation process, using over 50% of the volatile solids of the substrate with smaller particle sizes in the order of their pre-treatment levels, during the 35 days retention time. Also, as can be seen in the standard deviations and error bars in figure 5.9, sampling errors and variation between substrate biomass pre-treatment levels of methane production were still significant, similar to the trend in BPWSB. When comparing PTL4 to the others, it can be said that PTL4 has highest of methane yield, whereas PTL1 produces the least methane yield. The graphs produced by the different PTLs 1-4, and cellulose showed a normal degradation curve that was similar to the graphs from the BPWSB BMP test, indicating that both tests are valid. In addition, the results of GWSB's BMP testing shown in Figure 5.9, when PTL4 is compared to the others, it could be stated that PTL4 has reach the maximum level of methane production of about 274 ± 39 Nml/gVS as shown in appendix B1 and B2 respectively. Methane yield increased by a higher percentage (%) between PTL1 and PTL2 (11.1%), PTL1 and PTL3 (25.6%), PTL1 and PTL4 (34.8%), PTL2 and PTL3 (13%), PTL2 and PTL4 (21.3%), and PTL3 and PTL4 (7.3%). When the rate of GWSB production is compared to that of BPWSB, the yield of methane produced between the four PTLs is significantly lower, but it is consistent with the BPWSB percentage (%) output. This suggests that the kind of mechanical apparatus used has a substantial impact on how quickly biomass degrades. This agrees with the research of [187], who identified the particle size paradox by re-analysing prior studies and asserted that other factors other than the mean particle size play a vital role which

is due to how quickly particle size affects the relative rate of gas production per unit surface area for smaller particles. The grass waste substrate biomass (GWSB) test results are similar to that of [246] (209Nml/gVS) and [247], who found that grass waste produced 51% methane, which is equivalent to 199, 250 and 256Nml/gVS. These studies contrast with those of [248]–[251], which show a higher biogas yield 332, 368, 372 NmL/g VS and 298 to 467Nml/gVS.

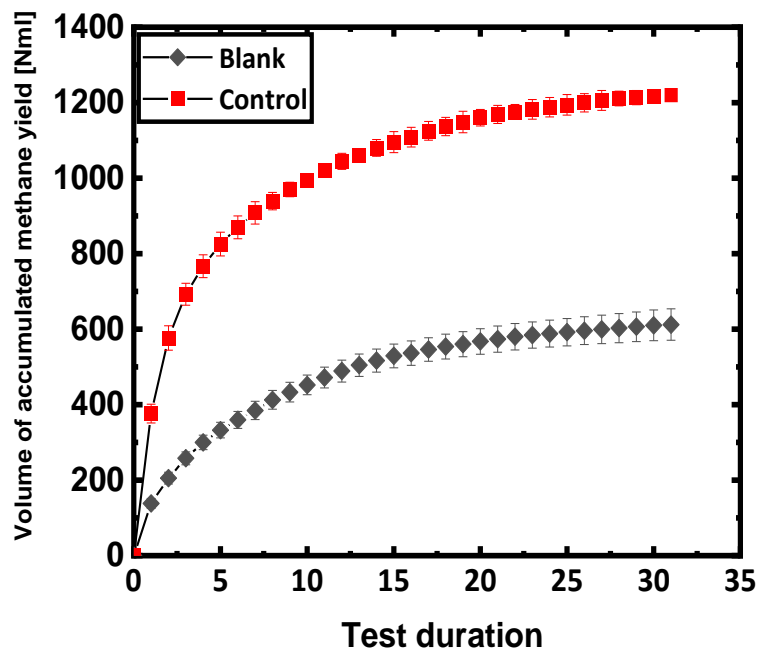


Figure 5.8a&b: Cumulative methane (CH₄) production for a triplicate sample of the blank, contains only 400ml inoculum and for control (cellulose and inoculum) digested during GWSB.

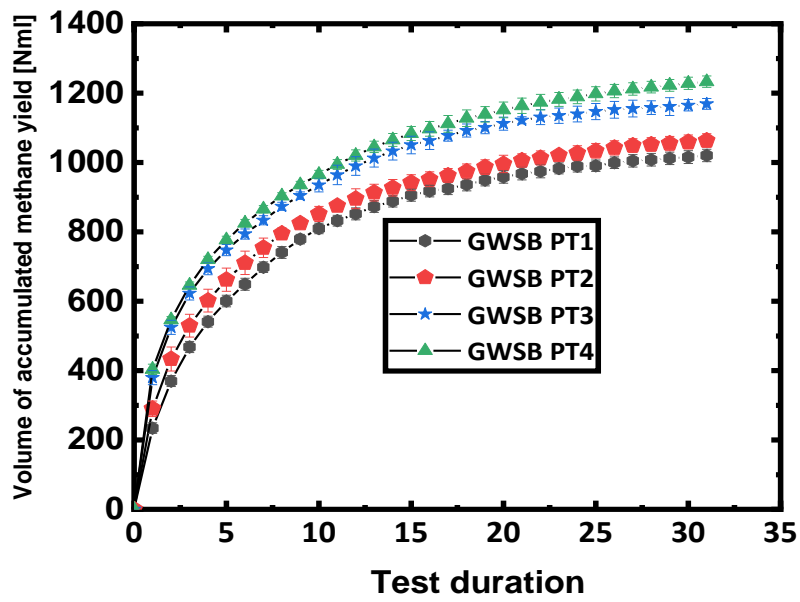


Figure 5.8b Cumulative methane (CH₄) production for a triplicate sample of the GWSB according to their mechanical breakdown pre-treatment levels including calculated measured among of the freshly active inoculum in grams (g).

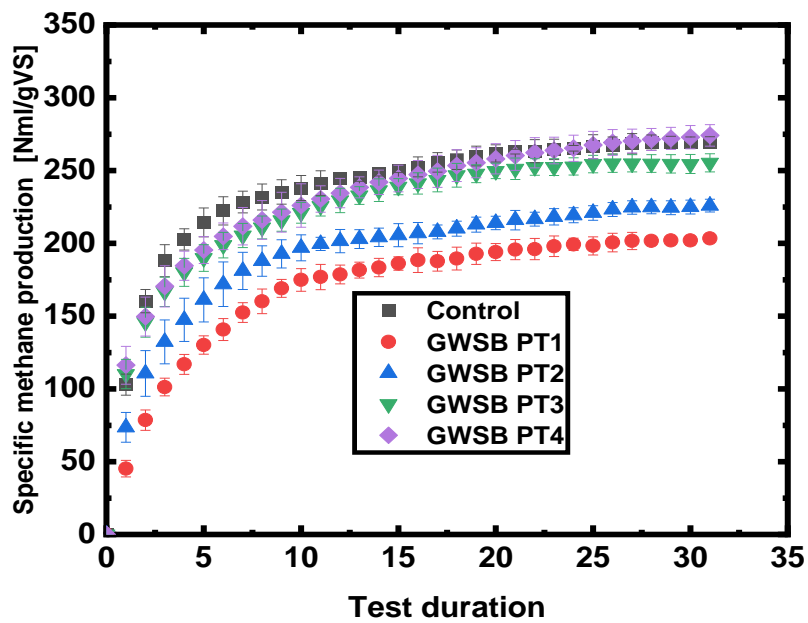


Figure 5.9 Specific methane (CH₄) production for grass waste substrate biomass (GWSB) with average control from triplicates (CH₄) subtracted from the inoculum and data expressed in terms of grams of volatile solid (gVS) added).

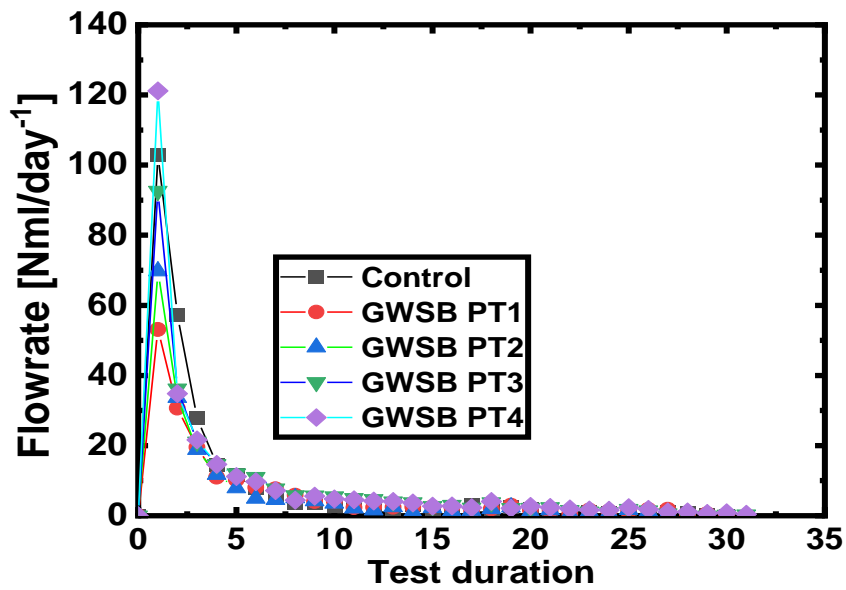


Figure 5.10 Cumulative flow rate and accumulated % volume of the methane production for GPWSB degradation after the subtraction of the inoculum CH₄ production.

Table 5. 7 Maximum biochemical methane (CH₄) achieved from grass waste substrate biomass.

Substrate biomass	Pre-treatment level	Units	BMP result	Inoculum measure	pH after digestion
Control		Nml/gVS	291.5 (0.5)	390	NM
GWSB	PT level 1	Nml/gVS	203.3 (1.1)	373	7.33(0.01)
	PT level 2	Nml/gVS	225.9 (1.4)	375	7.31(0.05)
	PT level 3	Nml/gVS	255.3 (0.8)	380	7.35(0.01)
	PT level 4	Nml/gVS	274.0 (1.4)	386	7.33(0.04)

Table 5. 8 Calculation of the grass waste substrate biomass volatile solids reduction

GWSB (PTLs)	VS			
	initial		Final	
PTL1	18.33	0.1834	9.632	0.09632
PTL2	18.34	0.1834	9.473	0.09473
PTL3	18.34	0.1834	8.692	0.08692
PTL4	18.34	0.1834	8.403	0.08403
AV	18.34	0.1834	9.133	0.09133
Batch anaerobic degradation: Calculated (%) Volatile solid reduction (VSR)				
$(\%) \text{ Volatile solid reduction (VSR)} = \frac{(VS_{Bin} - VS_{digestedout})}{(VS_{Bin} - (VS_{Bin} \times VS_{digestedout}))} \quad \text{where:}$ $\frac{(0.1834 - 0.09632)}{(0.1834 - (0.1834 \times 0.09632))} = \frac{(0.08708)}{(0.1834 - (0.0176651))} = \frac{0.08708}{0.16573} = 52.5\%$				
The amount of substrate biomass Volatile solid (VS) degraded				
PTL1	52.5 %			
PTL2	53.4%			
PTL3	57.6%			
PTL4	59.1%			
AV	55.2%			

5.2.1.1 Calculation of GWSB theoretical calorific value of biomass potential

The results of the GWSB proportion of the CH₄, CO₂, and carbon balance for each PTL are shown in appendix C1 to C4. The GWSB contains 69.7% methane (CH₄) and only 30.3% carbon dioxide (CO₂). Tables 5.9 and figure 5.11 display a comparison plot of GWSB's specific methane output based on both predicted and actual output. Theoretically, PTL4 produces 301 Nml/gVS more biogas than PTL3, PTL2, and PTL1 which like the pattern of the actual specific methane output. This is consistent with the research of [121], [160], [239], [240] where smaller particle sizes enhance the surface area for enzyme attack and optimize the altered material's carbon accessibility and hydrolysis. The results, as shown in Table 5.9 and Figure 5.11, indicate that the theoretical specific methane yield was higher than the actual methane production. Indicators of the %VS destruction can be found in the predicted compared to actual methane production in the digesters. The actual methane and predicted output work as an indicator the % of volatile solid reduction (VSR). Both anaerobic degradation and a specific methane output can increase with a higher volatile solid reduction (VSR) rate. Conversely, lower VSR rates will result in lower methane yield.

Table 5.9 Measured and predicted Maximum specific methane production with respective % volatile solids reduction.

GWSB (PTLs)	BMP experimental	BMP theoretical	% VSR
PTL1	203.3	268	52.5
PTL2	225.9	272	53.4
PTL3	255.3	294	57.6
PTL4	274.0	301	59.1
AV	239.1	283	55.2

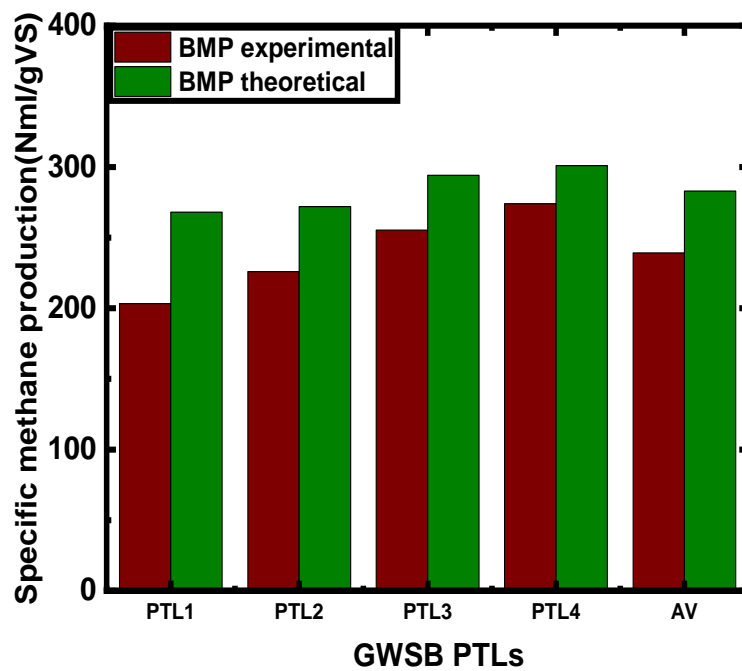


Figure 5.11 Compares the BMP of the GWSB with the theoretical methane yield at STP based on the experimentally determined volatile solids reduction (PTL1-4) and carbon feed material.

5.2.2 Grass waste substrate biomass BMP Kinetics

First order kinetics was used to obtain the parameter values for g and K , whereas the modified Gompertz model was used to obtain the parameter values for g , R and L . SPSS Statistical software was used for both methods. The results are shown in Figure 5.12, Tables 5.10 and 5.11 give the kinetic constants for equations 5.1 and 5.2. Equation 5.1 for the first order BMP kinetics shows a better fit as

compared to the modified Gompertz model presented in table 5.11 for pre-treatment levels 1-4, including the cellulose, with R squared (R²) values of 0.965, 0.994, 0.976, 0.942, and 0.922. The k values for all PTLs are identical, although PTL3 has a higher k value for first order kinetics (0.339). About k-value, the K-value of PTL3 is slightly higher than that of PTL4. This refutes the notion that the size distribution profiles are the only factors causing the disparity and supports previous studies [187] that suggests that factors other than the mean particle size also play significant roles. Similar to the results of BPWSB, Table 5.11 shows that the four PTLs had a relatively short lag time before the microbial organisms started to interact in the digester. A negative time lag (λ) was seen in the results which also holds for BPWSB. These results agreed with those of [241], [242]. The BMP test results also suggest that GWSB can be used as a potential material for anaerobic digestion (AD).

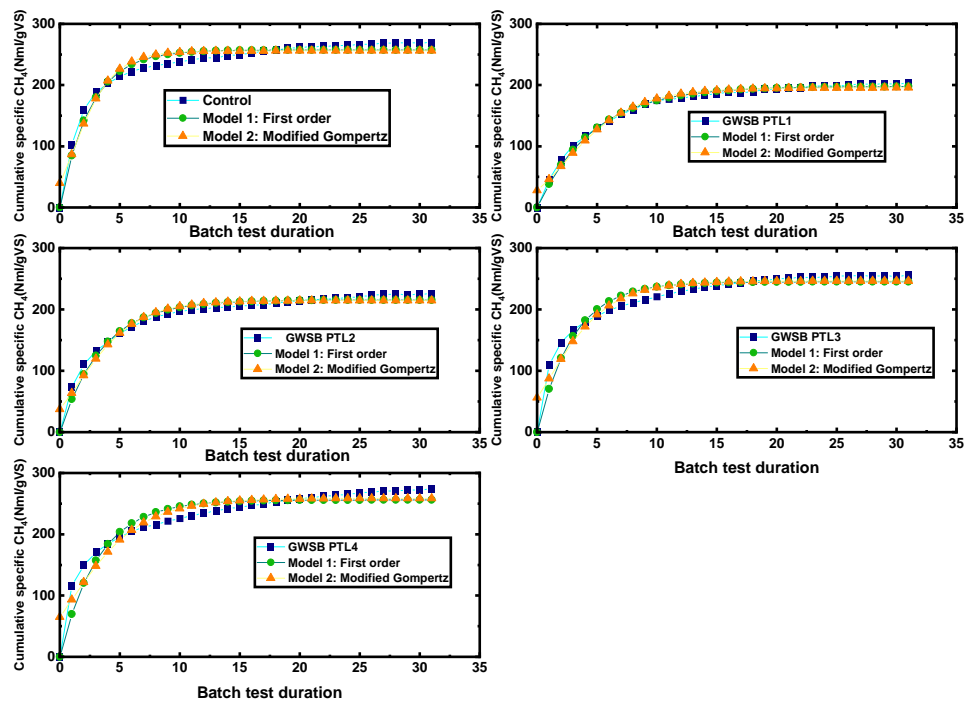


Figure 5.12 Experimental results for GWSB and the kinetics of specific CH₄ production for first order (model 1) and modified Gompertz (model 2)

Table 5. 10 First order kinetic parameters value from BMP modelling

Parameter Estimates					
Parameter	Estimate	Std. Error	95% Confidence Interval		R ²
			Lower Bound	Upper Bound	
Control					R²
g	257.46	2.26	252.83	262.081	965
k	0.401	0.024	0.353	0.449	
GWSB PTL1					R²
g	197.90	1.054	195.75	200.051	994
k	0.216	0.005	0.205	0.227	
GWSB PTL2					R²
g	215.6	1.82	211.9	219.282	976
k	0.289	0.013	0.261	0.316	
GWSB PTL3					R²
g	245.2	2.91	239.3	251.14	942
k	0.339	0.024	0.29	0.389	
GWSB PTL4					R²
g	256.134	3.63	248.7	263.54	922
k	0.318	0.026	0.264	0.371	

Table 5. 11 Modified Gompertz model kinetic parameters value from BMP modelling.

Parameter Estimates					
Parameters value	Estimate	Std. Error	95% Confidence Interval		R ²
			Lower Bound	Upper Bound	
	Control				
g	256.03	2.99	249.91	262.15	938
R	51.34	5.86	39.36	63.33	
L	-0.692	0.315	-1.337	-0.047	
GWSB PTL1					R²
g	195.7	1.9	191.79	199.56	977
R	21.78	1.39	18.95	24.61	
L	-1.1	0.312	-1.739	-0.461	
GWSB PTL2					R²
g	214.7	2.47	209.645	219.75	956
R	28.83	2.594	23.52	34.13	
L	-1.212	0.374	-1.977	-0.447	
GWSB PTL3					R²
g	246.4	3.547	239.144	253.66	922
R	32.024	3.806	24.24	39.81	
L	-1.734	0.526	-2.809	-0.659	
GWSB PTL4					R²
g	258.8	4.32	249.96	267.62	908
R	28.82	3.69	21.27	36.38	
L	-2.241	0.67	-3.611	-0.871	

5.2.3 ANOVA of Grass Waste Substrate Biomass

By comparing the average specific methane yields of the four PTLs 1-4 of GWSB, this study was conducted to determine whether there are any significant

variations. It was hypothesized that PTL4 of GWSB is more likely to yield a higher specific methane yield. The data from the batch test were analysed using an ANOVA with one way between subjects. The results are shown in Table 5.12. PTL4 significantly differs from other PTLs, according to the studies, $F(3,124) = 9.36$, $P=1.26E-05$. The post hoc analysis was carried out using Fisher LSD. According to the studies, PTL4 produced a significantly higher specific methane yield ($M=228.1$, $SD=56.7$) compared to PTL2 ($M =189.4$, $SD=49.7$) and PTL1 ($M=166.5$, $SD=49.4$), while PTL3 ($M =219.7$, $SD=53.6$) differed from PTL2 and PTL1. The specific methane yield, however, did not significantly differ between PTL4 and PTL3. Likewise, no significant differences exist between PTL2 and PTL1. According to the results, PTL1 has the lowest mean methane yield, and PTL4 has the highest specific methane yield when compared to other PTLs because of its larger surface area and lower PS. Box charts and fisher LSD plots were used to show the statistically significant differences between the PTLs (figures 5.13 and 5.14). Thus, increasing PTLs resulted in an increase in methane yield revealing that particle size affects methane yield. This supports the findings of other researchers, who conclude that smaller particle sizes enhance the surface area available for enzyme attack [36], [121], [160], [173], [239], [240]. It is comparable to the finding of the BPWSB.

Table 5. 12 One-way analysis of variance of the grass waste substrate biomass.

Descriptive Statistics					
	N Analysis	N Missing	Mean	Standard Deviation	SE of Mean
GWSB PT1	32	0	166.4738	49.36331	8.72628
GWSB PT2	32	0	189.3748	49.68444	8.78305
GWSB PT3	32	0	219.6887	53.57803	9.47135
GWSB PT4	32	0	228.1058	56.66388	10.01685
One Way ANOVA					
	DF	Mean Square	Sum of Squares	F Value	Prob>F
Model	3	77157.29	25719.1	9.36374	1.26E-05
Error	124	340587.1	2746.67		
Total	127	417744.4			
Fit Statistics					
	R-Square	Coeff Var	Root MSE	Data Mean	
	0.1847	0.26086	52.40868	200.9108	

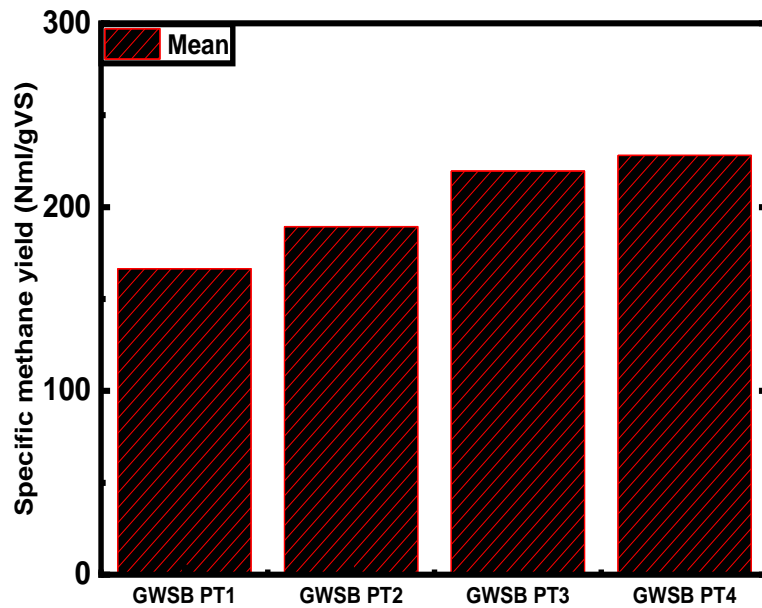


Figure 5.13 Means boxplot of the variation of the methane yield of GWSB four pre-treatment levels.

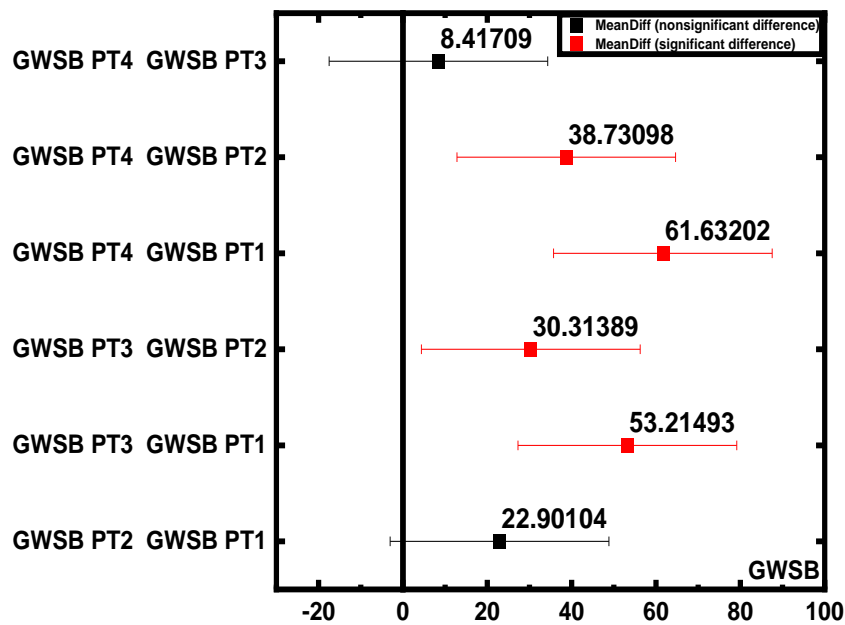


Figure 5.14 Fisher LSD means comparison plot for grass waste methane yield of four pre-treatment levels.

5.3 BMP Assay for Paper Waste Substrate Biomass (PWSB)

Figure 5.15a/b portrays the result of the cumulative methane yield of both the inoculum mechanically pre-treated, figure 5.16 shows specific methane yield of both the inoculum and control, while figure 5.17 presents the flow rate (in Nml/day) of PWSB. Also, their maximum BMP and % volatile solid reduction is presented in tables 5.13 and 5.14 respectively. From the results, it is observed that the pre-treatment levels PWSB followed a similar pattern of methane yield of BPWSB and GWSB, confirming further that particle sizes of feedstocks affect biodegradability and kinetics of waste biomass. However, the maximum yield of 273.8 Nml/gVS from PTL4 proves that paper wastes yielded less than banana peels and grass wastes. The graph of the flow rate clearly shows a peak flow and production at day 1 for all the PTLs, followed by a gradual decline in flow rate for the rest of the HRT. This is very interesting in the sense that the high flow rates reduce retention times on the one hand, thereby facilitates the AD process. On the other hand, it supports excessive production of ammonia which is unfavourable to the system. In addition, the summary of the maximum BMP achieved from the control and four pre-treatment levels of PWSB is presented in table 5.13 and the volatile solids reduction is shown in table 5. 14. According to the findings, PWSB pre-treatment levels yielded methane in a similar pattern to BPWSB and GWSB. Additionally, the results of the PWSB BMP test from the different PTLs 1-4, including the cellulose, yielded results that were similar to those of the BPWSB and GWSB BMP test in terms of shape, supporting the validity of the tests. Figure 5.16 shows the standard deviations and sampling error bars for pre-treatment levels of methane production in substrate biomass, and the result was still significant. When compared PTL4 to the others, PTL4 has the highest methane yield of about 273 ± 29 Nml/gVS. PTL4 produced SMP at rates that were higher than PTL1, PTL2, and PTL3 by 18.5%, 9.2%, and 3.4%. Specific methane yields for PTL3 were approximately 14.6% and 5.9% greater than those for PTL1 and PTL2, and the maximum methane yield for PTL2 was approximately

8.3% higher than that for PTL1. The best method for mechanical pre-treatment depends on the type of lignocellulosic material and mechanical apparatus cannot be proposed as a consistent strategy. The methane yield effects of paper waste PTL4 are similar to those of grass waste PTL4. The value of the methane yields obtained as shown in table 5.13 is similar to the results from [252], who compared 30 and 60 minutes of mechanical pre-treatment of paper waste and reported a 21% increase in methane production from 210Nml/gVS, which corresponds to the untreated paper, to 253 ml/gVS for 60 minutes, and those 30 minutes of pre-treatment had no effect on the methane yield. The results of shredding paper (PTL1) are congruent with those from [253], who found that waste paper yields 220Nml/gVS, and [252] who discovered that non-beaten paper yields 210Nml/gVS. Nonetheless, it does agree that smaller particles are more suited for the AD processes. According to [254], shredding wastepaper and cardboard does not increase the amount of biogas that is produced or the potential of methane. Using a thermophilic cellulose-degrading composite to pre-treat filter paper, wastepaper, newspapers, and cardboard yielded promising results. The pre-treated filter paper, wastepaper, newspaper, and cardboard produced 277, 287, 192, and 231 Nml/gVS of methane after 55 days of anaerobic digestion, respectively, with corresponding increases of 33%, 34%, 156%, and 141% over the untreated materials [255]. The methane yield of untreated paper wastes decreased from 132 NmL/gVS to 107 NmL/gVS as the S/I ratio rose from 0.5 to 0.7 during the wet digestion process, according to a previous report by [252]. Methane yields between 40 and 200 NmL/gVS [256] was observed in earlier research for wet digestion of untreated paper wastes while [257] achieved methane yield of about 229 Nml/gVS, This study's methane yield, which is a little higher than previous yields under wet digestion processes, which ranges from 231 to 274 Nml/gVS. This shows that the response rate and cumulative methane yield are significantly increased by particle size. On the other hand, particle size reduction has been demonstrated to improve gas production for substrates with a high content of fibres and low degradation rate, leading to a lower weight of

residue to be disposed of after digestion [55], [150], [179]. Additionally, it falls within the range of 107 to 369 Nml/gVS [209], [252], [253], [256]–[258] methane yields that have been reported in the literature data.

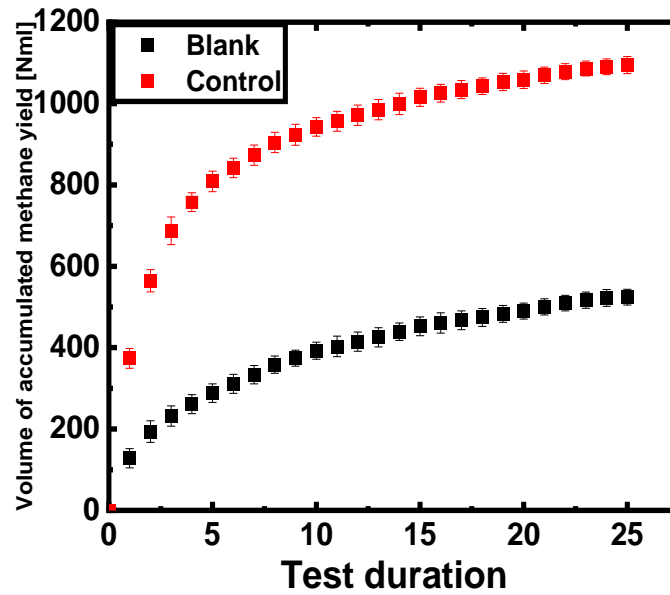


Figure 5.15a &b Cumulative methane (CH₄) production for a triplicate sample of the blank, contains only 400ml inoculum and for control (cellulose and inoculum) digested during PWSB.

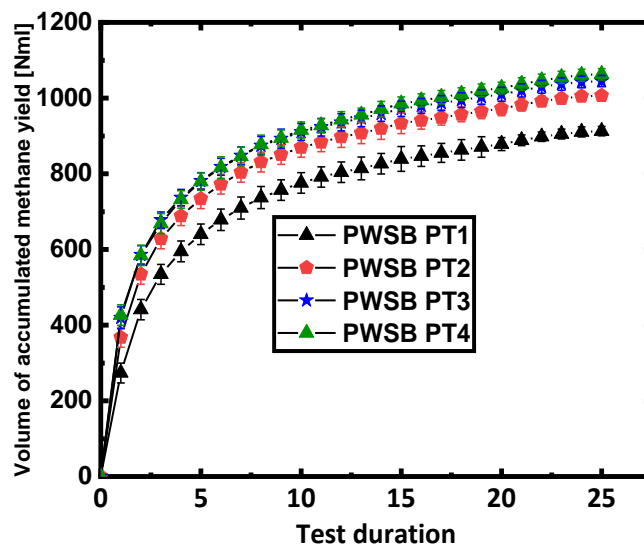


Figure 5-15b Cumulative methane (CH₄) production for a triplicate sample of the PWSB according to their mechanical breakdown pre-treatment levels including calculated measured among of the freshly active inoculum in grams (g).

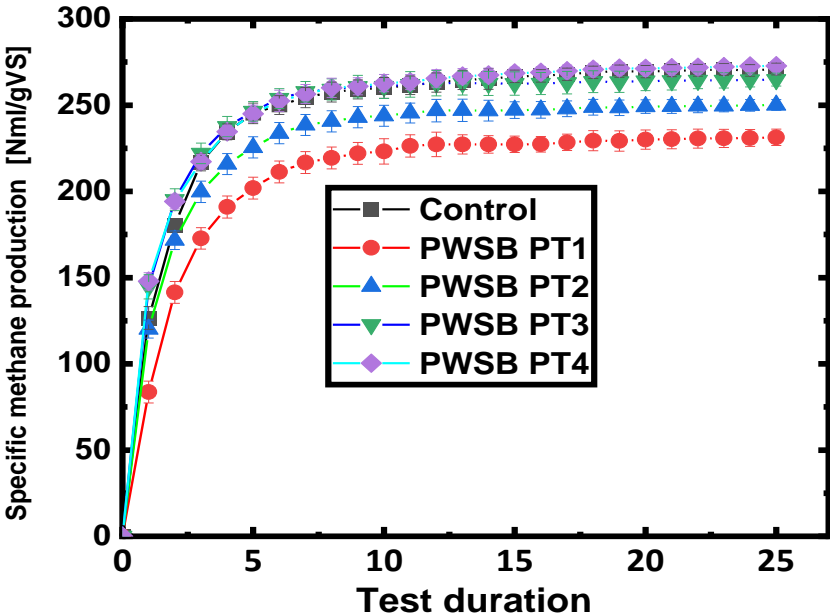


Figure 5.16 Specific methane (CH₄) production for paper waste substrate biomass (PWSB) with average control from triplicates (CH₄ subtracted from the inoculum and data expressed in terms of grams of volatile solid (gVS) added).

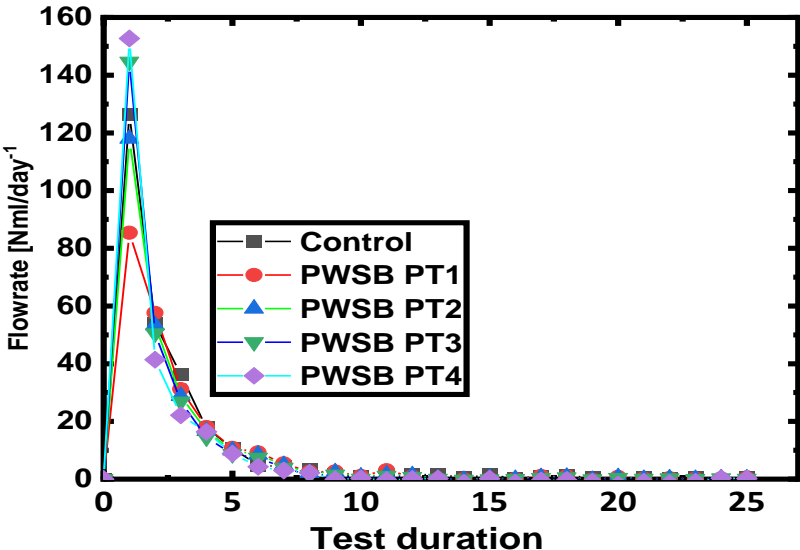


Figure 5.17 Cumulative flow rate and accumulated volume of the methane production for PWSB degradation after the subtraction of the inoculum CH₄ production.

Table 5. 13 Maximum biochemical methane (CH₄) achieved from the paper waste substrate biomass.

Substrate biomass	Pre-treatment level	Units	BMP result	Measure Inoculum (g)	pH after digestion
Control		Nml/gVS	270.9(4.7)	379	NM
PWSB	PT level 1	Nml/gVS	231 (5.6)	373	7.02(0.01)
	PT level 2	Nml/gVS	250.1 (3.4)	379	7.11(0.03)
	PT level 3	Nml/gVS	264..8 (3.7)	383	7.08(0.03)
	PT level 4	Nml/gVS	273.8(2.9)	384	7.13(0.01)

Table 5.14 Calculation of the volatile solid reduction of paper waste substrate biomass ultimate degradation.

PWSB (PTLs)	VS			
	initial		Final	
PTL1	20.33	0.2033	10.822	0.09632
PTL2	20.33	0.2033	10.652	0.09473
PTL3	20.33	0.2033	10.298	0.08692
PTL4	20.33	0.2033	10.087	0.08403
AV	20.33	0.2033	10.465	0.09133
Batch anaerobic degradation: Calculated (%) Volatile solid reduction (VSR)				
$(\%) \text{ Volatile solid reduction (VSR)} = \frac{(VS_{Bin} - VS_{digestedout})}{(VS_{Bin} - (VS_{Bin} \times VS_{digestedout}))}$ where:				
VS _{Bin} percentage (%) of volatile solid (VS) of biomass in the inflow				
VS _{digestedout} percentage (%) of volatile solids (VS) of digested in the outlet				
$\frac{(0.2033 - 0.10822)}{(0.2033 - (0.2033 \times 0.10822))} = \frac{(0.09508)}{(0.2033 - (0.0220011))} = \frac{0.09508}{0.181299} = 52.4\%$				
The amount of substrate biomass Volatile solid (VS) degraded				
PTL1	52.4 %			
PTL2	53.3%			
PTL3	55.0%			
PTL4	56.0%			
AV	54.2%			

5.3.1.1 Calculation of PWSB theoretical calorific value of biomass potential.

The PWSB proportion of CO₂ and CH₄ was calculated using the Buswell equations, as shown in the appendix D1 to D4. The carbon balance feed materials at 3gVS were also computed using a volatile solid reduction (VSR) derived from batch tests based on their

PTLs. PWSB has a methane content of 71.9% CH₄ and 28.1% CO₂. The study discovered that the theoretical value of the maximum specific methane output increases with the rise % volatile solid reduction (VSR). The actual methane output was found to be lower than the theoretical specific methane yield, as indicated in Table 5.15 and Figure 5.18. Hence, the % volatile solid reduction (VSR) is an indicator of the actual versus theoretical methane output in the digesters. A comparison plot of the specific methane output for GWSB based on actual and theoretical data is shown in Table 5.15 and Figure 5.18. Theoretically, PTL4, followed by PTL3, PTL2, and PTL1, has the highest methane output at roughly 287Nm³/gVS. This further supports the findings of previous studies [121], [160], [239], [240] which discovered that smaller particle size results in a larger surface area accessible to enzyme attack, which could boost carbon accessibility and hydrolysis of the treated feedstock. As shown in table 5.15, enhanced anaerobic degradation and a higher specific methane output would lead to higher volatile solid reduction (VSR) rates. On the other side, lower VSR rates will result in reduced methane yield.

Table 5. 15 Measured and predicted Maximum specific methane production with respective % volatile solids reduction.

PWSB (PTLs)	BMP experimental	BMP theoretical	% VSR
PTL1	231	269	52.4
PTL2	250.1	273	53.3
PTL3	264.8	282	55
PTL4	273.8	287	56
AV	254.9	277	54.2

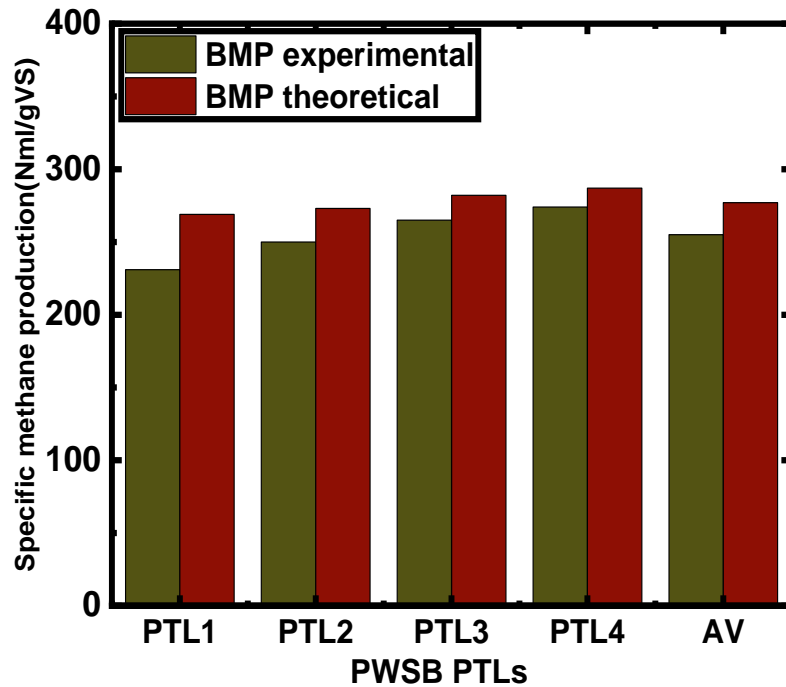


Figure 5.18 Compares the BMP of the PWSB with the theoretical methane yield at STP based on the experimentally determined volatile solids reduction (PTL1-4) and carbon feed material.

5.3.2 Paper waste substrate biomass BMP Kinetics

First order kinetics and a modified Gompertz model were used to determine the parameters for g and k , as well as g , R , and L . Both methods make use of SPSS, a statistical analysis software. The kinetic constants for equations 5.1 and 5.2 are listed in tables 5.16 and 5.17. The results of the predicted PWSB plot are shown in Figure 5.19. Equation 5.1 for the first order BMP kinetics gives a better fit, with R squared R^2 values of 0.956, 0.956, 0.956, and 0.956 when compared to the modified Gompertz model equation 5.2 (table 5.17). The k values for each PTLs are the identical, with PTL4 having a higher k value for first order kinetics because of its large surface area (0.59). Like the results for BPWSB and GWSB, PTL3 trails PTL4 in terms of k -value followed by PTL2 and PTL1. Similar to the outputs of BPWSB and GWSB, Table 5.17 displays the model's results for equation 5.2. The model's output also showed that the four PTLs had a short lag before bacteria began using the substrate.

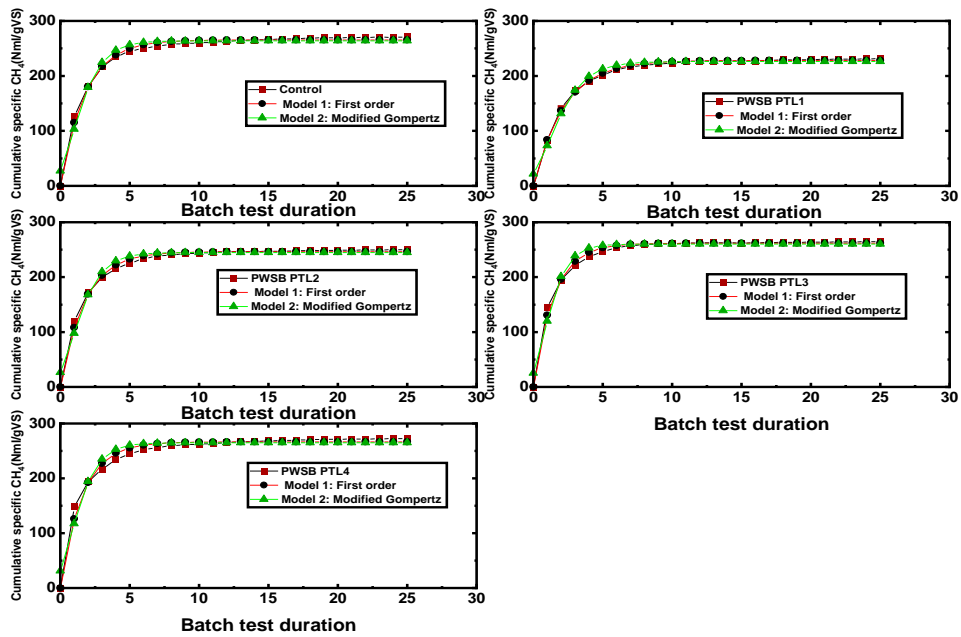


Figure 5.19 Experimental results for PWSB and the kinetics of specific CH₄ production for first order (model 1) and modified Gompertz (model 2)

Table 5. 16 First order kinetic parameters value from BMP modelling.

Parameter Estimates					
Parameters value	Estimate	Std. Error	95% Confidence Interval		R ²
			Lower Bound	Upper Bound	
Control					994
g	265.73	1.063	263.54	267.93	
k	0.568	0.016	0.534	0.602	
PWSB PTL1					998
g	228.37	0.516	227.31	229.44	
k	0.458	0.007	0.444	0.471	
PWSB PTL2					995
g	246.62	0.917	244.73	248.51	
k	0.579	0.016	0.546	0.611	
PWSB PTL3					995
g	261.89	0.944	259.95	263.84	
k	0.693	0.02	0.651	0.734	
PWSB PTL4					985
g	266.59	1.636	263.22	269.97	
k	0.64	0.03	0.578	0.703	

Table 5. 17 Modified Gompertz model kinetic parameters value from BMP modelling.

Parameter Estimates

Parameter	Estimate	Std. Error	95% Confidence Interval		R ²
			Lower Bound	Upper Bound	
Control					
g	263.99	2.19	259.45	268.53	974
R	85.77	7.67	69.91	101.63	
L	-0.206	0.15	-0.518	0.105	
PWSB PTL1					
g	226.40	1.64	222.995	229.79	983
R	60.81	4.25	52.01	69.6	
L	-0.201	0.14	-0.495	0.093	
PWSB PTL2					
g	245.07	2.06	240.81	249.33	973
R	80.14	7.27	65.096	95.19	
L	-0.224	0.15	-0.538	0.09	
PWSB PTL3					
g	260.37	2.09	256.05	264.697	973
R	105.64	10.23	84.47	126.81	
L	-0.138	0.132	-0.41	0.134	
PWSB PTL4					
g	265.04	2.703	259.45	270.64	958
R	94.09	10.84	71.67	116.504	
L	-0.249	0.178	-0.616	0.119	

5.3.3 ANOVA of Paper Waste Substrate Biomass

This study aims to investigate any significant differences in the average specific methane yield between the four PTLs 1-4 of PWSB. It was hypothesized that PTL4 of PWSB is more likely to produce a higher specific methane yield. A between subjects one-way ANOVA was used to analyse the batch test's data. Table 5.18 presents the results. The studies demonstrate that PTL4 significantly differs from other PTLs, $F(3,100) = 2.94$, $P = 0.03693$. Fisher LSD was used to conduct the post hoc analysis. The studies have found that PTL4 produced a significantly higher specific methane yield ($M = 255.21$, $SD = 57.7$) compared to PTL1 ($M = 204.5$, $SD = 53.5$). Likewise, PTL3 ($M = 241.9$, $SD = 56.2$) differed from PTL1 ($M = 204.5$, $SD = 53.5$). However, there were no significant differences between PTL4 and PTL3 and PTL4 and PTL2 in the specific methane yield. Also, no significant differences exist between PTL3 and PTL2 and PTL2 and PTL1. The findings suggest that PTL1 has the lowest mean methane yield, while PTL4 produces the highest specific methane yield compared to other PTLs due to its larger surface area and smaller PS. The statistically significant differences between the PTLs were displayed with

box charts and fisher LSD plots (figures 5.20 and 5.21). The results are similar with those of the BPWSB and GWSB which shows that during batch tests, particle size affects methane yield. The conclusion of the BPWSB and GWSB are comparable.

Table 5. 18 One-way analysis of variance of the grass waste substrate biomass.

Descriptive Statistics					
	N Analysis	N Missing	Mean	Standard Deviation	SE of Mean
PWSB PT1	26	0	204.51	53.54	10.41
PWSB PT2	26	0	225.24	54.58	10.70
PWSB PT3	26	0	241.93	56.20	11.02
PWSB PT4	26	0	245.25	57.67	11.31
One Way ANOVA					
	DF	Sum of Squares	Mean Square	F Value	Prob>F
Model	3	27168.36	9056.12	2.94	0.03693
Error	100	308259.3	3082.59		
Total	103	335427.7			
Fit Statistics					
	R-Square	Coeff Var	Root MSE	Data Mean	
	0.081	0.24221	55.5211	229.2311	

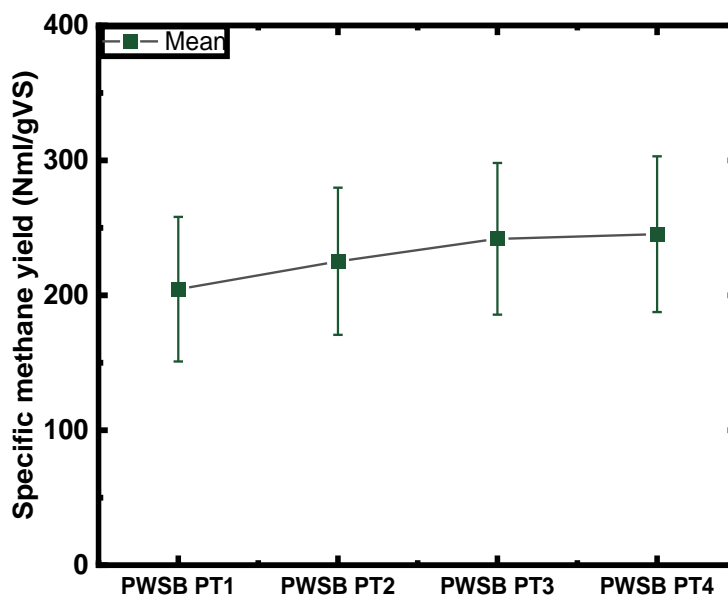


Figure 5.20 Means boxplot of the variation of the methane yield of GWSB four pre-treatment levels.

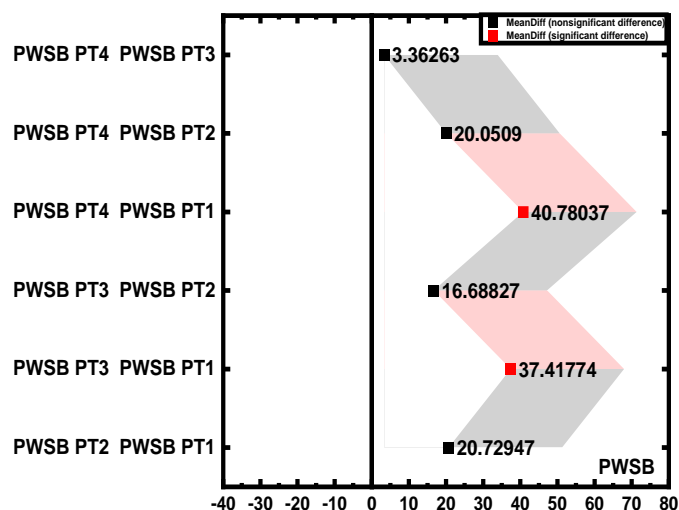


Figure 5.21 Fisher LSD means comparisons plot for grass waste methane yield of four pre-treatment levels.

5.4 BMP Assay for Tomato Waste Substrate Biomass (TWSB)

The batch testing results for the biomethane potential of TWSB are presented from figure 5.22a/b, to figure 5.24. Graphs of Accumulated methane yield, Specific methane yield and flow rate (figure 5.24) all plotted against the test duration are equally presented. The smallest particles (i.e., PTL 4) of the TWSB yielded more methane than other larger particles of the same TWSB. This agrees with [24], [179] and [173] that those smaller particles enhance the AD process. Aside from the above trend, a careful study of the flow rate over retention time shows that the feedstocks of the four PTLs attained their peak flow rate at day 1. This is due to their affinity to the organisms introduced into the batch for digestion. It is apt to take note that after the first 5 days, the flow of methane declined drastically. Hence, a BMP of 294.18 Nml/gVS was achieved from PTL 4 materials, under mesophilic temperature and pH variations as others. Also, the summary of the maximum BMP achieved from the inoculum and four pre-treatment levels of TWSB is presented in Table 5.19 and the percentage volatile solids reduction (VSR) is shown in Table 5. 20. The TWSB BMP test results from the various PTLs 1-4 along with cellulose, which showed the graphs followed a pattern like those from the BPWSB, GWSB, and PWSB BMP tests, further

supported the validity of the tests. BMP profile for the four-substrate biomass typically show a normal degradation curve. Figure 5.23 shows the standard deviations and sampling error bars for TWSB pre-treatment levels, and the result is still significant. PTL4 produces the most methane (294.2 ± 51 Nml/gVS) when compared to the other PTLs. Methane yields from other studies [237], [238], [259]–[262] that range from 199 to 384 NmL CH₄/gVS are comparable to those found in the current study, as shown by Table 5.19. The results found for PTL4 treated with a mincer and a grinder (PTL4), which comprised totally finer particles, are comparable to those of [173], where the particle size (PS) ranged from 1.3 to 20 mm and the most finely chopped particle size (PS) (1.3 mm) yields the maximum methane yield with a volatile solids reduction (VSR) of 60.3%. Methane yield rose from (PTL1) 233.1 Nml/gVS to (PTL4) 294 Nml/gVS with increases of 11.6%, 18.6%, and 26.2% for PTL2, PTL3 and PTL4 respectively. A further increase of 6.2%, 26.2%, and 6.4% in methane output was seen between PTL2 and PTL3, PTL2 and PTL4, and PTL3 and PTL4.

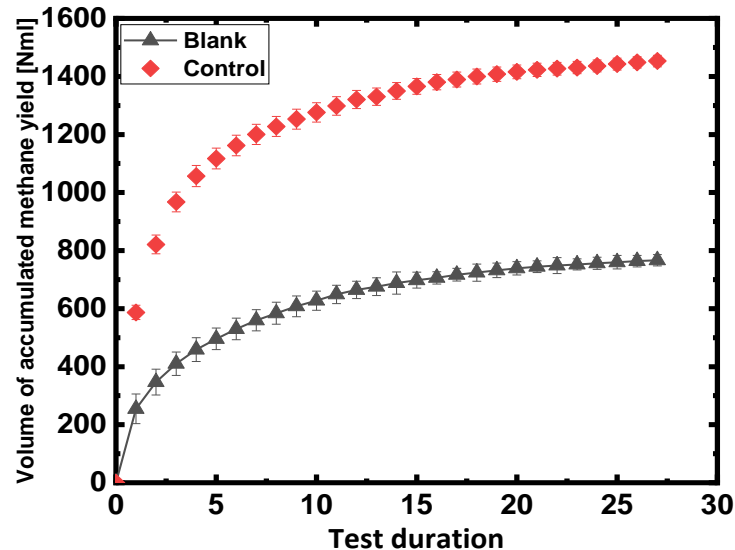


Figure 5.22a&b: Cumulative methane (CH₄) production for a triplicate sample of the blank , contains only 400ml inoculum and for control (cellulose and inoculum).

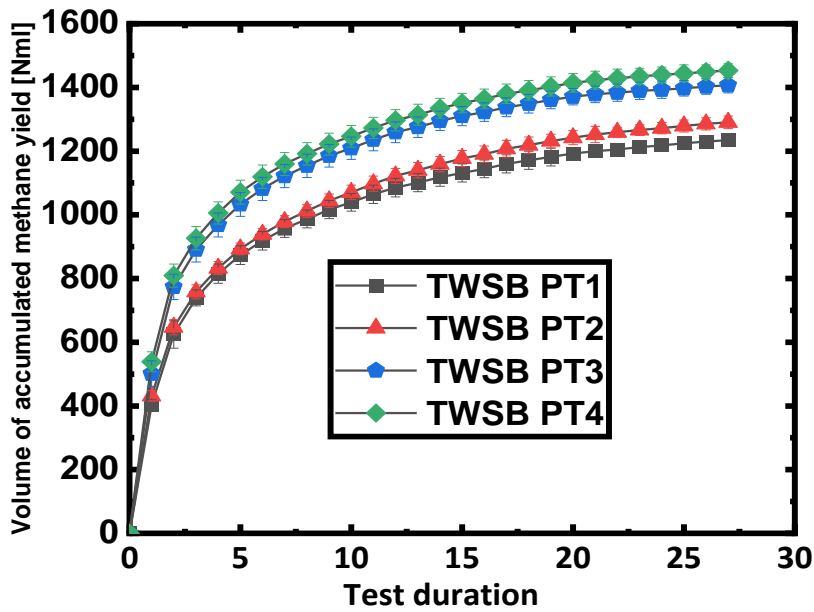


Figure 5-22b: Cumulative methane (CH₄) production for a triplicate sample of the TWSB according to their mechanical breakdown pre-treatment levels including calculated measured among of the freshly active inoculum in grams (g).

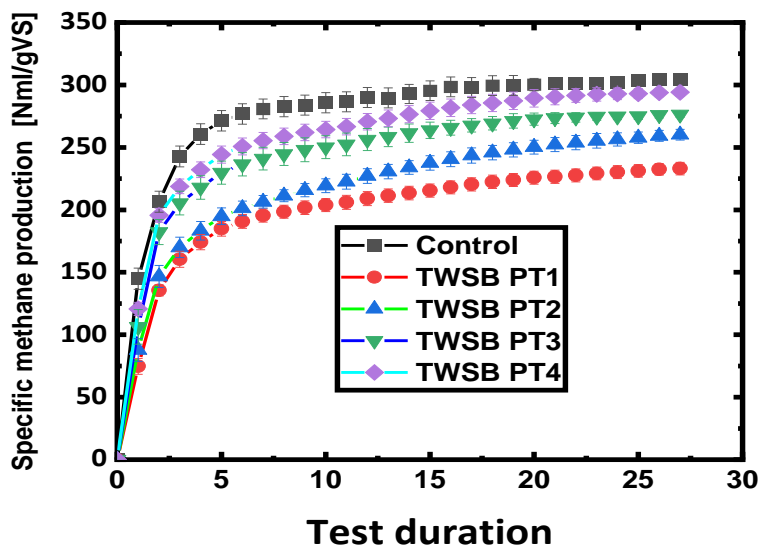


Figure 5.23 Specific methane (CH₄) production for paper waste substrate biomass (TWSB) with average control from triplicates (CH₄) subtracted from the inoculum and data expressed in terms of grams of volatile solid (gVS) added).

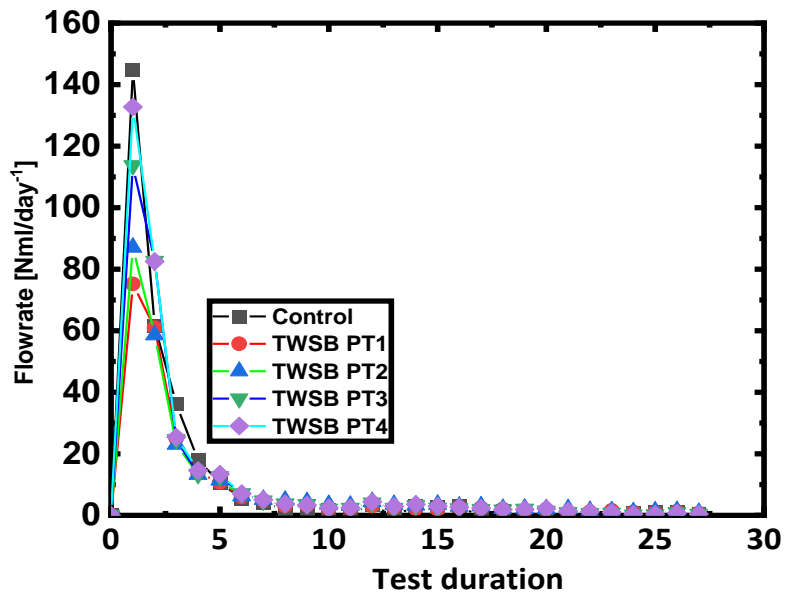


Figure 5.24: Cumulative flow rate and accumulated volume of the methane production for TWSB degradation after the subtraction of the inoculum CH₄ production.

Table 5. 19 Maximum Biochemical Methane (CH₄) Achieved From TWSB

Substrate biomass	Pre-treatment level	Units	BMP result	pH after digestion
Control		Nml/gVS	304.8(4.1)	NM
TWSB	PT level 1	Nml/gVS	233.1(2.0)	7.32
	PT level 2	Nml/gVS	260.2(0.1)	7.36
	PT level 3	Nml/gVS	276.4(1.6)	7.34
	PT level 4	Nml/gVS	294.2(7.0)	7.3

Table 5. 20 Calculation of volatile solid reduction of tomato waste substrate biomass ultimate degradation.

TWSB (PTLs)	VS			
	initial		Final	
PTL1	7.18	0.718	5.176	0.5176
PTL2	7.18	0.718	4.998	0.4998
PTL3	7.18	0.718	4.903	0.4903
PTL4	7.18	0.718	4.841	0.4841
AV	7.18	0.718	4.980	0.4980
Batch anaerobic degradation: Calculated (%) Volatile solid reduction (VSR)				
$(\%) \text{ Volatile solid reduction (VSR)} = \frac{(VS_{Bin} - VS_{digestedout})}{(VS_{Bin} - (VS_{Bin} \times VS_{digestedout}))} \quad \text{where:}$				
$VS_{Bin} \text{ percentage (\% of volatile solid (VS) of biomass in the inflow)}$				
$VS_{digestedout} \text{ percentage (\% of volatile solids (VS) of digested in the outlet)}$				
$\frac{(0.718 - 0.5176)}{(0.718 - (0.718 \times 0.5176))} = \frac{(0.2004)}{(0.718 - (0.346363))} = \frac{0.2004}{0.346363} = 57.9\%$				
The amount of substrate biomass Volatile solid (VS) degraded				
PTL1	57.9%			
PTL2	60.8%			
PTL3	62.2%			
PTL4	63.1%			
AV	61.0%			

5.4.1 Calculation of TWSB theoretical calorific value of biomass potential

The TWSB proportion of both CH₄ and CO₂ is shown in Table 5.30 as calculated using the Buswell equations. The carbon balance of the feed materials at 3gVS was also determined using a volatile solid reduction (VSR) derived from batch tests based on their PTLs, as shown in Appendix E1 to E4. TWSB has a methane content of 69.7% CH₄ and 30.3% CO₂. The results are consistent with those of the BPWSB, GWSB and PWSB. Volatile solid reduction (VSR) affects the theoretical value of the maximum specific methane output. The actual methane output was found to be lower than the predicted output, as shown in Appendix E1 to E2. Indicators of the % volatile solid reduction (VSR) can be found in the predicted compared to actual methane production in the digesters. A comparison graph showing the actual and predicted methane output of TWSB is shown in Tables 5.21 and figure 5.27. Theoretically, PTL4 (287Nml/gVS) produces higher methane than PTL3, PTL2, and PTL1. As shown in table 5.21, more degradation can lead to higher volatile solid reduction (VSR) rates, which in turn produce more specific methane output. Reduced VSR rates, on the other hand, will lead to lower

methane yield. This demonstrates that a high volatile solid reduction yields a higher methane output. The PTLs of the theoretical value and the actual methane yield are shown in Table 5.21, along with their percentage changes.

Table 5. 21 Measured and predicted Maximum specific methane production with respective % volatile solids reduction.

TWSB (PTLs)	BMP experimental	BMP theoretical	% VSR
PTL1	233.1	298	57.9
PTL2	260.2	313	60.8
PTL3	276.4	321	62.2
PTL4	294.2	325	63.1
AV	266.6	314	61.0

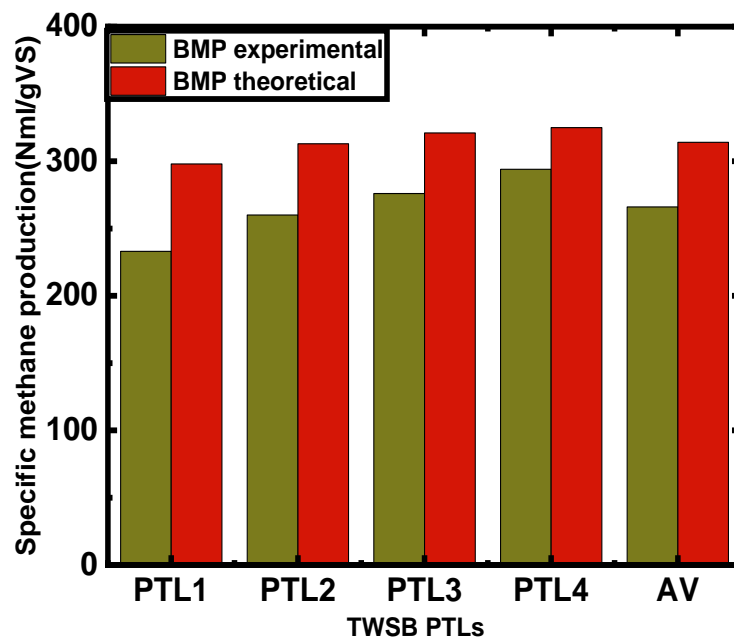


Figure 5.25 Compares the BMP of the TWSB with the theoretical methane yield at STP based on the experimentally determined volatile solids reduction (PTL1-4) and carbon feed material.

5.4.2 Tomato waste substrate biomass BMP Kinetics

A modified Gompertz model and first order kinetics were used to obtain the parameters for g , R and L , as well as g , and k . The statistical software SPSS is used

in both methods. The kinetic constants for equations 5.1 and 5.2 are shown in Tables 5.22 and 5.23. Figure 5.26 displays the results of the predicted and the actual methane output plot of TWSB. Equation 5.1 for first order BMP kinetics offers a better fit than the modified Gompertz model equation 5.2 as shown in table 5.23 to 5.23. PTL4's large surface area allows for a higher k value (0.59), similar to the results of BPWSB, GWSB, and PWSB. PTL1 was higher to PTL2, but PTL3 lagged PTL4 in terms of k-value. Results from the BPWSB, GWSB, and PWSB concur with those in Table 5.23. As a result, it can be claimed that TWSB is a viable fuel for anaerobic digestion (AD).

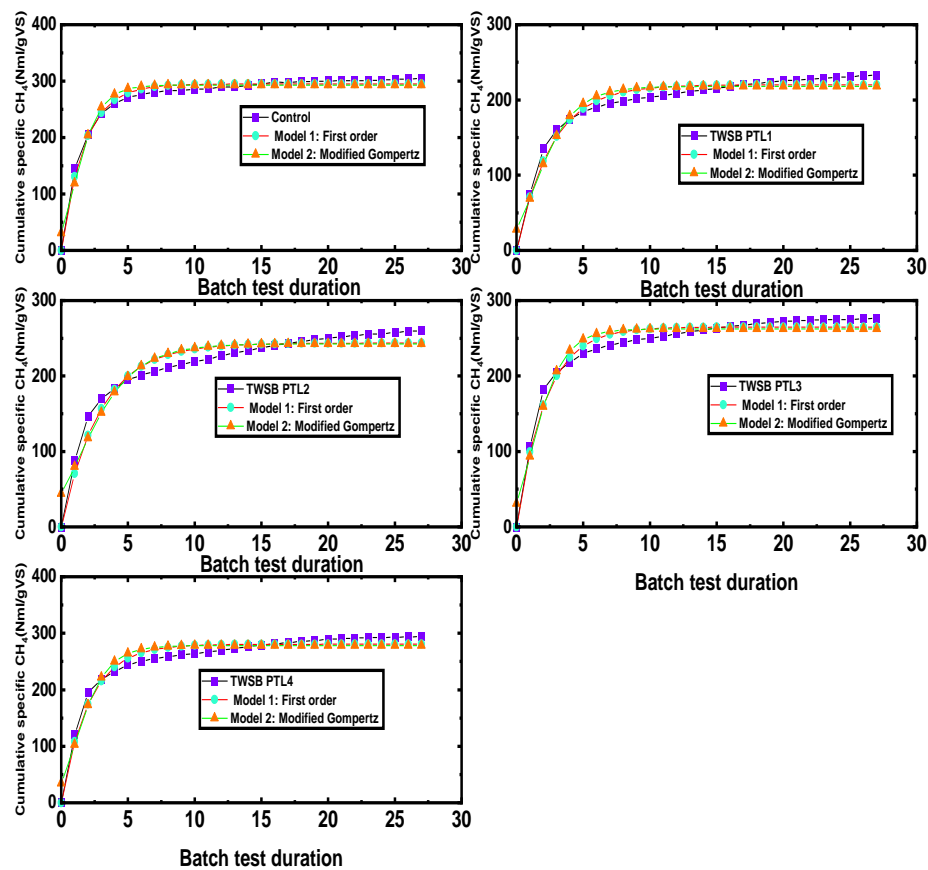


Figure 5.26 Experimental results for TWSB and the kinetics of specific CH₄ production for first order (model 1) and modified Gompertz (model 2).

Table 5. 22 First order kinetic parameters value from BMP modelling.

Parameter Estimates					
Parameters value	Estimate	Std. Error	95% Confidence Interval		R ²
			Lower Bound	Upper Bound	
Control					987
g	295.09	1.572	291.86	298.32	
k	0.586	0.024	0.537	0.635	
TWSB PTL1					971
g	220.40	2.104	216.074	224.72	
k	0.388	0.022	0.342	0.435	
TWSB PTL2					953
g	243.83	3.12	237.42	250.24	
k	0.344	0.025	0.293	0.395	
TWSB PTL3					973
g	265.096	2.257	260.46	269.74	
k	0.471	0.027	0.415	0.527	
TWSB PTL4					967
g	280.76	2.594	275.43	286.094	
k	0.488	0.031	0.424	0.552	

Table 5. 23 Modified Gompertz model kinetic parameters value from BMP modelling.

Parameter Estimates					
Parameter	Estimate	Std. Error	95% Confidence Interval		R ²
			Lower Bound	Upper Bound	
Control					966
g	293.25	2.554	287.99	298.51	
R	98.80	9.87	78.47	119.12	
L	-0.204	0.162	-0.538	0.131	
TWSB PTL1					946
g	218.18	2.812	212.39	223.97	
R	46.83	5.474	35.56	58.107	
L	-0.475	0.298	-1.09	0.139	
TWSB PTL2					946
g	242.834	3.976	234.65	251.02	
R	38.256	4.98	27.999	48.51	
L	-1.09	0.461	-2.039	-0.14	
TWSB PTL3					948
g	262.76	3.076	256.42	269.09	
R	70.50	8.431	53.14	87.868	
L	-0.327	0.244	-0.829	0.175	
TWSB PTL4					946
g	278.47	3.433	271.399	285.54	
R	75.91	9.681	55.97	95.84	
L	-0.356	0.256	-0.884	0.172	

5.4.3 ANOVA of Tomato Waste Substrate Biomass

The goal of this study is to ascertain whether there are any notable variations in the average specific methane yield between the four PTLs 1-4 of TWSB. According to a hypothesis, PTL4 of TWSB are more likely to yield a more specific methane yield. The collected data from the batch test were analysed using a between subjects one-way ANOVA. The results are shown in Table 5.44. The studies reveal that PTL4 significantly differs from other PTLs, $F(3,108) = 5.76$, $P = 0.00107$. The post hoc analysis was performed using Fisher LSD. The studies reveal that PTL4 produced a significantly higher specific methane yield ($M = 255.21$, $SD = 62.4$) compared to PTL2 ($M = 214.7$, $SD = 57.4$) and PTL1 ($M = 196.3$, $SD = 51.5$), while PTL3 ($M = 240.2$, $SD = 59.5$) differed from ($M = 196.3$, $SD = 51.5$). The specific methane yield of PTL4 and PTL3 did not, however, differ significantly. The differences between PTL2 and PTL1 are not significant. The results indicate that PTL4 produces a higher specific methane yield than other PTLs because of its greater surface area and smaller PS, whereas PTL1 has the lowest mean methane yield. Using box charts and fisher LSD plots, the statistically significant differences between the PTLs were shown (figures 5.27 and 5.28).

Table 5. 24 One-way analysis of variance of the grass waste substrate biomass.

Descriptive Statistics					
	N Analysis	N Missing	Mean	Standard Deviation	SE of Mean
TWSB PT1	28	0	196.28	51.47	9.73
TWSB PT2	28	0	214.70	57.39	10.85
TWSB PT3	28	0	240.22	59.46	11.24
TWSB PT4	28	0	255.21	62.39	11.79
One Way ANOVA					
	DF	Sum of Squares	Mean Square	F Value	Prob>F
Model	3	57811.04	19270.35	5.76	0.00107
Error	108	361029	3342.86		
Total	111	418840			
Fit Statistics					
	R-Square	Coeff Var	Root MSE	Data Mean	
	0.13803	0.25515	57.82	226.60	

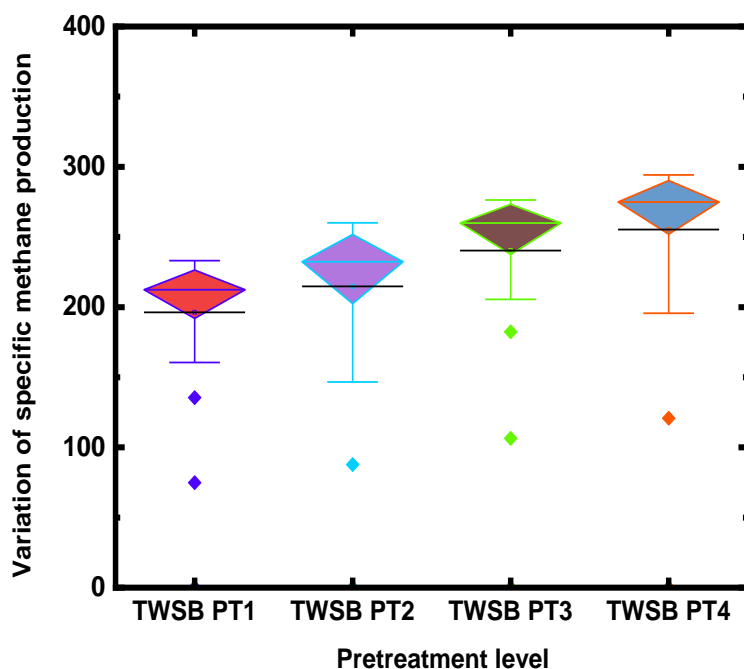


Figure 5.27 Means boxplot of the variation of the methane yield of GWSB four pre-treatment levels.

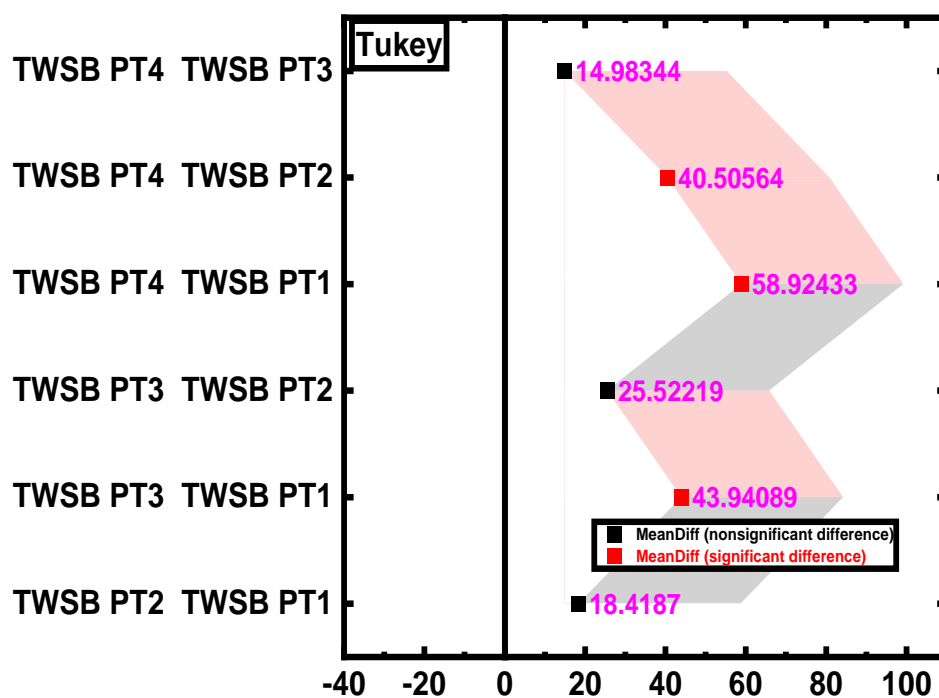


Figure 5.28 Tukey Test Means Comparisons plot for grass waste methane yield of four pre-treatment levels.

5.5 The effects of various mechanical devices on methane yield in biogas

The effects of different mechanical equipment on the production of biogas methane were studied. This study used four different substrates broken down into four PTLs (session 3.4.5) with increasing processing time of 2mins (PTL2) 3mins (PTL3) and 5mins (PTL4). As was previously noted, the substrate's PS size significantly affects how quickly it degrades [178]. The methane output of different particle sizes produced by various mechanical equipment followed a similar pattern: the higher the degradation rate, as a result, the higher the methane output. The methane potential for PTL1 of the non-treated GWSB and TWSB, manually chopped (BPWSB), and shredded (PWSB) feedstocks was tested. The manual chopping of BPWSB coarse material (PTL1) produced a methane production that was roughly 21%, 6.1%, and 5.2 more than that of GWSB, PWSB, and TWSB. The next best performing material was TWSB (non-treated), which outperformed PWSB and GWSB in terms of methane yield by 3.1% and 1%, respectively, while exceeding GWSB by 13.8% in terms of PWSB that had been shred. The biomass from the untreated GWSB produce the least methane. The measured methane output of the BPWSB was found to be much higher at roughly 20%, 8.4%, and 4.2% when compared to the GWSB, PWSB, and TWSB. This resulted from the maceration/mincing technique used to treat PTL2. The TWSB trailed closely after, outperforming the GWSB and PWSB by nearly 15% and 4%, respectively, while the PWSB exceeded the GWSB by 10.6%. The GWSB produce the least amount of methane. The BPWSB also produced significantly more methane than the GWSB, PWSB, and TWSB, at a rate of about 16% 11% 5%. This resulted from the grinding process used in PTL3 treatment. The TWSB outperformed the GWSB and PWSB by roughly 9.1% and 5%, respectively, whereas the PWSB outperformed the GWSB by 4.3%. Methane production is lowest in the biomass from the GWSB. Similarly, compared to the GWSB, PWSB, and TWSB, the BPWSB produced significantly more methane, at roughly 21% 21% 13%. This resulted from the processing of PTL4 using the combination mincer and

grinder methods. The PWSB and GWSB produced the lowest amount of methane. Compared to BPWSB and TWSB, the methane output from TWSB is almost 7.3% higher. This was due to the pre-treatment method's capacity to effectively decrease the material while also destroying the substrate. The size reduction caused an increase in methane production [94], [178]. The least efficient pre-treatment method also led to a rise in biogas production. When the results of the laboratory batch tests are compared, the mechanical pre-treatment methods, which uses a combination of a mincer and a grinder to treat PTL4, produces more methane and results in a higher volatile solid reduction (VSR), as opposed to the grinder and mincer used to treat PTL3 and PTL2, as well as the coarse/chopping/shredding and untreated material (PTL1). A grinder that was used to treat PTL3 material exhibited higher methane output than a mincer that was used to treat PTL2 material. The output of methane from coarse materials did not substantially increase. This is a result of the materials' size. Though, BPWSB that has been manually chopped outperforms the other three substrates in terms of methane yield, followed by TWSB that hasn't been treated, while PWSB that has been shred and non-treated GWSB have much less of an impact on the amount of methane output. When the methane yields for the various substrates were compared, it was discovered that BPWSB and TWSB performed best on average. The lowest amount of methane is produced in GWSB. The average methane production efficiencies for the BPWSB, GWSB, PWSB, and TWSB are shown in Table 5.3. The performances of the substrates at different pre-treatment degrees were compared. The results show that the PWSB did best at Pre-treatment level 1-3, while the BPWSB and TWSB did better overall at pre-treatment level 1-4. Although PTL4 of GWSB and PWSB were identical, GWSB produced the least amount of methane among PTL1-3.

5.5.1 Comparing the responses of the chosen substrates to various treatments in terms of methane yield and volatile solid reduction

Table 5.25 compares the four selected substrates, their responses to the various treatments, and the amount of methane produced. It reveals that the yields of

the untreated TWSB were similar to those of the PWSB that had been shred. The chopped BPWSB were significantly higher compared to those of untreated TWSB containing more smaller PS, GWSB, and shredded PWSB. Untreated TWSB produced significantly more methane than untreated GWSB, while chopped BPWSB produced significantly more methane than shredded PWSB. This could be attribute to substrates' lignin content, which inhibits anaerobic digestion [253]–[255]. The results from the shredded PWSB are like those from [252], [253] which showed that wastepaper yielded 210–217 Nml/gVS, though methane yield was slightly higher as shown in table 5.25 for PTL1. While the result of the minced treatment (PTL2) of TWSB was slightly higher than the PWSB, GWSB produced the least amount of methane, the output of the minced BPWSB was greater than that of the TWSB, GWSB, and PWSB. As evidenced by its high VSR in table 5.25, this showed that the treated materials have a greater impact on the biogas yields and kinetics. The rate of biogas production from minced banana peel was slightly higher than chopped banana peel, and the combined effect of the grinder and mincer was significantly greater than others three PTLs. Although the banana peel that had been ground was much higher than the banana peel that had been chopped and minced. A similar pattern was seen with grind treatment (PTL3), as well as the combined impact of the minced and grinded treatments, as shown in table 5.25. (PTL4) for all substrates. The combined effects of grinding and mincing showed a quick response to the rate of degradability and higher VSR because they produce particles with a greater surface area than the other three treatment methods. These were followed by ground, minced, and untreated TWSB, chopped BPWSB, untreated GWSB, and shredded PWSB, which initially did take a little longer to degrade due to its lesser surface area. On the other hand, as shown in table 5.25, the study's results agree with those of earlier research for the four selected biomass.

Table 5. 25 Comparison of the methane yield of the four-substrate biomass in Nml/gVS.

Substrate biomass	Treatment	PTLs	CH ₄ yield Nml/gVS	% Increase	VSR	% Increase	CH ₄ yield (literature data)	Reference
BPWSB	Manual Chopped	1	266.6	-	60.4		77-336 Nml/gVS	[36], [263]–[268]
	Mincing	2	293.9	10.2	61.9	0.6		
	Grinding	3	318.9	19.6	63.50	1.2		
	Mincing +grinding	4	334.2	25.4	66.70	2.4		
	AV		303.4		63.4			
GWSB	As Collected	1	201.9	-	52.5		117-467 Nml/gVS	[36], [248]–[251], [253], [269],
	Mincing	2	224.5	11.2	53.4	0.4		
	Grinding	3	253.8	25.7	57.4	2.4		
	Mincing +grinding	4	270.3	33.9	59.1	3.3		
	AV		237.6		55.2			
PWSB	Shredded	1	231.0		52.4		107-369 Nml/gVS	[209], [252], [253], [256]–[258]
	Mincing	2	250.1	8.3	53.3	0.4		
	Grinding	3	264.8	14.6	55.0	1.1		
	Mincing +grinding	4	273.8	18.5	56.0	1.6		
	AV		254.9		54.2			
TWSB	As Collected	1	233.1	-	57.9		199-384 Nml/gVS	[237], [238], [259]–[262]
	Mincing	2	260.2	11.6	60.8	1.2		
	Grinding	3	276.4	18.6	62.2	1.8		
	Mincing +grinding	4	294.2	26.2	63.0	2.2		
	AV		266.0		61.0			

5.6 Expected outcome of the batch test

The expected outcomes of the experiment were as follows:

- ❖ Decreased particle size will cause an increase in the ultimate methane potential for the same biomass source.
- ❖ Decreasing the particle size will cause an increase in the total surface area of the solid and the pore volumes [219], [270]. The modification of the lignocellulosic structure, such as the crystalline of the cellulose or lignin distribution as well as allowing higher biological process kinetics through the release of dissolved organic matter [271], [272].
- ❖ Fibrous biomass (e.g., paper), the maximum biogas potential of the fibrous materials will be more strongly affected by pre-treatment.

- ❖ Non-fibrous biomass samples (e.g., Banana peel) are expected to assist other fibrous biomass substrates to speed up hydrolysis steps that are generally accepted as the rate-limiting phase in anaerobic digestion (AD) in the breakdown of the lignocellulosic material. Thereby, the optimisation of this step might have great potential to greatly increase economic profitability.

5.6.1 The following conclusions can be made considering the results:

- ❖ The findings indicate that the same biomass source's greatest methane potential increases as particle size decreases.
- ❖ The results demonstrate that decreasing the particle size increases the substrates' total surface area and pore volumes.
- ❖ The study found that pre-treatment had a significant impact on fibrous biomass, like PWSB, which enhanced the potential for biogas methane output.
- ❖ The study discovered that the biomass samples significantly improve the hydrolysis steps, increasing the AD process's profitability.

5.7 Conclusion

The production of methane over time was similar for all four PTLs of each substrate, with PTL4 degrading more quickly than the other three PTLs. The specific methane output and volatile solids build-up of the four substrates used for the BMP test were the two main variations between them. Similar trends were seen in the flow rates for the four substrate sizes (measured in Nml/day), with PTL4 particles with more surface area producing more methane than PTL3 and 2 and 1 for each substrate. The differences are variations in particle size and substrate composition.

5.8 Semi-Continuous Testing; The effect of mechanical pre-treatment on degradation of complex organic matter

The semi-continuous testing was carried out with a hydraulic retention time (HRT) of twenty days according to each pre-treatment level of the substrate biomass used in the study and the reactor was fed once a day using manual mode. In an experimental semi-continuous test, three substrates were tested. This was done in accordance with their pre-treatment levels (PTLs). The substrates prepared for the batch and semi continuous tests that had been mechanically categorised into four (4) PTLs in session 3.2 (table3.1) were used. The test made use of PTLs 2-4 for each selected substrate for the semi- continuous test. The substrates consisted of grass waste substrate biomass (GWSB), banana peel waste substrate biomass (BPWSB), and paper waste substrate biomass (PWSB). A calculated daily amount of the influent substrates fed into the anaerobic digester with water addition is shown in Table 5.37 to 5.39. The variability of methane production was studied for 60 days for the three different substrates. This choice of trial length is because a shorter HRT is closely correlated with desirable capital cost reduction and process efficiency optimization. According to Rivard et al. [273], polymeric substrates require a digestion time of 60 to 90 days to be fully digested. The effect of particle size distribution on the operation and optimization of the AD process on the different pre-treatment levels and other relevant process parameters on anaerobic digestion of substrate waste biomass in the gas yield were also studied.

5.8.1 Feedstock Characterisation

Detailed characterisation of the three-substrate biomass used in this semi-continuous testing research was carried out. The results obtained from the characterisation of anaerobic digestion feedstocks are presented in tables 4.1 chapter 4. The anaerobic substrate biomass fed into the reactor was made as describe in session 3.6 to avoid a shortage of substrate during the feeding regime. This is to enable a good composition of the feedstock even though some

experimental difference is undeniable. Materials are easily mechanically broken down while some are not (PWSB and GWSB). The Calculated organic loading rates (OLRs) for the three substrates with water addition are shown in tables 5.26 to 5.28. However, the bioprocess laboratory-scale bioreactor was fed on a daily average value for 7-day week with an organic loading rate in wet 3gVS/day and the parameters measured during the semi-continuous testing is shown in table 5.29.

Table 5. 26: Calculated organic loading rate (OLR) of banana peel waste substrate biomass.

Substrate biomass (BPWSB)		
PTL2	PTL3	PTL4
Mass in	Mass in	Mass in
Reactor volume (RV) =1.7L		
Organic loading Reactor (OLR) 3kgVS/m³day		
Feed (f) :3*1.7=5.1		
Feed VS (FVS): 9.090=0.0909		
F/FVS: 56.11 g wet/day		
What about 5 days a week: 2*7/5=2.8		
Digester feed per day: 56.11+ 2.8 = 58.91 g wet/day		
Hydraulic retention Time (HRT): 28.86		
With water addition = Amount of water/day (ml) = 26.094		
Final HRT:RV/ (feed per day +H₂O)/1000 = 20		

Table 5. 27: Calculated organic loading rate (OLR) of grass peel waste substrate biomass.

Substrate biomass (GWSB)		
PTL2	PTL3	PTL4
Mass in	Mass in	Mass in
Reactor volume (RV) =1.7L		
Organic loading Reactor (OLR) 3kgVS/m³day		
Feed (f) :3*1.7=5.1		
Feed VS (FVS): 20.33=0.2033		
F/FVS: 27.81 g wet/day		
What about 5 days a week: 2*7/5=2.8		
Digester feed per day:27.81 + 2.8 =30.61g wet/day		
Hydraulic retention Time (HRT): 55.5		
With water addition = Amount of water/day (ml) = 54.39		
Final HRT: RV/ (feed per day +H₂O)/1000 = 20		

Table 5. 28: Calculated organic loading rate (OLR) of paper waste substrate biomass.

Substrate biomass (PWSB)		
PTL2	PTL3	PTL4
Mass in	Mass in	Mass in
Reactor volume (RV) =1.7L		
Organic loading Reactor (OLR) 3kgVS/m³day		
Feed (f) :3*1.7=5.1		
Feed VS (FVS): 20.33=0.2033		
F/FVS: 25.09 g wet/day		
What about 5 days a week: 2*7/5=2.8		
Digester feed per day:25.09 + 2.8 =27.89g wet/day		
Hydraulic retention Time (HRT): 60.96		
With water addition = Amount of water/day (ml) = 57.113		
Final HRT: RV/ (feed per day +H₂O)/1000 = 20		

Table 5. 29: Parameters measured during semi-continuous testing.

Physical And Chemical Parameters	Frequency	Reference
PH	Twice each week	[218]
Total Alkalinity (TA), Partial Alkalinity (PA) And Intermediate Alkalinity (IA)	Twice each week	2320B [218]
Total Solid (Ts) And Volatile Solid (VS)		[205]
Anaerobic Biogas Flow	Daily	Automatic Bioprocess
Biogas Composition	Daily	Automatic Bioprocess
Volatile Solid Destruction Measure (VSD)	Twice each week	

All digesters were initially inoculated and subjected to batch mode digestion until the stability of biogas production. The daily loading rate started with pre-treatment level 4 in the first 20 days. This was done for the anaerobic microbial organisms to feed on the substrate and improve the anaerobic degradability. After the first 20 days, the digester is fed with pre-treatment level 3 followed by pre-treatment level 2. Before feeding the freshly anaerobic substrate biomass for each substrate, an equal amount of digestate was withdrawn daily. This was done to maintain the recommendation headspace (300ml) by bioprocess and to avoid failure of the AD system while allowing the biomass substrate to have a vigorous mixture to promote the activity of a microbial organism in the bioreactors, to enhance the rate of methane production as well maintaining a constant volume of the bioreactor. The bioreactor system is well built with mechanical stirrers, and this presents an opportunity also for acclimatization of the freshly filtered digestate in the same vessel. The bioreactors were run in duplicate, and each duplicate was represented in the discussion according to its description, as shown in table 5.30.

Table 5. 30: Duplicate reactor used for semi-continuous testing of three substrate biomass degradation.

Bioreactors	Days of feeding			Substrate Biomass	Feeding sequence
	(1-20d)	(21-40d)	(41-58d)		
R1	PT4	PT3	PT2	GWSB	PT4 PT3 and PT2
R2	PT4	PT3	PT2	GWSB	PT4 PT3 and PT2
R3	PT4	PT3	PT2	BPWSB	PT4 PT3 and PT2
R4	PT4	PT3	PT2	BPWSB	PT4 PT3 and PT2
R5	PT4	PT3	PT2	PWSB	PT4 PT3 and PT2
R6	PT4	PT3	PT2	PWSB	PT4 PT3 and PT2

5.9 Grass Waste Substrate Biomass

5.9.1 Biogas output methane production of the GWSB

The results show that a temperature shock occurs for the semi-continuous test incubation digesters (R1-R2) around day 22/23, and the methane content of the biogas decreases significantly. This could be explained by the nature of the substrates and the pattern of the feed. The methane content of the biogas produced increased steadily after the system recovered, with peaks and drops as PS decreased over time. Figures 5.29 show the percentage (%) and daily average production of methane (CH₄) from semi-continuous testing of GWSB, respectively. Appendix F1 shows the experimental results, which show a daily average biogas methane flow rate of about 1149 ml/day for 9 weeks. Figure 5.33 clearly shows how HRT has affected biogas production. The biogas methane (CH₄) content was found at his peak on day 8 which is about 68.5% for R1 and on day 3 about 67.4% respectively for R2. The minimum biogas methane (CH₄) content was found on day 23 which is about 25.5% for R1 and on day 23 about 30.3% (R2). The lowest biogas methane (CH₄) content was discovered on day 23, which is around 25.5% for R1 and approximately 30.3% (R2). Methane output from biogas was seen to be fairly steady over time. The biogas methane content of R2 were more stable than R1. The results also show that PTL4 processed for five minutes in a combined effect of a mincer and grinder yields the peak biogas methane content for R1 and R2, respectively. PTL4 may have broken down more quickly and the concentration of methane (CH₄) in the biogas may have increased due to the increased activities and population of microorganisms in both R1

and R2. The available surface area may have contributed to the peak biogas methane concentration seen in R1 and R2. Also, the spikes in PTL4 may be due to smaller PS being digested more quickly. Even so, biogas methane content production gradually reduced with time though not distinctly. This could be attributed to being the frequency of the particles size distribution from pre-treatment level 4, followed by pre-treatment level 3 with HRT 21 -40 days and pre-treatment level 2 with HRT 41-58 days. Biogas produced by PTL3 grinders, which have larger PS with lesser surface area, had a much-reduced methane content. The biogas may have been affected by HRT due to larger PS which take longer time digest. The biogas's methane concentration rose after days 23 and 49 (R1 and R2) because of the particle size distributions in PT3 and PT2, which gradually reduced over time and made it simpler for the microbe to acclimatize. The proportions of biogas methane (CH₄) in the test samples of grass waste substrate biomass (GWSB) were 55.1% for R1 and 58.9% for R2. Typically, biogas made from grass waste substrate biomass (GWSB) contains 57% methane (CH₄). This implies that anaerobic digester was working correctly. The effect of hydraulic retention time (HRT) on the anaerobic digestion of wheat straw was also noted by [274]. Using HRT of 20, 40, and 60 days, the results showed that the average biogas production was 46.8, 79.9, and 89.1 mL/g total solid as well as 55.2, 94.3, and 105.2 mL/g volatile solids, respectively. The HRT of 20 had the lowest methane contents of the three reactors, ranging from 14.2% to 28.5%. A 20-day HRT for the anaerobic digestion of maize was also reported by [275]. The present results support [276] 's assertion that when the HRT was less than 2 days, the anaerobic sequential batch reactor treating a dilute waste stream did fail because the HRT was too short to allow for microorganism growth to exceed the limits.

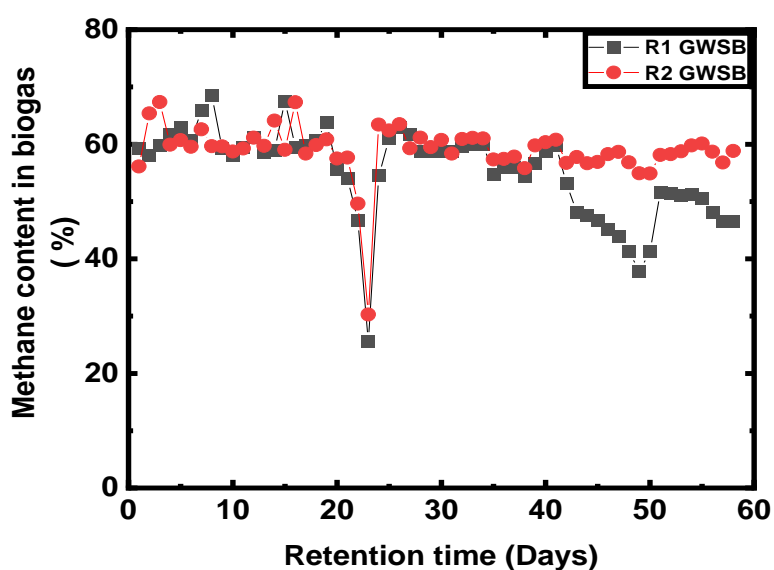


Figure 5.29: Percentage biogas methane CH₄ content produced from the degradation of GWSB (R1 and R2).

5.9.2 The specific production rate of methane (CH₄) in semi-continuous testing of GWSB

The result of specific methane production for the GWSB bioreactors is shown in figure 5.30. Specific methane production for both reactors rose from 211.3 Nml/gVS to 333 Nml/gVS within the first five (5) days of the experiment. Thereafter methane yield declined in both reactors to about 280Nml/gVS. The initial increase in methane production up to 333Nml/gVS could be due to the degradation of the readily organic component of the grass waste. The specific methane yield significantly dropped to 67.8 Nml/gVS at the start of PTL3, after which both reactors recovered. Again, large PS with lesser surfaces are to account for the decline in methane production since they take more time to digest and affect the biogas output. As a result, HRT affected the amount of methane produced by biogas. Also, it can be due to temperature shock. Specific methane production was relatively higher in R2 as compared to R1, and this trend was consistent for the duration of the experiment. This tends to suggest that the digestion processes for R2 worked better. It is impossible to conclude

that a shorter HRT influenced the production. It can be observed that after the start of PTL3, R1 and R2's specific methane production could no longer remain steady. A decline from 255Nml/gVS to 200Nml/gVS was observed for R2 while 250 Nml/gVS to 200Nml/gVS was observed for R1 following the commencement of PTL2 to the termination of the experiment. The decrease in the specific methane yield when PTL3 is added to the digester is like the behaviour observed when the digester is fed with PTL2. This development has showed that beyond a certain level, further particle size reduction of lignocellulosic substrate does not ensure the corresponding yield in biogas. Large PS take longer to digest, which suggests that HRT affects the production of biogas. Methane-producing archaeobacteria regenerate more slowly than acidogenesis and hydrolase-producing bacteria. To prevent methanogens from being washed away, HRT needs to be long enough. According to [276], the failure of the anaerobic sequential batch reactor treating a diluted waste stream was caused by the HRT being too short to allow microorganisms to multiply over their limiting thresholds. As shown in figure 5.31, the biogas output was affected by HRT. Additionally, the production of biogas may not match the PTLs due to the mechanically processed materials being fed into the digester in a sequence of smaller (more) to larger (less) particle size reduction (PSR). The specific methane production rate decreases in both bioreactors between day 40 and 60. The possible explanation of the reduction in methane production could be the feeding of PTL2 which has a larger size distribution than PTL3 and PTL4. During the period, PTL2 undergoes degradation to PTL3, and then to PTL4. Figure 5.31 shows that PTL4 and PTL3 produce more biogas than PTL2, which produces the least amount. This suggests that, even though the digester was affected by HRT, reduced particle size and a related increase in the surface area have made organic material more accessible for microbial breakdown, hence boosting the biogas output. The average specific methane production of grass waste substrate biomass is shown in Figure 5.31 along with standard deviation error bars. PTL4 has the highest effect on specific methane as shown in figure 5.31, with a specific methane of 321 ± 30 Nml/gVS. From the graph, methane production almost reduced to 50 Nml/gVS, because of the influence of HRT

and temperature shock. PTL4 had the greatest methane production rate from the daily feeding, followed by PTL3 and PTL2, in that order. Previous research has shown that changing the feeding sequence can increase operational stability while also changing the diversity, dynamism, and evenness of the microbial communities [277]. Studies by Lemmer and [278]–[280] have explored how changes in feed affected the biogas production rate in terms of rise and fall of biogas over time.

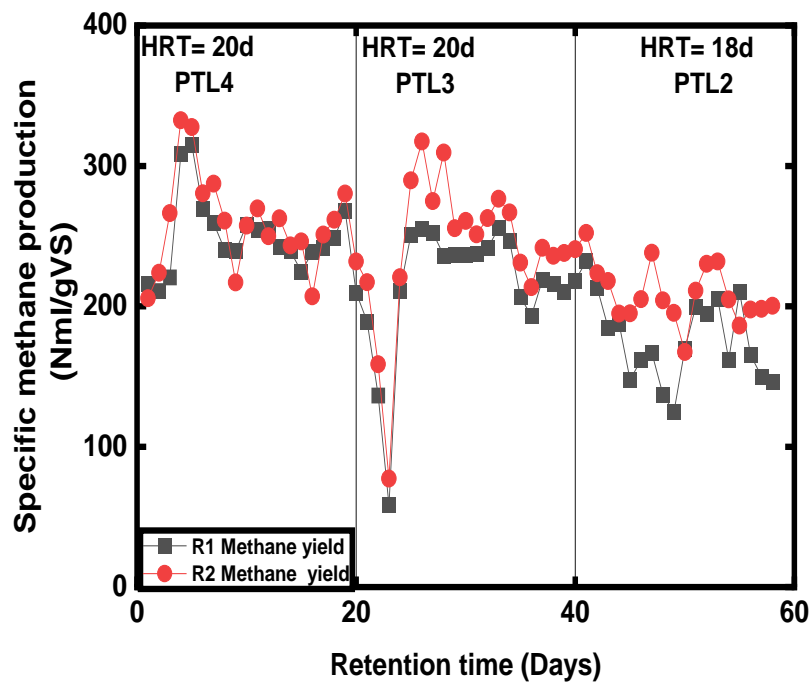


Figure 5.30: Semi-continuous testing showing specific CH₄ production of GWSB (R1 and R2).

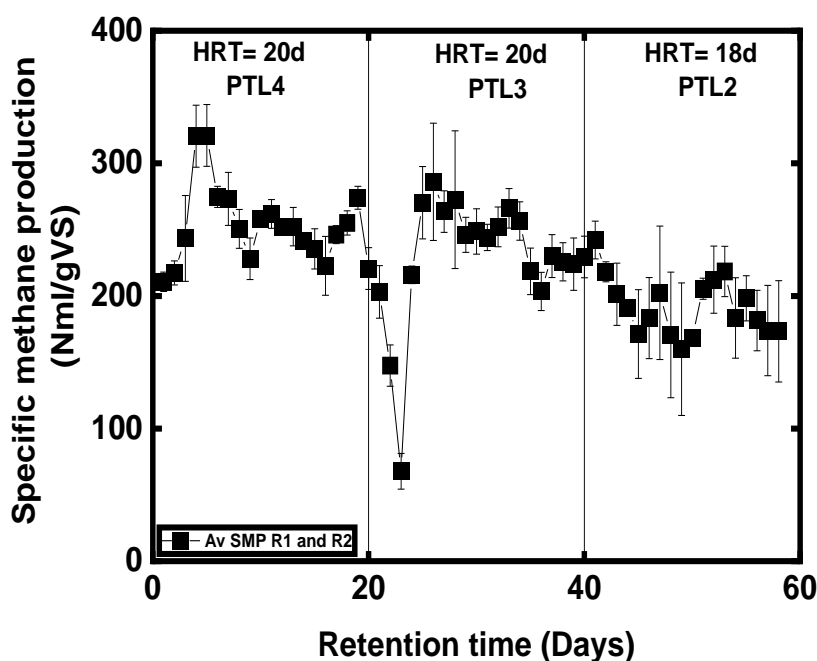


Figure 5.31: Semi-continuous testing showing average specific CH₄ production from GWSB in a bioreactor (R1 and R2).

5.10 Banana Peeled Waste Substrate Biomass

5.10.1 Percentage and Average Methane Production Rate of BPWSB

The results of the semi-continuous test of the BPWSB biogas methane (CH₄) content are shown as a percent (%) in figures 5.32. On days 23 for reactors R3 and R4, temperature shock caused the biogas's methane content to drop significantly. Both the composition of the substrates and the order of the feed could explain this. The daily average methane in biogas flow rate for the nine weeks was about 1102ml/day (see appendix F2). The results reveal that HRT had an impact on the biogas methane content. Methane (CH₄) content was found to be present in about 69% of the biogas produced by reactor R3 on day 5 and roughly 64% of the biogas produced by reactor R4 on day 18. On day 23, reactor R3 produced about 31% of the biogas' methane content, whereas reactor R4 produced about 30%. The highest biogas methane content of reactor R3 and R4 falls

within PTL4 which has more fine particles (PS) while PTL3 has lowest amount of biogas methane concentration as shown in figure 5.32. When the digester was fed with larger particle size (PS) processed using a grinder (PTL3) and mincer (PTL2), a reduced in the amount of biogas produced was observed with each of the feed PTLs tested. Because of the microbial attack on their surfaces, the three PTLs of the BPWSB were considered to differ from each other. Several studies have shown that when particle size increases, the surface area exposed to the bacteria to produce biogas reduces [178], [186], [212]. This was demonstrated by the fact that PTL4 digesters processed using a combination of a mincer and a grinder for five minutes produced a higher biogas methane (CH₄) content than PTL3 and PTL2 digesters. This agrees with existing literature [36], [173], [176], [178], [183], [209], [281]–[284] that the smaller particles contribute more to biodegradation in terms of their specific surface area than the larger particles. Because, it has been concluded by the researcher, that biodegradation hydrolysis of substrate biomass is a surface-related mechanism since most of the hydrolytic anaerobic microbial organism is said to be attached to the surface of the biomass substrate during degradation using extracellular enzymes. After day 20, when the digester is fed with a larger PS, methane output starts to decline (PTL3).

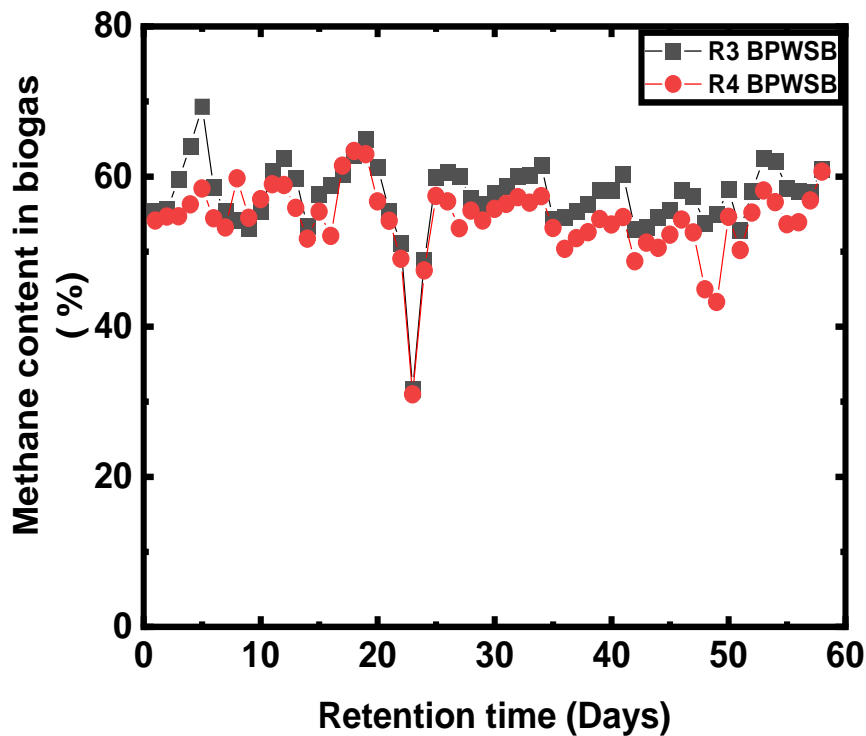


Figure 5.32: Methane (CH_4) content of biogas production of the degradation of BPWSB (R3 and R6)

5.10.2 The specific production rate of methane (CH_4) in semi-continuous testing of BPWSB

The specific methane output for BPWSB for reactors R3 and R4 is shown in figure 5.33. The result reveals that, despite the two reactors' output trends being identical, R3's methane flowrate was consistently higher than those of R4 throughout the test. The specific methane production for R3 rose from 201 Nml/gVS to 291 Nml/gVS during the first five (5) days of the experiment, and for R4, it rose from 176 Nml/gVS to 252 Nml/gVS on the eleventh (11) day. Methane flow rates for both reactors fell by more than 50% between days 23. This could be the result of a significant shift in the system's kinetics after the start of pre-treatment level PTL3 or because of the destabilisation of the AD system discussed in session 5.6.1. A similar drop-in methane flow rate was also observed around day 45 for reactor R4 following the commencement of pre-treatment level PT2.

After day 23, when the reactor was recovered, the digester was fed with required amount of PTL3, R3 continued to produce methane. From day 30 to day 47, the methane flowrate in reactor (R4) consistently decreased, suggesting that some of the substrate biomass had been washed off. As a result, it was evident that HRT had an impact on the amount of methane produced which also holds for GWSB. According to [276], the failure of the anaerobic sequential batch reactor treating a diluted waste stream was caused by the HRT being too short to allow microorganisms to multiply over their limiting thresholds. It is also observed from both reactors that the commencement of a new pre-treatment level was always followed by a sudden decline in the specific production rate of methane. Both R3 and R4 exhibit a similar trend in biogas output by responding to the changing feed with a sudden rapid fall after each feed PTLs. There was a decrease in reaction to the fed of reactor with PTL3 and PTL2, followed by a fair consistent increase. This can be explained by the PTLs' feeding sequence, as shown in table 5.29, and the physiochemical properties of the substrate. The larger particles take longer to digest and will consequently have an extended effect on the biogas rate of production. The anaerobic digestion of the smaller particle size (PTL4) produces the peaks in the biogas output after feeding. Besides the disturbance in the kinetics of the reactor, a change in the microorganism's food ratio could also cause a decline in the specific production rate of methane. The observed results showed that PTL4 material, which was processed for five minutes using a combination of a mincer and a grinder, had a higher specific methane production than PTL3 (grinder) and PTL2 (mincer) while PTL2 had the lowest specific methane output. The average specific methane production of BPWSB is presented in figure 5.34 along with standard deviation error bars. PTL4 achieved a specific methane yield of $262 \pm 21 \text{ Nml/gVS}$ and has the highest effect on biogas production. With peaks and troughs in methane output, daily PTL4 feeding of the digester promotes the methane production to continually increase. PTL3 achieved roughly $254 \pm 12 \text{ Nml/gVS}$, while PTL1 had the lowest methane output at approximately $229 \pm 28 \text{ Nml/gVS}$.

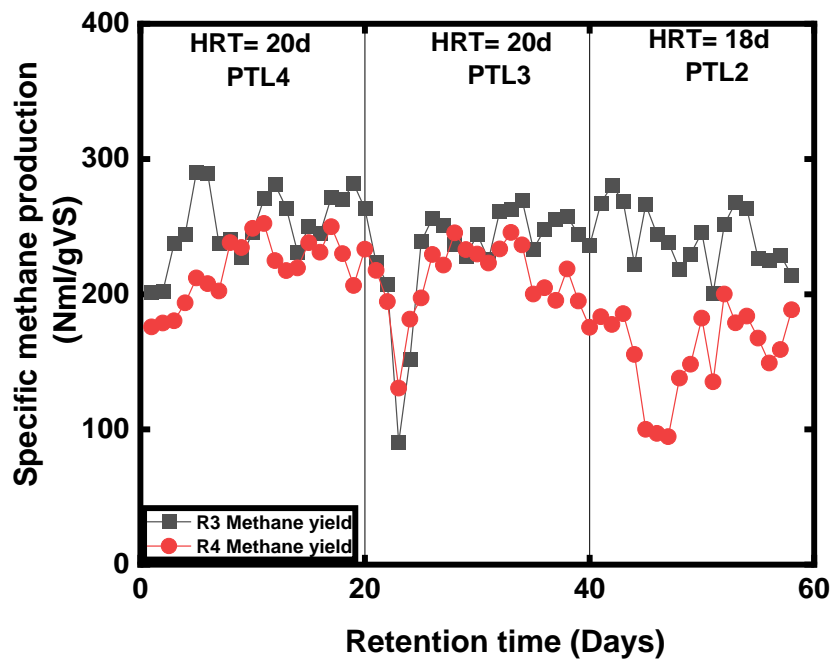


Figure 5.33: Specific methane (CH₄) production of the degradation of BPWSB (R3 And R4).

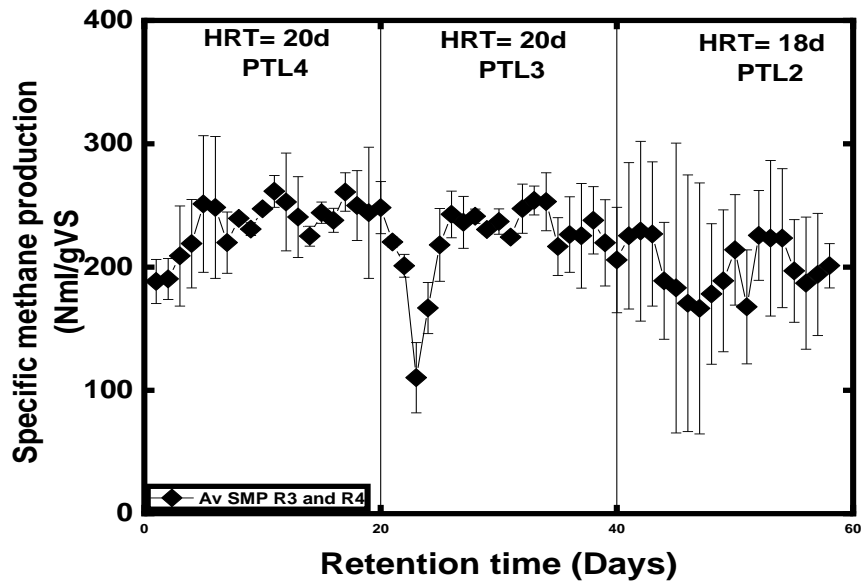


Figure 5.34: Semi-continuous testing showing average specific CH₄ production of BPWSB degradation.

5.11 Paper Waste Substrate Biomass

5.11.1 Percentage and average production rate of paper waste substrate biomass

The results from the lab-scale analysis of paper waste substrate biomass are displayed in figures 5.35. Appendix F3 shows that the daily average flowrate of biogas methane output is around 955 ml/day. On days 23, a temperature shock significantly reduced the methane content of the biogas in reactors R3 and R4. The composition of the substrates and the feed order can both be used to explain this. Both reactors R5 and R6 have a similar trend of biogas methane output. R5 seems to be more stable than R6. On days 13 and 27, correspondingly, for reactors R5 and R6, the highest biogas methane concentration (CH₄) was recorded. These values are approximately 64% and 66%, respectively. This reveals that the pre-treatment levels 4 and 3 had the highest output rates for R5 and R6. Since PTL4 contained more dense PS with a larger surface area than PTL3 did, one explanation for PTL4 processed with a combination of mincer and grinder could be an increase in microbial population and action. For PTL3, this could be revealed by the actions of the anaerobic microbes and the residual materials during the degradation of the biomass substrate of pre-treatment level 4. On day 23, the biogas methane content for reactors R5 and R6 was found to be the lowest, at roughly 32% for R5 and 34% for R6, respectively. Reduced biogas was produced when the digester was fed with larger particle size (PS) treated using a grinder (PTL3) and mincer (PTL2). This This can be driven by the fact that large PS require longer to breakdown and will have a substantial effect on the biogas. As a result, HRT might have affected the biogas's methane concentration. The results are similar to those of GWSB and BPWSB. The output of the biogas methane is driven to gradually increase until the end of the test by both reactors R5 and R6, which produce methane in peaks and valleys. The results are similar to those of grass and banana peel waste substrate biomass.

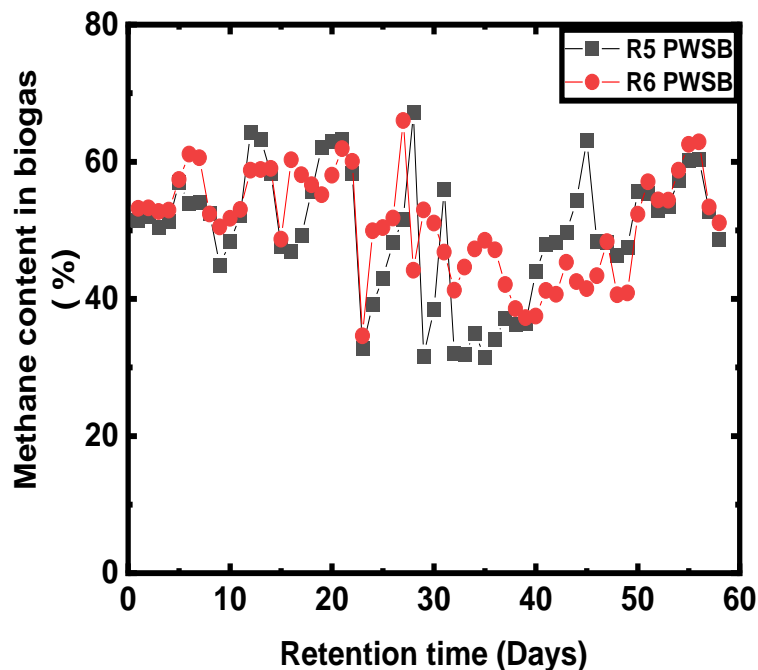


Figure 5.35: Percentage biogas methane CH₄ production of the degradation of PWSB (R5 and R6)

5.11.2 The specific production rate of the methane (CH₄) in semi-continuous testing of PWSB

The results of a specific methane output for the PWSB are shown in Figure 5.36. Methane output initially increased at all pre-treatment levels before decreasing. R6 had a higher biogas spike on day 9 (250 ml/gVS/day) than it did on day 6, when R5 had a higher spike (243 ml/gVS/day). PTL4 has the highest specific methane production of reactors R5 and R6 and contains more fine particles (PS). This can be explained by the fact that the rate of biogas production has increased due to the digestion of smaller particles, which have a more larger surface area available for enzymatic hydrolysis. When reactor R6 is compared to R5, reactor R5 produced reduced methane at a rate of 32 ml/gVS/day as opposed to 54 ml/gVS/day for reactor R6. The methane production profile at day 20 is similar in both R5 and R6, demonstrating that the particle size distribution of PT4 is similar. The methane

production profiles for pre-treatment levels PTL3 and PTL2 are different. A possible explanation could be a slight difference in the particle size distribution which is predicted by the increase in the methane production in R6 between day 20-40 compared to R5, and the decrease in the methane production in R6 when PT2 is fed into the digester, while the methane production in R5 increases with the addition of PT2. The specific methane outputs of both reactors had a sudden drop before rising when the digesters were fed with PTL3 grinder substrate which is like the behaviour seen when the digester is fed with PT2. Large PS with lesser surface area may be a contributing factor in this decrease in methane production because they take longer to metabolise and hence affect the rate at which biogas is produced. As seen in figure 5.39, there were peaks and troughs in the methane output which suggest that HRT had an impact on the rate of biogas production. The cumulative methane amount produced by the microbial breakdown of paper waste is shown in Figure 5.37 along with standard deviation error bars. The output of methane increases when PTL4 is fed to the digester after being minced and grind for five minutes, but it gradually decreases over time. After day 20, the breakdown of the residual PTL4 and the added PTL3 causes methane production to rise. Methane output starts to recover after a steep decline on day 23. Methane production exhibits a sharp drop between days 30 and 40, which is followed by a gradual rise between days 40 and 60 (PTL2). The decrease in methane output could be attributed to large PS with smaller surface areas since they metabolise more slowly, which slows down the production of biogas. As seen in Figure 5.40, HRT had a clear effect on the production rate of methane. PTL4 has the highest effect on production, producing an average of approximately $247 \pm 18 \text{ ml/CH}_4/\text{gVs/day}$ of specific methane from paper waste.

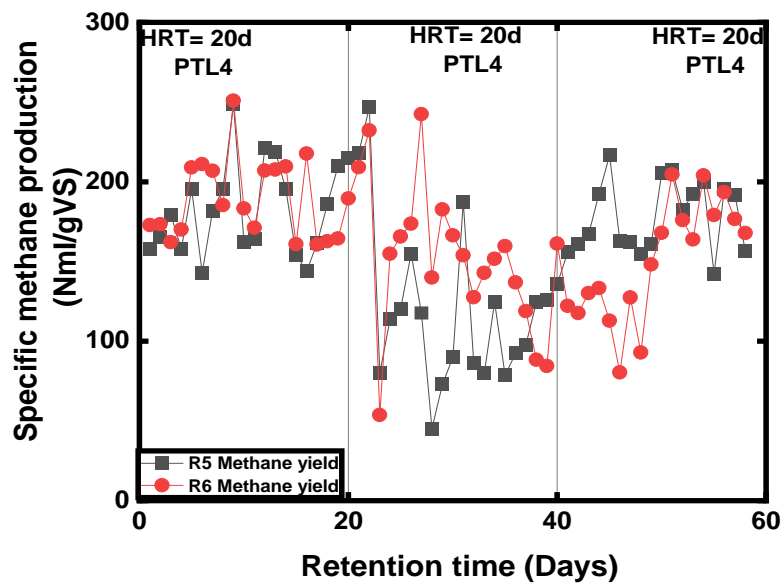


Figure 5.36: Semi-continuous testing showing specific CH₄ production of the PWSB.

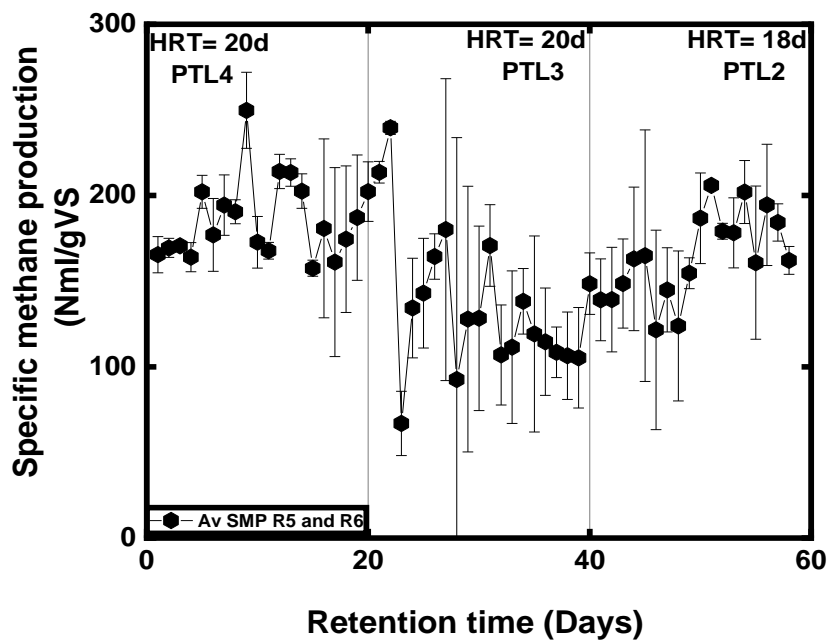


Figure 5.37: Semi-continuous testing showing average specific CH₄ production of PWSB.

5.12 Performance of reactor R1 to R6

Biogas methane content in a reactor is affected by the kind of substrate used and how efficiently each stage of the anaerobic digestion process is working in that reactor under steady - state conditions [285]. The six (6) reactors used for the semi-continuous test was carried out in duplicate as shown in session 3.9 (Table 3.5) for each sample reactor, although R2, R3 and R6 had a higher methane content indicating that its digestion activities were more effective as compared to R1, R4 and R5 of the same substrate. It is possible to conclude from these results how short HRT and the change in feed PTLs in the reactor affected this operation given that this was the case throughout the test duration. Similarly, PTL4 exhibits a similar trend in production for the first 20 days in R1 and R2, however PTL3 and PTL2 for days 21 through 40 and days 41 through 58, reactor R2 produce more methane. Additionally, when compared to reactor R3 displays a similar trend in high methane output from days 1 through 58 in all three PTLs (PTL4, PTL3, and PTL2), when compared to R4. Reactor R5 produced higher methane in PTL2 than reactor R6, however when R5 and R6 were compared in terms of output, R6 produced more methane in PTL4 and R3. PTL4 typically produces more methane during the first 20 days of output than PTL3 and PTL2 as shown in table 5.31 and figure 5.38.

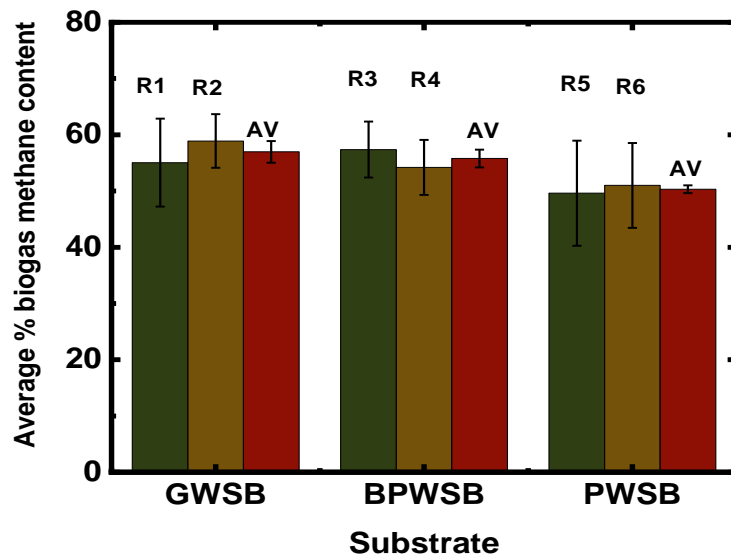


Figure 5.38: The average % of biogas methane content for GWSB, BPWSB, and PWSB duplicate reactors R1 to R6

Table 5. 31 Average% biogas methane content for reactor R1 to R6 PTLs

	GWSB	BPWSB	PWSB
PTL4			
R1	61.10±3.02	59.12±4.17	53.92±5.63
R2	60.84±2.97	56.72±3.28	55.62±3.59
AV	60.97±0.13	57.92±1.28	54.77±0.85
PTL3			
R1	55.73±7.99	55.78±6.38	42.42±10.97
R2	57.88±7.00	52.86±5.71	47.70±8.13
AV	56.80±1.08	54.32±1.46	45.06±2.69
PTL2			
R1	47.56±4.29	57.19±2.96	52.83±4.95
R2	57.88±1.56	52.89±4.22	49.52±7.59
AV	52.72±5.16	55.04±2.15	51.17±1.66
AV substrate	57	56	50

5.13 Conclusions

The reactions to changing feed when PTLs with less surface area PS are fed, along with the effects of short HRT on the methane content and specific methane yield, are the most obvious similarities between the reactors R1 to R6. The methane production profiles of the PWSB differed significantly. While PS with more surface area (PTL4) outperformed the other three PTLs with lesser surface area, GWSB

outperformed both BPWSB and GWSB. Also, for all substrates, the spike in methane yield was greater for the GWSB compared to the other substrates, as well as between PTL4 and the other two PTLs.

5.14 Stability operations of a semi-continuous test

The stability performance of the digester operations is presented in Figures 5.39, 5.40, and 5.41, which also reveal how HRT affects the pH levels of the GWSB, BPWSB, and PWSB during anaerobic digestion. The performance of anaerobic digestion is significantly influenced by pH, especially for lignocellulosic substrates like PWSB. The pH profile of the slurry in the digester shows that there are pH fluctuations. With HRT of 20 days, pH levels for PTL4 range from 7.33 to 7.45, but pH values for PTL3 and PTL2 ranged from 7.36 to 7.42 and from 7.20 to 7.35 for GWSB. Additionally, the pH levels in the BPWSB vary between 7.30 and 7.32 with an HRT of 20 days for PTL4, whereas the pH ranges for PTL3 and PTL2 were 7.25 to 7.34 and 7.28 to 7.31, respectively. The pH levels in the PWSB range from 7.2 to 7.3 for PTL4, however they were 6.61 to 7.23 and 6.8 to 7.0 for PTL3 and PTL2, respectively. The optimum pH range in an anaerobic digester is 6.8 to 7.2 in the anaerobic digestion process. However, a range of 6.5 to 8.0 may be tolerated by the digestion process [286], [287]. The pH profile reveals a drop in pH of the slurry in R5 and R6 from 7.3 to 6.61 between days 25 and 48. The decline in methane output driven on by HRT may also be explained by a decline in the pH of the digester slurry. Also, the pH of the digester slurry for BPWSB and GWSB showed a very slight variation in pH; however, this pH concentration did not drop below 7.2 or rise above 7.5, which is within the allowable range for steady - state operation. On the other hand, the lowest pH value with HRT of 20 days was 6.61, which was still within a fair limit suitable for substrate degradation and beneficial for methane production. Based on the initial pH and pH endpoints, the three alkalinity ratio indicators (PA, IA, and TA) suggested by [219] were used as a stability indicator as described in session 3.4.3 (table 3.3). The results demonstrate that the

digester fluctuates even though the feed is changed from PTL4 which contains small PS and more surface area to PTL3 and PTL2 which contain large PS and less surface area. An increase in the IA/PA ratio, which may indicate the build-up of volatile fatty acids (VFAs) in the reactor for all three substrates, showed that the pH in the reactor was relatively stable over time. According to literature data [219] the IA:PA ratio increasing from 0.2 to 0.4 suggests a steady mode of operation for the reactor but rising over 0.4 indicates an unstable digester. As demonstrated in figures 5.41 to 5.43, the gradually increasing IA: PA level showed there was a disturbance in the digester for the BPWSB, GWSB, and PWSB. The PA and IA in the semi-continuous reactors were within the permissible range of 0.3 for the first four weeks of digestion operations, but gradually increased to 0.42 (BPWSB), 0.41 (GWSB), and 0.45 (PWSB), revealing that the reactor had become more unstable over time.

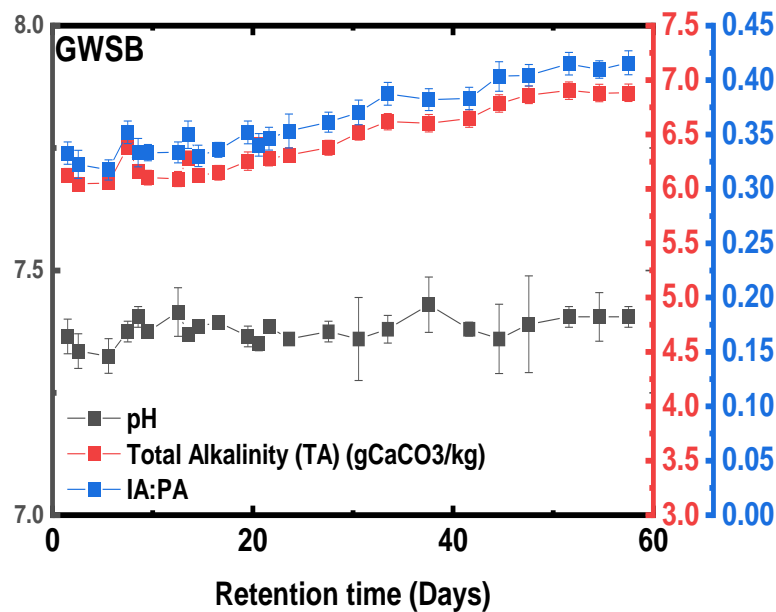


Figure 5.39: shows the pH, total and IA:PA alkalinity, for the GWSB digester during the semi-continuous test.

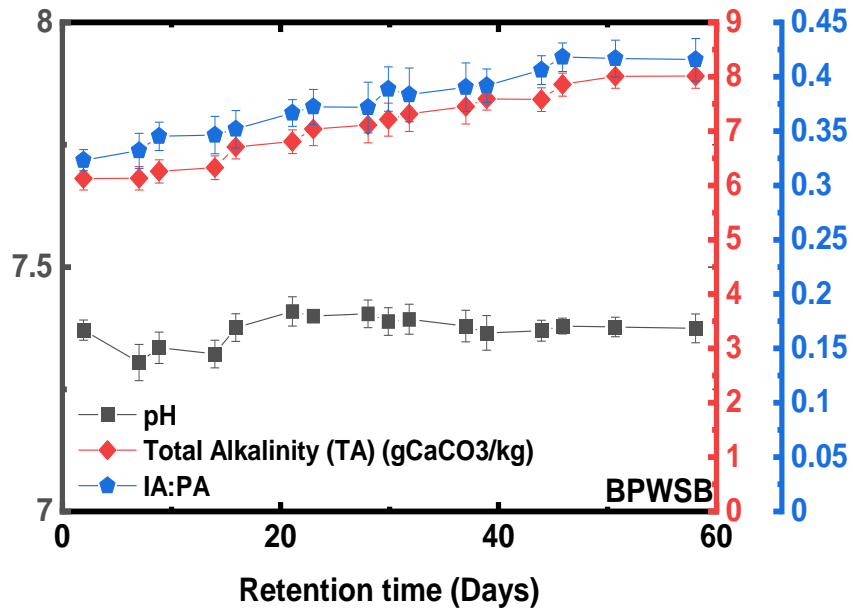


Figure 5.40 shows the pH, total and IA:PA alkalinity, for the GWSB digester during the semi-continuous test.

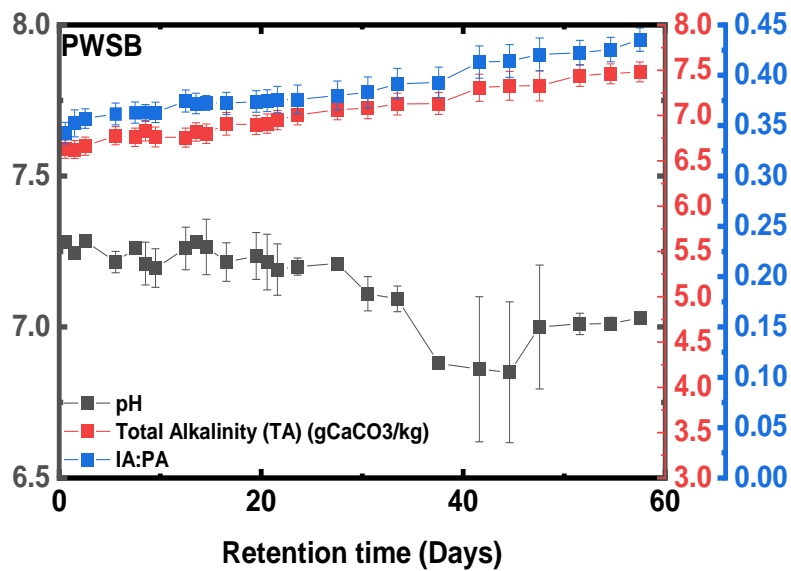


Figure 5.41: shows the pH, total and IA:PA alkalinity, for the GWSB digester during the semi-continuous test.

Conclusions: Overall, the changeover from large surface area PTL4 to smaller surface area PTL3 and PTL2 feed affected the process stability indicators such as pH, total and partial alkalinity, and IA/PA ratio, as well as shorter HRT, which reduce the substrate destruction and biogas in methane output.

5.15 Comparison of experimental and theoretical methane and energy yield

Equations [3.7], [3.8] and [3.9], and were used to determine the theoretical gas composition and theoretical calorific value based on data for the elemental analysis of the four selected substrate biomass. The dried substance's heating value (CV) was also calculated. The results are compared, as shown in table 5.6. The energy value of the substrate is computed using equations 3.8 and 3.9 of the Dulong formula as shown in appendix G1 and G2. The result of the two equations demonstrates good agreement with a minor discrepancy from the value produced by the two equations 3.8 and 3.9. Despite the short duration of the HRT, which demonstrated the substrate's rapid degradation rate, and the BMP results, which suggested that the peak of gas produced occurs within the first five days, semi-continuous test of the three chosen substrates revealed enhanced methane output. Both BPWSB and PWSB produced methane in the same patterns. The result shown in table 5.32 demonstrates that, despite increased methane production between PTLs due to PS, there were differences in the methane output for the BPWSB and PWSB as the batch test produced more methane than the semi-continuous test, which may have been influenced by short HRT compared to the GWSB where the methane output is higher in the semi continuous test output. The organic material and increased unit surface area exposed to enzyme attack may have contributed to this by improving carbon bioavailability and hydrolysis of the treated substrate. Additionally, according to [160], [288]–[290], the particle size of a substrate may have an influence on the efficiency of biological processes like anaerobic digestion (AD) . Larger surface area is exposed to enzyme attack on smaller particles per unit of time, that could boost the processed material's carbon accessibility and hydrolysis [61], [160], [240], [291].

Table 5. 32: An overview of digester performance

Substrate	Parameter	Value			
		PTL1	PTL2	PTL3	PTL4
	Pre-treatment levels				
BPWSB	BMP (Batch test)	245	271	293	332
	Semi continuous test	-	229	253	262
	Theoretical specific methane production	321	327	339	353
	Empirical formula	$C_{32.64}H_{56.57}N_1$			
	Molar mass of empirical formula	463.04			
	% Measured biogas methane CH ₄ content	-	55	54	58
	Theoretical %biogas methane CH ₄ content	71			
	Calculated CV (energy value) MJ kg ⁻¹ VS (equation 3.6)	22			
	Calculated CV (energy value) MJ kg ⁻¹ VS (equation 3.7)	20			
	Average batch test specific methane CH ₄ production	285			
	Average semi continuous test specific methane CH ₄ production	248			
	Average % measured biogas methane CH ₄ content of substrate	56			
	Average theoretical specific methane CH ₄ production of substrate	353			
	Average digester pH	7.32			
GWSB	BMP (Batch test)	203	225	255	274
	Semi continuous test	-	242	286	321
	Theoretical specific methane production	268	272	294	301
	Empirical formula	$C_{14.84}H_{26.2}N_1$			
	Molar mass of empirical formula	218.65			
	% Measured biogas methane CH ₄ content	-	53	57	61
	Theoretical %biogas methane CH ₄ content	70			
	Calculated CV (energy value) MJ kg ⁻¹ VS (equation 3.6)	22			
	Calculated CV (energy value) MJ kg ⁻¹ VS (equation 3.7)	20			
	Average batch test specific methane CH ₄ production	239			
	Average semi continuous test specific methane CH ₄ production	283			
	Average % measured biogas methane CH ₄ content of substrate	57			
	Average digester pH	7.33			

Continues

Substrate	Parameter	Value			
		PTL1	PTL2	PTL3	PTL4
	Pre-treatment levels				
PWSB	BMP (Batch test)	231	250	264	274
	Semi continuous test	-	206	240	250
	Theoretical specific methane production (Buswell 1952)	269	273	282	287
	Empirical formula	C₁H₂			
	Molar mass of empirical formula	14.03			
	% Measured biogas methane CH ₄ content	-	51	45	55
	Theoretical %biogas methane CH ₄ content (Buswell 1952)	72			
	Calculated CV (energy value) MJ kg ⁻¹ VS (equation 3.6)	21			
	Calculated CV (energy value) MJ kg ⁻¹ VS (equation 3.7)	19			
	Average batch test specific methane CH ₄ production	255			
	Average semi continuous test specific methane CH ₄ production	232			
	Average % measured biogas methane CH ₄ content of substrate	50			
	Average digester pH	7.09			
TWSB	BMP (Batch test)	233	260	276	294
	Semi continuous test	-	-	-	-
	Theoretical specific methane production	298	313	321	325
	Empirical formula	C_{22.62}H_{38.49}N₁			
	Molar mass of empirical formula	324.5			
	% Measured biogas methane CH ₄ content	-	-	-	-
	Theoretical % biogas methane CH ₄ content	70			
	Calculated CV (energy value) MJ kg ⁻¹ VS (equation 3.6)	21			
	Calculated CV (energy value) MJ kg ⁻¹ VS (equation 3.7)	19			
	Average batch test specific methane CH ₄ production	266			
	Average digester pH	7.33			
	- Not measured				

5.16 Comparison of batch and semi-continuous tests

The semi-continuous test lasted 58 days for the three substrate biomass pre-treatment levels before the experiment was terminated, whereas the batch test lasted 30 days during degradation for each substrate PTLs. After the BMP test, the data from the bioprocess software differed, which would have been caused by the organic matter and the bacteria' activity in the reactor. HRT of 20 days for GWSB, BPWSB, and 18 days for PWSB was used to make the batch test comparable to the semi-continuous test. This allowed for easier comparison. The average specific methane output of the three chosen feedstocks, such as GWSB, BPWSB, and PWSB, is shown in Table 5.33 using three PTLs (PTL2, PTL3, and PTL4) from the PSD classification class used in the semi-continuous test. A batch test is used to compare the semi-continuous methane output performance.

The semi-continuous and batch tests produced contradictory results. Table 5.33 demonstrates that while the batch test provided a higher methane output for BPWSB and PWSB, the semi-continuous test yielded a higher methane output for all PTLs (PT4-PT2) for GWSB. comparing the substrate performances at different PTLs. As shown in Table 5.33, the results of the batch tests showed that, on average, BPWSB performed best at PTL4 and PTL3, PWSB performed better at PTL2, and GWSB produced the lowest amount of methane across all PTLs. Similar to batch tests, GWSB performed best in the semi-continuous test at PTL4 and PTL3, however, PTL2 had the best results from BPWSB. The methane output for GWSB averagely performed best for the semi continuous test than the batch test. This might be explained by the microbial activity. On the other hand, this supports the discoveries of [187] who, using results from previous studies, identified the particle size paradox. Their study showed that other characteristics other than the mean size play a critical role because the relative rate of gas production per unit surface area rapidly decreases with decreasing particle size for smaller particles. Result of the BPWSB and PWSB of the semi continuous test can be explained by the change in feed from PTL4 with greater units of surface area compared to PTL3

and PTL2 with lesser unit surface area. Also, the operating condition (HRT) of the digester could also affect the rate of biogas methane output. The results showed that batch test yielded the highest methane output ($295 \pm 34 \text{ Nml/gVS}$) for BPWSB as compared to semi-continuous test ($253 \pm 29 \text{ mlCH}_4/\text{gVS/day}$) for GWSB, which falls within PTL4. Similarly, smaller particle size results in a higher unit surface area that is exposed to enzymatic attack, which could also boost carbon availability and hydrolysis of the mechanical treated material [61], [157], [240], [291]. Finally, it is noteworthy that GWSB outperformed the other two substrate and is best suited for anaerobic digestion (AD) in terms of providing the optimal amount of specific methane. Also, from the experiment, the paper waste substrate biomass (PWSB) produced less methane when compared with the other two (2) substrate. The physical significance of these could be poor microbial activities on the reactor content. Hence, making the sampling of the effluent less accurate as the solid particles could not be actively degraded by the microbes. This creates curiosity for physicochemical characteristic of the paper waste sample. Paper, which is a by-product of wood is known to be rich in lignin. Lignin is considered as the most recalcitrant to biological deconstruction due to its irregular, complex, and highly heterogeneous aromatic structure [292].

Table 5. 33 Average specific methane output from batch and semi-continuous tests of GWSB, BPWSB and PWSB across the duration of the study.

	PTLs	HRT (days)	Substrate biomass		
			GWSB	PWSB	BPWSB
Batch test	PT4	20	218 \pm 37 Nml/gVS	251 \pm 31 Nml/gVS	295 \pm 34 Nml/gVS
	PT3	20	212 \pm 36 Nml/gVS	248 \pm 29 Nml/gVS	259 \pm 38 Nml/gVS
	PT2	18	117 \pm 37 Nml/gVS	228 \pm 33 Nml/gVS	223 \pm 35 Nml/gVS
Semi-continuous test	PT4	20	253 \pm 29 Nml/gVS	186 \pm 22 Nml/gVS	235 \pm 20 Nml/gVS
	PT3	20	228 \pm 48 Nml/gVS	136 \pm 40 Nml/gVS	221 \pm 32 Nml/gVS
	PT2	18	192 \pm 21 Nml/gVS	164 \pm 24 Nml/gVS	199 \pm 22 Nml/gVS

5.17 Comparison of reactors performances for semi continuous testing

The study's goal is to assess whether there is a variation in methane yield among reactors R1 and R2 from GWSB semi-continuous test results. This hypothesis was tested by comparing the specific methane yields of R1 and R2. An independent samples t-test was used to test this hypothesis. Table 5.34 reveals that the average specific methane yields in reactor R2 (M=237.2, SD=43.04) are significantly greater than those in reactor R1 (M=214.2, SD=46.05), $t(114) = 2.78$, $p = 0.006$. The magnitude of the effect is medium (Cohen's $d = 0.516$). These results suggest that R2 produced more methane than R1, which could be attributed to a higher microbial population in the digester.

Table 5. 34 Specific Methane yield differences in reactors R1 and R2

Group Statistics								
R	N	M	SD	SEM	t	df	p	Cohen's d
1	58	214.2	46.05	6.05	-2.78	114	0.0064	-0.516
2	58	237.2	43.04	5.65				
R=Reactor=Mean, SD= Std. Deviation, SEM= Std. Error Mean, df= difference								

Using data from the BPWSB semi-continuous test, the study's goal is to determine if specific methane yield differs between reactors R1 and R2. comparing R2 and R1's specific methane yields allowed us to test this hypothesis. This was explored using an independent samples t-test. The average specific methane yields in reactor R1 (M=237.2, SD=43.04) are significantly higher than those in reactor R1 (M=214.2, SD=46.05), as shown in table 5.35, with a $t(114) = 6.81$, $p < 0.006$. Cohen's d value of 0.516 indicates a medium-sized effect. Due to a higher microbial population in the digester, these results indicate that R2 produced more methane than R1, which could be explained by this.

Table 5. 35 Specific Methane yield differences in reactors R3 and R4

Group Statistics								
R	N	M	SD	SEM	t	df	p	Cohen's d
1	58	241.8	32.27	4.24	6.81	114	<0.001	1.265
2	58	196.7	38.82	5.1				
R=Reactor=Mean, SD= Std. Deviation, SEM= Std. Error Mean, df= difference								

Reactors R1 and R2's Specific methane yields were compared (Table 5.36). Specific methane yields in reactor R2 (M=164.2, SD=40.61) were, on average, higher than those in reactor R1 (M=159.7, SD=46.12). An independent t-test revealed that this difference was statistically significant; the results were $t(114) = 0.558$, $P = 0.578$. The small size of the effect is indicated by the Cohen's d value of 0.261. These results show that R2 produced more methane than R1 due to a higher population of microbe in the digester.

Table 5. 36 Specific Methane yield differences in reactors R5 and R6

Group Statistics								
R	N	M	SD	SEM	t	df	p	Cohen's d
1	58	159.7	46.12	6.06	-0.558	114	0.578	0.261
2	58	164.2	40.61	5.33				
R=Reactor=Mean, SD= Std. Deviation, SEM= Std. Error Mean, df= difference								

5.17.1 Performance of the three substrates in terms of methane production

The BPWSB M=225.7 (SD=43.2) specific methane yield was correlated with the GWSB (N=58). Comparatively, the BPWSB M=219.5 (SD=29.5) was associated with the numerically smaller GWSB (N=58). As shown in table 5.37, an independent samples t test was carried out to determine the hypothesis that the GWSB and BPWSB were associated to statistically significant differences in the mean of the BPWSB. The independent samples t tests revealed statistically significant results, with a value of, $t(114) = .942$, $P = .0348$. As a result, the GWSB was associated to a statistically larger mean than the BPWSB. Based on the Cohen's d (1992) guideline, the Cohen's d was estimated at .175, which is a very low value. Table 5.37 Also displays the mean at 95% confidence intervals. The specific methane yield from the GWSB, M=225.7 (SD=43.2), was correlated with the GWSB (N=58). The numerically smaller PWSB (N=58) was correlated with the PWSB M=161.9 (SD=37.1). The hypothesis that the GWSB and PWSB were associated to statistically significant differences in the mean of the PWSB was examined using an independent samples t test. With a value of, $t(114) = 8.530$, $P < 0.001$, the independent samples t tests produced statistically significant results. The GWSB

was thus related to a statistically higher mean than the PWSB. The Cohen's d was estimated at 1.584, which is a large value based on the Cohen's d (1992) guideline. The mean analysed at 95% confidence intervals are shown in Table 5.37. While the BPWSB (N=58) was correlated with the specific methane yield from the BPWSB, M=219.2 (SD=29.5). The PWSB M=161.9 (SD=37.1) was correlated with the numerically smaller PWSB (N=58). To determine whether the GWSB and BPWSB were connected to statistically significant differences in the mean of the BPWSB, an independent samples t test was conducted. Independent samples t tests produced results that were statistically significant, with a value of $t(114) = 9.214$, $P < 0.001$. Thus, compared to the PWSB, the BPWSB was statistically associated with a higher mean. According to the Cohen's d (1992) formula, the Cohen's d was calculated to be 1.711, which is a large value. Table 5.37 shows the average.

Table 5. 37 An independent samples t test of the three-substrate used for semi-continuous test

Group Statistics								
S	N	M	SD	SEM	t	df	p	Cohen's d
GWSB	58	225.7	43.2	5.67	0.942	114	0.348	0.175
BPWSB	58	219.2	29.5	3.87				
S	N	M	SD	SEM	t	df	p	Cohen's d
GWSB	58	225.7	43.2	5.67	8.53	114	<0.001	1.584
PWSB	58	161.9	37.1	4.87				
S	N	M	SD	SEM	t	df	p	Cohen's d
BPWSB	58	219.2	29.5	3.87	9.214	114	<0.001	1.711
PWSB	58	161.9	37.1	4.87				

S=Substrate =Mean, SD= Std. Deviation, SEM= Std. Error Mean, df= difference

5.17.2 Results of the analysis of variance: Average specific methane potential of the GWSB.

The study's aim is to determine whether there is significant variance in the average specific methane yield of GWSB based on their chosen PTLs (4-2) from the PSD characterisation. Based on the hypothesis, PTL4 with smaller PSD and more surface area will probably produce more specific methane yield than larger PS with less surface area. The semi-continuous test experimental data were analysed using a between-subjects one-way ANOVA. The results revealed a

significant variation in the specific methane yield between the three (3) pre-treatment levels, with $F(2, 55) = 13.8$ and $P = 1.42E-05$. The effect size is 33% as shown in table 5.38. Post hoc analysis was performed using Fisher's LSD. The studies reveal that PTL4 ($M=253, SD=29.8$) has a significantly higher specific methane yield than PTL3 ($M=229, SD=49.2$) and PTL2 ($M=192, SD=21.9$). Based on the Fisher's LSD results, PTL3 and PTL2 both differ significantly from PTL4 ($M = -24.4, SEM = 11.4, P = 0.00273$) and from PTL2 ($M = -60.99, SEM = 11.7, P = 2.73E-06$), respectively, while PTL2 differs significantly from PTL3 ($M = -36.61, SEM = 11.7, P = 0.0036$). The results indicate that PTL4 is more likely to produce more specific methane yields than PTL3 and PTL2 because it has more smaller PS and more surface area. This could suggest that PTL4 of the GWSB produces a higher specific methane yield than other methods owing to the activity of the microbial population in the reactor. As shown in figures 5.42 and 5.43, the results were presented using a box chart and post hoc test Fisher LSD.

Table 5. 38 Results of the analysis of variance: Average specific methane potential of the GWSB.

ANOVAOneWay (19/01/2023 13:03:15)								
Descriptive Statistics of GWSB								
	N Analysis	N Missing	Mean	Standard Deviation	SE of Mean			
PT4	20	0	253.03	29.8	6.7			
PT3	20	0	228.66	49.2	10.9			
PT2	18	2	192.04	21.9	5.2			
Overall ANOVA								
	DF	Sum of Squares	Mean Square	F Value	Prob>F	η^2		
Model	2	35507.9	17753.9	13.8	1.42E-05	.334		
Error	55	70906.7	1289.2					
Total	57	106414.6						
Fit Statistics								
	R-Square	Coeff Var	Root MSE	Data Mean				
	0.334	0.16	35.9	225.7				
				Prob	Alpha	Sig	LCL	UCL
Homogeneity of Variance Test Levene's Test (Absolute Deviations)								
	DF	Sum of Squares	Mean Square	F Value	Prob>F			
Model	2	2127.9	1063.9	1.67	.1972			
Error	55	34985.9	636.1					
Means Comparison								
	MeanDiff	SEM	t Value	Prob	Alpha	Sig	LCL	UCL
PT3 PT4	-24.38	11.4	-2.15	0.036	0.05	1	-47.13	-1.62
PT2 PT4	-60.99	11.7	-5.23	2.73E-06	0.05	1	-84.37	-37.61
PT2 PT3	-36.61	11.7	-3.14	0.00273	0.05	1	-59.99	-13.24

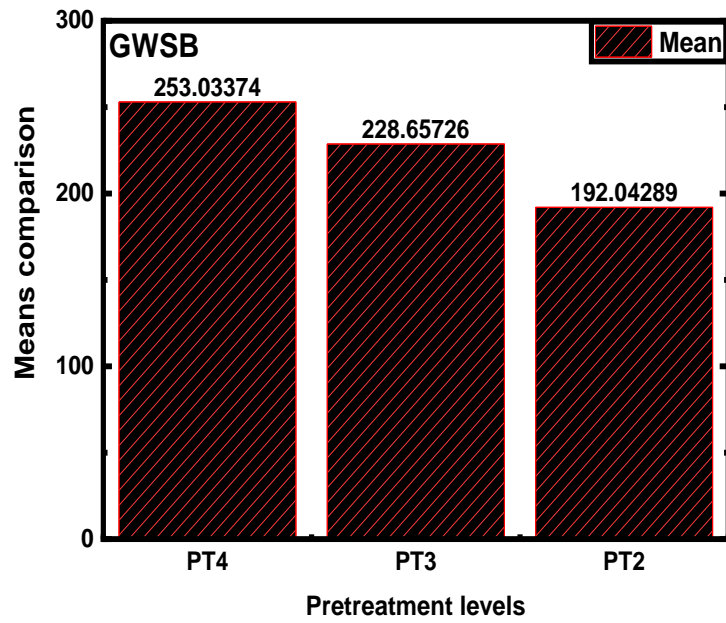


Figure 5.42: Means bar chart of the GWSB average specific methane yield's variation.

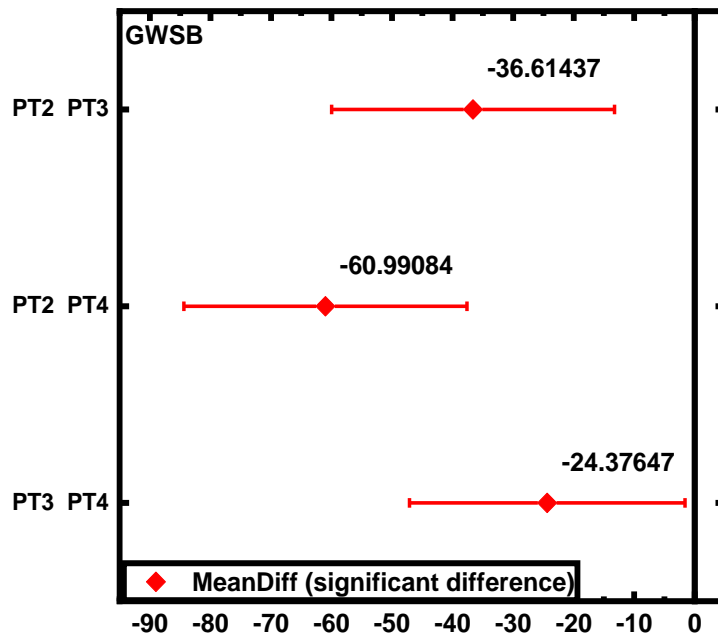


Figure 5.43: Means Comparison plot using fisher LSD.

5.17.3 Results of the analysis of variance: Average specific methane potential of the BPWSB.

The purpose of the study is to determine how well the chosen PTLs (4-2) from the PSD characterisation represent a significant variation in the average specific methane yield of BPWSB. According to the hypothesis, PTL4 will likely produce a higher specific methane yield than larger PS with lower surface area. Using a between-subjects one-way ANOVA, the experimental data from the semi-continuous test were analysed. With $F(2, 55) = 9.10$ and $P = 3.87E-04$, the results reveal a significant difference in the specific methane yield between the three (3) pre-treatment levels. The effect is .25% in size. Fisher's LSD was used for post hoc analysis as shown in table 5.39. The study reveals that PTL4 ($M=235.5$, $SD=20.9$) has a significantly higher specific methane yield when compared to PTL3 ($M=220.8$, $SD=32.8$) and PTL2 ($M=199.5.8$, $SD=22.2$). Fisher's LSD results showed that PTL2 differ significantly from PTL4 ($M= -35.9$, $SEM=8.45$), $t=-4.25$, $P= 8.26E-05$) and PTL2 differ significantly from PTL3 ($M= -21.2$, $SEM=8.45$), $t=- 2.5$, $P= 0.01494$), respectively, while PT2 differs significantly from PT3 ($M= -36.61$, $SEM= 11.7$, $P=-0.0036$). PTL3 also have no significant variation from PTL4 ($M= -14.7$, $SEM=8.22$), $t=-1.79$, $P= 7.94E-02$). As a result of its larger surface area and smaller PS than PTL3 and PTL2, PTL4 is more likely to produce more specific methane yields, according to the results. This might imply that PTL4 of the BPWSB produces a higher specific methane yield than those of other processes because the microbe in the reactor is active. Figures 5.44 and 5.45 present the findings using a SD as error and a post hoc fisher LSD plot, respectively.

Table 5. 39. Results of the analysis of variance: Average specific methane potential of the BPWSB.

ANOVAOneWay (19/01/2023 13:40:42)								
Descriptive Statistics of BPWSB								
	N Analysis	N Missing	Mean	Standard Deviation	SE of Mean			
PT4	20	0	235.4598	20.94647	4.68377			
PT3	20	0	220.7538	32.82749	7.34045			
PT2	18	2	199.515	22.24403	5.24297			
Overall ANOVA								
	DF	Sum of Squares	Mean Square	F Value	Prob>F			
Model	2	12310.84	6155.419	9.0951	3.87E-04			
Error	55	37223.12	676.784					
Total	57	49533.96						
Fit Statistics								
	R-Square	Coeff Var	Root MSE	Data Mean				
	0.24853	0.11866	26.01507	219.2335				
Means Comparison								
	MeanDiff	SEM	t Value	Prob	Alpha	Sig	LCL	UCL
PT3 PT4	-14.7061	8.22669	-1.7876	7.94E-02	0.05	0	-31.1927	1.7806
PT2 PT4	-35.9448	8.45212	-4.25276	8.26E-05	0.05	1	-52.8832	-19.0064
PT2 PT3	-21.2388	8.45212	-2.51283	0.01494	0.05	1	-38.1772	-4.30034
Homogeneity of Variance Test Levene's Test (Absolute Deviations)								
	DF	Sum of Squares	Mean Square	F Value	Prob>F			
Model	2	179.4294	89.71471	0.29927	0.74256			
Error	55	16487.72	299.7767					

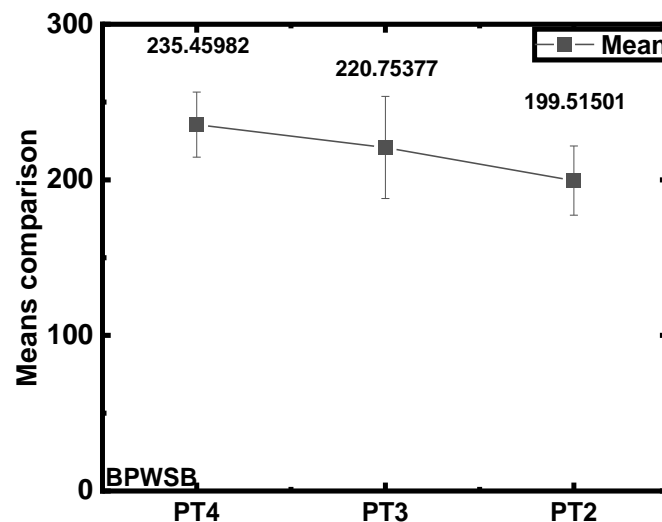


Figure 5.44: Means plot SD as error for the BPWSB average specific methane yield's variation.

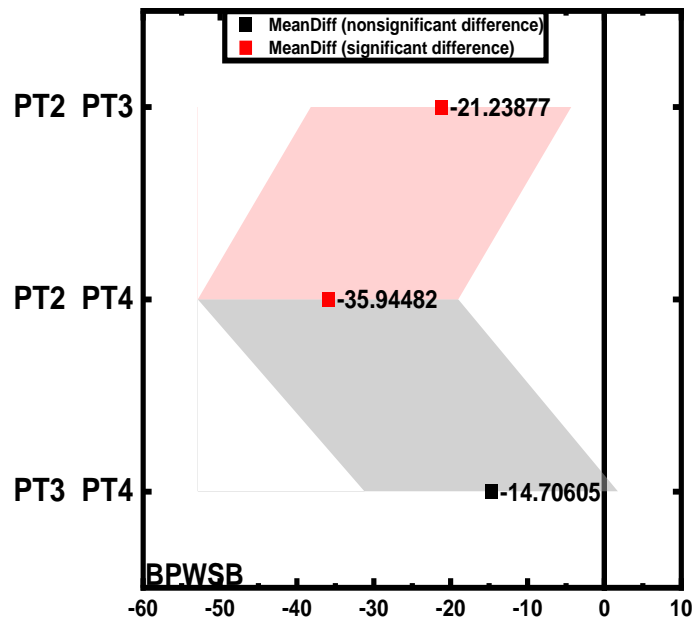


Figure 5.45: Means Comparison plot using Fisher LSD.

5.17.4 Results of the analysis of variance: Average specific methane potential of the PWSB.

The goal of the study is to evaluate how well the PSD characterisation's PTLs (4-2) chosen PTLs (4-2) represent a significant variation in the average specific methane yield of PWSB. The hypothesis suggests that PTL4 will probably yield a greater specific methane yield than larger PS with a smaller surface area. The experimental data from the semi-continuous test were analysed with a between-subjects one-way ANOVA. As shown in table 5.40, the results revealed a significant difference in the specific methane yield between the three (3) pre-treatment levels, with $F(2, 55) = 12.9$, $P = 2.62E-05$. Post hoc analysis was performed using Fisher's LSD. According to the data analysis, PTL4 ($M = 185.9$, $SD = 23.0$) has a significantly higher average specific methane yield than PTL2 ($M = 164.1$, $SD = 25.3$) and PTL3 ($M = 136.0$, $SD = 41.3$). There is .32% influence. Fisher's LSD analysis indicate that PTL3 and PTL2 significantly differ from PTL4 ($M = -24.4$, $SEM = 11.4$, $P = 0.00273$) and from PTL2 ($M = -60.99$, $SEM = 11.7$, $P = 2.73E-06$), respectively,

while PT2 significantly differs from PT3 (M= -36.61, SEM= 11.7, P=-0.0036). The results suggest that PTL4 is more likely to yield more specific methane yields due to its greater surface area and smaller PS than PTL3 and PTL2. Because the microbe in the reactor is active, this could mean that PTL4 of the PWSB has a greater specific methane yield than those of other processes. PTL3 and PTL2, on the other hand, which are comparable in that they both contain larger PS and less surface area, are more likely to yield the same amount of a specific methane. A box chart and a means comparisons plot fisher were used to display the results, as shown in figures 46 and 47.

Table 5. 40 Results of the analysis of variance: Average specific methane potential of the PWSB.

ANOVAOneWay (19/01/2023 23:00:49)								
Descriptive Statistics of PWSB								
	N Analysis	N Missing	Mean	Standard Deviation	SE of Mean			
PT4	20	0	185.8772	23.03612	5.15103			
PT3	20	0	136.0314	41.32925	9.2415			
PT2	18	2	164.0909	25.26574	5.95519			
Overall ANOVA								
	DF	Sum of Squares	Mean Square	F Value	Prob>F			
Model	2	24968.2	12484.1	12.86087	2.62E-05			
Error	55	53388.71	970.7039					
Total	57	78356.91						
Fit Statistics								
	R-Square	Coeff Var	Root MSE	Data Mean				
	0.31865	0.19241	31.15612	161.9277				
Means Comparison								
	MeanDiff	SEM	t Value	Prob	Alpha	Sig	LCL	UCL
PT3 PT4	-49.8458	9.85243	-5.05924	5.01E-06	0.05	1	-69.5905	-30.1011
PT2 PT4	-21.7864	10.12241	-2.15229	0.03578	0.05	1	-42.0721	-1.50059
PT2 PT3	28.05948	10.12241	2.77202	0.00759	0.05	1	7.77372	48.34524
Homogeneity of Variance Test Levene's Test (Absolute Deviations)								
	DF	Sum of Squares	Mean Square	F Value	Prob>F			
Model	2	1832.04	916.0198	2.51949	0.08975			
Error	55	19996.53	363.5732					

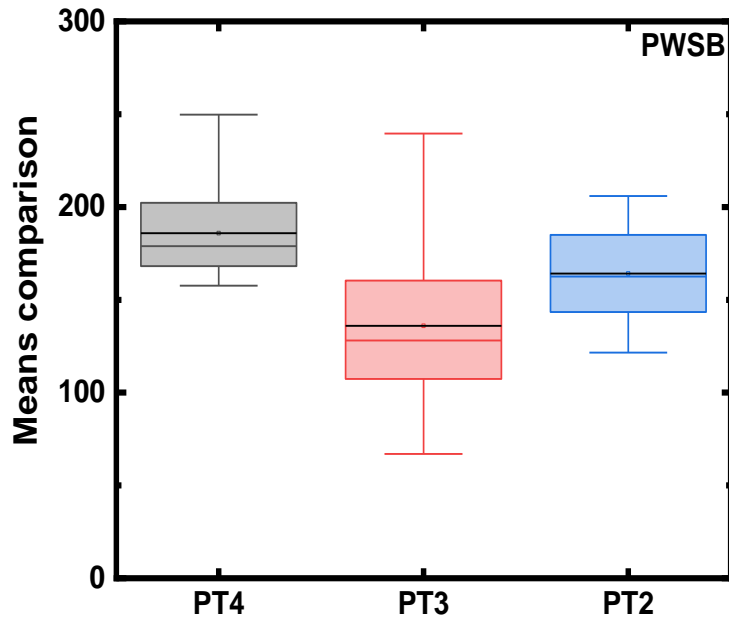


Figure 5.46: Means boxplot of the PWSB average specific methane yield's variation.

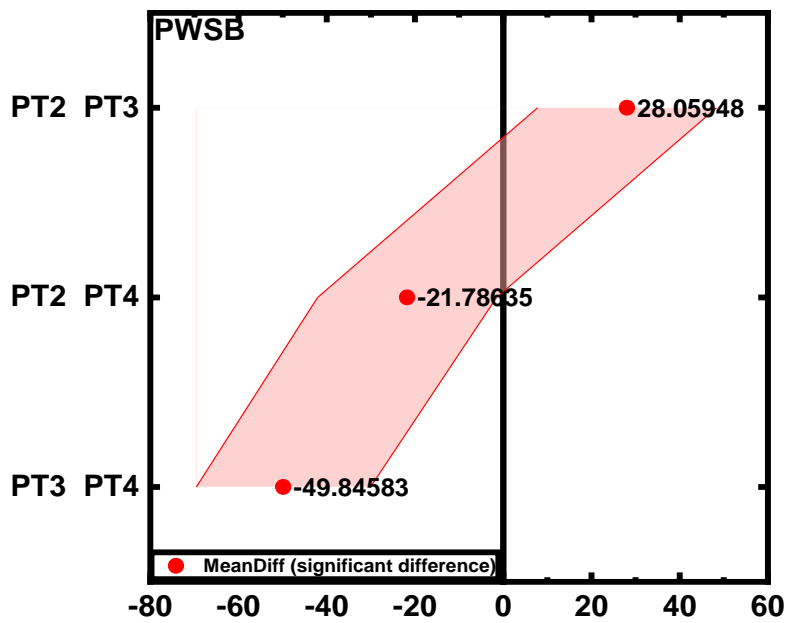


Figure 5.47: Means Comparison plot using fisher LSD.

Conclusion: One-way ANOVA and Post-hoc Fisher LSD were used to analyse the experimental data from the semi-continuous test, and they showed that PTL4 produced more specific methane yield than PTL3 and PTL2 because of its greater surface area and smaller PS. On the other hand, PTL3 and PTL2, which are comparable in that they both contain larger PS and have less surface area, are more likely to produce the same amount of a specific methane yield for all substrates.

5.18 A comparison of the specific methane yields of four substrate pre-treatment levels used in the batch test.

The study's goal is to ascertain whether there are any notable differences between the four PTLs for substrates that were selected to be used in a batch test. It was proposed that BPWSB are more likely to produce greater methane in their various PTLs than others substrate biomass. The data was collected over a 25-day test period for all substrates for the analysis. This is because some substrate's data was recorded for longer than 25 days. After that, a between-subjects one-way ANOVA was used to analyse the data. The Fisher LSD was used in the post-hoc analysis. The results revealed a significant variation between the four PTL1-4 of each substrate, with $F(15,400) = 7.22$ and $4.01E-14$. Specific methane yields differ significantly between the four pre-treatment levels, according to the studies, as shown in appendix I1. TWSB PTL1 had a higher specific methane yield than the other substrates ($M=210.07$, $SD=55.8$), while GWSB PTL1 had the lowest ($M=210.07$, $SD=55.8$). According to the study results, the specific methane yields for BPWSB, TWSB, and PWSB are comparable but not identical. The highest specific methane yield was produced by BPWSB for PTL2 ($M=225.6$, $SD=57.7$), while the lowest was produced by GWSB ($M=181.2$, $SD=51.9$). The results suggest that the specific methane yields for BPWSB, TWSB, and PWSB are similar but not identical. Again, BPWSB PTL3 ($M=255$, $SD=63.5$) differed significantly from the others, whereas GWSB had the lowest specific methane yield ($M=211.7$, $SD=56.6$). Likewise, BPWSB PTL4 outperformed the other substrates ($M=290.3$, $SD=69.3$),

while GWSB PTL4 has the least ($M=218.3$, $SD=69.4$).

Table 5. 41 Results of the analysis of variance between the four substrates used in the batch test for a period of 25 days.

ANOVAOneWay (24/01/2023 13:00:23)					
Descriptive Statistics					
	N Analysis	N Missing	Mean	Standard Deviation	SE of Mean
GWSBPTL1	26	0	158.3043	51.48986	10.09799
BWSBPTL1	26	0	207.244	53.02007	10.39809
PWSBPTL1	26	0	204.5089	53.53726	10.49952
TWSBPTL1	26	0	210.0675	55.84928	10.95294
GWSBPTL2	26	0	181.2355	51.89785	10.17801
BWSBPTL2	26	0	225.5784	57.65218	11.30652
PWSBPTL2	26	0	225.2383	54.58297	10.7046
TWSBPTL2	26	0	221.9227	63.1478	12.3843
GWSBPTL3	26	0	211.6531	56.57955	11.09616
BWSBPTL3	26	0	254.9541	63.46653	12.44681
PWSBPTL3	26	0	241.9266	56.20291	11.0223
TWSBPTL3	26	0	243.6956	63.3382	12.42164
GWSBPTL4	26	0	218.0484	58.4785	11.46858
BWSBPTL4	26	0	290.333	69.35201	13.60105
PWSBPTL4	26	0	245.2892	57.69149	11.31423
TWSBPTL4	26	0	251.3372	71.54467	14.03106
	DF	Sum of Squares	Mean Square	F Value	Prob>F
Model	15	375970.6	25064.7	7.22483	4.01E-14
Error	400	1387699	3469.247		
Total	415	1763669			
	R-Square	Coeff Var	Root MSE	Data Mean	
	0.21318	0.26241	58.90031	224.4585	
	DF	Sum of Squares	Mean Square	F Value	Prob>F
Model	15	9939.717	662.6478	0.33693	0.99121
Error	400	786679.8	1966.699		

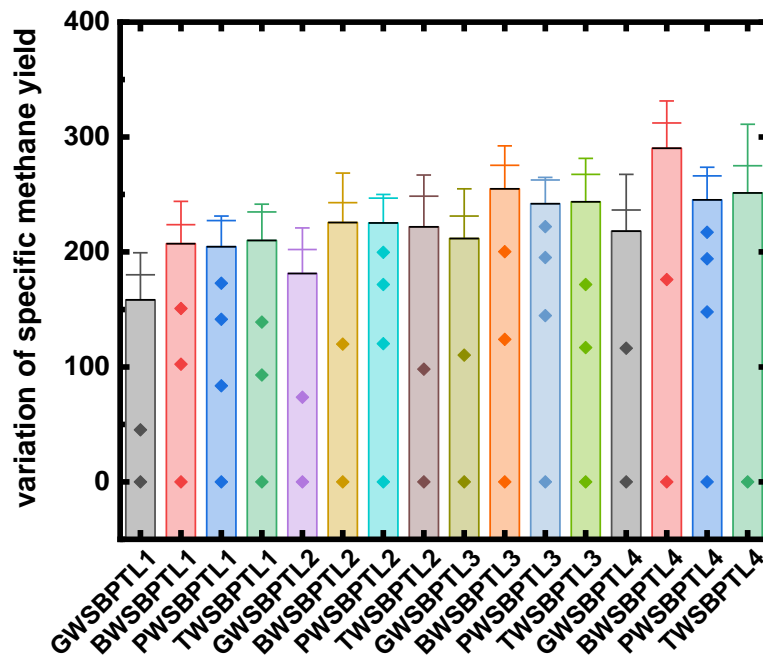


Figure 5.48: Means bar plot of the average specific methane yields of four substrate from batch test

5.19 Expected outcome of the semi-continuous test

The expected outcomes of semi-continuous test were as follows:

- ❖ It is expected that after applying different feedstock enhancement solutions to the various feedstocks investigated, such as the pre-treatment, it should show a viable method for upgrading the biogas yield of the feedstock and thereby enhancing the overall anaerobic digestion (AD) process.
- ❖ It is expected that increasing the pre-treatment intensity will result in a greater specific yield of biogas since decreasing the particle size will increase the total surface area of the solids by the opening of the compact structure leading to higher biodegradability and an increase in the biogas [155], [174], [175].
- ❖ It is expected that the effect of pre-treatment on the maximum OLR and maximum volumetric biogas production could be to increase or decrease the maximum biogas

production from a continuous system, depending on which is the predominant effect, or eventual failure mechanism. More intensive pre-treatment could lead to an increased tendency for foaming to occur in the system, thus reducing the maximum biogas production. However, the increased biodegradability of the material subject to pre-treatment could lead to enhancement of the maximum biogas production.

- ❖ The increase in pre-treatment intensity (i.e., PS1-PS3) will result in a reduced tendency to foaming. This is because several scientific researchers [20], [159], [176], [177] have reported that organic overloading of digesters can be a reason for foaming. This is because of the excess compounds not being degraded by the bacteria within the digesters, thereby leading to the potential accumulation of hydrophobic or surface-active by-products that will promote foaming. Hence, increasing the substrate surface area through pre-treatment intensity will assist in providing more access to microbial degradation, since the rate and degree of degradation increases after size reduction.

5.20 Based on the findings, it is possible to draw the following conclusions:

- ❖ The increasing pre-treatment intensity of substrates led to a greater specific surface area while enhancing the process' output and increasing the production of biogas by decreasing the size of the particle size and increasing the total surface area of the substrates.
- ❖ The highest amount of biogas produced increased because of the pre-treated material's greater biodegradability, which was influenced by the hydraulic retention time (HRT) and change in feed.
- ❖ The results reveal that intensive pre-treatment had no detrimental effects on the anaerobic digestion system (e.g., foaming).
- ❖ The study showed that an increase in pre-treatment intensity causes a decrease in the tendency to foam (PS2-PS4).

Anaerobic Degradation Model Describing the Change in Particle Size Distribution

6 Process Modelling

Bacterial degradation plays a key role during anaerobic digestion. Most waste is homogenous, so during size reduction each particle size fraction behaves differently. Additionally, when materials are tested experimentally, they do not completely degrade. However, this session will present a result of particle size distribution obtained from literature data, degradation model describing changes in the PSD of substrates over time using the Surface-Based Kinetics model for spherical particles in a continuous anaerobic digestion system.

6.1 Model Description

The model enhances the anaerobic digestion proposed by [176] for the calibration of the results that were obtained from batch experiments of a single feedstock to study the effects of the particle size distribution (PSD) on the anaerobic digestion (AD) of selected waste biomass from both batch and continuous testing. This research work presents a particle size distribution (PSD) based degradation model describing changes in the PSD of substrates over time, using the surface-based kinetics model for a spherical particle in a batch using literature data. A model calculation for the particle size distribution (PSD) is based on the mass fraction considering the time of stability. However, most literature data have assumed that particles of a substrate are spherical and are degraded from the outside.

If the total mass is $\frac{4\pi R^3 np}{3}$ **equation 6.1**

Where the n = number of particles and ρ = particle density and total surface area ($4\pi nR^2$) of spherical particles in a digester is substituted into 3.1 such that the decrease of the average particle radius with time can be written as follows:

$$R_t - R_o = -\frac{K_{sbk} * t}{\rho} \dots \dots \dots \text{equation 6.2}$$

[24], [174], [176], [200]

Where r = complex organic solid particles radius [L], assumed to be time dependent as indicated the formation proposed by [174] :

r_o =initial organic solid particle radius [L], specified as the initial condition for model application.

ρ =density of the substrate (kg/m^3),

r_t =average particle radius at time= $t(m)$

t =time (days),

K_{sbk} =surface-based hydrolysis constant ($kg/m^2 \text{ day}$). From the equation 6.2 above the current particle size distribution-based model is calculated based on the frequency over time as follows:

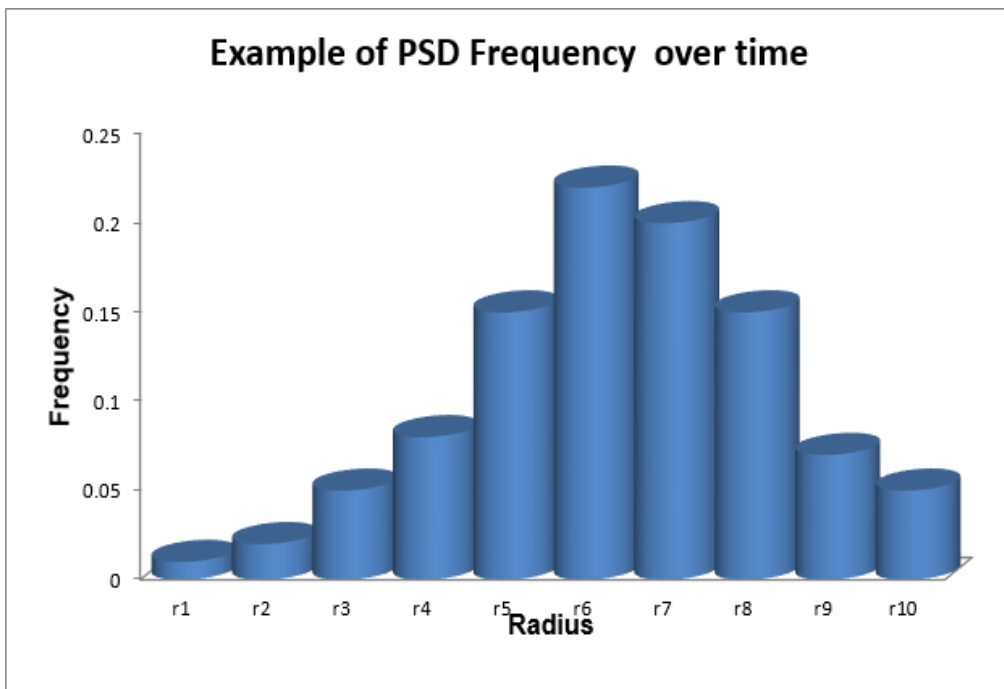


Figure 6.1 Demonstrates the feedstock radius frequency as a function of time

Such that the sum = 1, Overtime the particle size distribution-based model changes, using a spherical particle. However, the model was limited to 10

fractions of the PSD due to the large range of the particle size (100). This makes describing the PSD's middle point, as well as its upper and lower ends, much easier to characterise, with 10 values suggesting a good overview of the distribution. This was done to allow the study of the effects of the response of the particle size distribution on the rate of methane production by using fewer kinetic model runs.

6.1.1 The purpose of the particle size distribution-based degradation model

This model attempts to deal with particle size distribution and its effects on kinetics and biogas. Taking the particle size distribution (PSD) each fraction of the PSD is modelled by a completely mixed state variable degrading kinetics. While its specific surface area increase. The model depicts the degradation of complex organic matter and in turn, the surface area limiting the kinetics. It is a single reaction model, from complex organic matter to methane. A single reaction model that is governed by kinetics. The previous model has dealt with a single particle size followed by degradation. This is to account for the degradation and methane production. The biomass as PSD is describe as shown in figure 6.2. The PSD-based model is calculated from equation 6.2 below based on its frequency over time such that the sum of $\sum_1^{10} f_i = 1$. Using a spherical particle, the PSD changes over time, and equation 6.4 describes the changes. The case of $i=1$ and $i=10$ is slightly different.

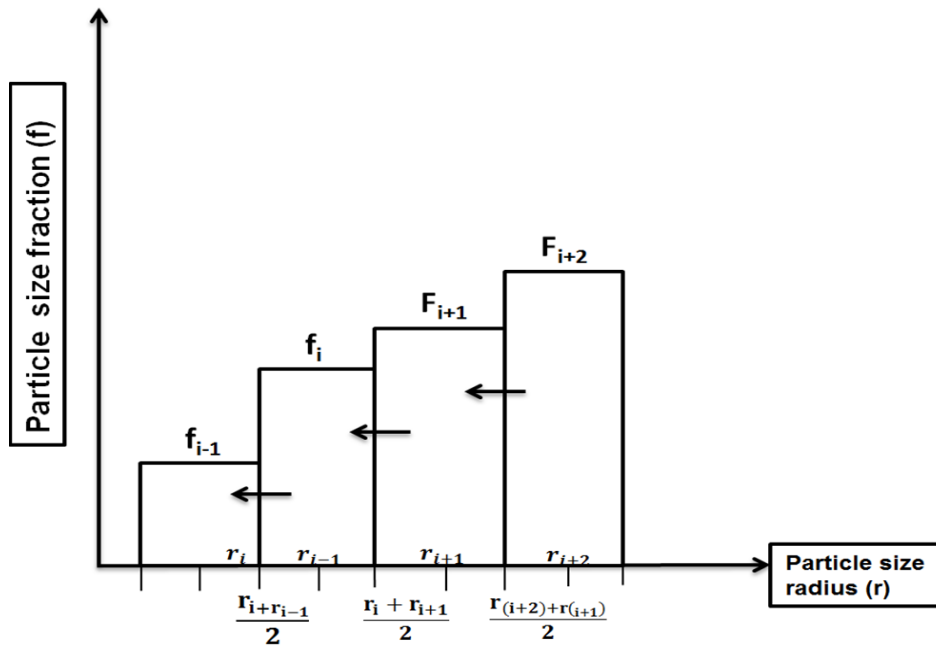


Figure 6.2 displays the feedstock PSD over time.

$$R_t - R_o = - \frac{K_{sbk} * t}{\rho} \dots \dots \dots \text{equation 6.2}$$

Where:

ρ is the substrate density (kg/m³),

R_t is the average particle radius at time t (m),

R_o is the average radius at time 0 (m),

t is the time (days),

and K_{sbk} is the surface-based hydrolysis constant (kg/m².day) [174], [175].

From the figure 6.2 above, the mass balance can be derived. However, there is need to determine the consumption and production rate of a particular size radius.

For the consumption of particle size r_i where, $i=1,2, 3,\dots,10$.

Simplifying equation 6.2 gives.

$$= \frac{K_{sbk}}{\rho} \left(\frac{f_{(i+1)}}{\frac{1}{2}(r_{i+2} - r_i)} \right) - \left(\frac{f_i}{\frac{1}{2}(r_{i+1} + r_{i-1})} \right) \dots \dots \dots \text{equation 6.3}$$

Production *Consumption*

For the production time

$$\frac{K_{sbk}}{\rho} \left(\frac{f_2}{\frac{1}{2}(r_3 - r_1)} \right) \text{Production only}$$

$$\left(\frac{f_i}{\frac{1}{2}(r_{max} + r_9)} \right) \text{Consumption}$$

r_{max} is the maximum particle size and in this case is set to be

$$r_{max} = r_{10} + \frac{r_{10} - r_9}{2}$$

$$f = \left\{ \begin{matrix} f_1 \\ f_2 \\ f_3 \\ f_4 \\ f_5 \\ f_6 \\ f_7 \\ f_8 \\ f_9 \\ f_{10} \end{matrix} \right\} = \text{Act like a completely mixed state variable}$$

Since the digester behaves like a the completely mixed state variable, mass balance analysis is given as:

$$\frac{df}{dt} = D (f_{in-f}) + \rho_f \dots \dots \dots \text{equation 6.4}$$

Where D is the dilution rate

Where $\rho_f = \left\{ \begin{array}{l} \rho_{f_1} \\ \rho_{f_2} \\ \rho_{f_3} \\ \rho_{f_4} \\ \rho_{f_5} \\ \rho_{f_6} \\ \rho_{f_7} \\ \rho_{f_8} \\ \rho_{f_9} \\ \rho_{f_{10}} \end{array} \right\}$ The mass fraction of each particle size is calculated as

follows:

$$a^* \text{ For a spherical particle} = \frac{3}{\rho r}$$

Where a^* is the specific surface area of the particle

Since particle size distribution has an impact on the degradation of complex organic matter, the disintegrated constant for surface-based AD System was modelled by introducing a parameter which describes the integration process.

The concentration of the individual particle is a function of the particle size distribution and the frequency. Hence, it can be calculated as:

$$\text{Mass fraction } C_i = \frac{f_i r_i^3}{\sum_1^{10} (f_i r_i^3)} \text{ --- equation 6.5}$$

Derived from the equation for mass of a particle.

$$C_v = \left\{ \begin{array}{l} C_1 \\ C_2 \\ C_3 \\ C_4 \\ C_5 \\ C_6 \\ C_7 \\ C_8 \\ C_9 \\ C_{10} \end{array} \right\} \text{ Such that } \sum_1^{10} C_I = C$$

Where C is the total concentration of organic matter and C_v is the vector of the individual concentration of the particle.

Therefore, each mass fraction degrades by the following rate equation.

$$\rho_{C_i} = -K_{sbk} a^* C_i = -\frac{K_{sbk}^3}{\rho r_i} C_i \dots \dots \dots \text{equation 6.6}$$

Where C acts as a completely mixed state variable such that

$$\frac{dC}{dt} = D (C_{in} - C) + \rho_c \dots \dots \dots \text{equation 6.7}$$

Finally, methane output is calculated by the following equation.

$$m = k_m \sum_1^{10} \rho C_i$$

And $c = \sum_1^{10} C_i \dots \dots \dots \text{equation 6.8}$ as previously stated.

6.1.2 Kinetic Model of Anaerobic Digestion

6.1.3 Purpose of this Model

This model attempts to deal with particle size distribution and its effects on the kinetics and biogas. Previous model has dealt with a single particle size follow by degradation. This is to account for the degradation and methane production, it is a very simple model, but could be enhanced and could be linked into anaerobic digestion model no1(ADM1) from hydrolysis into the soluble organic matter.

6.1.4 Model parameter definition

The following model parameter definition is used in the particle size distribution model:

- **Parameter**
- ❖ Particle size range and categories in m

- ❖ r_{\max} is used to set the maximum particle size for PS distribution calculations.
- ❖ Rate constant based on surface area (K_{sbk})
- ❖ Density (ρ)
- ❖ Specific methane production in m^3 methane/kg VS destroyed (km)

➤ **Initial conditions**

- ❖ Initial condition of particle size distribution (F_{ini})
- ❖ Initial VS concentrations (C_{ini}) % kg m^{-3}
- Inlet conditions of feedstock
 - ❖ Dilution rate
 - ❖ Particle size distribution of feedstock (F_{in})
 - ❖ Inlet VS concentrations (C_{in}) % kg m^{-3} (fresh)

6.2 Limitation of the particle size distribution-based model

- ❖ All particle sizes have different degradability.
- ❖ All particle sizes have a different shape.
- ❖ **All particle sizes have different kinetic.**

6.3 Modelling Results

6.3.1 Selection and processing of experimental data from the literature

The PSD-based degradation model was evaluated using both the raw and digested slurry. The data for the present work, however, only contain the raw slurry because post-digestion PSD (digested slurry) could not be collected. digested pig slurry. As a result, study was conducted utilising data from [183]. on the particle size and metal distributions in anaerobically digested pig slurry. The anaerobic reactor was operated at 37°C for approximately 15 days. Using the Cilas 1180 L n°516 laser diffraction system, the particle size distribution of two slurries raw slurry and digested slurry was examined before any separation treatment. The results showed how much of the solids' total volume was occupied by the particle volume distribution. The distribution of particle sizes in the raw and digested

slurries is represented by a histogram of the relative frequency per volume class versus the volume class of the particles (Figure 6.1). According to Houghton et al.[283] the quantity of particles can determine the specific area in each particle size class as a percentage of the total cumulative specific surface area, assuming the particles are spherical and non-porous. Using a digitizer software. The individual volume fractions of the particles were summed up to 100%. The dry matter content (DM) and volatile solid (VS) for the raw slurry (RS) and digested slurry (DS) are 27%, 673 and 16% and 591 respectively [183] . The mass concentration (C_i) in kg/m^3 of each particle size radius was estimated from the percentage volume fraction by multiplying with the total VS shown in table 6.1

Table 6. 1 Calculation example of the mass concentration (C_i)

		Raw slurry	Volatile solid	Digested slurry	Volatile solid
% Fresh matter	Dm	27		16	
g kg ⁻¹ DM	VS	673/1000	0.673	591/1000	0.591
		27*0.673		16*0.591	
Calculations					
Total particle volume		0.081353		0.009280	
		(V/100) *(DM*VS)			
		(0.081353/100) *(27*0.673)		(0.009280/100) *(16*0.591)	
C_i		0.014783		0.000878	

Note

% Fresh matter
g kg⁻¹ DM (VS) from Source [183].
The mass concentration (C_i)

To estimate the frequency of each particle size distribution, the mass concentration was divided by the particle size radius. Since the total particle size consists of 100 fractions, the mathematical model can accommodate only 10 fractions. The frequency of the particle size radius was partitioned into 10 of 10 fractions, each and plotted against the respective concentrations (figure 6.2). The

weighted average particle size range of each of the 10 fractions was estimated by multiplying each particle size radius by its frequency and dividing the product by the weighted average frequency as shown in table 6.2 examples. The spread sheet calculation is shown in appendix G. The concentration of the particle size distribution (10 fractions) was estimated by multiplying the individual weighted average frequency by the weighted average particle size radius. The mass fraction of the particle size distribution (10 fractions) was then calculated by dividing the individual concentration by the total concentration of the particle size distribution (10 fractions). Finally, the initial concentration used for the simulation was obtained by multiplying the mass fraction by the volatile solid content of the feedstock. The same procedure was used to estimate the inert fraction of the particle size distribution (10 fractions).

Table 6. 2 Calculation example of the weighted average particle size range of each of the 10 fractions

	99					10 fractions		
	PSD	Total particle size volume	Ci	Ci/r ³	fi	fi	Fi*ri	ri average
1	28.1955	0.081353	0.014783	6.59E-07	0.808993		22.80996	
2	50.0968	0.027555	0.005007	3.98E-08	0.048852		2.447321	
3	71.9891	0.054981	0.009991	2.68E-08	0.032849		2.364774	
4	90.752	0.082394	0.014972	2E-08	0.024572		2.229943	
5	115.783	0.091609	0.016646	1.07E-08	0.013156		1.523208	
6	137.679	0.109923	0.019974	7.65E-09	0.009388		1.292599	
7	156.447	0.128224	0.0233	6.08E-09	0.007464		1.167738	
8	181.477	0.137439	0.024974	4.18E-09	0.005126		0.930202	
9	203.379	0.146642	0.026646	3.17E-09	0.003886		0.790236	
10	225.275	0.164956	0.029974	2.62E-09	0.003216	0.957501	0.724524	37.89081

Hence Ci the mass concentration = (TPSV/100) * (DM* VS)

(0.081353/100) * (27*0.673)

Where TPVS = Total PS volume

% Fresh matter 27

g kg-1 DM (VS) from source [183].

Ci/r³ = mass concentration ci divided by the PSD

Fi = Ci/r³/the sum of Ci/r³

Where fi = fraction of fi into 10 of 10

$F_i \cdot r_i = f_i \cdot \text{PSD}$ and $r_i \text{ average} = F_i \cdot r_i / f_i$

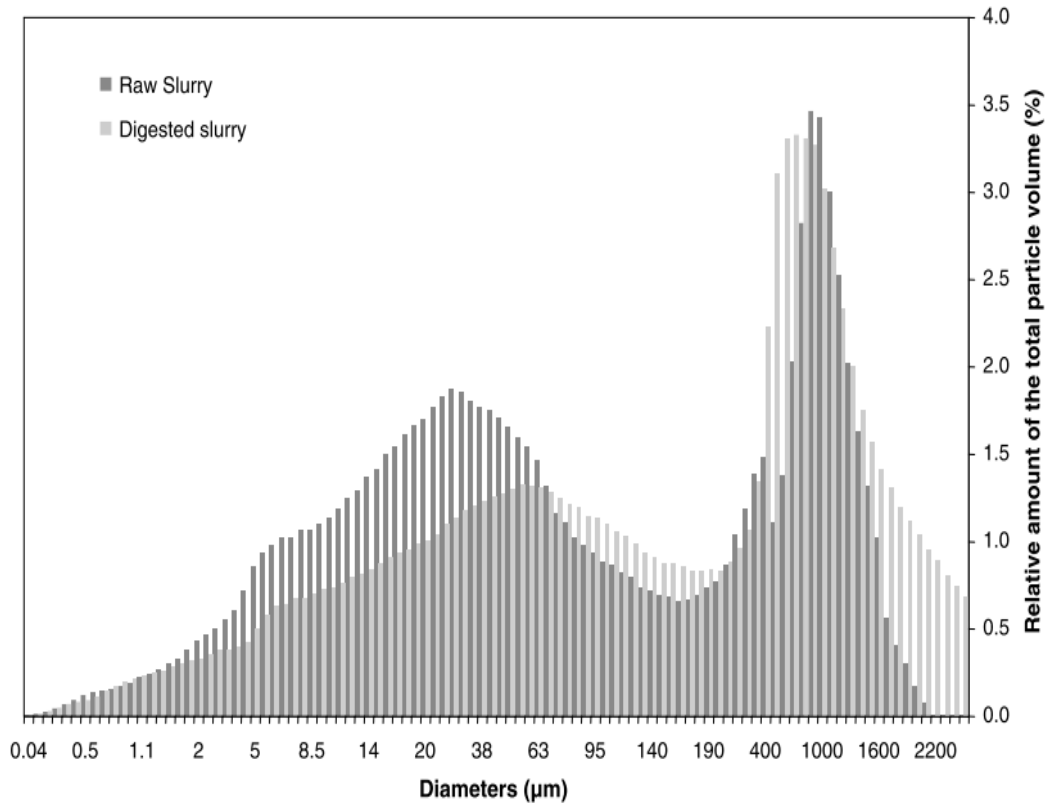


Figure 6.3 Experimental data for PSD used for extraction

Source [183].

The result in figure 6.3 shows the distribution of particle size in both raw and digester slurries. In both slurries, two peaks were observed. The first peak occurs at the particle diameter of 28µm for raw slurry and 53µm for digested slurry. The second peak in the graph for both slurries occur at 950µm (raw) and 700µm (digested) respectively. The first peak corresponds to "supracolloids" (1-100µm, including bacterial floc, single cells, and organic residues), and the second peak to settleable (>100 µm, consist of mainly organic residue), according to terminology proposed by Levine, cited by [183], [293], [294]. This confirms the fact that only the smaller particles are degraded during AD leading to a shift in the amount (in volume) occupied by the large particles in the slurry which is about 92%. The graph also shows that the particle diameter of the smaller particles is usually less than

1um. In general, the graph depicts a bimodal distribution of particles in both slurries with larger particles in more proportion than the smaller particles.

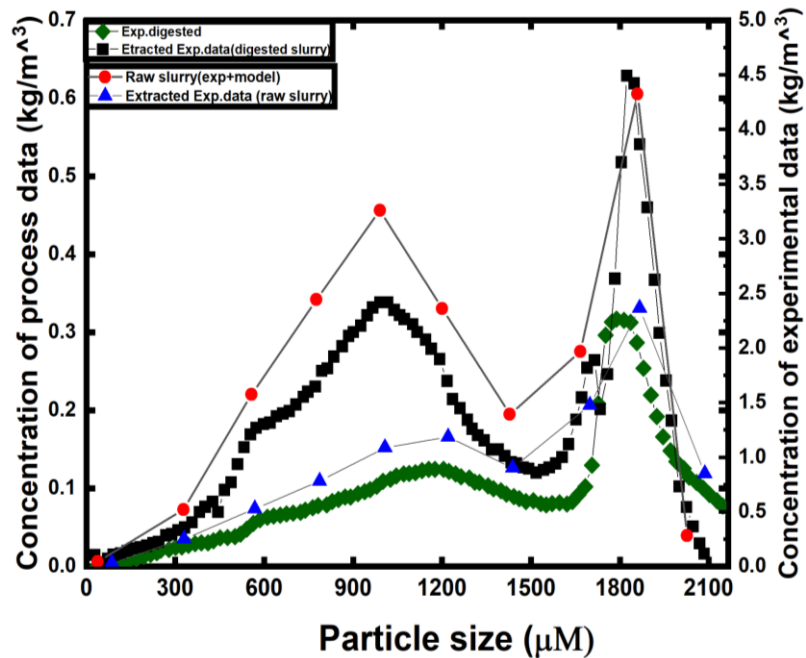


Figure 6.4: Converted experimental data of PSD digested slurry and model output digested slurry.

Figure 6.4 shows the distribution of particle size for raw and digested slurries from experiments and the output of a model. Two peaks are observed in the following experiments: raw slurry (exp.+ model), digested slurry (exp.), digested slurry (extracted exp. Data). As shown by the simulated results, the raw slurry (extracted exp. Data) had three peaks with the peak at PS=1700μm being quite insignificant as compared to those at PS = 1000 and approximate 1850μm for the raw slurries. The results reveal that there are two distinct peaks at 1700 um and 1850 um, which can be attributed to the PS's class (large size). At the point of occurrence of the peak at PS=1000μm, a concentration of 3.26kg/m³ was observed for the raw slurry (exp+ model) and a concentration of 2.5kg/m³ for the raw slurry (extract.

exp data). The digested slurries (exp and ext. exp.) had their first peaks at PS approximately 1200 μm with concentrations of 1.2 kg/m^3 and 0.9 kg/m^3 respectively. Also, the digested slurries had their second peak at PS between 1800 -1850 μm with concentrations of 2.35 and 2.25 kg/m^3 respectively. The raw slurries (exp. +model and extracted exp. Data) had their second peaks at PS approximately equal to 1850 μm with concentrations of 4.32 and 4.5 kg/m^3 respectively. Generally, the graphical distribution shows an unequal mode of particles in both slurries with larger particles in more proportion than the smaller particles. This confirms the existing report of [183]. However, the same trend in the particle size distribution of larger diameters was also found by [282] in anaerobically digested domestic sewage where the generation of bacterial flocs and filaments during anaerobic digestion leads to a slight increase in the relative volume occupied by the largest particle.

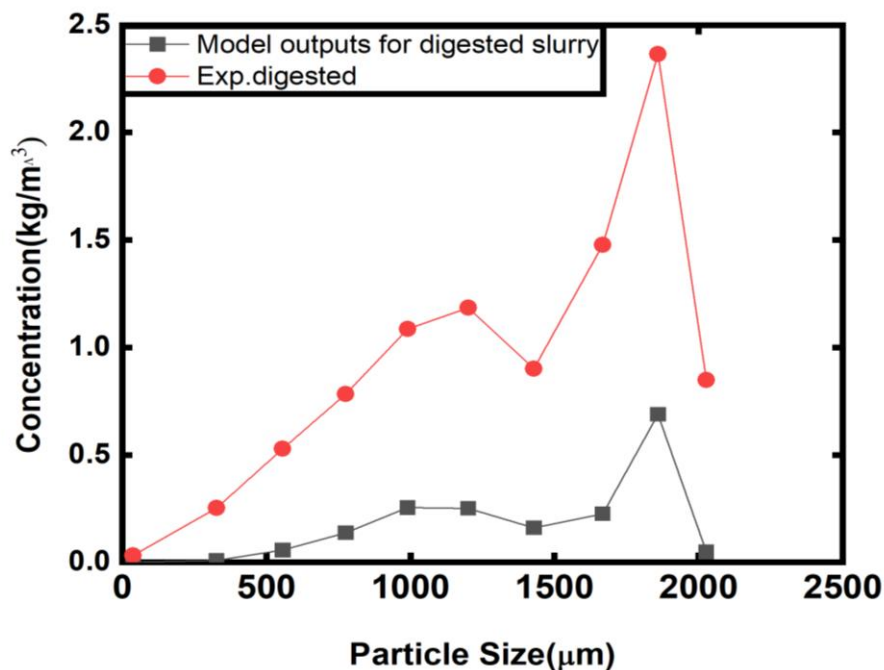


Figure 6.5: Experimental digester slurry and model output of digested slurry at 100% degradability.

As shown in Figure 6.5, the results from the simulation demonstrated the ability of the model to predict similar behaviour observed in the experiment of [183]. [183]. The model simulation also reveals that the feedstock is completely degradable (i.e., Achieves 100% degradation). This is explained by the biochemical makeup of the substrate and the composition of the feedstock.

6.3.2 Modelling the effect of particle size distribution at a different percentage of biodegradability factor

Different degradability factors (table 6.3) and a kinetic constant $K_{sbk} = 0.28$ were used to model the experimental data. The output of the model and experimental data is shown in Figure 6.6. All model outputs reveal a bimodal distribution curve when compared to the experimental digested slurry; the output result has two peaks at various degradability factors. The two speak suggest the presence of bimodal particle distribution which could be because of the differences in particle sizes. Bimodal particle size distribution has been reported by [183] that found out that the differences peaks correspond differently to particle size distribution. Also, the bimodal particle size distribution results from the formation of bacterial flocs, filament as well as undigested organics that settle at the bottom of digestion. Hence, the results indicated the same trend with the first peak occurring about 1000-micron particle size and a second peak about 1800-micron particle size.

Table 6. 3 Assume degradability factor (exp.+ model), for digested output with 0.28 kinetic constants K_{sbk} .

Degradability factor
0.4
0.5
0.6
0.7
0.8
0.9

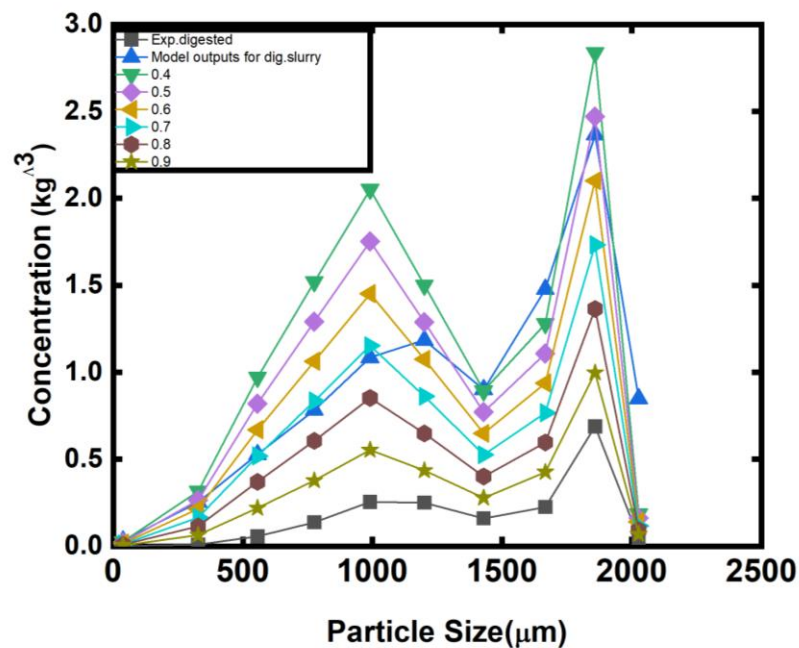


Figure 6.6: Particle size distribution (PSD) result, Experimental digested and model output for digested slurry.

As a result, the graph shows that the degradability factor of 0.7 best fits the experimental data results in the first peak when the particle size radius is between 0 and 1000 micrometres, and that the degradability of the organic matter is 70% of the total VS fed into the digester. Suggesting that the particles of smaller particle size distribution degrade at that rate of 0-1000 micrometre range. This agrees with existing literature [283] that the smaller particles contribute more (to biodegradation) in terms of their specific surface area than the larger particles. However, in the second peak, when the particle size radius is between 1500-2000 micrometre, corresponding to larger-size particles, model results best fit the experimental data at the degradability factor of 0.5 of the total volatile solid, indicating 50% biodegradation. The model result also reveals that larger-size particles degrade slowly. Hence, it could be suggested that the actual degradability factor for the model that would reproduce the experimental curve/data lies between 0.5-0.7. This is in line with the previously existing

literature [295] which reviewed the kinetic relationships for the design of anaerobic digesters for pig manure. For low influent VS concentrations, the researcher discovered that the K value remains constant at 0.6. The fact that K increases significantly for volatile solid (VS) concentrations above 55kgm⁻³ (5.5%VS). As a result, it seems that the equation 6.72 below can be used to estimate the K value for anaerobic digestion (AD) of pig manure slurry. To determine this value, a sensitivity analysis was performed in the degradability factor range of 0.5 and 0.7 but at varying hydrolysis constants. According to the current research, the design of a digester used to treat pig slurry with degradability factor above 0.7 can be detrimental to the process.

$$K = 0.6 + 0.0006e^{(0.1185S T_0)}$$

-----equation 6.72

6.3.3 Modelling the effect of particle size distribution with a constant biodegradability factor and variation in K_{sbk}

From Figures 6.7 and 6.8, the results of the sensitivity analysis obtained by varying the hydrolysis constant K_{sbk} and under constant biodegradability factor are shown in Figures 6.7 and 6.8, respectively. The K_{sbk} was varied at a factor of ±0.5, a value that was chosen due to a lack of empirical, experimental data that makes it difficult to have confidence in the model. The model result shows a weak sensitivity of the hydrolysis constant. This is because the hydraulic retention time of 15 days is sufficient for complete degradation except at lower hydrolysis constant. The model result shows that, at 70% degradability factor, hydrolysis constant values K_{sbk} best fit is achieved at lower hydrolysis constant (0.14) and the worst fit obtained at hydrolysis constant of 0.42 respectively (Figure 6. 6). Similarly, the trend was observed for the 50% degradability factor, except that in general, the 70% modelling curve is a much better fit to the experimental digested curve than the 50% modelling curve. The result agrees with research pieces of literature that smaller particles can enhance the substrates biodegradability by offering a large surface area for microbial action [36], [173], [178], [200], [281], [282]. However, it should be noted that in all cases, degradation was not constant,

but varies across the particle sizes. Non-constant degradation across particle sizes could be the result of differences in the physical characteristics of waste, such as the feedstock composition, ease of splitting, input particle size distribution, durability, and biochemical makeup of the feedstock. Further, because the experiment was performed with pig slurry which has undergone two kinds of digestion processes (pig digestion and anaerobic digestion), it is expected that if the larger particles are more degradable, they should have completely degraded. Similar to this study, the physical and biochemical differences between the substrates of banana peels, tomatoes, and grass led to non-constant degradation of the feedstock, with paper waste becoming less biodegradable in comparison to the other three feedstocks, which may have been caused by difficulties with bacterial metabolism during digestion. The carbon accessibility and hydrolysis of the processed material may be enhanced by the smaller particle size because a larger unit surface area is exposed to enzymatic attack [160], [239], [240], [296]. The particle size paradox was discovered by [187] using a reanalysis of data from earlier studies. The fact that the relative rate of gas production per unit surface area rapidly decreases with decreasing particle size for smaller particles reveals that factors other than the mean particle size play a key role in the process and can equally be a contributing factor to non-constant degradation during the test.

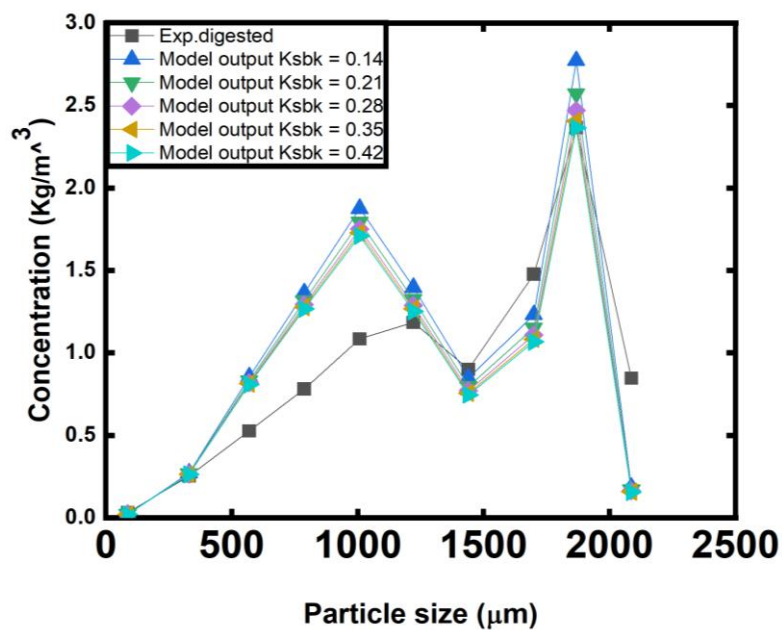


Figure 6.7: Variation of hydrolysis constant (K_{sbk}) at 50% degradability constant.

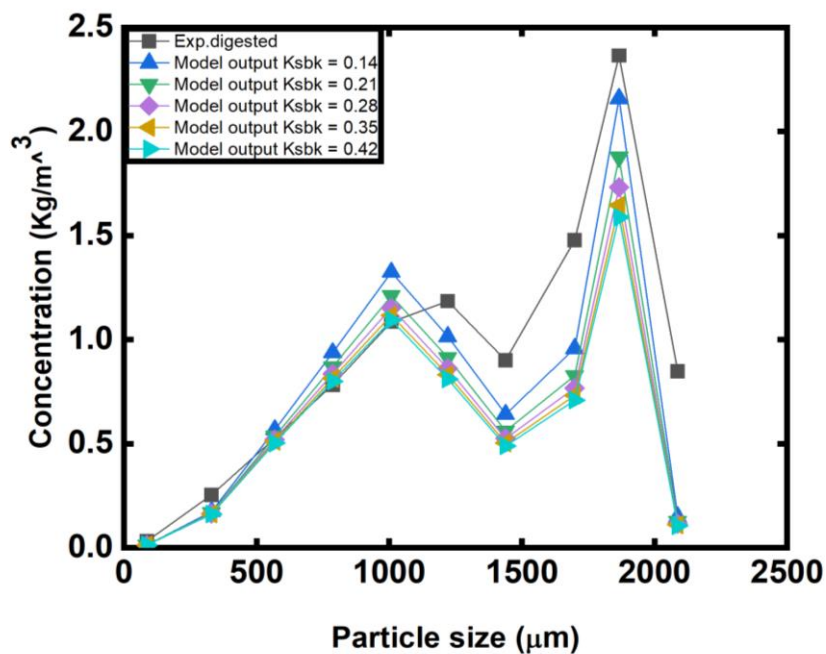


Figure 6.8: Variation of hydrolysis constant (K_{sbk}) at 70% degradability constant.

6.3.4 Cumulative model output of particle size distribution of total surface area contribution of digested slurry.

Figure 6.7 and table 6-4, shows the distribution of the total surface area contribution of digested slurry. The plot of the particle size distribution shows that the solids are uniformly graded (with a uniformity coefficient of about 0.46). The result reveal that the digested slurry had a slightly lower total specific surface area (0.3853 m²/g) than the area contribution degradable (0.4605 m²/g). However, a comparison of the plots of the total specific surface area and the area of inert slurry shows little or near insignificant biodegradation, consequently poor biogas yield. This is evident in VS feed still found in the effluent digested slurry. This implies that there is too much inert in the influent biomass, which cannot be degraded. It can also be argued that at the end of the anaerobic digestion process, there is a distribution of particles in the effluent with large particle sizes having an increasing concentration in the effluent. This is due to the utilization of smaller particles in the AD process which results in the formation of dense particles. Thus, suggesting that a measurement of the VS that contributes to biogas production could be estimated, by evaluating the effluent VS leaving the digester.

Table 6. 4 Experimental digester slurry and model output of digested slurry at 100% degradability.

Average	r(m)	Experimental digested slurry	Area contribution inert	Total specific surface area	Area contribution degradable
	5.57E-04	0.96862	0.8527	0.85835	0.86244
	7.76E-04	0.8812	0.70061	0.70941	0.75029
	9.90E-04	0.74632	0.53133	0.54181	0.63022
	0.0012	0.56691	0.3543	0.36466	0.50008
	0.00143	0.43699	0.24846	0.25765	0.38278
	0.00167	0.3606	0.19606	0.20408	0.30715
	0.00186	0.25288	0.13254	0.13841	0.20206
	0.00203	0.01567	0.0075	0.0079	0.04904
AV	0.0013	0.5286	0.3779	0.3853	0.4605

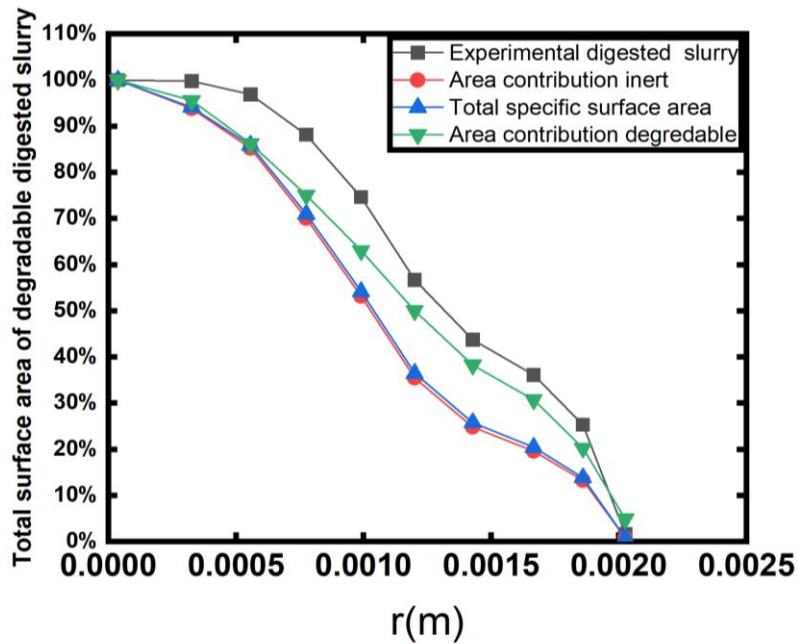


Figure 6.9: Cumulative model output of particle size distribution of total surface area contribution of digested slurry.

6.4 Physical Interpretation of Model Results

Following the results obtained from the simulation in sections 6.5 and 6.6. The particle size with a larger range is slowly degradable, while the smaller fraction is more degradable. The difference in the degradability can be attributed to an increase in the surface area figure (6.9) available for the degradation in the smaller particle size range. The model simulation results, when compared to the experiment, demonstrated the model's ability to completely describe the experimental results. This suggests that the composition of the feedstock, ease of splitting, and input particle size distribution may all contribute to the physical effects.

6.4.1 All Particle sizes have different degradability and shape.

Following the results obtained from the simulation test in sections 6.3 and 6.4, fractions with larger particle sizes are slowly degradable, while the smaller fraction is more degradable. This agrees with existing literature [283] that the smaller particles contribute more (to biodegradation) in terms of their specific surface area than the larger particles. It is also reported that substrate utilization rate coefficient doubled with a decrease in the average PS 2.14mm to 1.02mm indicating that PS is an important factor in the AD of food waste [281]. Also, the particle size paradox was found after reanalysing data from earlier studies [187]. The results show that factors other than the mean particle size are important because the relative rate of gas production per unit surface area drops off dramatically as particle sizes decrease. In agreement with this, [297] stated that biodegradability enhancement may result from both the increase in the available surface area of the substrate and the formation of biodegradable compounds from lignin. It should be noted from Figure 6.6 that while particle size fractions of 1000 microns attend 70 per cent degradability, PS of 1500 micron and 1800micron achieved 40 per cent and 50 per cent degradability, respectively. It could be that the 1500-micron PS fraction contains a high amount of lignin which restricts biodegradation. According to [36], cellulose in the lingo-cellulosic polymeric form is not available for bacterial attack, or what [59] described inaccessibility of the cellulose in the lignocellulose complex [173]. Also suggested that the ligneous structure within an organic complex tends to shield cellulosic materials from enzymatic hydrolysis. When any of these conditions exist, it becomes possible that smaller-size fractions could be less degraded than larger fractions.[204] found that the surface area of particles will vary in size. This implies that substrates giving different microbial growth rates and substrates degradation rates must be composed of different sizes as well as the chemical composition of the substrate. Biodegradability is also a function of the particle shape. Particles with different shapes have different biodegradability. According to Hills and

Nakano[173], the sphericity of particles varies between 1.0 for spheres, cubes, and short cylinders, and 0.28 for Formica flakes. This indicates that particle shape has a pronounced effect on biodegradability. However, differences in particle shape could result from the milling process where some particles that pass the screen are most probably smaller or even dissolved, whereas others may have been larger having passed through longitudinally [173]. [20] equally reported that differences in the particle shape could be because of the particles not being uniform in all dimensions, or that some of the particles are naturally present in the finer particles rather than being physically changed because of the action of the machine.

7 Conclusions and recommendations.

Based on the experimental results, the following conclusions can be drawn.

- ❖ Before experimental testing, the types of digesters employed, feedstocks, the process of breaking down the organic substrates and degree of particle size reduction must all be carefully considered as this can become a bottleneck.
- ❖ A combine effect mincer and a grinder for PTL4 were used to process the four substrates tested, including paper waste with a high lignin content, and it was discovered that this resulted in a significant improvement in processing efficiency.
- ❖ The mincer can effectively decrease the size of feedstock, particles large or smaller than the jaw opening, however, the output may comprise particulates that are highly irregular in shape - folded, twisted, clumped, thin, and so on
- ❖ A higher pre-treatment level led to a higher production of methane because of the smaller size of the particles. Therefore, optimising the size of the substrate and the growth of microbial organisms may boost the amount of methane produced.
- ❖ The BMP test results showed that BPWSB has a high potential for use as feedstock in an anaerobic digestion (AD) system to produce renewable energy, with a specific methane yield of $332 \pm 36 \text{ Nml/gVS}$ and volatile solid reduction of 67%.
- ❖ This study showed that smaller particle size reduction increased methane yield also with fibres like PWSB (PT4).
- ❖ The performance of a semi-continuous mesophilic digester decreases as large PS is fed into it. The IA/PA ratio, which shows the reactor's rising instability, increased gradually from 0.3 to 0.42 (BPWSB), 0.41 (GWSB), and 0.45 (PWSB). The specific methane yield decreased from 321 Nml/gVs to 68 Nml/gVs (GWSB), 262 Nml/gVs to 77 Nml/gVs (BPWSB), and 247 Nml/gVs to 59 Nml/gVs (PWSB)
- ❖ A 20-day HRT in a semicontinuous CSTR was used to study the effect of PSD in anaerobic digestion of three substrate biomass such as GWSB, BPWSB, and PWSB

according to their chosen pre-treatment levels 2 to 4. The study discovered that the peak and trough in biogas production indicated that HRT may have an impact on the amount of methane, pH level, and alkalinity.

- ❖ The three-substrate biomass showed fair digestion stability over time during the 20-day HRT digestion. The results indicated that HRT plays a significant role in determining the efficiency and stability of anaerobic digestion of organic matter.

- ❖ The pre-treatment method undoubtedly has an impact on particle size. A variety of PSD can be produced by the combined effect of different mechanical devices.

- ❖ The semi-continuous and batch tests produced contradictory experimental results. The batch test shows that BPWSB is necessary for a highly effective anaerobic degradation process as shown by an increase in specific methane production across pre-treatment level 4,3 and PT2. The batch results demonstrated that PTL4 has the highest specific methane production of approximately 295 ± 34 Nml/gVS when compared to the semi continuous test, which had a 235 ± 20 Nml/gVs.

- ❖ Batch test provided a higher methane output for BPWSB and PWSB, the semi-continuous test yielded a higher methane output for all PTLs (PT4-PT2) for GWSB

- ❖ The batch tests result revealed that, on average, BPWSB performed best at PTL4 and PTL3, PWSB performed better at PTL2, and GWSB produced the least amount of methane overall. Like batch tests, GWSB performed best in the semi-continuous test at PTL4 and PTL2, but PTL3 had the best results from BPWSB. The semi-continuous test had a better average methane output performance for GWSB than the batch test. A possible explanation for this is microbial activity. On the other hand, this confirms findings from earlier research that other factors besides mean size play an important role.

- ❖ Comparing the simulated results and the experimental data for different degradability reveals that large particles degrade slowly while the smaller

fractions degrade more rapidly. This demonstrates a kind of bimodal distribution with a lower and upper bound of degradability. Hence, suggesting that the smaller particle sizes may be one step towards more efficient conversion.

❖ The difference in the degradability can be attributed to the increase in surface area available for the degradation in the smaller particle size range.

8 Further Works

- ❑ The studies on the effects of carefully chosen combined mechanical equipment are incredibly rare. More study is required to better understand the combined effects of mechanical pre-treatment methods and the AD potential for biochemical methane output.
- ❑ More study on different mechanical treatment techniques using different substrate biomass is needed to examine the effects of varying HRT on the anaerobic digestion of various organic materials in semicontinuous CSTR.
- ❑ According to the findings of this study, the bioreactor should be fed twice a day during testing rather than once a day. This could help in decreasing the shock. This may maintain bioreactor stability while also increasing the rate of biogas production rate.
- ❑ It was not possible to dig deeper into the effect of PSD and shape on methane production from complex organic matter using experimental data, or to improve and integrate a PSD-based degradation model into the ADM1 model for anaerobic digestion to determine which best describes the experimental data due to time constraints and challenges. This research could be expanded upon to have a deeper understanding of the model.

9 References

- [1] FGN, 'Ngerian power baseline report', pp. 1–36, 2015.
- [2] C. E. Nnaji, C. C. Uzoma, and J. O. Chukwu, 'The Role of Renewable Energy Resources in Poverty Alleviation and Sustainable Development in Nigeria', *Sol. Energy*, vol. 3, no. September, pp. 31–37, 2010.
- [3] B. Fashola, 'Investment opportunities in the nigerian power sector', pp. 1–67, 2016.
- [4] K. Monson, S. R. Esteves, and A. J. Guwy, 'Anaerobic Digestion of Biodegradable Municipal Wastes: A Review, Sustainable Environmental Research Center, Welsh Assembly Government.', 2007.
- [5] B. A. S. Sambo, 'Matching Electricity Supply with Demand in Nigeria', pp. 32–36, 2008.
- [6] A. S. Sambo, 'Strategic Developments In Renewable Energy In Nigeria', *Int. Assoc. Energy Economics*, pp. 15–19, 2009.
- [7] E. Salminen and J. Rintala, 'Anaerobic digestion of organic solid poultry slaughterhouse waste--a review.', *Bioresour. Technol.*, vol. 83, no. 1, pp. 13–26, 2002, doi: 10.1016/S0960-8524(01)00199-7.
- [8] D. Batstone and J. Keller, 'The IWA Anaerobic Digestion model No 1 (ADM1)', *Water Sci. Technol.*, vol. 45, no. 10, pp. 65–73, 2002.
- [9] R. M. Jingura and R. Matengaifa, 'Optimization of biogas production by anaerobic digestion for sustainable energy development in Zimbabwe', *Renew. Sustain. Energy Rev.*, vol. 13, no. 5, pp. 1116–1120, 2009, doi: 10.1016/j.rser.2007.06.015.
- [10] T. D. Reynolds and P. A. Richards, *Unit operations and processes in environmental engineering*. PWS Pub. Co, 1996.
- [11] AG Rother, 'Background — Chair of Microbial Diversity — TU Dresden', *Institute of microbiology, Chair of general microbiology Technische Universität Dresden*, 2016. [Online]. Available: <https://tu-dresden.de/mn/biologie/mikro/mikdiv/forschung/Projects/methanogenesis>. [Accessed: 26-Aug-2022].
- [12] P. Weiland, 'Biogas production: Current state and perspectives', *Appl. Microbiol. Biotechnol.*, vol. 85, no. 4, pp. 849–860, 2010, doi: 10.1007/s00253-009-2246-7.
- [13] B. Schink, 'Energetics of syntrophic cooperation in methanogenic degradation', *Microbiol. Mol. Biol. Rev.*, vol. 61, no. 2, pp. 262–280, 1997, doi: 10.1128/mnbr.61.2.262-280.1997.
- [14] D. R. Boone, D. P. Chynoweth, R. A. Mah, P. H. Smith, and A. C. Wilkie, 'Ecology and microbiology of biogasification', *Biomass and Bioenergy*, vol. 5, no. 3–4, pp. 191–202, Jan. 1993, doi: 10.1016/0961-9534(93)90070-K.
- [15] M. Walker, C. J. Banks, and S. Heaven, 'The development of a mesh bioreactor for the anaerobic digestion of biodegradable municipal waste', *Water Sci. Technol.*, vol. 59, no. 4, pp. 729–735, 2008.
- [16] I. Angelidaki and W. Sanders, 'Assessment of the anaerobic biodegradability of macropollutants', *Rev. Environ. Sci. Biotechnol.*, vol. 3, no. 2, pp. 117–129, 2004,

- doi: 10.1007/s11157-004-2502-3.
- [17] K. G. Gollakota and K. K. Meher, 'Effect of particle size, temperature, loading rate and stirring on biogas production from castor cake (oil expelled)', *Biol. Wastes*, vol. 24, no. 4, pp. 243–249, 1988, doi: 10.1016/0269-7483(88)90109-7.
- [18] K. K. Moorhead and R. A. Nordstedt, 'Batch anaerobic digestion of water hyacinth: Effects of particle size, plant nitrogen content, and inoculum volume', *Bioresour. Technol.*, vol. 44, no. 1, pp. 71–76, 1993, doi: 10.1016/0960-8524(93)90211-S.
- [19] M. E. Griffin, K. D. McMahon, R. I. Mackie, and L. Raskin, 'Methanogenic population dynamics during start-up of anaerobic digesters', *Biotechnol. Bioeng.*, vol. 57, no. 3, pp. 346–355, 1998.
- [20] Y. Zhang and C. J. Banks, 'Impact of different particle size distributions on anaerobic digestion of the organic fraction of municipal solid waste', *Waste Manag.*, vol. 33, no. 2, pp. 297–307, 2013, doi: 10.1016/j.wasman.2012.09.024.
- [21] L. A. Fdez.-Güelfo, C. Álvarez-Gallego, D. Sales Márquez, and L. I. Romero García, 'The effect of different pretreatments on biomethanation kinetics of industrial Organic Fraction of Municipal Solid Wastes (OFMSW)', *Chem. Eng. J.*, vol. 171, no. 2, pp. 411–417, 2011, doi: 10.1016/j.cej.2011.03.095.
- [22] A. Cesaro and V. Belgiorno, 'Pretreatment methods to improve anaerobic biodegradability of organic municipal solid waste fractions', *Chem. Eng. J.*, vol. 240, pp. 24–37, 2014, doi: 10.1016/j.cej.2013.11.055.
- [23] Y. A. Vetter, J. W. Deming, P. A. Jumars, and B. B. Krieger-Brockett, 'A predictive model of bacterial foraging by means of freely released extracellular enzymes', *Microb. Ecol.*, vol. 36, no. 1, pp. 75–92, 1998, doi: 10.1007/s002489900095.
- [24] G. Esposito, L. Frunzo, A. Panico, and F. Pirozzi, 'Modelling the effect of the OLR and OFMSW particle size on the performances of an anaerobic co-digestion reactor', *Process Biochem.*, vol. 46, no. 2, pp. 557–565, 2011, doi: 10.1016/j.procbio.2010.10.010.
- [25] S. Jain, A. K. Lala, S. K. Bhatia, and A. P. Kudchadker, 'Modelling of hydrolysis controlled anaerobic digestion', *J. Chem. Technol. Biotechnol.*, vol. 53, no. 4, pp. 337–344, 1992, doi: 10.1002/jctb.280530404.
- [26] V. A. Vavilin, S. V. Rytov, and L. Y. Lokshina, 'A description of hydrolysis kinetics in anaerobic degradation of particulate organic matter', *Bioresour. Technol.*, vol. 56, no. 2–3, pp. 229–237, 1996, doi: 10.1016/0960-8524(96)00034-X.
- [27] X. Tong, L. H. Smith, and P. L. McCarty, 'Methane fermentation of selected lignocellulosic materials', *Biomass*, vol. 21, no. 4, pp. 239–255, 1990, doi: 10.1016/0144-4565(90)90075-U.
- [28] E. Morgenroth, R. Kommedal, and P. Harremoës, 'Processes and modelling of hydrolysis of particulate organic matter in aerobic wastewater treatment - a review', *Water Sci. Technol.*, vol. 45(6), no. 6, pp. 25–40, 2002.
- [29] H. Song, W. P. Clarke, and L. L. Blackall, 'Concurrent microscopic observations and activity measurements of cellulose hydrolyzing and methanogenic populations during the batch anaerobic digestion of crystalline cellulose', *Biotechnol. Bioeng.*, vol. 91, no. 3, pp. 369–378, 2005, doi: 10.1002/bit.20517.

- [30] D. J. Batstone, P. D. Jensen, and Editor-in-Chief: Peter Wilderer, '4.17 - Anaerobic Processes', no. 1, pp. 615–639, 2011.
- [31] I. Ramsay and Q. Government, 'Modelling and control of high-rate anaerobic wastewater treatment systems', no. January 1997, 1997.
- [32] J. a Eastman and J. F. Ferguson, 'Solubilization of particulate organic carbon during the acid phase of anaerobic digestion', *J. Water Pollut. Control Fed.*, vol. 53, no. 3, pp. 352–366, 1981, doi: 10.2307/25041085.
- [33] J. Mata-Alvarez, 'Biomethanization of the Organic Fraction of Municipal Solid Wastes | IWA Publishing', 2002. [Online]. Available: <https://www.iwapublishing.com/books/9781900222143/biomethanization-organic-fraction-municipal-solid-wastes>. [Accessed: 14-Aug-2018].
- [34] V. A. Vavilin, B. Fernandez, J. Palatsi, and X. Flotats, 'Hydrolysis kinetics in anaerobic degradation of particulate organic material: An overview', *Waste Manag.*, vol. 28, no. 6, pp. 939–951, 2008, doi: 10.1016/j.wasman.2007.03.028.
- [35] L. P. Griffin, 'Anaerobic Digestion of Organic Waste: The Impact of Operating Conditions on Hydrolysis Efficiency and Microbial Community Composition', p. 103, 2012.
- [36] S. K. Sharma, I. M. Mishra, M. P. Sharma, and J. S. Saini, 'Effect of particle size on biogas generation from biomass residues', *Biomass*, vol. 17, no. 4, pp. 251–263, 1988, doi: 10.1016/0144-4565(88)90107-2.
- [37] L. Appels, J. Baeyens, J. Degrève, and R. Dewil, 'Principles and potential of the anaerobic digestion of waste-activated sludge', *Prog. Energy Combust. Sci.*, vol. 34, no. 6, pp. 755–781, 2008, doi: 10.1016/j.pecs.2008.06.002.
- [38] A. Molino, F. Nanna, Y. Ding, B. Bikson, and G. Braccio, 'Biomethane production by anaerobic digestion of organic waste', *Fuel*, vol. 103, pp. 1003–1009, 2013, doi: 10.1016/j.fuel.2012.07.070.
- [39] F. Di Maria, 'The Recovery of Energy and Materials From Food Waste by Codigestion with Sludge: Internal Environment of Digester and Methanogenic Pathway', *Food Bioconversion*, vol. 2, pp. 95–125, Jun. 2017, doi: 10.1016/B978-0-12-811413-1.00003-6.
- [40] A. Wellinger, J. Murphy, and D. Baxter, *The biogas handbook: science, production and applications*, 1st Editio. Woodhead Publishing Series in Energy, 2013.
- [41] C. Eliyan, 'Anaerobic Digestion of Municipal Solid Waste in Thermophilic Continuous Operation', no. May 2007, 2007.
- [42] J. B. Van, 'A Short History of Anaerobic Digestion', 2022. [Online]. Available: <https://extension.psu.edu/a-short-history-of-anaerobic-digestion>. [Accessed: 04-Aug-2022].
- [43] A. M. Buswell and W. D. Hatfield, 'TMENT OF REGISTRATION AND EDUCATION [Printed by authority of the State of Illinois .]', no. 32, 1936.
- [44] Danish Ministry of Energy and Environment, 'Energy 21; The Danish Government's Action Plan for Energy 1996. Copenhagen, Denmark.', 1996.
- [45] A. Lettinga, G.; Van Haandel, 'Anaerobic treatment for energy production and environmental protection.', " *Chapter 19 in Renewable Energy: Sources for Fuels*

- and Electricity*. Covelo, CA: Island Press., 1992. [Online]. Available: <https://www.semanticscholar.org/paper/Anaerobic-treatment-for-energy-production-and-Lettinga-Haandel/eed92cdd08e531dbb48a8479229bf57e4484b3c1>. [Accessed: 04-Aug-2022].
- [46] M. N. Nnabuchi, F. O. Akubuko, C. Augustine, and G. Z. Ugwu, 'Assessment of the Effect of Co-Digestion of Chicken Dropping and Cow Dung on Biogas Generation', *Glob. J. Sci. Front. Res. Phys. Sp. Sci.*, vol. 12, no. 7, pp. 238–243, 2012.
- [47] E. Dahlquist, 'Technologies for Converting Biomass to Useful Energy Series: Sustainable Energy Developments 4 Erik Dahlquist', p. 499, 2013, doi: 10.1007/978-81-322-2211-8.
- [48] H. W. Doelle and H. W., 'Biotechnology and Human Development in Developing Countries', *Electron. J. Biotechnol.*, vol. 4, no. 3, pp. 0–0, Dec. 2001, doi: 10.2225/vol4-issue3-fulltext-9.
- [49] E. Epstein, 'Disposal and Management of Solid Waste', *Dispos. Manag. Solid Waste*, pp. 128–133, Jan. 2015, doi: 10.1201/B18070-14/DISPOSAL-MANAGEMENT-SOLID-WASTE-ELIOT-EPSTEIN.
- [50] Y. Vögeli, C. Riu, A. Gallardo, S. Diener, and C. Zurbrügg, *Anaerobic Digestion of Biowaste in Developing Countries*. 2014.
- [51] C. Mao, Y. Feng, X. Wang, and G. Ren, 'Review on research achievements of biogas from anaerobic digestion', *Renew. Sustain. Energy Rev.*, vol. 45, pp. 540–555, May 2015, doi: 10.1016/j.rser.2015.02.032.
- [52] GLOBALPETROLPRICES.COM, 'Nigeria diesel prices, 06-Aug-2018 | GlobalPetrolPrices.com', 2016. [Online]. Available: https://www.globalpetrolprices.com/Nigeria/diesel_prices/. [Accessed: 13-Aug-2018].
- [53] Jeanger P. Juanga and A, 'Optimizing dry Anaerobic Digestion of Organic Fraction of Municipal Solid Waste', *Tesis Dr.*, no. Asian Institute of Technology, p. 160p., 2005.
- [54] D. J. Caruana and A. E. Olsen, *Anaerobic digestion : processes, products, and applications*. Nova Science Publishers, 2011.
- [55] J. Mata-Alvarez, S. Macé, and P. Llabrés, 'Anaerobic digestion of organic solid wastes. An overview of research achievements and perspectives', *Bioresour. Technol.*, vol. 74, no. 1, pp. 3–16, 2000, doi: 10.1016/S0960-8524(00)00023-7.
- [56] C. R. Lohri, L. Rodić, C. Zurbrügg, L. Rodic, and C. Zurbrugg, 'Feasibility assessment tool for urban anaerobic digestion in developing countries', *J. Environ. Manage.*, vol. 126, pp. 122–131, 2013, doi: 10.1016/j.jenvman.2013.04.028.
- [57] R. Steffen, O. Szolar, and R. Braun, 'Feedstocks for anaerobic digestion', *Inst. Agrobiotechnology ...*, pp. 1–29, 1998.
- [58] C. C. Ngumah, J. N. Ogbulie, J. C. Orji, and E. S. Amadi, 'Biogas potential of organic waste in Nigeria', *J. Urban Environ. Eng.*, vol. 7, no. 1, pp. 110–116, 2013, doi: 10.4090/juee.2013.v7n1.110116.

- [59] J. M. Owens and D. Chynoweth, 'Biochemical methane potential of municipal solid waste (MSW) components', *Water Sci. Technol.*, vol. 27, no. 2, pp. 1–14, 1993.
- [60] L. Appels *et al.*, 'Anaerobic digestion in global bio-energy production: Potential and research challenges', *Renew. Sustain. Energy Rev.*, vol. 15, no. 9, pp. 4295–4301, 2011, doi: 10.1016/j.rser.2011.07.121.
- [61] V. N. Gunaseelan, 'Anaerobic digestion of biomass for methane production: A review', *Biomass and Bioenergy*, vol. 13, no. 1–2, pp. 83–114, 1997, doi: 10.1016/S0961-9534(97)00020-2.
- [62] C. G. Gunnerson, D. C. Stuckey, M. Greeley, and R. T. Skrinde, 'Anaerobic digestion: Principles and practices for biogas systems'. The World Bank, Washington, DC, 01-Jan-1986.
- [63] H. Bouallagui, Y. Touhami, R. Ben Cheikh, and M. Hamdi, 'Bioreactor performance in anaerobic digestion of fruit and vegetable wastes', *Process Biochem.*, vol. 40, no. 3–4, pp. 989–995, 2005, doi: 10.1016/j.procbio.2004.03.007.
- [64] V. Riau, M. Á. De la Rubia, and M. Pérez, 'Temperature-phased anaerobic digestion (TPAD) to obtain class A biosolids: A semi-continuous study', *Bioresour. Technol.*, vol. 101, no. 8, pp. 2706–2712, 2010, doi: 10.1016/j.biortech.2009.11.101.
- [65] A. Khalid, M. Arshad, M. Anjum, T. Mahmood, and L. Dawson, 'The anaerobic digestion of solid organic waste', *Waste Manag.*, vol. 31, no. 8, pp. 1737–1744, 2011, doi: 10.1016/j.wasman.2011.03.021.
- [66] S. E. Nayono, *Anaerobic digestion of organic solid waste for energy production*. 2009.
- [67] M. Kim and R. E. Speece, 'Reactor configuration-part i comparative process stability and efficiency of mesophilic anaerobic digestion', *Environ. Technol. (United Kingdom)*, vol. 23, no. 6, pp. 631–642, Jun. 2002, doi: 10.1080/09593330.2002.9619248.
- [68] SHEFALI VERMA, 'Anaerobic Digestion of Biodegradable Organics in Municipal Solid Wastes', *Found. Sch. Eng. Appl. Sci. Columbia Univ.*, no. May, pp. 1–56, 2002, doi: 10.1016/j.biotechadv.2010.10.005.
- [69] F. Monnet, 'An Introduction to Anaerobic Digestion of Organic Wastes', *Remade Scotl. Rep.*, no. November, pp. 1–48, 2003, doi: 10.1007/978-3-319-24708-3_2.
- [70] E. Sánchez, R. Borja, P. Weiland, L. Travieso, and A. Martín, 'Effect of substrate concentration and temperature on the anaerobic digestion of piggery waste in a tropical climate', *Process Biochem.*, vol. 37, no. 5, pp. 483–489, 2001, doi: 10.1016/S0032-9592(01)00240-0.
- [71] G. Lyberatos and I. V Skiadas, 'Modelling of anaerobic digestion - a review', *Glob. NEST J.*, vol. 1, no. 2, pp. 63–76, 1999, doi: 10.2478/v10026-008-0011-9.
- [72] W. I. Warburton and Sri Suhartini, 'ePrints Soton', *Soc. Sci.*, pp. 1–283, 2000, doi: 10.1109/fie.2016.7757408.
- [73] Metcalf & Eddy (2003), 'Wastewater Engineering Treatment and Reuse. 4th Edition, McGraw-Hill, New York. - References - Scientific Research Publishing'.

- [Online]. Available: [https://www.scirp.org/\(S\(351jmbntvnsjt1aadkposzje\)\)/reference/ReferencesPapers.aspx?ReferenceID=1570731](https://www.scirp.org/(S(351jmbntvnsjt1aadkposzje))/reference/ReferencesPapers.aspx?ReferenceID=1570731). [Accessed: 06-Aug-2022].
- [74] E. Kwietniewska and J. Tys, 'Process characteristics, inhibition factors and methane yields of anaerobic digestion process, with particular focus on microalgal biomass fermentation', *Renew. Sustain. Energy Rev.*, vol. 34, pp. 491–500, 2014, doi: 10.1016/j.rser.2014.03.041.
- [75] X. Gómez, M. J. Cuetos, J. Cara, A. Morán, and A. I. García, 'Anaerobic co-digestion of primary sludge and the fruit and vegetable fraction of the municipal solid wastes: Conditions for mixing and evaluation of the organic loading rate', *Renew. Energy*, vol. 31, no. 12, pp. 2017–2024, Oct. 2006, doi: 10.1016/J.RENENE.2005.09.029.
- [76] P. G. Stroot, K. D. McMahon, R. I. Mackie, and L. Raskin, 'Anaerobic codigestion of municipal solid waste and biosolids under various mixing conditions - II: Microbial population dynamics.', *Water Res.*, vol. 35, no. 7, pp. 1804–1816, 2001, doi: 10.1016/S0043-1354(00)00439-5.
- [77] R. Al Seadi, T., Ruiz, D., Prassl, H., Kottner, M., Finsterwaldes, T., Volke, S. and Janssens, 'Handbook of Biogas. University of Southern Denmark, Esbjerg. - References - Scientific Research Publishing', 2008. [Online]. Available: [https://www.scirp.org/\(S\(lz5mqp453edsnp55rrgjt55\)\)/reference/referencespapers.aspx?referenceid=1437252](https://www.scirp.org/(S(lz5mqp453edsnp55rrgjt55))/reference/referencespapers.aspx?referenceid=1437252). [Accessed: 06-Aug-2022].
- [78] ZAKI ABEDBEEN, 'SLUDGE TREATMENT IN WASTEWATER: AEROBIC AND ANAEROBIC DIGESTION', 2010. [Online]. Available: <https://www.slideshare.net/zakiabedeen/anaerobic-aerobic-digestion>. [Accessed: 13-Aug-2018].
- [79] G. N. Demirer and S. Chen, 'Effect of retention time and organic loading rate on anaerobic acidification and biogasification of dairy manure', *J. Chem. Technol. Biotechnol.*, vol. 79, no. 12, pp. 1381–1387, 2004, doi: 10.1002/jctb.1138.
- [80] R. Borja, C. J. Banks, and Z. Wang, 'Effect of organic loading rate on anaerobic treatment of slaughterhouse wastewater in a fluidised-bed reactor', *Bioresour. Technol.*, vol. 52, no. 2, pp. 157–162, 1995, doi: 10.1016/0960-8524(95)00017-9.
- [81] B. Zhang, L. L. Zhang, S. C. Zhang, H. Z. Shi, and W. M. Cai, 'The influence of pH on hydrolysis and acidogenesis of kitchen wastes in two-phase anaerobic digestion', *Environ. Technol.*, vol. 26, no. 3, pp. 329–340, 2005, doi: 10.1080/09593332608618563.
- [82] Z. H. Hu, G. Wang, and H. Q. Yu, 'Anaerobic degradation of cellulose by rumen microorganisms at various pH values', *Biochem. Eng. J.*, vol. 21, no. 1, pp. 59–62, 2004, doi: 10.1016/j.bej.2004.05.004.
- [83] H. J. M. Op den Camp, G. J. M. Verkley, H. J. Gijzen, and G. D. Vogels, 'Application of rumen microorganisms in the anaerobic fermentation of an organic fraction of domestic refuse', *Biol. Wastes*, vol. 30, no. 4, pp. 309–316, Jan. 1989, doi: 10.1016/0269-7483(89)90059-1.
- [84] R.E.Speece, 'Anaerobic Biotechnology and Odor/Corrosion Control for

- Municipalities and Industries: Amazon.com: Books', *Archae Press*, 2008. [Online]. Available: <https://www.amazon.com/Anaerobic-Biotechnology-Corrosion-Municipalities-Industries/dp/B001P77CW6>. [Accessed: 13-Aug-2018].
- [85] G. F. Parkin and W. F. Owen, 'Fundamentals of Anaerobic Digestion of Wastewater Sludges', *J. Environ. Eng.*, vol. 112, no. 5, pp. 867–920, Oct. 1986, doi: 10.1061/(ASCE)0733-9372(1986)112:5(867).
- [86] R. E. Speece, 'Anaerobic biotechnology for industrial wastewaters', p. 394, 1996.
- [87] J. KIM *et al.*, 'Effects of Various Pretreatments for Enhanced Anaerobic Digestion with Waste Activated Sludge', *J. Biosci. Bioeng.*, vol. 95, no. 3, pp. 271–275, 2003, doi: 10.1263/jbb.95.271.
- [88] B. K. Angelidaki, I., Ellegaard, L. & Ahring, 'Applications of the anaerobic digestion process.', *In: Ahring, B. K. (ed.) Biomethanation II: Advances in Biochemical Engineering Biotechnology. Berlin, Germany: Springer.*, 2003. [Online]. Available: [https://www.scirp.org/\(S\(351jmbntvnsjt1aadkposzje\)\)/reference/referencespapers.aspx?referenceid=200383](https://www.scirp.org/(S(351jmbntvnsjt1aadkposzje))/reference/referencespapers.aspx?referenceid=200383). [Accessed: 06-Aug-2022].
- [89] K. V. Rajeshwari, M. Balakrishnan, A. Kansal, K. Lata, and V. V. N. Kishore, 'State-of-the-art of anaerobic digestion technology for industrial wastewater treatment', *Renew. Sustain. energy Rev.*, vol. 4, no. 2, pp. 135–156, 2000, doi: 10.1016/S1364-0321(99)00014-3.
- [90] A. Khalid, M. Arshad, M. Anjum, T. Mahmood, and L. Dawson, 'The anaerobic digestion of solid organic waste', *Waste Manag.*, vol. 31, no. 8, pp. 1737–1744, Aug. 2011, doi: 10.1016/J.WASMAN.2011.03.021.
- [91] A. Veeken, S. Kalyuzhnyi, H. Scharff, and B. Hamelers, 'Effect of pH and VFA on Hydrolysis of Organic Solid Waste', *J. Environ. Eng.*, vol. 126, no. 12, pp. 1076–1081, 2000, doi: 10.1061/(asce)0733-9372(2000)126:12(1076).
- [92] C. P. L. Grady Jr., G. T. Daigger, N. G. Love, and C. D. M. Filipe, 'BIOLOGICAL WASTEWATER TREATMENT', 2011.
- [93] M. J. Cuetos, X. Gómez, M. Otero, and A. Morán, 'Anaerobic digestion of solid slaughterhouse waste (SHW) at laboratory scale: Influence of co-digestion with the organic fraction of municipal solid waste (OFMSW)', *Biochem. Eng. J.*, vol. 40, no. 1, pp. 99–106, 2008, doi: 10.1016/j.bej.2007.11.019.
- [94] I. Angelidaki, L. Ellegaard, and B. K. Ahring, 'Applications of the anaerobic digestion process', *Adv. Biochem. Eng. Biotechnol.*, vol. 82, pp. 1–33, 2003, doi: 10.1007/3-540-45838-7_1.
- [95] H.-W. Yen and D. E. Brune, 'Anaerobic co-digestion of algal sludge and waste paper to produce methane', *Bioresour. Technol.*, vol. 98, pp. 130–134, 2007, doi: 10.1016/j.biortech.2005.11.010.
- [96] Chongrak Polprasert, 'Organic Waste Recycling | IWA Publishing', *John Wiley & sons. ISBN: 0-471-96434-4.*, 1996. [Online]. Available: <https://www.iwapublishing.com/books/9781843391210/organic-waste-recycling>. [Accessed: 29-Dec-2022].
- [97] Y. Chen, J. J. Cheng, and K. S. Creamer, 'Inhibition of anaerobic digestion

- process: A review', *Bioresour. Technol.*, vol. 99, no. 10, pp. 4044–4064, 2008, doi: 10.1016/j.biortech.2007.01.057.
- [98] L. A. de Baere, M. Devocht, P. Van Assche, and W. Verstraete, 'Influence of high NaCl and NH₄Cl salt levels on methanogenic associations', *Water Res.*, vol. 18, no. 5, pp. 543–548, 1984, doi: 10.1016/0043-1354(84)90201-X.
- [99] S. Sung and T. Liu, 'Ammonia inhibition on thermophilic anaerobic digestion', *Chemosphere*, vol. 53, no. 1, pp. 43–52, 2003, doi: 10.1016/S0045-6535(03)00434-X.
- [100] D. C. Stuckey, W. F. Owen, P. L. McCarty, and G. F. Parkin, 'Anaerobic toxicity evaluation by batch and semi-continuous assays', *J. Water Pollut. Control Fed.*, vol. 52, no. 4, pp. 720–729, 1980.
- [101] Y. Chen, J. J. Cheng, and K. S. Creamer, 'Inhibition of anaerobic digestion process: A review', *Bioresour. Technol.*, vol. 99, no. 10, pp. 4044–4064, Jul. 2008, doi: 10.1016/j.biortech.2007.01.057.
- [102] J. Yang and R. E. Speece, 'The effects of chloroform toxicity on methane fermentation', *Water Res.*, vol. 20, no. 10, pp. 1273–1279, 1986, doi: 10.1016/0043-1354(86)90158-2.
- [103] Pascale RENARD. Christine BOUJLLON. Henry NAVEAU and Edmond-Jacques NYNS*, 'Toxicity of a mixture of polychlorinated organic compounds towards an unacclimated methanogenic consortium', *Pap. Knowl. . Towar. a Media Hist. Doc.*, vol. 3, no. April, pp. 49–58, 2015.
- [104] H. J. Heipieper, F. J. Weber, J. Sikkema, H. Keweloh, and J. A. M. de Bont, 'Mechanisms of resistance of whole cells to toxic organic solvents', *Trends Biotechnol.*, vol. 12, no. 10, pp. 409–415, 1994, doi: 10.1016/0167-7799(94)90029-9.
- [105] J. Sikkema, J. A. M. De Bont, and B. Poolman, 'Interactions of cyclic hydrocarbons with biological membranes', *J. Biol. Chem.*, vol. 269, no. 11, pp. 8022–8028, 1994.
- [106] Y. Chen, J. J. Cheng, and K. S. Creamer, 'Inhibition of anaerobic digestion process: A review', 2007, doi: 10.1016/j.biortech.2007.01.057.
- [107] R. M. Sterritt and J. N. Lester, 'Interactions of heavy metals with bacteria', *Sci. Total Environ.*, vol. 14, no. 1, pp. 5–17, 1980, doi: 10.1016/0048-9697(80)90122-9.
- [108] S. W. Davis and S. E. Powers, 'Alternative Sorbents for Removing MTBE from Gasoline-Contaminated Ground Water', *J. Environ. Eng.*, vol. 126, no. July, p. 354, 2000, doi: 10.1061/(ASCE)0733-9372(2000)126.
- [109] P. J. He, F. Lü, L. M. Shao, X. J. Pan, and D. J. Lee, 'Kinetics of enzymatic hydrolysis of polysaccharide-rich particulates', *J. Chinese Inst. Chem. Eng.*, vol. 38, no. 1, pp. 21–27, 2007, doi: 10.1016/j.jcice.2006.07.001.
- [110] A. J. Mawson, R. L. Earle, and V. F. Larsen, 'Degradation of acetic and propionic acids in the methane fermentation', *Water Res.*, vol. 25, no. 12, pp. 1549–1554, 1991, doi: 10.1016/0043-1354(91)90187-U.
- [111] S. Babel, K. Fukushi, and B. Sitanrassamee, 'Effect of acid speciation on solid waste liquefaction in an anaerobic acid digester', *Water Res.*, vol. 38, no. 9, pp.

- 2416–2422, 2004, doi: 10.1016/j.watres.2004.02.005.
- [112] C. J. Banks and E. I. Stentiford, 'Biodegradable municipal solid waste: biotreatment options', *Proc. Inst. Civ. Eng. - Waste Resour. Manag.*, vol. 160, no. 1, pp. 11–18, 2007, doi: 10.1680/warm.2007.160.1.11.
- [113] G. Tchobanoglous, H. Theisen, and S. A. Vigil, *Integrated solid waste management : engineering principles and management issues*. McGraw-Hill, 1993.
- [114] P. Vandevivere, L. De Baere, and W. Verstraete, 'Types of anaerobic digester for solid wastes', *Biomethanization Org. fraction Munic. solid wastes*, no. January 2002, pp. 111–140, 2003.
- [115] N. Rilling, 'Anaerobic Fermentation of Wet and Semidry Garbage Waste Fractions', *undefined*, pp. 355–373, Jul. 2005, doi: 10.1002/3527604286.CH14.
- [116] P. Weiland, 'One- and two-step anaerobic digestion of solid agroindustrial residues', *Water Sci. Technol.*, vol. 27, no. 2, pp. 145–151, 1993, doi: 10.2166/wst.1993.0093.
- [117] N. Rilling, 'Anaerobic Fermentation of Wet and Semidry Garbage Waste Fractions', *Environ. Biotechnol.*, pp. 355–373, Jul. 2005, doi: 10.1002/3527604286.CH14.
- [118] N. H. Heo, S. C. Park, and H. Kang, 'Effects of mixture ratio and hydraulic retention time on single-stage anaerobic co-digestion of food waste and waste activated sludge', *J. Environ. Sci. Heal. - Part A Toxic/Hazardous Subst. Environ. Eng.*, vol. 39, no. 7, pp. 1739–1756, 2004, doi: 10.1081/ESE-120037874.
- [119] K. H. Hansen, I. Angelidaki, and B. K. Ahring, 'Anaerobic digestion of swine manure: Inhibition by ammonia', *Water Res.*, vol. 32, no. 1, pp. 5–12, 1998, doi: 10.1016/S0043-1354(97)00201-7.
- [120] B. Demirel and P. Scherer, 'Production of methane from sugar beet silage without manure addition by a single-stage anaerobic digestion process', *Biomass and Bioenergy*, vol. 32, no. 3, pp. 203–209, Mar. 2008, doi: 10.1016/j.biombioe.2007.09.011.
- [121] V. Nallathambi Gunaseelan, 'Anaerobic digestion of biomass for methane production: A review', *Univers. J. Environ. Res. Technol.*, vol. 13, no. 1/2, pp. 83–114, 1997.
- [122] A. Sambhuanth Ghosh, 1 Member, 'IMPROVED SLUDGE GASIFICATION BY TWO-PHASE ANAEROBIC DIGESTION', vol. 113, no. 6, pp. 1265–1284, 1987.
- [123] A. J. Ward, P. J. Hobbs, P. J. Holliman, and D. L. Jones, 'Optimisation of the anaerobic digestion of agricultural resources', *Bioresour. Technol.*, vol. 99, no. 17, pp. 7928–7940, 2008, doi: 10.1016/j.biortech.2008.02.044.
- [124] T. Forster-Carneiro, M. Pérez, and L. I. Romero, 'Anaerobic digestion of municipal solid wastes: Dry thermophilic performance', *Bioresour. Technol.*, vol. 99, no. 17, pp. 8180–8184, 2008, doi: 10.1016/j.biortech.2008.03.021.
- [125] C. Sambhunath Ghosh and both of I. Donald L. Klass, Barrington, 'Two Phase Anaerobic Digestion. USA patent application United States Patent', no. 19, pp. 2–7, 1977.
- [126] F. G. Pohland and S. Ghosh, 'Developments in Anaerobic Stabilization of Organic

- Wastes - The Two-Phase Concept', <http://dx.doi.org/10.1080/00139307109434990>, vol. 1, no. 4, pp. 255–266, 1971, doi: 10.1080/00139307109434990.
- [127] T. Liu, 'Anaerobic digestion of solid substrates in an innovative two-phase plug-flow reactor (TPPFR) and a conventional single-phase continuously stirred-tank reactor', *Water Sci. Technol.*, vol. 38, no. 8–9, pp. 453–461, Jan. 1998, doi: 10.1016/S0273-1223(98)00723-9.
- [128] S. Ghosh, M. P. Henry, A. Sajjad, M. C. Mensinger, and J. L. Arora, 'Pilot-scale gasification of municipal solid wastes by high-rate and two-phase anaerobic digestion (TPAD)', *Water Sci. Technol.*, vol. 41, no. 3, pp. 101–110, 2000, doi: 10.2166/wst.2000.0061.
- [129] H. B. Nielsen, Z. Mladenovska, P. Westermann, and B. K. Ahring, 'Comparison of Two-Stage Thermophilic (68°C/55°C) Anaerobic Digestion with One-Stage Thermophilic (55°C) Digestion of Cattle Manure', *Biotechnol. Bioeng.*, vol. 86, no. 3, pp. 291–300, 2004, doi: 10.1002/bit.20037.
- [130] B. Dearman, P. Marschner, and R. H. Bentham, 'Methane production and microbial community structure in single-stage batch and sequential batch systems anaerobically co-digesting food waste and biosolids', *Appl. Microbiol. Biotechnol.*, vol. 69, no. 5, pp. 589–596, 2006, doi: 10.1007/s00253-005-0076-9.
- [131] H. Shahriari, M. Warith, M. Hamoda, and K. Kennedy, 'Evaluation of single vs. staged mesophilic anaerobic digestion of kitchen waste with and without microwave pretreatment', *J. Environ. Manage.*, vol. 125, pp. 74–84, 2013, doi: 10.1016/j.jenvman.2013.03.042.
- [132] L. De Baere, 'Anaerobic digestion of solid waste: State-of-the-art', *Water Sci. Technol.*, vol. 41, no. 3, pp. 283–290, 2000, doi: 10.2166/wst.2000.0082.
- [133] J. Von Sachs, U. Meyer, P. Rys, and H. Feitkenhauer, 'New approach to control the methanogenic reactor of a two-phase anaerobic digestion system', *Water Res.*, vol. 37, no. 5, pp. 973–982, 2003, doi: 10.1016/S0043-1354(02)00446-3.
- [134] H. Bouallagui, Y. Touhami, R. Ben Cheikh, and M. Hamdi, 'Bioreactor performance in anaerobic digestion of fruit and vegetable wastes', *Process Biochem.*, vol. 40, no. 3–4, pp. 989–995, 2005, doi: 10.1016/j.procbio.2004.03.007.
- [135] Joshua Rapport Ruihong Zhang Bryan M. Jenkins Robert B. Williams, 'Current Anaerobic Digestion Technologies Used for Treatment of Municipal Organic Solid Waste', no. March, 2008.
- [136] A. Mtz.-Viturcia, J. Mata-Alvarez, and F. Cecchi, 'Two-phase continuous anaerobic digestion of fruit and vegetable wastes', *Resour. Conserv. Recycl.*, vol. 13, no. 3–4, pp. 257–267, 1995, doi: 10.1016/0921-3449(94)00048-A.
- [137] R. E. Speece, M. Duran, G. Demirer, H. Zhang, and T. DiStefano, 'The role of process configuration in the performance of anaerobic systems', *Water Sci. Technol.*, vol. 36, no. 6–7, pp. 539–547, Sep. 1997, doi: 10.2166/WST.1997.0634.
- [138] H. K. Ong, P. F. Greenfield, and P. C. Pullammanapllil, 'An operational strategy for improved biomethanation of cattle-manure slurry in an unmixed, single-

- stage, digester', *Bioresour. Technol.*, vol. 73, no. 1, pp. 87–89, 2000, doi: 10.1016/S0960-8524(99)00139-X.
- [139] Y. Park, F. Hong, J. Cheon, T. Hidaka, and H. Tsuno, 'Comparison of thermophilic anaerobic digestion characteristics between single-phase and two-phase systems for kitchen garbage treatment', *J. Biosci. Bioeng.*, vol. 105, no. 1, pp. 48–54, 2008, doi: 10.1263/jbb.105.48.
- [140] S. Wan, L. Sun, Y. Douieb, J. Sun, and W. Luo, 'Anaerobic digestion of municipal solid waste composed of food waste, wastepaper, and plastic in a single-stage system: Performance and microbial community structure characterization', *Bioresour. Technol.*, vol. 146, pp. 619–627, 2013, doi: 10.1016/j.biortech.2013.07.140.
- [141] P. Fox and F. G. Pohland, 'Anaerobic treatment applications and fundamentals: Substrate specificity during phase separation', *Water Environ. Res.*, vol. 66, no. 5, pp. 716–724, 1994, doi: 10.2175/WER.66.5.8.
- [142] N. Mosier *et al.*, 'Features of promising technologies for pretreatment of lignocellulosic biomass', *Bioresour. Technol.*, vol. 96, no. 6, pp. 673–686, 2005, doi: 10.1016/j.biortech.2004.06.025.
- [143] M. Carlsson, A. Lagerkvist, and F. Morgan-Sagastume, 'The effects of substrate pre-treatment on anaerobic digestion systems: A review', *Waste Manag.*, vol. 32, no. 9, pp. 1634–1650, 2012, doi: 10.1016/j.wasman.2012.04.016.
- [144] P. Bardos, 'Composting of Mechanically Segregated Fractions of Municipal Solid Waste – A Review', *SITA Environ. Trust*, vol. 30, no. November, p. 143, 2004.
- [145] N. Goldstein and L. F. Diaz, 'Size reduction equipment review', *Biocycle*, vol. 46, no. 1, pp. 48–53, 2005.
- [146] J. G. Abert, 'Municipal Waste Processing in Europe', no. 37, 1985.
- [147] L. Kratky and T. Jirout, 'Biomass Size Reduction Machines for Enhancing Biogas Production', *Chem. Eng. Technol.*, vol. 34, no. 3, pp. 391–399, 2011, doi: 10.1002/ceat.201000357.
- [148] Department for Environment Food & Rural Affairs (DEFRA), 'Mechanical Biological Treatment of Municipal Solid Waste', no. February, 2013.
- [149] S. Sud and A. Kamath, 'Methods of Size Reduction and Factors Affecting Size Reduction in Pharmaceuticals', *Int. Res. J. Pharm.*, vol. 4, no. 8, pp. 57–64, 2013, doi: 10.7897/2230-8407.04810.
- [150] A. Banks, C.J., Zhang, Y., Heaven, S., Watson, G., Powrie, W., Stentiford, E., Hobbis, P., Bulson, H., Muller, W., Niesar, M. and Bockreis, 'Particle size requirements for effective bioprocessing of biodegradable municipal waste': .Particle size requirements for effective bioprocessing of biodegradable municipal waste, 2010.
- [151] M. G. Shashidhar, T. P. K. Murthy, K. G. Girish, and B. Manohar, 'Grinding of coriander seeds: Modeling of particle size distribution and energy studies', *Part. Sci. Technol.*, vol. 31, no. 5, pp. 449–457, Sep. 2013, doi: 10.1080/02726351.2013.772546.
- [152] G. Dodbiba, A. Shibayama, J. Sadaki, and T. Fujita, 'Combination of triboelectrostatic separation and air tabling for sorting plastics from a multi-

- component plastic mixture', *Mater. Trans.*, vol. 44, no. 12, pp. 2427–2435, 2003, doi: 10.2320/matertrans.44.2427.
- [153] Nora Goldstein and Luis F. Diaz, 'Size Reduction Equipment Review - BioCycle BioCycle', *BioCycle January 2005, Vol. 46, No. 1, p. 48*, 2005. [Online]. Available: <https://www.biocycle.net/2005/01/21/size-reduction-equipment-review/>. [Accessed: 14-Aug-2018].
- [154] J. Zhang, W. Hou, and J. Bao, 'Reactors for high solid loading pretreatment of lignocellulosic biomass', *Adv. Biochem. Eng. Biotechnol.*, vol. 152, no. March, pp. 75–90, 2016, doi: 10.1007/10_2015_307.
- [155] Defra, 'Mechanical Biological Treatment of Municipal Solid Waste', no. February, pp. 1–57, 2013.
- [156] M. J. Taherzadeh and K. Karimi, *Pretreatment of lignocellulosic wastes to improve ethanol and biogas production: A review*, vol. 9, no. 9. 2008.
- [157] Y. Zhang, S. Kusch-Brandt, S. Gu, and S. Heaven, 'Particle Size Distribution in Municipal Solid Waste Pre-Treated for Bioprocessing', doi: 10.3390/resources8040166.
- [158] D. T. Sponza and O. N. Ağdağ, 'Effects of shredding of wastes on the treatment of municipal solid wastes (MSWs) in simulated anaerobic recycled reactors', *Enzyme Microb. Technol.*, vol. 36, no. 1, pp. 25–33, 2005, doi: 10.1016/j.enzmictec.2004.03.021.
- [159] M. C. Di Lonardo, F. Lombardi, and R. Gavasci, 'Characterization of MBT plants input and outputs: A review', *Rev. Environ. Sci. Biotechnol.*, vol. 11, no. 4, pp. 353–363, 2012, doi: 10.1007/s11157-012-9299-2.
- [160] Y. Zhang, S. Kusch-Brandt, S. Gu, and S. Heaven, 'Particle size distribution in municipal solid waste pre-treated for bioprocessing', *Resources*, vol. 8, no. 4, 2019, doi: 10.3390/resources8040166.
- [161] R. Lornage, E. Redon, T. Lagier, I. Hébé, and J. Carré, 'Performance of a low cost MBT prior to landfilling: Study of the biological treatment of size reduced MSW without mechanical sorting', *Waste Manag.*, vol. 27, no. 12, pp. 1755–1764, 2007, doi: 10.1016/j.wasman.2006.10.018.
- [162] M. J. Krause, G. W. Chickering, T. G. Townsend, and P. Pullammanappallil, 'Effects of temperature and particle size on the biochemical methane potential of municipal solid waste components', *Waste Manag.*, vol. 71, pp. 25–30, 2018, doi: 10.1016/j.wasman.2017.11.015.
- [163] Y. Zhang and C. J. Banks, 'Impact of different particle size distributions on anaerobic digestion of the organic fraction of municipal solid waste', *Waste Manag.*, vol. 33, no. 2, pp. 297–307, 2013, doi: 10.1016/j.wasman.2012.09.024.
- [164] D. Dr.K Fricke und Dr.W Muller, Ing. C. Bartetzko, D. Ing. U. Einzmann, and D. I. K. Kellner-aschenbrenner, '6Wdelolvlhuxqj Yrq 5Hwvp • Oo Gxufk Phfdqvlvk Elrorjlvfkh % Hkdqgoxqj Xqg \$ Xvzlunxqjhq Dxi Glh ' Hsrqlhuxqj', 1999.
- [165] L. A. Fdez.-Güelfo, C. Álvarez-Gallego, D. Sales Márquez, and L. I. Romero García, 'Biological pretreatment applied to industrial organic fraction of municipal solid wastes (OFMSW): Effect on anaerobic digestion', *Chem. Eng. J.*, vol. 172, no. 1, pp. 321–325, 2011, doi: 10.1016/j.cej.2011.06.010.

- [166] H. Carrère, B. Sialve, and N. Bernet, 'Improving pig manure conversion into biogas by thermal and thermo-chemical pretreatments', *Bioresour. Technol.*, vol. 100, no. 15, pp. 3690–3694, 2009, doi: 10.1016/j.biortech.2009.01.015.
- [167] V. Penaud, J. P. Delgenès, and R. Moletta, 'Thermo-chemical pretreatment of a microbial biomass: Influence of sodium hydroxide addition on solubilization and anaerobic biodegradability', *Enzyme Microb. Technol.*, vol. 25, no. 3–5, pp. 258–263, 1999, doi: 10.1016/S0141-0229(99)00037-X.
- [168] J. Ariunbaatar, 'Methods to enhance anaerobic digestion of food waste', 2014.
- [169] H. Li, C. Li, W. Liu, and S. Zou, 'Optimized alkaline pretreatment of sludge before anaerobic digestion', *Bioresour. Technol.*, vol. 123, pp. 189–194, 2012, doi: 10.1016/j.biortech.2012.08.017.
- [170] T. V. Fernandes, G. J. Klaasse Bos, G. Zeeman, J. P. M. Sanders, and J. B. van Lier, 'Effects of thermo-chemical pre-treatment on anaerobic biodegradability and hydrolysis of lignocellulosic biomass', *Bioresour. Technol.*, vol. 100, no. 9, pp. 2575–2579, 2009, doi: 10.1016/j.biortech.2008.12.012.
- [171] L. Neves, R. Ribeiro, R. Oliveira, and M. M. Alves, 'Enhancement of methane production from barley waste', *Biomass and Bioenergy*, vol. 30, no. 6, pp. 599–603, 2006, doi: 10.1016/j.biombioe.2005.12.003.
- [172] C. A. O'Sullivan, P. C. Burrell, W. P. Clarke, and L. L. Blackall, 'Structure of a cellulose degrading bacterial community during anaerobic digestion', *Biotechnol. Bioeng.*, vol. 92, no. 7, pp. 871–878, 2005, doi: 10.1002/bit.20669.
- [173] D. J. Hills and K. Nakano, 'Effects of particle size on anaerobic digestion of tomato solid wastes', *Agric. Wastes*, vol. 10, no. 4, pp. 285–295, 1984, doi: 10.1016/0141-4607(84)90004-0.
- [174] W. Sanders, *Anaerobic hydrolysis digestion of complex substrates*. 2001.
- [175] F. Liotta *et al.*, 'Effect of moisture on disintegration kinetics during anaerobic digestion of complex organic substrates', *Waste Manag. Res.*, vol. 32, no. 1, pp. 40–48, 2014, doi: 10.1177/0734242X13513827.
- [176] F. Liotta, 'Bio-methanation tests and mathematical modelling to assess the role of moisture content on anaerobic digestion of organic waste Flavia Liotta To cite this version : Degree of Doctor in Environmental Technology Thèse – Tesi di Dottorato – PhD thesis In fro', 2014.
- [177] I. S. Kim, D. H. Kim, and S. H. Hyun, 'Effect of particle size and sodium ion concentration on anaerobic thermophilic food waste digestion', *Water Sci. Technol.*, vol. 41, no. 3, pp. 67–73, 2000.
- [178] A. Mshandete, L. Björnsson, A. K. Kivaisi, M. S. T. Rubindamayugi, and B. Mattiasson, 'Effect of particle size on biogas yield from sisal fibre waste', *Renew. Energy*, vol. 31, no. 14, pp. 2385–2392, 2006, doi: 10.1016/j.renene.2005.10.015.
- [179] L.M. Palmowski* and J. A. Müller, 'Influence of the size reduction of organic waste on their anaerobic digestion', *Water Sci Technol*, vol. 41, no. 3, pp. 155–162, 2000, doi: 10.2166/wst.2000.0067.
- [180] I. Angelidaki and B. K. Ahring, 'Methods for increasing the biogas potential from the recalcitrant organic matter contained in manure', *Water Sci. Technol.*, vol.

- 41, no. 3, pp. 189–194, 2000.
- [181] A. Hajji and M. Rhachi, 'The influence of particle size on the performance of anaerobic digestion of municipal solid waste', *Energy Procedia*, vol. 36, pp. 515–520, 2013, doi: 10.1016/j.egypro.2013.07.059.
- [182] C. Perez Lopez, R. Kirchmayr, M. Neureiter, and R. Braun, 'Oth_Copenhagen2_Perez.pdf'. 2005.
- [183] C. E. Marcato, E. Pinelli, P. Pouech, P. Winterton, and M. Guiresse, 'Particle size and metal distributions in anaerobically digested pig slurry', *Bioresour. Technol.*, vol. 99, no. 7, pp. 2340–2348, 2008, doi: 10.1016/j.biortech.2007.05.013.
- [184] H. Hartmann and B. K. Ahring, 'Strategies for the anaerobic digestion of the organic fraction of municipal solid waste: An overview', *Water Sci. Technol.*, vol. 53, no. 8, pp. 7–22, 2006, doi: 10.2166/wst.2006.231.
- [185] A. Nopharatana, P. C. Pullammanappallil, and W. P. Clarke, 'Kinetics and dynamic modelling of batch anaerobic digestion of municipal solid waste in a stirred reactor', *Waste Manag.*, vol. 27, no. 5, pp. 595–603, 2007, doi: 10.1016/j.wasman.2006.04.010.
- [186] M. Kayhanian and S. Hardy, 'The impact of four design parameters on the performance of a high-solids anaerobic digestion of municipal solid waste for fuel gas production', *Environ. Technol.*, vol. 15, no. 6, pp. 557–567, 1994, doi: 10.1080/09593339409385461.
- [187] P. M. Mason and D. C. Stuckey, 'Biofilms, bubbles and boundary layers – A new approach to understanding cellulolysis in anaerobic and ruminant digestion', *Water Res.*, vol. 104, pp. 93–100, 2016, doi: 10.1016/j.watres.2016.07.063.
- [188] J. U. Hernández-Beltrán, I. O. Hernández-De Lira, M. M. Cruz-Santos, A. Saucedo-Luevanos, F. Hernández-Terán, and N. Balagurusamy, 'Insight into pretreatment methods of lignocellulosic biomass to increase biogas yield: Current state, challenges, and opportunities', *Appl. Sci.*, vol. 9, no. 18, 2019, doi: 10.3390/app9183721.
- [189] N. Ganidi, S. Tyrrel, and E. Cartmell, 'Anaerobic digestion foaming causes--a review.', *Bioresour. Technol.*, vol. 100, no. 23, pp. 5546–5554, 2009, doi: 10.1016/j.biortech.2009.06.024.
- [190] M. Barjenbruch and O. Kopplow, 'Enzymatic, mechanical and thermal pre-treatment of surplus sludge', *Adv. Environ. Res.*, vol. 7, no. 3, pp. 715–720, 2003, doi: 10.1016/S1093-0191(02)00032-1.
- [191] K. R. Pagilla, K. C. Craney, and W. H. Kido, 'Causes and effects of foaming in anaerobic sludge digesters', *Water Sci. Technol.*, vol. 36, no. 6–7, pp. 463–470, Jan. 1997, doi: 10.1016/S0273-1223(97)00556-8.
- [192] A. D. Wheatley, K. A. Johnson, and C. I. Winstanley, 'Foaming in activated sludge plants treating dairy waste', *Environ. Technol. Lett.*, vol. 9, no. 3, pp. 181–190, 1988, doi: 10.1080/09593338809384556.
- [193] W. Environment, 'Vyw © f distance learning', vol. 22, no. 6, 2022.
- [194] L. Moeller, K. Goersch, J. Neuhaus, A. Zehnsdorf, and R. A. Mueller, 'Comparative review of foam formation in biogas plants and ruminant bloat', *Energy. Sustain. Soc.*, vol. 2, no. 1, pp. 1–9, 2012, doi: 10.1186/2192-0567-2-12.

- [195] N. Massart, R. Bates, and G. Neun, 'THE ROOT CAUSE OF EXCESSIVE ANAEROBIC DIGESTER FOAMING', *Proc. Water Environ. Fed.*, vol. 2006, no. 2, pp. 1099–1117, Jan. 2006, doi: 10.2175/193864706783797078.
- [196] William P F Barber, 'Foaming during anaerobic digestion: Causes and Solutions | Environmental XPRT', 2005. [Online]. Available: <https://www.environmental-expert.com/articles/foaming-during-anaerobic-digestion-causes-and-solutions-152218>. [Accessed: 14-Aug-2018].
- [197] A. Moeller, Lucie; Herbes, Carsten; Müller, Roland A. and Zehnsdorf, 'Formation and removal of foam in the process of anaerobic digestion. L', vol. 2, 2010.
- [198] F. Vardar-Sukan, 'Foaming: Consequences, prevention and destruction', *Biotechnol. Adv.*, vol. 16, no. 5–6, pp. 913–948, 1998, doi: 10.1016/S0734-9750(98)00010-X.
- [199] D. J. Batstone, J. Keller, R. B. Newell, and M. Newland, 'Modelling anaerobic degradation of complex wastewater. II: Parameter estimation and validation using slaughterhouse effluent', *Bioresour. Technol.*, vol. 75, no. 1, pp. 75–85, 2000, doi: 10.1016/S0960-8524(00)00019-5.
- [200] G. Esposito, L. Frunzo, A. Panico, and G. d'Antonio, 'Mathematical modelling of disintegration-limited co-digestion of OFMSW and sewage sludge', *Water Sci. Technol.*, vol. 58, no. 7, pp. 1513–1519, 2008, doi: 10.2166/wst.2008.509.
- [201] G. Esposito, 'Bio-Methane Potential Tests To Measure The Biogas Production From The Digestion and Co-Digestion of Complex Organic Substrates', *Open Environ. Eng. J.*, vol. 5, no. 1, pp. 1–8, 2012, doi: 10.2174/1874829501205010001.
- [202] S. G. Pavlostathis and E. Giraldo-Gomez, 'Kinetics of anaerobic treatment: A critical review', *Crit. Rev. Environ. Control*, vol. 21, no. 5–6, pp. 411–490, Jan. 1991, doi: 10.1080/10643389109388424.
- [203] C. Yaw Tzuu and R. R. Dague, 'Effects of particulate size in anaerobic acidogenesis using cellulose as a sole carbon source', *Water Environ. Res.*, vol. 66, no. 5, pp. 670–678, 1994.
- [204] P. N. Hobson, 'A model of some aspects of microbial degradation of particulate substrates', *J. Ferment. Technol.*, vol. 65, no. 4, pp. 431–439, 1987, doi: 10.1016/0385-6380(87)90140-3.
- [205] W. F. Owen, D. C. Stuckey, J. B. Healy, L. Y. Young, and P. L. McCarty, 'Bioassay for monitoring biochemical methane potential and anaerobic toxicity', *Water Res.*, vol. 13, no. 6, pp. 485–492, 1979, doi: 10.1016/0043-1354(79)90043-5.
- [206] P. D. Jensen, H. Ge, and D. J. Batstone, 'Assessing the role of biochemical methane potential tests in determining anaerobic degradability rate and extent', *Water Sci. Technol.*, vol. 64, no. 4, pp. 880–886, 2011, doi: 10.2166/wst.2011.662.
- [207] S. J. Lim and P. Fox, 'Biochemical methane potential (BMP) test for thickened sludge using anaerobic granular sludge at different inoculum/substrate ratios', *Biotechnol. Bioprocess Eng.*, vol. 18, no. 2, pp. 306–312, 2013, doi: 10.1007/s12257-012-0465-8.
- [208] I. Angelidaki *et al.*, 'Defining the biomethane potential (BMP) of solid organic

- wastes and energy crops: A proposed protocol for batch assays', *Water Sci. Technol.*, vol. 59, no. 5, pp. 927–934, 2009, doi: 10.2166/wst.2009.040.
- [209] J. M. Owens and D. P. Chynoweth, 'Biochemical methane potential of municipal solid waste (MSW) components', *Water Sci. Technol.*, vol. 27, no. 2, pp. 1–14, 1993, doi: 10.2166/wst.1993.0065.
- [210] M. Badshah, D. M. Lam, J. Liu, and B. Mattiasson, 'Use of an Automatic Methane Potential Test System for evaluating the biomethane potential of sugarcane bagasse after different treatments', *Bioresour. Technol.*, vol. 114, pp. 262–269, Jun. 2012, doi: 10.1016/j.biortech.2012.02.022.
- [211] M. O. Aremu and S. E. Agarry, 'Enhanced biogas production from poultry droppings using corn-cob and waste paper as cosubstrate.', *Int. J. Eng. Sci. Technol.*, vol. 5, no. 2, pp. 247–253, 2013.
- [212] S. K. Sharma, I. M. Mishra, M. P. Sharma, and J. S. Saini, 'Effect of particle size on biogas generation from biomass residues', *Biomass*, vol. 17, no. 4, pp. 251–263, 1988, doi: 10.1016/0144-4565(88)90107-2.
- [213] L. M. Palmowski and J. A. Müller, 'Anaerobic degradation of organic materials - Significance of the substrate surface area', *Water Sci. Technol.*, vol. 47, no. 12, 2003.
- [214] F. Liotta *et al.*, 'Effect of total solids content on methane and volatile fatty acid production in anaerobic digestion of food waste', *Waste Manag. Res.*, vol. 32, no. 10, pp. 947–953, 2014, doi: 10.1177/0734242X14550740.
- [215] A. Nopharatana, P. C. Pullammanappallil, and W. P. Clarke, 'Kinetics and dynamic modelling of batch anaerobic digestion of municipal solid waste in a stirred reactor', *Waste Manag.*, vol. 27, no. 5, pp. 595–603, 2007, doi: 10.1016/j.wasman.2006.04.010.
- [216] R. Valencia-Vázquez, M. E. Pérez-López, M. G. Vicencio-de-la-Rosa, M. A. Martínez-Prado, and R. Rubio-Hernández, 'Knowledge and technology transfer to improve the municipal solid waste management system of Durango City, Mexico', *Waste Manag. Res.*, vol. 32, no. 9, pp. 848–856, 2014, doi: 10.1177/0734242X14546035.
- [217] D. T. Sponza and O. N. Ağdağ, 'Effects of shredding of wastes on the treatment of municipal solid wastes (MSWs) in simulated anaerobic recycled reactors', *Enzyme Microb. Technol.*, vol. 36, no. 1, pp. 25–33, Jan. 2005, doi: 10.1016/J.ENZMICTEC.2004.03.021.
- [218] American Public Health Association, *Standard methods for the examination of water & wastewater*. American Public Health Association, 2005.
- [219] L. E. Ripley and W. C. Boyle, 'Improved Alkalimetric Monitoring for Anaerobic Digestion of High-Strength Wastes', 1986.
- [220] N. Curry and P. Pillay, 'Biogas prediction and design of a food waste to energy system for the urban environment', *Renew. Energy*, vol. 41, pp. 200–209, 2012, doi: 10.1016/j.renene.2011.10.019.
- [221] A. M. Buswell and H. F. Mueller, 'Mechanism of Methane Fermentation', *Ind. Eng. Chem.*, vol. 44, no. 3, pp. 550–552, Mar. 1952, doi: 10.1021/IE50507A033/ASSET/IE50507A033.FP.PNG_V03.

- [222] R. D. Paode, J. I. Liu, and T. M. Holsen, 'Modeling the Energy Content of Municipal Solid Waste Using Multiple Regression Analysis', *J. Air Waste Manag. Assoc.*, vol. 46, no. 7, pp. 650–656, 1996, doi: 10.1080/10473289.1996.10467499.
- [223] D. Komilis, A. Evangelou, G. Giannakis, and C. Lymperis, 'Revisiting the elemental composition and the calorific value of the organic fraction of municipal solid wastes', *Waste Manag.*, vol. 32, no. 3, pp. 372–381, 2012, doi: 10.1016/j.wasman.2011.10.034.
- [224] D. M. Mason and K. N. Gandhi, 'Formulas for calculating the calorific value of coal and coal chars: Development, tests, and uses', *Fuel Process. Technol.*, vol. 7, no. 1, pp. 11–22, 1983, doi: 10.1016/0378-3820(83)90022-X.
- [225] A. Friedl, E. Padouvas, H. Rotter, and K. Varmuza, 'Prediction of heating values of biomass fuel from elemental composition', *Anal. Chim. Acta*, vol. 544, no. 1-2 SPEC. ISS., pp. 191–198, 2005, doi: 10.1016/j.aca.2005.01.041.
- [226] C. Sheng and J. L. T. Azevedo, 'Estimating the higher heating value of biomass fuels from basic analysis data', *Biomass and Bioenergy*, vol. 28, no. 5, pp. 499–507, 2005, doi: 10.1016/j.biombioe.2004.11.008.
- [227] M. Barjenbruch, H. Hoffmann, O. Kopplow, J. Tränckner, Y. Zhang, and C. J. Banks, 'Minimizing of foaming in digesters by pre-treatment of the surplus-sludge', *Waste Manag.*, vol. 42, no. 2, pp. 297–307, 2000, doi: 10.1016/j.wasman.2012.09.024.
- [228] K. R. Pagilla, K. C. Craney, and W. H. Kido, 'Causes and effects of foaming in anaerobic sludge digesters', *Water Sci. Technol.*, vol. 36, no. 6–7, pp. 463–470, Sep. 1997, doi: 10.2166/wst.1997.0624.
- [229] J. A. Serna-Jiménez, F. Luna-Lama, Á. Caballero, M. de los Á. Martín, A. F. Chica, and J. Á. Siles, 'Valorisation of banana peel waste as a precursor material for different renewable energy systems', *Biomass and Bioenergy*, vol. 155, no. October, 2021, doi: 10.1016/j.biombioe.2021.106279.
- [230] S. K. Cho, D. H. Kim, Y. M. Yun, K. W. Jung, H. S. Shin, and S. E. Oh, 'Statistical optimization of mixture ratio and particle size for dry co-digestion of food waste and manure by response surface methodology', *Korean J. Chem. Eng.*, vol. 30, no. 7, pp. 1493–1496, Jul. 2013, doi: 10.1007/S11814-013-0096-6.
- [231] J. Siciliano-Jones and M. R. Murphy, 'Specific Gravity of Various Feedstuffs as Affected by Particle Size and In Vitro Fermentation', *J. Dairy Sci.*, vol. 74, no. 3, pp. 896–901, 1991, doi: 10.3168/jds.S0022-0302(91)78238-6.
- [232] A. P. Hooper and J. G. Welch, 'Effects of Particle Size and Forage Composition on Functional Specific Gravity', *J. Dairy Sci.*, vol. 68, no. 5, pp. 1181–1188, 1985, doi: 10.3168/jds.S0022-0302(85)80945-0.
- [233] T. Thamsiroj and J. D. Murphy, 'Difficulties associated with monodigestion of grass as exemplified by commissioning a pilot-scale digester', *Energy and Fuels*, vol. 24, no. 8, pp. 4459–4469, 2010, doi: 10.1021/ef1003039.
- [234] M. E. Montingelli, K. Y. Benyounis, B. Quilty, J. Stokes, and A. G. Olabi, 'Influence of mechanical pretreatment and organic concentration of Irish brown seaweed for methane production', *Energy*, vol. 118, pp. 1079–1089, 2017, doi:

- 10.1016/j.energy.2016.10.132.
- [235] X. Kang *et al.*, 'The effect of mechanical pretreatment on the anaerobic digestion of Hybrid Pennisetum', *Fuel*, vol. 252, no. May, pp. 469–474, 2019, doi: 10.1016/j.fuel.2019.04.134.
- [236] L. Melville, A. Weger, S. Wiesgickl, and M. Franke, 'Anaerobic Digestion', *Transform. Biomass Theory to Pract.*, vol. 9781119973270, pp. 31–59, Sep. 2014, doi: 10.1002/9781118693643.CH2.
- [237] A. J. Ward, P. J. Hobbs, P. J. Holliman, and D. L. Jones, 'Optimisation of the anaerobic digestion of agricultural resources', *Bioresour. Technol.*, vol. 99, no. 17, pp. 7928–7940, Nov. 2008, doi: 10.1016/j.biortech.2008.02.044.
- [238] V. N. Gunaseelan, 'Biochemical methane potential of fruits and vegetable solid waste feedstocks', *Biomass and Bioenergy*, vol. 26, no. 4, pp. 389–399, 2004, doi: 10.1016/j.biombioe.2003.08.006.
- [239] O. Parthiba Karthikeyan, E. Trably, S. Mehariya, N. Bernet, J. W. C. Wong, and H. Carrere, 'Pretreatment of food waste for methane and hydrogen recovery: A review', *Bioresour. Technol.*, vol. 249, no. July 2017, pp. 1025–1039, 2018, doi: 10.1016/j.biortech.2017.09.105.
- [240] S. O. Dahunsi, 'Mechanical pretreatment of lignocelluloses for enhanced biogas production: Methane yield prediction from biomass structural components', *Bioresour. Technol.*, vol. 280, pp. 18–26, May 2019, doi: 10.1016/J.BIORTECH.2019.02.006.
- [241] B. Rincón, C. J. Banks, and S. Heaven, 'Biochemical methane potential of winter wheat (*Triticum aestivum* L.): Influence of growth stage and storage practice', *Bioresour. Technol.*, vol. 101, no. 21, pp. 8179–8184, 2010, doi: 10.1016/j.biortech.2010.06.039.
- [242] S. Jijai, G. Srisuwan, S. O-thong, I. Norli, and C. Siripatana, 'Iranica Journal of Energy & Environment Effect of Substrate and Granules / Inocula Sizes on Biochemical Methane Potential and Methane Kinetics', vol. 7, no. 2, pp. 94–101, 2016.
- [243] C. J. Banks and S. Heaven, 'Optimisation of biogas yields from anaerobic digestion by feedstock type', *Biogas Handb. Sci. Prod. Appl.*, pp. 131–165, Jan. 2013, doi: 10.1533/9780857097415.1.131.
- [244] V. Nallathambi Gunaseelan, 'Biomass estimates, characteristics, biochemical methane potential, kinetics and energy flow from *Jatropha curcus* on dry lands', *Biomass and Bioenergy*, vol. 33, no. 4, pp. 589–596, 2009, doi: 10.1016/j.biombioe.2008.09.002.
- [245] D. Access *et al.*, 'Origin Booklet Flipbook Proof', 2018. [Online]. Available: <https://www.originlab.com/brochure/>. [Accessed: 06-Jan-2022].
- [246] D. P. Chynoweth, C. E. Turick, J. M. Owens, D. E. Jerger, and M. W. Peck, 'Biochemical methane potential of biomass and waste feedstocks', *Biomass and Bioenergy*, vol. 5, no. 1, pp. 95–111, 1993, doi: 10.1016/0961-9534(93)90010-2.
- [247] V. Prabhudessai, A. Ganguly, and S. Mutnuri, 'Biochemical Methane Potential of Agro Wastes', *J. Energy*, vol. 2013, pp. 1–7, 2013, doi: 10.1155/2013/350731.
- [248] E. Allen, D. M. Wall, C. Herrmann, and J. D. Murphy, 'A detailed assessment of

- resource of biomethane from first, second and third generation substrates', *Renew. Energy*, vol. 87, no. 2016, pp. 656–665, 2016, doi: 10.1016/j.renene.2015.10.060.
- [249] G. Liu, R. Zhang, H. M. El-Mashad, and R. Dong, 'Effect of feed to inoculum ratios on biogas yields of food and green wastes', *Bioresour. Technol.*, vol. 100, no. 21, pp. 5103–5108, 2009, doi: 10.1016/j.biortech.2009.03.081.
- [250] A. S. Nizami, N. E. Korres, and J. D. Murphy, 'Review of the integrated process for the production of grass biomethane', *Environmental Science and Technology*, vol. 43, no. 22. American Chemical Society, pp. 8496–8508, 15-Nov-2009, doi: 10.1021/es901533j.
- [251] J. Murphy, G. Bochmann, P. Weiland, and A. Wellinger, 'Biogas from Crop Digestion', *IEA Bioenergy - Task 37*, no. August 2016, p. 24, 2011.
- [252] C. Rodriguez, A. Alaswad, Z. El-Hassan, and A. G. Olabi, 'Mechanical pretreatment of waste paper for biogas production', *Waste Manag.*, vol. 68, pp. 157–164, Oct. 2017, doi: 10.1016/j.wasman.2017.06.040.
- [253] W. E. Eleazer, W. S. Odle, Y. S. Wang, and M. A. Barlaz, 'Biodegradability of municipal solid waste components in laboratory- scale landfills', *Environ. Sci. Technol.*, vol. 31, no. 3, pp. 911–917, 1997, doi: 10.1021/es9606788.
- [254] S. Pommier, A. M. Llamas, and X. Lefebvre, 'Analysis of the outcome of shredding pretreatment on the anaerobic biodegradability of paper and cardboard materials', *Bioresour. Technol.*, vol. 101, no. 2, pp. 463–468, Jan. 2010, doi: 10.1016/J.BIORTECH.2009.07.034.
- [255] X. Yuan *et al.*, 'Effect of pretreatment by a microbial consortium on methane production of waste paper and cardboard', *Bioresour. Technol.*, vol. 118, pp. 281–288, Aug. 2012, doi: 10.1016/j.biortech.2012.05.058.
- [256] T. Meyer and E. A. Edwards, 'Anaerobic digestion of pulp and paper mill wastewater and sludge', *Water Res.*, vol. 65, pp. 321–349, Nov. 2014, doi: 10.1016/J.WATRES.2014.07.022.
- [257] A. T. Jansson, R. J. Patinvoh, I. S. Horváth, and M. J. Taherzadeh, 'Dry anaerobic digestion of food and paper industry wastes at different solid contents', *Fermentation*, vol. 5, no. 2, pp. 1–10, 2019, doi: 10.3390/fermentation5020040.
- [258] D. Brown, J. Shi, and Y. Li, 'Comparison of solid-state to liquid anaerobic digestion of lignocellulosic feedstocks for biogas production', *Bioresour. Technol.*, vol. 124, pp. 379–386, Nov. 2012, doi: 10.1016/J.BIORTECH.2012.08.051.
- [259] P. S. Calabrò, R. Greco, A. Evangelou, and D. Komilis, 'Anaerobic digestion of tomato processing waste: Effect of alkaline pretreatment', *J. Environ. Manage.*, vol. 163, pp. 49–52, 2015, doi: 10.1016/j.jenvman.2015.07.061.
- [260] E. Dinuccio, P. Balsari, F. Gioelli, and S. Menardo, 'Evaluation of the biogas productivity potential of some Italian agro-industrial biomasses', *Bioresour. Technol.*, vol. 101, no. 10, pp. 3780–3783, 2010, doi: 10.1016/j.biortech.2009.12.113.
- [261] A. González-González and F. Cuadros, 'Continuous biomethanization of agrifood industry waste: A case study in Spain', *Process Biochem.*, vol. 48, no. 5–6, pp.

- 920–925, 2013, doi: 10.1016/j.procbio.2013.03.013.
- [262] R. Sarada and K. Nand, 'Start-up anaerobic digestion of tomato-processing wastes for methane generation', *Biol. Wastes*, vol. 30, no. 3, pp. 231–237, 1989, doi: 10.1016/0269-7483(89)90124-9.
- [263] N. Barirdiya, D. Somayaji, and S. Khanna, 'Biomethanation of banana peel and pineapple waste', *Bioresour. Technol.*, vol. 58, no. 1, pp. 73–76, 1996, doi: 10.1016/S0960-8524(96)00107-1.
- [264] N. Pisutpaisal, S. Boonyawanich, and H. Saowaluck, 'Feasibility of biomethane production from banana peel', *Energy Procedia*, vol. 50, pp. 782–788, 2014, doi: 10.1016/j.egypro.2014.06.096.
- [265] W. Zheng, K. Phoungthong, F. Lü, L. M. Shao, and P. J. He, 'Evaluation of a classification method for biodegradable solid wastes using anaerobic degradation parameters', *Waste Manag.*, vol. 33, no. 12, pp. 2632–2640, Dec. 2013, doi: 10.1016/j.wasman.2013.08.015.
- [266] P. Buffiere, D. Loisel, N. Bernet, and J. P. Delgenes, 'Towards new indicators for the prediction of solid waste anaerobic digestion properties', *Water Sci. Technol.*, vol. 53, no. 8, pp. 233–241, 2006, doi: 10.2166/wst.2006.254.
- [267] P. Tumutegyeize, F. I. Muranga, J. Kawongolo, and F. Nabugoomu, 'Optimization of biogas production from banana peels: Effect of particle size on methane yield', *African J. Biotechnol.*, vol. 10, no. 79, pp. 18243–18251, Dec. 2011, doi: 10.5897/AJB11.2442.
- [268] V. N. Gunaseelan, 'Biochemical methane potential of fruits and vegetable solid waste feedstocks', *Biomass and Bioenergy*, vol. 26, no. 4, pp. 389–399, 2004, doi: 10.1016/j.biombioe.2003.08.006.
- [269] Y. Li *et al.*, 'Evaluating methane production from anaerobic mono- and co-digestion of kitchen waste, corn stover, and chicken manure', *Energy and Fuels*, vol. 27, no. 4, pp. 2085–2091, Apr. 2013, doi: 10.1021/EF400117F.
- [270] J. C. Motte *et al.*, 'Total solids content: A key parameter of metabolic pathways in dry anaerobic digestion', *Biotechnol. Biofuels*, vol. 6, no. 1, pp. 1–9, 2013, doi: 10.1186/1754-6834-6-164.
- [271] J.-C. Motte *et al.*, 'Total solids content: a key parameter of metabolic pathways in dry anaerobic digestion', *Biotechnol. Biofuels*, vol. 6, no. 1, p. 164, 2013, doi: 10.1186/1754-6834-6-164.
- [272] P. Shanmugam and N. J. Horan, 'Simple and rapid methods to evaluate methane potential and biomass yield for a range of mixed solid wastes', *Bioresour. Technol.*, vol. 100, no. 1, pp. 471–474, 2009, doi: 10.1016/j.biortech.2008.06.027.
- [273] C. J. Rivard, F. Bordeaux, J. M. Henson, and P. H. Smith, 'Effects of addition of soluble oxidants on the thermophilic anaerobic digestion of biomass to methane', *Appl. Biochem. Biotechnol.*, vol. 17, no. 1–3, pp. 245–262, Apr. 1988, doi: 10.1007/BF02779161.
- [274] X. S. Shi *et al.*, 'Effect of Hydraulic Retention Time on Anaerobic Digestion of Wheat Straw in the Semicontinuous Continuous Stirred-Tank Reactors', *Biomed Res. Int.*, vol. 2017, 2017, doi: 10.1155/2017/2457805.

- [275] C. Banks, 'Renewable energy from crops and agrowastes', *Www.Cropgen.Soton.Ac.Uk*, 2007.
- [276] J. Ma *et al.*, 'Methanosarcina domination in anaerobic sequencing batch reactor at short hydraulic retention time', *Bioresour. Technol.*, vol. 137, pp. 41–50, 2013, doi: 10.1016/j.biortech.2013.03.101.
- [277] J. De Vrieze, W. Verstraete, and N. Boon, 'Repeated pulse feeding induces functional stability in anaerobic digestion', *Microb. Biotechnol.*, vol. 6, no. 4, pp. 414–424, 2013, doi: 10.1111/1751-7915.12025.
- [278] W. Laperrière, B. Barry, M. Torrijos, B. Pechiné, N. Bernet, and J. P. Steyer, 'Optimal conditions for flexible methane production in a demand-based operation of biogas plants', *Bioresour. Technol.*, vol. 245, no. September, pp. 698–705, 2017, doi: 10.1016/j.biortech.2017.09.013.
- [279] E. Mauky, H. F. Jacobi, J. Liebetrau, and M. Nelles, 'Flexible biogas production for demand-driven energy supply - Feeding strategies and types of substrates', *Bioresour. Technol.*, vol. 178, pp. 262–269, 2015, doi: 10.1016/j.biortech.2014.08.123.
- [280] A. Lemmer and J. Krümpel, 'Demand-driven biogas production in anaerobic filters', *Appl. Energy*, vol. 185, pp. 885–894, 2017, doi: 10.1016/j.apenergy.2016.10.073.
- [281] K. Izumi, Y. ki Okishio, N. Nagao, C. Niwa, S. Yamamoto, and T. Toda, 'Effects of particle size on anaerobic digestion of food waste', *Int. Biodeterior. Biodegrad.*, vol. 64, no. 7, pp. 601–608, 2010, doi: 10.1016/j.ibiod.2010.06.013.
- [282] T. a Elmitwalli, J. Soellner, A. D. E. Keizer, G. Zeeman, and G. Lettinga, 'Biodegradability and Change of Physical Characteristics of Particles During Anaerobic Digestion of Sewage', *Water Res.*, vol. 35, no. 5, pp. 1311–1317, 2001, doi: 10.1016/S0043-1354(00)00377-8.
- [283] J. I. Houghton and T. O. M. Stephenson, 'Particle Size Analysis of Digested Sludge', *Water Res.*, vol. 36, no. 18, pp. 4643–4647, 2002.
- [284] P. Harmsen, W. Huijgen, L. López, and R. Bakker, *Literature Review of Physical and Chemical Pretreatment Processes for Lignocellulosic Biomass*, no. September. 2010.
- [285] A. Wellinger, J. Murphy, and D. Baxter, *The biogas handbook: science, production and applications*. .
- [286] A. E. Cioabla, I. Ionel, G.-A. A. Dumitrel, and F. Popescu, 'Comparative study on factors affecting anaerobic digestion of agricultural vegetal residues', *Biotechnol. Biofuels*, vol. 5, no. ii, pp. 1–9, 2012, doi: 10.1186/1754-6834-5-39.
- [287] A. C. van Haandel and J. G. M. van der Lubbe, 'Handbook of Biological Wastewater Treatment: Design and Optimisation of Activated Sludge Systems', *Water Intell. Online*, vol. 11, Jan. 2012, doi: 10.2166/9781780400808.
- [288] Yadvika, Santosh, T. R. Sreekrishnan, S. Kohli, and V. Rana, 'Enhancement of biogas production from solid substrates using different techniques - A review', *Bioresour. Technol.*, vol. 95, no. 1, pp. 1–10, 2004, doi: 10.1016/j.biortech.2004.02.010.
- [289] H. Hartmann and B. K. Ahring, 'Strategies for the anaerobic digestion of the

- organic fraction of municipal solid waste: An overview', *Water Sci. Technol.*, vol. 53, no. 8, pp. 7–22, 2006, doi: 10.2166/wst.2006.231.
- [290] S. Panigrahi and B. K. Dubey, 'A critical review on operating parameters and strategies to improve the biogas yield from anaerobic digestion of organic fraction of municipal solid waste', *Renew. Energy*, vol. 143, pp. 779–797, 2019, doi: 10.1016/j.renene.2019.05.040.
- [291] O. Parthiba Karthikeyan, E. Trably, S. Mehariya, N. Bernet, J. W. Wong, and H. Carrere, 'Pretreatment of food waste for methane and hydrogen recovery: A review', 2017, doi: 10.1016/j.biortech.2017.09.105.
- [292] P. N. Hobson and A. M. Robertson, 'Waste treatment in agriculture', p. 257, 1977.
- [293] H. K. Shon, S. Vigneswaran, and S. A. Snyder, 'Effluent Organic Matter (EfOM) in Wastewater: Constituents, Effects, and Treatment', <http://dx.doi.org/10.1080/10643380600580011>, vol. 36, no. 4, pp. 327–374, Jul. 2007, doi: 10.1080/10643380600580011.
- [294] A. Rodriguez Andara and J. M. Lomas Esteban, 'Transition of particle size fractions in anaerobic digestion of the solid fraction of piggery manure', *Biomass and Bioenergy*, vol. 23, no. 3, pp. 229–235, Sep. 2002, doi: 10.1016/S0961-9534(02)00043-0.
- [295] Y. R. Chen, 'Kinetic analysis of anaerobic digestion of pig manure and its design implications', *Agric. Wastes*, vol. 8, no. 2, pp. 65–81, 1983, doi: 10.1016/0141-4607(83)90105-1.
- [296] V. Nallathambi Gunaseelan and V. N. Gunaseelan, 'Anaerobic digestion of biomass for methane production: A review', *Biomass and Bioenergy*, vol. 13, no. 1–2, pp. 83–114, 1997, doi: 10.1016/S0961-9534(97)00020-2.
- [297] S. Antognoni *et al.*, 'Potential Effects of Mechanical Pre-treatments on Methane Yield from Solid Waste Anaerobically Digested', *Int. J. Environ. Bioremediation Biodegrad.*, vol. 1, no. 1, pp. 20–25, 2013, doi: 10.12691/ijebb-1-1-4.

10 Appendices

Particle Size Characterisation

Appendix A1: The photograph of each pre-treatment level of banana peel waste substrate biomass (1-4)



BPWSB PT1



BPWSB PT2



BPWSB PT3



BPWSB PT4

Appendix A2: The photograph of each pre-treatment level of grass waste substrate biomass (1-4).



GWSB PT1



GWSB PT2



GWSB PT3



GWSB PT4

Appendix A3: The photograph of each pre-treatment level of paper waste substrate biomass (1-4).



PWSB PTL1



PWSB PTL2



PWSB PTL3



PWSB PTL4

Appendix A4: The photograph of each pre-treatment level of tomato waste substrate biomass (1-4).



TWSB PT1



TWSB PT2



TWSB PT3



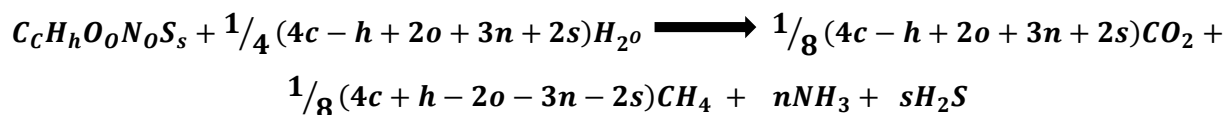
TWSB PT4

Batch testing

Calculation of the theoretical calorific value of BPWSB potential

Table B1 BPWSB Proportion of CH₄ and CO₂ and Carbon balance for each PTLs

Based on the Buswell equation from 1952, the proportion of methane (CH₄) to carbon-dioxide (CO₂) is used to calculate the products of anaerobic digestion of an overall organic matter with known chemical composition $C_cH_hO_oN_nS_s$



Biomass		Atomic Weight	Elemental Composition (%ODM)
BPWSB	C	12	40.1
	H	1	5.82
	O	16	-
	N	14	1.43
	S	32	-

Where $C_{40/12}H_{5.82/1}O_{0/16}N_{1.43/14}S_{0/32}$

$C_{3.3342}H_{5.82}O_0N_{0.102143}S_0$

calculating the coefficients for methane CH₄ and carbon dioxide CO₂.

$$\frac{1}{8}(4c - h + 2o + 3n + 2s)$$

$$\frac{1}{8}(4 * 3.3342 - 5.82 + 2 * 0 + 3 * 0.102143 + 2 * 0) = 0.97790$$

$$\frac{1}{8}(4c + h - 2o - 3n - 2s)$$

$$\frac{1}{8}(4 * 3.3342 + 5.82 - 2 * 0 - 3 * 0.102143 - 2 * 0) = 2.35623$$

$$2.35623 / (2.35623 + 0.97790) = 0.7067 * 100 = 70.7\%$$

CH₄ = 70.7%

CO₂ = 29.3%

Carbon balance

Table **B2** Predicted biogas production for BPWSB based on volatile solid reduction from experimental data for PTL1- 2

Carbon balance: BPWSB	
PTL1 @60.6% Volatile solids reduction (VSR)	PTL2 @61.7% Volatile solids reduction (VSR)
3gVS contains 40.1g of carbon of which 60.6% is degraded = 0.401gC/gVS	3gVS contains 40.1g of carbon of which 61.7% is degraded = 0.401gC/gVS
$(0.606\% \times 0.401) = 0.243006 \text{ gC/gVS}$	$(0.617\% \times 0.401) = 0.24742 \text{ gC/gVS}$
70.7% of carbon is converted to methane = $0.243006 \times 0.707 = 0.171805 \text{ gC/gVS}$	70.7% of carbon is converted to methane = $0.24742 \times 0.707 = 0.17492 \text{ gC/gVS}$
= 0.171805 gC is $(0.171805 / 12) = 0.01432$ moles C and 1 mole of C \equiv 1 mole of CH ₄ so 1gVS produces 0.01432 moles of methane	= 0.17492 gC is $(0.17492 / 12) = 0.01458$ moles C and 1 mole of C \equiv 1 mole of CH ₄ so 1gVS produces 0.01458 moles of methane
• 1 mole of gas occupies 22.4 litres at STP => 0.01432 moles occupy $(0.01432 \times 22.4) = 0.35299$ litres.	• 1 mole of gas occupies 22.4 litres at STP => 0.01458 moles occupy $(0.01458 \times 22.4) = 0.32652$ litres.
Therefore, specific methane production = 321 Nml/gVS	Therefore, specific methane production = 327Nml/gVS

Table **B3** Shows the predicted biogas production for BPWSB based on volatile solid reduction from experimental data for PTL3- 4

Carbon balance: BPWSB	
PTL3 @64% Volatile solids reduction (VSR)	PTL4 @66.7% Volatile solids reduction (VSR)
3gVS contains 40.1g of carbon of which 64% is degraded = 0.401gC/gVS	3gVS contains 40.1g of carbon of which 66.7% is degraded = 0.401gC/gVS
$(0.64 \% \times 0.401) = 0.25664 \text{ gC/gVS}$	$(0.667\% \times 0.401) = 0.26747 \text{ gC/gVS}$
70.7% of carbon is converted to methane = $0.25664 \times 0.707 = 0.18144448 \text{ gC/gVS}$	70.7% of carbon is converted to methane = $0.26747 \times 0.707 = 0.189099169 \text{ gC/gVS}$
= 0.18144448 gC is $(0.18144448 / 12) = 0.0151203733$ moles C and 1 mole of C \equiv 1 mole of CH ₄ so 1gVS produces 0.0151204 moles of methane	= 0.189099169 gC is $(0.189099169 / 12) = 0.0157582641$ moles C and 1 mole of C \equiv 1 mole of CH ₄ so 1gVS produces 0.015595 moles of methane
• 1 mole of gas occupies 22.4 litres at STP => 0.0151204 moles occupy $(0.0151204 \times 22.4) = 0.33669$ litres.	• 1 mole of gas occupies 22.4 litres at STP => 0.0157583 moles occupy $(0.0157583 \times 22.4) = 0.35299$ litres.
Therefore, specific methane production = 339 Nml/gVS	Therefore, specific methane production = 353 Nml/gVS

Table **B4** shows the predicted BPWSB based average biogas production using volatile solid reduction from experimental data for PTL3- 4

Carbon balance: BPWSB
63.4% Volatile solids reduction (VSR)
3 gVS contains 40.1g of carbon of which 63.4% is degraded = 0.401gC/gVS
$(0.634\% \times 0.401) = 0.254234 \text{ gC/gVS}$
70.7% of carbon is converted to methane = $0.254234 \times 0.707 = 0.179743438 \text{ gC/gVS}$
= 0.179743438 gC is $(0.179743438 / 12) = 0.0149786198$ moles C and 1 mole of C \equiv 1 mole of CH ₄ so 1gVS produces 0.014979 moles of methane
<ul style="list-style-type: none"> • 1 mole of gas occupies 22.4 litres at STP => 0.0157583 moles occupy $(0.014979 \times 22.4) = 0.3355$ litres.
Therefore, specific methane production = 353 Nml/gVS

Table **B5** Shows the Biogas production using assume volatile solid reduction

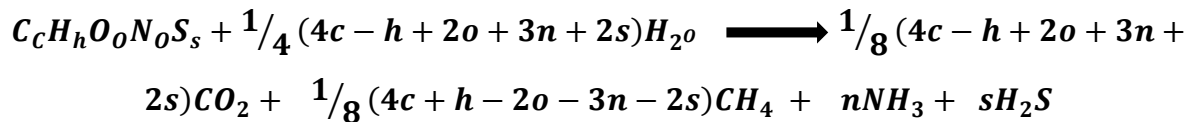
Carbon balance: Assuming 70 and 75 % Volatile solids reduction (VSR)	
BPWSB@70%	BPWSB@75%
3 gVS contains 40.1g of carbon of which 70% is degraded = 0.401gC/gVS	3 gVS contains 40.1g of carbon of which 75% is degraded = 0.401gC/gVS
$(0.70\% \times 0.401) = 0.2807 \text{ gC/gVS}$	$(0.75\% \times 0.401) = 0.30075 \text{ gC/gVS}$
70.7% of carbon is converted to methane = $0.2807 \times 0.707 = 0.1984549 \text{ gC/gVS}$	70.7% of carbon is converted to methane = $0.30075 \times 0.707 = 0.21263025 \text{ gC/gVS}$
= 0.1984549 gC is $(0.1984549 / 12) = 0.0165379083$ moles C and 1 mole of C \equiv 1 mole of CH ₄ so 1gVS produces 0.016538 moles of methane	= 0.21263025 gC is $(0.21263025 / 12) = 0.0177191875$ moles C and 1 mole of C \equiv 1 mole of CH ₄ so 1gVS produces 0.016538 moles of methane
<ul style="list-style-type: none"> • 1 mole of gas occupies 22.4 litres at STP => 0.016538 moles occupy $(0.016538 \times 22.4) = 0.37045$ litres. 	<ul style="list-style-type: none"> • 1 mole of gas occupies 22.4 litres at STP => 0.017712 moles occupy $(0.017712 \times 22.4) = 0.397$ litres.
Therefore, specific methane production = 370 Nml/gVS	Therefore, specific methane production = 397Nml/gVS

Calculation of the theoretical calorific value of GWSB potential

Table C1 GWSB Proportion of CH₄ and CO₂ and Carbon balance for each PTLs

GWSB Proportion of CH₄ and CO₂ and Carbon balance for each PTLs

Based on the Buswell equation from 1952, the proportion of methane (CH₄) to carbon-dioxide (CO₂) is used to calculate the products of anaerobic digestion of an overall organic matter with known chemical composition $C_cH_hO_oN_nS_s$



Biomass	Atomic Weight		Elemental Composition (%ODM)
BPWSB	C	12	39.19
	H	1	5.8
	O	16	-
	N	14	3.08
	S	32	-

Where $C_{39.2/12}H_{5.8/1}O_{0/16}N_{3.08/14}S_{0/32}$

$C_{3.3342}H_{5.82}O_0N_{0.22}S_0$

calculating the coefficients for methane CH₄ and carbon dioxide CO₂.

$$\frac{1}{8}(4c - h + 2o + 3n + 2s)$$

$$\frac{1}{8}(4 * 3.26667 - 5.8 + 2 * 0 + 3 * 0.22 + 2 * 0) = 0.99084$$

$$\frac{1}{8}(4c + h - 2o - 3n - 2s)$$

$$\frac{1}{8}(4 * 3.3342 + 5.8 - 2 * 0 - 3 * 0.22 - 2 * 0) = 2.27584$$

$$2.27584 / (2.27584 + 0.99084) = 0.69668 * 100 = 69.7\%$$

$$CH_4 = 69.7\%$$

$$CO_2 = 30.3\%$$

Carbon balance

Table C2 Predicted biogas production for GWSB based on volatile solid reduction from experimental data for PTL1- 2

Carbon balance: GWSB	
PTL1 @52.5% Volatile solids reduction (VSR)	PTL2 @53.4% Volatile solids reduction (VSR)
3 gVS contains 39.2g of carbon of which 52.5% is degraded = 0.392gC/gVS	3 gVS contains 39.2g of carbon of which 53.4% is degraded = 0.392gC/gVS
$(0.525\% \times 0.392) = 0.2058 \text{ gC/gVS}$	$(0.534\% \times 0.392) = 0.20933 \text{ gC/gVS}$
69.7% of carbon is converted to methane = $0.2058 \times 0.697 = 0.1434426 \text{ gC/gVS}$	69.7% of carbon is converted to methane = $0.20933 \times 0.697 = 0.14590 \text{ gC/gVS}$
= 0.1434426 gC is $(0.1434426 / 12) = 0.01195$ moles C and 1 mole of C \equiv 1 mole of CH ₄ so 1gVS produces 0.01195 moles of methane	= 0.14590 gC is $(0.14590 / 12) = 0.0121585$ moles C and 1 mole of C \equiv 1 mole of CH ₄ so 1gVS produces 0.0121585 moles of methane
<ul style="list-style-type: none"> • 1 mole of gas occupies 22.4 litres at STP => 0.01195 moles occupy $(0.01195 \times 22.4) = 0.26776$ litres. 	<ul style="list-style-type: none"> • 1 mole of gas occupies 22.4 litres at STP => 0.0121585 moles occupy $(0.0121585 \times 22.4) = 0.2723$ litres.
Therefore, specific methane production = 268 Nml/gVS	Therefore, specific methane production = 272 Nml/gVS

Table C3 Shows the predicted biogas production for GWSB based on volatile solid reduction from experimental data for PTL3- 4

Carbon balance: GWSB	
PTL3@57.6% Volatile solids reduction (VSR)	PTL3@59.1% Volatile solids reduction (VSR)
3 gVS contains 39.2g of carbon of which 57.6% is degraded = 0.392gC/gVS	3 gVS contains 39.2g of carbon of which 59.1% is degraded = 0.392gC/gVS
$(0.576\% \times 0.392) = 0.2258 \text{ gC/gVS}$	$(0.591\% \times 0.392) = 0.231672 \text{ gC/gVS}$
69.7% of carbon is converted to methane = $0.2258 \times 0.697 = 0.157377 \text{ gC/gVS}$	69.7% of carbon is converted to methane = $0.231672 \times 0.697 = 0.16147538 \text{ gC/gVS}$
= 0.157377 gC is $(0.157377 / 12) = 0.0131148$ moles C and 1 mole of C \equiv 1 mole of CH ₄ so 1gVS produces 0.0131148 moles of methane	= 0.16147538 gC is $(0.16147538 / 12) = 0.013456282$ moles C and 1 mole of C \equiv 1 mole of CH ₄ so 1gVS produces 0.013456282 moles of methane
<ul style="list-style-type: none"> • 1 mole of gas occupies 22.4 litres at STP => 0.0131148 moles occupy $(0.0131148 \times 22.4) = 0.29377$ litres. 	<ul style="list-style-type: none"> • 1 mole of gas occupies 22.4 litres at STP => 0.013456282 moles occupy $(0.013456282 \times 22.4) = 0.3014$ litres.
Therefore, specific methane production = 294 Nml/gVS	Therefore, specific methane production = 301 Nml/gVS

Table C4 Shows the predicted GWSB based average biogas production using volatile solid reduction from experimental data for GWSB

Carbon balance: GWSB
@55.2% Volatile solids reduction (VSR)
3 gVS contains 39.2g of carbon of which 55.2% is degraded = 0.392gC/gVS
$(0.555\% * 0.392) = 0.21756 \text{ gC/gVS}$
69.7% of carbon is converted to methane = $0.20933 * 0.697 = 0.15163932 \text{ gC/gVS}$
= 0.15163932 gC is $(0.15163932 / 12) = 0.01263661$ moles C and 1 mole of C = 1 mole of CH ₄ so 1gVS produces 0.01263661 moles of methane
<ul style="list-style-type: none"> • 1 mole of gas occupies 22.4 litres at STP => 0.01263661 moles occupy $(0.01263661 * 22.4) = 0.2831$ litres.
Therefore, specific methane production = 283 Nml/gVS

Table C5 Show the Biogas production using assume volatile solid reduction

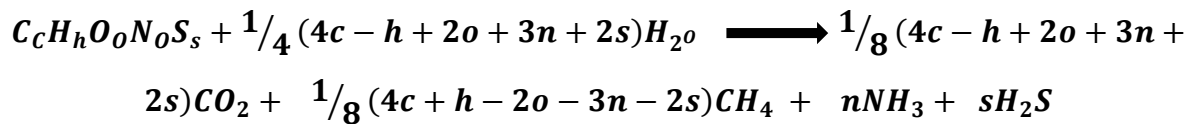
Carbon balance: Assuming 70 and 75 % Volatile solids reduction (VSR)	
GWSB @70%	GWSB @75%
3 gVS contains 39.2g of carbon of which 70 % is degraded = 0.392gC/gVS	3 gVS contains 39.2g of carbon of which 75 % is degraded = 0.392gC/gVS
$= (0.70\% * 0.392) = 0.2744 \text{ gC/gVS}$	$(0.75\% * 0.392) = 0.294 \text{ gC/gVS}$
69.7% of carbon is converted to methane = $0.2744 * 0.697 = 0.19126 \text{ gC/gVS}$	69.7% of carbon is converted to methane = $0.294 * 0.697 = 0.20492 \text{ gC/gVS}$
= 0.1912568 gC is $(0.1912568 / 12) = 0.015938$ moles C and 1 mole of C \equiv 1 mole of CH ₄ so 1gVS produces 0.015938 moles of methane	= 0.20492 gC is $(0.20492 / 12) = 0.0170765$ moles C and 1 mole of C \equiv 1 mole of CH ₄ so 1gVS produces 0.01263661 moles of methane
<ul style="list-style-type: none"> • 1 mole of gas occupies 22.4 litres at STP => 0.015938 moles occupy $(0.015938 * 22.4) = 0.3570$ litres. 	<ul style="list-style-type: none"> • 1 mole of gas occupies 22.4 litres at STP => 0.0170765 moles occupy $(0.0170765 * 22.4) = 0.3825$ litres.
Therefore, specific methane production = 357 Nml/gVS	Therefore, specific methane production = 383 Nml/gVS

Calculation of the theoretical calorific value of PWSB potential

Table D1 PWSB Proportion of CH₄ and CO₂ and Carbon balance for each PTLs

PWSB Proportion of CH₄ and CO₂ and Carbon balance for each PTLs

Based on the Buswell equation from 1952, the proportion of methane (CH₄) to carbon-dioxide (CO₂) is used to calculate the products of anaerobic digestion of an overall organic matter with known chemical composition $C_cH_hO_oN_nS_s$



Biomass		Atomic Weight	Elemental Composition (%ODM)
BPWSB	C	12	38.19
	H	1	5.57
	O	16	-
	N	14	-
	S	32	-

Where $C_{38.2/12}H_{5.57/1}O_{0/16}N_{0/14}S_{0/32}$



calculating the coefficients for methane CH₄ and carbon dioxide CO₂.

$$\frac{1}{8}(4c - h + 2o + 3n + 2s)$$

$$\frac{1}{8}(4 * 3.1833 - 5.57 + 2 * 0 + 3 * 0 + 2 * 0) = 0.8954$$

$$\frac{1}{8}(4c + h - 2o - 3n - 2s)$$

$$\frac{1}{8}(4 * 3.1833 + 5.57 - 2 * 0 - 3 * 0 - 2 * 0) = 2.2879$$

$$2.2879 / (2.2879 + 0.8954) = 0.71872 * 100 = 71.9\%$$

$$CH_4 = 71.9\%$$

$$CO_2 = 28.1\%$$

Carbon balance

Table D2 Predicted biogas production for PWSB based on volatile solid reduction from experimental data for PTL1- 2

Carbon balance: PWSB	
PTL1 @52.4% Volatile solids reduction (VSR)	PTL2 @53.3% Volatile solids reduction (VSR)
3 gVS contains 38.2g of carbon of which 52.4% is degraded = 0.382gC/gVS	3 gVS contains 38.2g of carbon of which 53.3% is degraded = 0.382gC/gVS
$(0.524\% \times 0.382) = 0.20017 \text{ gC/gVS}$	$(0.533\% \times 0.382) = 0.20361 \text{ gC/gVS}$
71.9% of carbon is converted to methane = $0.2058 \times 0.719 = 0.143922 \text{ gC/gVS}$	71.9% of carbon is converted to methane = $0.20933 \times 0.719 = 0.1463956 \text{ gC/gVS}$
= 0.143922 gC is $(0.143922 / 12) = 0.011994$ moles C and 1 mole of C = 1 mole of CH ₄ so 1gVS produces 0.011994 moles of methane	= 0.1463956 gC is $(0.1463956 / 12) = 0.0121996$ moles C and 1 mole of C = 1 mole of CH ₄ so 1gVS produces 0.0121996 moles of methane
• 1 mole of gas occupies 22.4 litres at STP => 0.011994 moles occupy $(0.011994 \times 22.4) = 0.2687$ litres.	• 1 mole of gas occupies 22.4 litres at STP => 0.0121996 moles occupy $(0.0121996 \times 22.4) = 0.2733$ litres.
Therefore, specific methane production = 269 Nml/gVS	Therefore, specific methane production = 273 Nml/gVS

Table D3 Shows the predicted biogas production for PWSB based on volatile solid reduction from experimental data for PTL3- 4

Carbon balance: PWSB	
PTL3@55% Volatile solids reduction (VSR)	PTL3@56% Volatile solids reduction (VSR)
3 gVS contains 38.2g of carbon of which 55% is degraded = 0.382gC/gVS	3 gVS contains 38.2g of carbon of which 56% is degraded = 0.382gC/gVS
$(0.55\% \times 0.382) = 0.2101 \text{ gC/gVS}$	$(0.56\% \times 0.382) = 0.21392 \text{ gC/gVS}$
71.9% of carbon is converted to methane = $0.2101 \times 0.719 = 0.151062 \text{ gC/gVS}$	71.9% of carbon is converted to methane = $0.231672 \times 0.719 = 0.1538085 \text{ gC/gVS}$
= 0.151062gC is $(0.151062/12) = 0.0125885$ moles C and 1 mole of C = 1 mole of CH ₄ so 1gVS produces 0.0125885 moles of methane	= 0.1538085 gC is $(0.1538085 / 12) = 0.0128174$ moles C and 1 mole of C = 1 mole of CH ₄ so 1gVS produces 0.0128174 moles of methane
• 1 mole of gas occupies 22.4 litres at STP => 0.0125885 moles occupy $(0.0125885 \times 22.4) = 0.28198$ litres.	• 1 mole of gas occupies 22.4 litres at STP => 0.0128174 moles occupy $(0.0128174 \times 22.4) = 0.28711$ litres.
Therefore, specific methane production = 282 Nml/gVS	Therefore, specific methane production = 287Nml/gVS

Table D4 Shows the predicted PWSB based average biogas production using volatile solid reduction from experimental data

Carbon balance: PWSB
@55.2% Volatile solids reduction (VSR)
3 gVS contains 38.2g of carbon of which 55.2% is degraded = 0.382gC/gVS
$(0.54.2\% \times 0.382) = 0.20628 \text{ gC/gVS}$
71.9% of carbon is converted to methane = $0.20628 \times 0.719 = 0.14832 \text{ gC/gVS}$
= 0.14832 gC is $(0.14832 / 12) = 0.01235961$ moles C and 1 mole of C \equiv 1 mole of CH ₄ so 1gVS produces 0.01235961moles of methane
• 1 mole of gas occupies 22.4 litres at STP => 0.01235961 moles occupy $(0.01235961 \times 22.4) = 0.27686$ litres.
Therefore, specific methane production = 277 Nml/gVS

Table D5 Show the Biogas production using assume volatile solid reduction

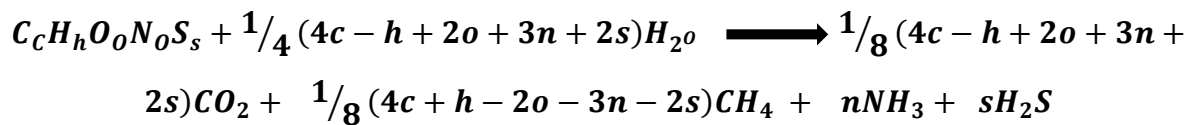
Carbon balance: Assuming 70 and 75 % Volatile solids reduction (VSR)	
PWSB @70%	PWSB @75%
3 gVS contains 38.2g of carbon of which 70 % is degraded = 0.382gC/gVS	3 gVS contains 38.2g of carbon of which 75 % is degraded = 0.382gC/gVS
$= (0.70\% \times 0.382) = 0.2674 \text{ gC/gVS}$	$(0.75\% \times 0.382) = 0.2865 \text{ gC/gVS}$
71.9% of carbon is converted to methane = $0.2674 \times 0.719 = 0.192261 \text{ gC/gVS}$	71.9% of carbon is converted to methane = $0.2865 \times 0.719 = 0.205994 \text{ gC/gVS}$
= 0.192261 gC is $(0.192261 / 12) = 0.01602172$ moles C and 1 mole of C \equiv 1 mole of CH ₄ so 1gVS produces 0.01602172 moles of methane	= 0.205994 gC is $(0.205994 / 12) = 0.01716613$ moles C and 1 mole of C \equiv 1 mole of CH ₄ so 1gVS produces 0.01716613 moles of methane
• 1 mole of gas occupies 22.4 litres at STP => 0.01602172 moles occupy $(0.01602172 \times 22.4) = 0.35888$ litres.	• 1 mole of gas occupies 22.4 litres at STP => 0.01716613 moles occupy $(0.01716613 \times 22.4) = 0.3845$ litres.
Therefore, specific methane production = 359 Nml/gVS	Therefore, specific methane production = 385 Nml/gVS

Calculation of the theoretical calorific value of TWSB potential

Table E1 TWSB Proportion of CH₄ and CO₂ and Carbon balance for each PTLs

PWSB Proportion of CH₄ and CO₂ and Carbon balance for each PTLs

Based on the Buswell equation from 1952, the proportion of methane (CH₄) to carbon-dioxide (CO₂) is used to calculate the products of anaerobic digestion of an overall organic matter with known chemical composition $C_cH_hO_oN_nS_s$



Biomass		Atomic Weight	Elemental Composition (%ODM)
TWSB	C	12	39.55
	H	1	5.65
	O	16	-
	N	14	2.04
	S	32	-

Where $C_{39.6/12}H_{5.65/1}O_{0/16}N_{2.04/14}S_{0/32}$



calculating the coefficients for methane CH₄ and carbon dioxide CO₂.

$$\frac{1}{8}(4c - h + 2o + 3n + 2s)$$

$$\frac{1}{8}(4 * 3.3 - 5.65 + 2 * 0 + 3 * 0.145714 + 2 * 0) = 0.9984$$

$$\frac{1}{8}(4c + h - 2o - 3n - 2s)$$

$$\frac{1}{8}(4 * 3.3 + 5.65 - 2 * 0 - 3 * 0.145714 - 2 * 0) = 2.30161$$

$$2.30161 / (2.30161 + 0.9984) = 0.697455 * 100 = 69.7\%$$

$$CH_4 = 69.7\%$$

$$CO_2 = 30.3\%$$

Carbon balance

Table E2 Predicted biogas production for PWSB based on volatile solid reduction from experimental data for PTL1- 2

Carbon balance: TWSB	
PTL1 @57.9% Volatile solids reduction (VSR)	PTL2 @60.8% Volatile solids reduction (VSR)
3gVS contains 39.6g of carbon of which 57.9% is degraded = 0.396gC/gVS	3 gVS contains 39.6g of carbon of which 60.8% is degraded = 0.396gC/gVS
$(0.579 \times 0.396) = 0.229284 \text{ gC/gVS}$	$(0.608 \times 0.396) = 0.240768 \text{ gC/gVS}$
69.7% of carbon is converted to methane = $0.229284 \times 0.697 = 0.159811 \text{ gC/gVS}$	69.7% of carbon is converted to methane = $0.240768 \times 0.697 = 0.16782 \text{ gC/gVS}$
= 0.159811 gC is $(0.159811 / 12) = 0.01331758$ moles C and 1 mole of C \equiv 1 mole of CH ₄ so 1gVS produces 0.01331758 moles of methane	= 0.16782 gC is $(0.16782 / 12) = 0.013985$ moles C and 1 mole of C \equiv 1 mole of CH ₄ so 1gVS produces 0.013985 moles of methane
• 1 mole of gas occupies 22.4 litres at STP => 0.01331758 moles occupy $(0.01331758 \times 22.4) = 0.2983$ litres.	• 1 mole of gas occupies 22.4 litres at STP => 0.013985 moles occupy $(0.013985 \times 22.4) = 0.31326$ litres.
Therefore, specific methane production = 298 Nml/gVS	Therefore, specific methane production = 313 Nml/gVS

Table E3 Shows the predicted biogas production for TWSB based on volatile solid reduction from experimental data for PTL3- 4

Carbon balance: TWSB	
PTL3@62.2% Volatile solids reduction (VSR)	PTL3@63.1% Volatile solids reduction (VSR)
3 gVS contains 39.6g of carbon of which 62.2% is degraded = 0.382gC/gVS	3 gVS contains 38.2g of carbon of which 63.1% is degraded = 0.396gC/gVS
$(0.622 \times 0.396) = 0.246312 \text{ gC/gVS}$	$(0.631 \times 0.396) = 0.249876 \text{ gC/gVS}$
69.7% of carbon is converted to methane = $0.246312 \times 0.697 = 0.1716795 \text{ gC/gVS}$	69.7% of carbon is converted to methane = $0.249876 \times 0.697 = 0.174164 \text{ gC/gVS}$
= 0.1716795gC is $(0.1716795 / 12) = 0.0143066$ moles C and 1 mole of C \equiv 1 mole of CH ₄ so 1gVS produces 0.0143066 moles of methane	= 0.174164gC is $(0.174164 / 12) = 0.014514$ moles C and 1 mole of C \equiv 1 mole of CH ₄ so 1gVS produces 0.014514 moles of methane
• 1 mole of gas occupies 22.4 litres at STP => 0.0143066 moles occupy $(0.0143066 \times 22.4) = 0.3205$ litres.	• 1 mole of gas occupies 22.4 litres at STP => 0.014514 moles occupy $(0.014514 \times 22.4) = 0.32511$ litres.
Therefore, specific methane production = 321 Nml/gVS	Therefore, specific methane production = 325Nml/gVS

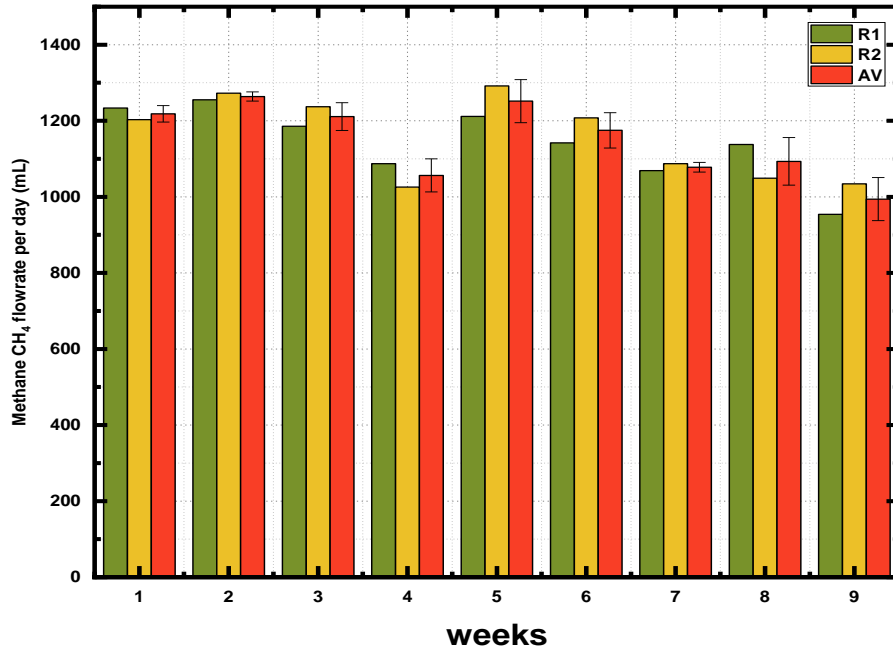
Table E4 Shows the predicted TWSB based average biogas production using volatile solid reduction from experimental data for PTL3- 4

Carbon balance: GWSB
@55.2% Volatile solids reduction (VSR)
3 gVS contains 39.6g of carbon of which 61% is degraded = 0.396gC/gVS
$(0.61\% * 0.396) = 0.24156 \text{ gC/gVS}$
69.7% of carbon is converted to methane = $0.24156 * 0.697 = 0.168367 \text{ gC/gVS}$
= 0.168367 gC is $(0.168367 / 12) = 0.014031$ moles C and 1 mole of C \equiv 1 mole of CH ₄ so 1gVS produces 0.014031moles of methane
• 1 mole of gas occupies 22.4 litres at STP => 0.014031 moles occupy $(0.014031 * 22.4) = 0.31429$ litres.
Therefore, specific methane production = 314 Nml/gVS

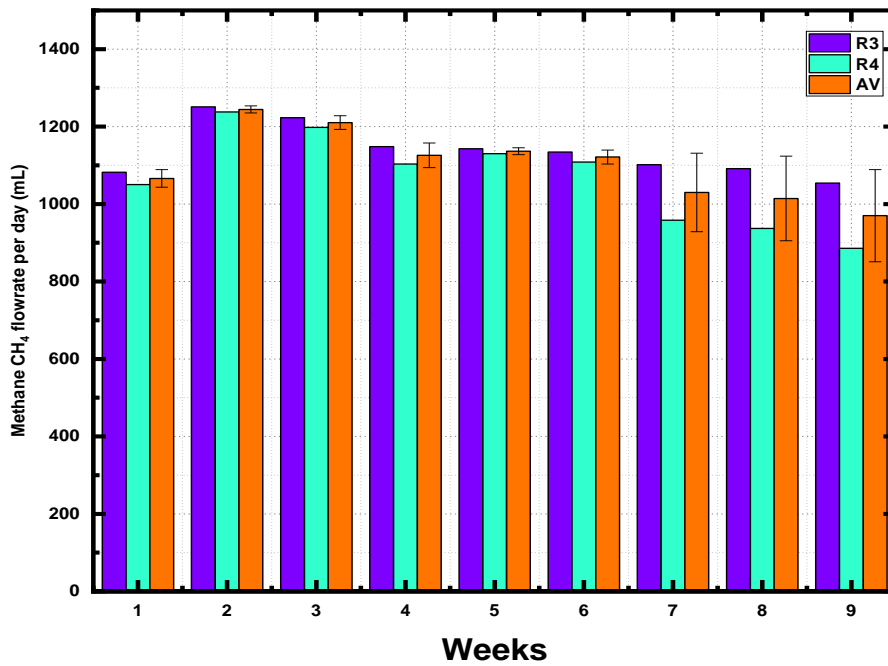
Table E5 Show the Biogas production using assume volatile solid reduction

Carbon balance: Assuming 70 and 75 % Volatile solids reduction (VSR)	
TWSB @70%	TWSB @75%
3 gVS contains 396g of carbon of which 70 % is degraded = 0.396gC/gVS	3 gVS contains 396g of carbon of which 75 % is degraded = 0.396gC/gVS
$= (0.70\% * 0.396) = 0.2772 \text{ gC/gVS}$	$(0.75\% * 0.396) = 0.297 \text{ gC/gVS}$
69.7 % of carbon is converted to methane = $0.2772 * 0.697 = 0.19321 \text{ gC/gVS}$	69.7% of carbon is converted to methane = $0.297 * 0.697 = 0.207009 \text{ gC/gVS}$
= 0.19321 gC is $(0.19321/12) = 0.0161007$ moles C and 1 mole of C \equiv 1 mole of CH ₄ so 1gVS produces 0.0161007 moles of methane	= 0.207009 gC is $(0.207009/12) = 0.0172508$ moles C and 1 mole of C \equiv 1 mole of CH ₄ so 1gVS produces 0.0172508 moles of methane
• 1 mole of gas occupies 22.4 litres at STP => 0.0161007 moles occupy $(0.0161007 * 22.4) = 0.3607$ litres.	• 1 mole of gas occupies 22.4 litres at STP => 0.0172508 moles occupy $(0.0172508 * 22.4) = 0.3864$ litres.
Therefore, specific methane production = 361 Nml/gVS	Therefore, specific methane production = 386 Nml/gVS

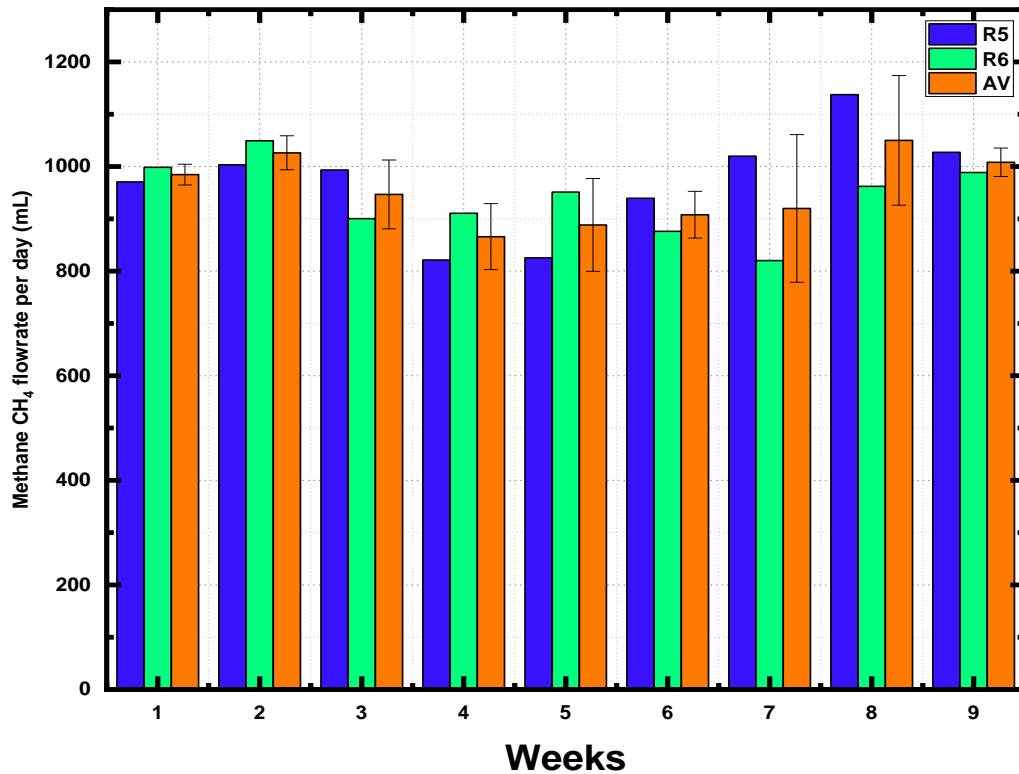
Semi continuous testing.



Appendix F1 Daily average banana peel waste substrate biomass (GWSB) methane flow rate above 1149ml/day for 9 weeks,



Appendix F2 Daily average paper waste substrate biomass (BPWSB) methane flow rate above 1149ml/day for 9 weeks



Appendix F3 Daily average paper waste substrate biomass (PWSB) methane flow rate above 955ml/ day for 9 weeks.

G1 = Calculation of calorific value modified Dulong formulas

$$337C + 1419(H - \frac{1419}{8}O) + 93S + 23.26N$$

$$GWSB = 337(39.19) = 13207$$

$$1419(5.8) - \frac{0}{8} = 8230$$

$$23.26(3.08) = 72$$

$$\text{Energy value} = 337(39.19) + 1419(5.8 - \frac{1419}{8}O) + 23.26(3.08) = 22 \text{ MJ/kgVS}$$

$$BPWSB = 337(40.01) = 13483$$

$$1419(5.82) - \frac{0}{8} = 8259$$

$$23.26(1.43) = 33.3$$

$$\text{Energy value} = 337(40.01) + 1419(5.82 - \frac{1419}{8}O) + 23.26(1.43) = 22 \text{ MJ/kgVS}$$

$$PWSB = 337(38.19) = 12870$$

$$1419 (5.57) - \frac{0}{8} = 7904$$

$$23.26(0) = 23.26$$

$$\text{Energy value} = 337(38.19) + 1419(5.57 - 1419 \frac{0}{8}) + 23.26(0) = 21 \text{ MJ/kgVS}$$

$$\text{TWSB} = 337(39.55) = 13328$$

$$1419 (5.65) - \frac{0}{8} = 8017$$

$$23.26(2.04) = 48$$

$$\text{Energy value} = 337(38.19) + 1419(5.65 - 1419 \frac{0}{8}) + 23.26(2.04) = 21 \text{ MJ/kgVS}$$

OR.

$$\text{G2} = 34.1\text{C} + 102\text{H} + 6.3\text{N} + 19.1(0) - 9.850/100$$

$$\text{GWSB} = 34.1(39.19) + 102(5.8) + 6.3(3.08) + 19.1\text{S} - 9.85(0)/100 = 20 \text{ MJ/kgVS}$$

$$\text{BPWSB} = 34.1(40.01) + 102(5.82) + 6.3(1.43) + 19.1(0) - 9.85(0)/100 = 20 \text{ MJ/kgVS}$$

$$\text{PWSB} = 34.1(38.19) + 102(5.57) + 6.3(0) + 19.1(0) - 9.85(0)/100 = 19 \text{ MJ/kgVS}$$

$$\text{TWSB} = 34.1(39.55) + 102(5.65) + 6.3(2.04) + 19.1(0) - 9.85(0)/100 = 19 \text{ MJ/kgVS}$$

Process modelling

Appendix H1: MATLAB Simulation Code

```
% Initialises workspace variables for particle size distribution AD model
% Note that F is the frequency distribution of particles with radius
% Partitioning set using R - to use a mass fraction-based particle size
% Distribution we would need to calculate on a frequency basis before using
% This model. F is relative frequency and therefore should sum to 1
% Particle size range and categories in m
R = [1e-5 3e-5 1e-4 3e-4 1e-3 3e-3 1e-2 3e-2 1e-1 3e-1]';
rmax = ((3*R(max(size(R)))) + R(max(size(R)-1)))/2; % rmax is used to set the
maximum particle size for PS distribution calculations
% Particle size distribution of feedstock
Fin = [1 0 0 0 0 0 0 0 0]';
% Initial condition of particle size distribution
Fini = [0.0 0.0 0.0 0.0 0.2 0.3 0.4 0.1 0.0 0.0]';
% Inlet VS concentration
Cin = [0 250]; % kg m-3
% Initial VS concentration
Cini = 200; % kg m-3
% Dilution rate
D = [0 0];
% Rate constant based on surface area
Ksbk = 0.5;
% Density
rho = 1000;
% Specific methane production in m3 methane/kg VS destroyed
km = 0.5;
```


Table H3 Extracted parameters and estimates for the particle size distribution of the raw slurry

Total particle volume (PSD), created by Plot Digitizer, 2.5.1							
Date: 17/01/2021, 17:18:17							
	PSD um	Total particle volume	Ci	Ci/r^3	fi	fi	Fi*ri
1	28.1955	0.081353	0.014783	6.59497E-07	0.809207		22.816
2	50.0968	0.027555	0.005007	3.98244E-08	0.048865		2.44797
3	71.9891	0.054981	0.009991	2.67788E-08	0.032858		2.365401
4	90.752	0.082394	0.014972	2.00311E-08	0.024578		2.230534
5	115.783	0.091609	0.016646	1.07246E-08	0.013159		1.523611
6	137.679	0.109923	0.019974	7.65357E-09	0.009391		1.292941
7	156.447	0.128224	0.0233	6.0848E-09	0.007466		1.168047
8	181.477	0.137439	0.024974	4.17853E-09	0.005127		0.930449
9	203.379	0.146642	0.026646	3.16752E-09	0.003887		0.790445
10	225.275	0.164956	0.029974	2.62185E-09	0.003217	0.957755	0.724716
11	244.047	0.174145	0.031644	2.17706E-09	0.002671		0.651913
12	269.06	0.219807	0.039941	2.05056E-09	0.002516		0.676969
13	287.832	0.228997	0.041611	1.74498E-09	0.002141		0.616279
14	309.724	0.256422	0.046594	1.56823E-09	0.001924		0.595979
15	331.621	0.274736	0.049922	1.36889E-09	0.00168		0.557002
16	356.638	0.311287	0.056564	1.24697E-09	0.00153		0.545672
17	381.638	0.384283	0.069828	1.25625E-09	0.001541		0.588266
18	400.396	0.420808	0.076465	1.19122E-09	0.001462		0.585235
19	425.413	0.457358	0.083107	1.07945E-09	0.001324		0.563456
20	444.172	0.384567	0.06988	7.97439E-10	0.000978	0.017768	0.434606
21	466.055	0.539531	0.098038	9.68465E-10	0.001188		0.553819
22	487.934	0.594292	0.107989	9.29599E-10	0.001141		0.556549
23	509.778	0.721946	0.131185	9.9024E-10	0.001215		0.619396
24	531.625	0.840488	0.152725	1.01647E-09	0.001247		0.66305
25	553.487	0.931695	0.169298	9.98459E-10	0.001225		0.678086
26	572.241	0.977331	0.177591	9.47728E-10	0.001163		0.665441
27	597.262	1.00477	0.182577	8.56941E-10	0.001051		0.628004
28	619.164	1.01397	0.184248	7.76224E-10	0.000952		0.589711
29	641.047	1.05962	0.192544	7.30902E-10	0.000897		0.574905
30	662.944	1.07793	0.195871	6.72262E-10	0.000825	0.010905	0.546843
31	684.84	1.09625	0.1992	6.20185E-10	0.000761		0.521143
32	706.724	1.1419	0.207495	5.87838E-10	0.000721		0.509746
33	731.732	1.19667	0.217447	5.55005E-10	0.000681		0.498306
34	747.361	1.23318	0.224081	5.36802E-10	0.000659		0.492256
35	772.379	1.26973	0.230723	5.00724E-10	0.000614		0.474544
36	794.231	1.37916	0.250607	5.00211E-10	0.000614		0.487469
37	812.998	1.39746	0.253932	4.72552E-10	0.00058		0.471396
38	834.8864	1.47956	0.268851	4.61986E-10	0.000567		0.473264
39	862.993	1.55257	0.282117	4.38943E-10	0.000539		0.464796
40	884.864	1.62555	0.295379	4.26334E-10	0.000523	0.006258	0.462885
41	900.496	1.65295	0.300358	4.11333E-10	0.000505		0.454487
42	925.509	1.69862	0.308656	3.89344E-10	0.000478		0.442141
43	947.379	1.7716	0.321917	3.78594E-10	0.000465		0.440092
44	966.129	1.82635	0.331866	3.68008E-10	0.000452		0.436254
45	991.146	1.8629	0.338508	3.47661E-10	0.000427		0.422805
46	1016.18	1.863	0.338526	3.22611E-10	0.000396		0.402251
47	1038.11	1.80842	0.328608	2.9373E-10	0.00036		0.374143
48	1056.91	1.77205	0.321999	2.72735E-10	0.000335		0.353692
49	1072.57	1.74478	0.317044	2.56946E-10	0.000315		0.338154
50	1100.75	1.70845	0.310442	2.32764E-10	0.000286	0.004017	0.314377

	ri average	ri (m)	fi*ri^3	ci/ctot	ci	fi*ri3	ci
1						18138.41	0.01508045
2						6143.644	0.005107885
3						12258.53	0.010191858
4						18370.51	0.01527342
5						20425.08	0.01698161
6						24508.36	0.020376486
7						28588.74	0.023768952
8						30643.31	0.025477142
9						32695.2	0.027183107
10	37.89081	3.78908E-05	52102.213	0.002436	0.044264	36778.48	0.030577983
11						38827.25	0.032281353
12						49008.02	0.040745743
13						51057.01	0.042449298
14						57171.67	0.047533085
15						61254.95	0.050927961
16						69404.34	0.05770344
17						85679.47	0.071234748
18						93823.06	0.078005407
19						101972.2	0.0847807
20	327.2886	0.000327289	622930.71	0.029124	0.529219	85742.79	0.071287393
21						120293.5	0.100013154
22						132502.9	0.11016423
23						160964.6	0.133827521
24						187394.6	0.155801716
25						207730.1	0.172708807
26						217905.1	0.181168377
27						224022.8	0.186254759
28						226074.1	0.187960168
29						236252.1	0.196422333
30	557.1699	0.00055717	1886161.7	0.088185	1.602415	240334.5	0.199816468
31						244419.1	0.203212456
32						254597.2	0.211674622
33						266808.7	0.221827366
34						274949	0.228595245
35						283098.1	0.235370538
36						307496.6	0.255655636
37						311576.7	0.259047917
38						329881.7	0.274266839
39						346159.9	0.287800742
40	775.8805	0.00077588	2923147.9	0.136668	2.483401	362431.5	0.301329084
41						368540.6	0.306408237
42						378723.2	0.31487411
43						394994.7	0.328402452
44						407201.7	0.338551489
45						415350.9	0.345326782
46						415373.2	0.345345319
47						403204.1	0.335227795
48						395095.1	0.328485869
49						389015	0.323430814
50	990.4195	0.000990419	3902532	0.182458	3.315451	380914.8	0.316696302

Continues

51	1116.42	1.65385	0.300521	2.15969E-10	0.000265		0.295768
52	1144.61	1.59929	0.290607	1.93791E-10	0.000238		0.272168
53	1163.42	1.53559	0.279032	1.77192E-10	0.000217		0.252946
54	1191.62	1.46281	0.265807	1.57092E-10	0.000193		0.229688
55	1216.73	1.30802	0.23768	1.3195E-10	0.000162		0.196993
56	1235.57	1.18054	0.214516	1.13725E-10	0.00014		0.172414
57	1260.64	1.11686	0.202945	1.01299E-10	0.000124		0.15669
58	1285.71	1.03496	0.188063	8.84857E-11	0.000109		0.139593
59	1301.39	0.971239	0.176484	8.00723E-11	9.82E-05		0.127861
60	1320.19	0.925759	0.16822	7.31084E-11	8.97E-05	0.00137	0.118427
61	1342.11	0.889403	0.161613	6.68518E-11	8.2E-05		0.11009
62	1367.17	0.825816	0.150059	5.87212E-11	7.21E-05		0.098506
63	1389.08	0.825816	0.150059	5.59861E-11	6.87E-05		0.095423
64	1411.01	0.780348	0.141797	5.04751E-11	6.19E-05		0.087388
65	1432.94	0.734881	0.133535	4.53849E-11	5.57E-05		0.079797
66	1451.72	0.725847	0.131894	4.31097E-11	5.29E-05		0.07679
67	1473.64	0.698603	0.126943	3.96675E-11	4.87E-05		0.071725
68	1492.42	0.689569	0.125302	3.7695E-11	4.63E-05		0.069027
69	1517.47	0.662338	0.120353	3.44428E-11	4.23E-05		0.064131
70	1542.5	0.680665	0.123684	3.37005E-11	4.14E-05	0.000572	0.063784
71	1561.26	0.698966	0.127009	3.33741E-11	4.1E-05		0.063934
72	1583.16	0.726391	0.131993	3.3264E-11	4.08E-05		0.064617
73	1605.04	0.77204	0.140287	3.39282E-11	4.16E-05		0.066818
74	1626.9	0.863248	0.156861	3.64277E-11	4.47E-05		0.072718
75	1651.85	1.03647	0.188337	4.17853E-11	5.13E-05		0.084692
76	1670.55	1.19145	0.216498	4.64383E-11	5.7E-05		0.095188
77	1689.23	1.40109	0.254592	5.28176E-11	6.48E-05		0.109475
78	1714.23	1.45587	0.264546	5.25163E-11	6.44E-05		0.110461
79	1733.18	1.1097	0.201644	3.87305E-11	4.75E-05		0.082365
80	1758.09	1.35582	0.246366	4.53375E-11	5.56E-05	0.000509	0.097801
81	1782.8	2.03019	0.368906	6.5104E-11	7.99E-05		0.142415
82	1804.3	2.85033	0.517933	8.81755E-11	0.000108		0.195211
83	1822.78	3.46088	0.628877	1.0384E-10	0.000127		0.232244
84	1847.84	3.40632	0.618962	9.81005E-11	0.00012		0.222424
85	1866.83	2.97815	0.54116	8.31785E-11	0.000102		0.19053
86	1892.08	2.53178	0.46005	6.79182E-11	8.33E-05		0.157679
87	1917.37	2.02163	0.36735	5.2115E-11	6.39E-05		0.122607
88	1933.2	1.64812	0.29948	4.14512E-11	5.09E-05		0.098324
89	1955.27	1.31108	0.238236	3.18704E-11	3.91E-05		0.076461
90	1974.18	1.0287	0.186925	2.42945E-11	2.98E-05	0.000805	0.058849
91	1999.44	0.564106	0.102504	1.28237E-11	1.57E-05		0.031461
92	2024.55	0.418423	0.076032	9.16239E-12	1.12E-05		0.022761
93	2046.52	0.281839	0.051213	5.97492E-12	7.33E-06		0.015004
94	2068.49	0.163478	0.029706	3.35643E-12	4.12E-06		0.008519
95	2084.17	0.09065	0.016472	1.81948E-12	2.23E-06	4.07E-05	0.004653
97		98.02528	17.81217	8.14992E-07	1		

51						368643.6	0.301488457
52						356576.6	0.296461254
53						342374.1	0.28465315
54						326147.1	0.271161882
55						291635.2	0.242468376
56						263212.4	0.218837339
57						249014.3	0.207032943
58						230754	0.191851096
59						216546.8	0.1800391
60	1216.435	0.001216435	2466356.6	0.115312	2.095328	206406.6	0.171608447
61						198300.7	0.164869116
62						184123.4	0.153081959
63						184123.4	0.153081959
64						173985.9	0.144653532
65						163848.6	0.136225289
66						161834.4	0.134550652
67						155760	0.129500417
68						153745.8	0.127825779
69						147674.4	0.122777954
70	1428.162	0.001428162	1665701.1	0.077878	1.41512	151760.6	0.12617524
71						155841	0.129567706
72						161955.6	0.134651493
73						172133.5	0.143113473
74						192469.2	0.160020749
75						231090.6	0.192131005
76						265644.9	0.220859732
77						312386.1	0.259720812
78						324599.8	0.269875411
79						247418	0.20570569
80	1666.996	0.001666996	2356679.5	0.110184	2.00215	302292.7	0.251329088
81						452649.8	0.37633742
82						635507.6	0.528367216
83						771635.4	0.641545201
84						759470.8	0.631431384
85						664006.3	0.552061279
86						564483.9	0.46931743
87						450741.2	0.374750648
88						367463.7	0.305512897
89						292317.5	0.24303561
90	1859.369	0.001859369	5174622.5	0.241933	4.396173	229358.2	0.190690676
91						125772.7	0.104568635
92						93291.31	0.077563298
93						62838.63	0.052244648
94						36448.94	0.030304005
95	2026.518	0.002026518	338384.89	0.015821	0.28748	20211.26	0.01680384
97						21855650	18.171
			21388619				

Table H4 Extracted data and calculations for the digested slurry's particle size distribution

Total particle volume (PSD), created by Plot Digitizer, 2.5.1										
Date: 17/01/2020, 17:18:17										
	99 um					10 fractions				
	PSD	Total particle volume	Ci	Ci/r ³	fi	fi	Fi*ri	ri average	r(m)	fi*ri ³
1	37.5837	0.00928	0.000878	1.65296E-08	0.260349		9.784874			
2	56.3555	0.01847	0.001746	9.75784E-09	0.153691		8.661312			
3	81.3817	0.036796	0.003479	6.45554E-09	0.101678		8.274714			
4	103.283	0.045999	0.00435	3.94791E-09	0.062181		6.422291			
5	128.305	0.073437	0.006944	3.28771E-09	0.051783		6.644016			
6	147.072	0.091738	0.008675	2.72689E-09	0.04295		6.316723			
7	168.973	0.100941	0.009545	1.97844E-09	0.031161		5.265434			
8	193.99	0.137491	0.013001	1.78092E-09	0.02805		5.441476			
9	215.883	0.164916	0.015594	1.54994E-09	0.024412		5.2702			
10	237.78	0.18323	0.017326	1.28878E-09	0.020299	0.776555	4.826664	86.1597	8.62E-05	496688.94
11	250.279	0.219729	0.020778	1.32532E-09	0.020874		5.22444			
12	278.439	0.228957	0.02165	1.00293E-09	0.015797		4.398402			
13	300.332	0.256382	0.024243	8.94932E-10	0.014096		4.233363			
14	322.233	0.265585	0.025114	7.50587E-10	0.011822		3.809471			
15	344.13	0.283899	0.026845	6.58724E-10	0.010375		3.570425			
16	366.022	0.311324	0.029439	6.00342E-10	0.009456		3.460982			
17	387.923	0.320527	0.030309	5.19201E-10	0.008178		3.172303			
18	409.829	0.320617	0.030318	4.40439E-10	0.006937		2.843036			
19	428.592	0.34803	0.03291	4.18015E-10	0.006584		2.821823			
20	450.48	0.384567	0.036365	3.97789E-10	0.006265	0.110384	2.822423	329.366	0.000329	3944041.9
21	475.51	0.393783	0.037236	3.46326E-10	0.005455		2.593814			
22	500.541	0.402998	0.038107	3.03872E-10	0.004786		2.395658			
23	519.299	0.439522	0.041561	2.96781E-10	0.004674		2.427431			
24	541.174	0.503394	0.047601	3.00334E-10	0.00473		2.559973			
25	563.039	0.585489	0.055364	3.10178E-10	0.004885		2.750698			
26	584.923	0.631138	0.05968	2.98219E-10	0.004697		2.747439			
27	609.94	0.667688	0.063137	2.7824E-10	0.004382		2.673009			
28	631.837	0.686002	0.064868	2.57168E-10	0.004051		2.559272			
29	653.738	0.695205	0.065739	2.35293E-10	0.003706		2.422739			
30	675.635	0.713519	0.06747	2.18764E-10	0.003446	0.044813	2.327997	568.0961	0.000568	8216152.1
31	697.536	0.722721	0.06834	2.01362E-10	0.003172		2.212272			
32	722.567	0.731936	0.069212	1.83462E-10	0.00289		2.08794			
33	738.2	0.759336	0.071803	1.78492E-10	0.002811		2.07533			
34	763.217	0.795886	0.075259	1.69283E-10	0.002666		2.03496			
35	781.98	0.823299	0.077851	1.62809E-10	0.002564		2.005245			
36	810.14	0.832527	0.078724	1.48056E-10	0.002332		1.889206			
37	828.894	0.878163	0.083039	1.45809E-10	0.002297		1.903611			
38	850.787	0.905589	0.085632	1.39052E-10	0.00219		1.863334			
39	872.675	0.942126	0.089087	1.34048E-10	0.002111		1.84249			
40	891.451	0.942203	0.089095	1.25765E-10	0.001981	0.025014	1.765837	786.7705	0.000787	12182214
41	916.464	0.987865	0.093413	1.21355E-10	0.001911		1.751733			
42	938.356	1.01529	0.096006	1.16197E-10	0.00183		1.717339			
43	957.119	1.0427	0.098598	1.12452E-10	0.001771		1.69523			
44	979.002	1.08835	0.102914	1.09679E-10	0.001728		1.69123			
45	1000.88	1.15222	0.108954	1.08667E-10	0.001712		1.71306			
46	1025.9	1.17966	0.111549	1.03312E-10	0.001627		1.669352			
47	1044.65	1.2253	0.115864	1.01634E-10	0.001601		1.672253			
48	1069.67	1.25274	0.118459	9.67874E-11	0.001524		1.630656			

Continues

49	1088.45	1.26193	0.119328	9.25374E-11	0.001458		1.586425			
50	1110.35	1.27113	0.120198	8.78047E-11	0.001383	0.016545	1.535576	1007.141	0.001007	16901686
51	1132.24	1.29855	0.122791	8.45962E-11	0.001332		1.50863			
52	1154.14	1.31687	0.124523	8.09981E-11	0.001276		1.472404			
53	1176.04	1.31696	0.124532	7.65621E-11	0.001206		1.418174			
54	1204.21	1.31708	0.124543	7.13203E-11	0.001123		1.352723			
55	1223	1.28982	0.121965	6.66741E-11	0.00105		1.284332			
56	1244.92	1.25346	0.118527	6.14319E-11	0.000968		1.204561			
57	1263.71	1.21709	0.115088	5.7028E-11	0.000898		1.135087			
58	1291.89	1.19899	0.113376	5.25831E-11	0.000828		1.069955			
59	1310.69	1.1444	0.108214	4.80602E-11	0.000757		0.992154			
60	1326.34	1.13535	0.107359	4.60122E-11	0.000725	0.010163	0.961216	1220.007	0.00122	18455249
61	1354.53	1.08991	0.103062	4.14698E-11	0.000653		0.884738			
62	1373.32	1.05354	0.099623	3.8463E-11	0.000606		0.831972			
63	1398.37	1.02631	0.097048	3.54911E-11	0.000559		0.781692			
64	1417.17	0.980827	0.092747	3.25862E-11	0.000513		0.72736			
65	1442.22	0.944485	0.089311	2.9772E-11	0.000469		0.67629			
66	1461.01	0.917228	0.086733	2.78116E-11	0.000438		0.639988			
67	1482.94	0.880872	0.083295	2.55417E-11	0.000402		0.596577			
68	1507.97	0.890087	0.084167	2.45449E-11	0.000387		0.582973			
69	1533.02	0.853744	0.08073	2.24074E-11	0.000353		0.541045			
70	1551.8	0.835599	0.079014	2.11445E-11	0.000333	0.004713	0.516806	1438.44	0.001438	14027409
71	1570.57	0.8539	0.080745	2.08422E-11	0.000328		0.515577			
72	1595.6	0.863115	0.081616	2.00911E-11	0.000316		0.504919			
73	1620.65	0.844996	0.079903	1.87713E-11	0.000296		0.479156			
74	1639.4	0.88152	0.083357	1.89184E-11	0.000298		0.488499			
75	1661.27	0.972727	0.091981	2.00622E-11	0.000316		0.524942			
76	1683.12	1.08216	0.102329	2.14612E-11	0.000338		0.568935			
77	1704.88	1.37382	0.129908	2.62154E-11	0.000413		0.703953			
78	1726.38	2.20307	0.208322	4.0488E-11	0.000638		1.100922			
79	1750.96	3.13256	0.296215	5.51796E-11	0.000869		1.521767			
80	1772.78	3.31488	0.313455	5.62614E-11	0.000886	0.004698	1.570939	1698.432	0.001698	23018552
81	1788.41	3.35139	0.316907	5.54027E-11	0.000873		1.560601			
82	1813.45	3.33327	0.315194	5.2852E-11	0.000832		1.509595			
83	1835.37	3.30603	0.312618	5.05642E-11	0.000796		1.461708			
84	1857.41	3.03277	0.286779	4.47531E-11	0.000705		1.309258			
85	1879.49	2.68662	0.254047	3.82643E-11	0.000603		1.132733			
86	1904.7	2.32226	0.219593	3.17789E-11	0.000501		0.953364			
87	1923.62	2.03076	0.192029	2.69779E-11	0.000425		0.817375			
88	1945.66	1.75751	0.16619	2.25634E-11	0.000355		0.691457			
89	1970.79	1.56626	0.148106	1.93486E-11	0.000305		0.600599			
90	1989.63	1.42056	0.134328	1.70549E-11	0.000269	0.005663	0.534461	1866.625	0.001867	36832933
91	2014.71	1.32954	0.125721	1.53734E-11	0.000242		0.48784			
92	2033.55	1.21117	0.114528	1.36191E-11	0.000215		0.436211			
93	2058.62	1.13838	0.107645	1.23386E-11	0.000194		0.40007			
94	2080.56	1.05647	0.0999	1.10924E-11	0.000175		0.363494			
95	2102.51	0.974554	0.092154	9.91515E-12	0.000156		0.328345			
96	2127.58	0.892653	0.084409	8.76461E-12	0.000138		0.293705			
97	2146.4	0.819838	0.077524	7.83977E-12	0.000123		0.265038			
98	2171.46	0.756161	0.071503	6.98339E-12	0.00011		0.238843			
99	2193.39	0.701582	0.066342	6.28693E-12	9.9E-05		0.217194			
						0.001452	0	2086.706	0.002087	13196887
		100.5033	9.503594	6.34901E-08	1					147271814

	ci/ctot	ci
1		
2		
3		
4		
5		
6		
7		
8		
9		
10	0.003373	0.031891
11		
12		
13		
14		
15		
16		
17		
18		
19		
20	0.026781	0.253238
21		
22		
23		
24		
25		
26		
27		
28		
29		
30	0.055789	0.527541
31		
32		
33		
34		
35		
36		
37		
38		
39		
40	0.082719	0.782193
41		
42		
43		
44		
45		
46		
47		
48		
49		
50	0.114765	1.08522
51		
52		
53		
54		
55		
56		

57		
58		
59		
60	0.125314	1.184971
61		
62		
63		
64		
65		
66		
67		
68		
69		
70	0.095248	0.900669
71		
72		
73		
74		
75		
76		
77		
78		
79		
80	0.1563	1.477971
81		
82		
83		
84		
85		
86		
87		
88		
89		
90	0.250102	2.364962
91		
92		
93		
94		
95		
96		
97		
98		
99		
100	0.089609	0.847343

Hence C_i the mass concentration = $(TPSV/100) * (DM * VS)$
 $(0.081353/100) * (27 * 0.673)$
Where TPVS = Total PS volume
% Fresh matter 27
g kg⁻¹ DM (VS) from source [183].
 C_i/r^3 = mass concentration c_i divided by the PSD
 $F_i = C_i/r^3 / \text{the sum of } C_i/r^3$
Where f_i = fraction of f_i into 10 of 10
 $F_i * r_i = f_i * \text{PSD}$ and r_i average = $F_i * r_i / f_i$
 $f_i * r_i^3 = 0.957501 * 37.89081^3 = 52,088$
 $c_i / c_{tot} = 0.002396 * (27 * 0.673)$
 $c_i = c_i / c_{tot} * (27 * 0.673) = 0.002396 * (27 * 0.673) = 0.04353$

Appendix I1

Table I1 As Post Hoc means comparison using fisher LSD

	MeanDiff	SEM	t Value	Prob	Alpha	Sig	LCL	UCL
BWSBPTL1 GWSBPTL1	48.93969	16.33601	2.99582	0.00291	0.05	1	16.82453	81.05485
PWSBPTL1 GWSBPTL1	46.20458	16.33601	2.82839	0.00491	0.05	1	14.08943	78.31974
PWSBPTL1 BWSBPTL1	-2.7351	16.33601	-0.16743	0.86712	0.05	0	-34.8503	29.38005
TWSBPTL1 GWSBPTL1	51.76322	16.33601	3.16866	0.00165	0.05	1	19.64807	83.87838
TWSBPTL1 BWSBPTL1	2.82354	16.33601	0.17284	0.86286	0.05	0	-29.2916	34.93869
TWSBPTL1 PWSBPTL1	5.55864	16.33601	0.34027	0.73383	0.05	0	-26.5565	37.6738
GWSBPTL2 GWSBPTL1	22.93124	16.33601	1.40372	0.16118	0.05	0	-9.18392	55.04639
GWSBPTL2 BWSBPTL1	-26.0085	16.33601	-1.59209	0.11215	0.05	0	-58.1236	6.1067
GWSBPTL2 PWSBPTL1	-23.2734	16.33601	-1.42467	0.15503	0.05	0	-55.3885	8.84181
GWSBPTL2 TWSBPTL1	-28.832	16.33601	-1.76493	0.07834	0.05	0	-60.9472	3.28317
BWSBPTL2 GWSBPTL1	67.27409	16.33601	4.11815	4.64E-05	0.05	1	35.15894	99.38925
BWSBPTL2 BWSBPTL1	18.33441	16.33601	1.12233	0.26239	0.05	0	-13.7808	50.44956
BWSBPTL2 PWSBPTL1	21.06951	16.33601	1.28976	0.19788	0.05	0	-11.0457	53.18467
BWSBPTL2 TWSBPTL1	15.51087	16.33601	0.94949	0.34294	0.05	0	-16.6043	47.62603
BWSBPTL2 GWSBPTL2	44.34286	16.33601	2.71442	0.00693	0.05	1	12.2277	76.45802
PWSBPTL2 GWSBPTL1	66.93405	16.33601	4.09733	5.06E-05	0.05	1	34.8189	99.04921
PWSBPTL2 BWSBPTL1	17.99437	16.33601	1.10152	0.27133	0.05	0	-14.1208	50.10952
PWSBPTL2 PWSBPTL1	20.72947	16.33601	1.26894	0.2052	0.05	0	-11.3857	52.84463
PWSBPTL2 TWSBPTL1	15.17083	16.33601	0.92867	0.35362	0.05	0	-16.9443	47.28599
PWSBPTL2 GWSBPTL2	44.00282	16.33601	2.69361	0.00737	0.05	1	11.88766	76.11798
PWSBPTL2 BWSBPTL2	-0.34004	16.33601	-0.02082	0.9834	0.05	0	-32.4552	31.77512
TWSBPTL2 GWSBPTL1	63.61841	16.33601	3.89437	1.15E-04	0.05	1	31.50326	95.73357
TWSBPTL2 BWSBPTL1	14.67873	16.33601	0.89855	0.36943	0.05	0	-17.4364	46.79388
TWSBPTL2 PWSBPTL1	17.41383	16.33601	1.06598	0.28708	0.05	0	-14.7013	49.52899
TWSBPTL2 TWSBPTL1	11.85519	16.33601	0.72571	0.46844	0.05	0	-20.26	43.97035
TWSBPTL2 GWSBPTL2	40.68718	16.33601	2.49064	0.01316	0.05	1	8.57202	72.80234
TWSBPTL2 BWSBPTL2	-3.65568	16.33601	-0.22378	0.82304	0.05	0	-35.7708	28.45948
TWSBPTL2 PWSBPTL2	-3.31564	16.33601	-0.20297	0.83927	0.05	0	-35.4308	28.79952
GWSBPTL3 GWSBPTL1	53.34883	16.33601	3.26572	0.00119	0.05	1	21.23367	85.46399
GWSBPTL3 BWSBPTL1	4.40914	16.33601	0.2699	0.78737	0.05	0	-27.706	36.5243
GWSBPTL3 PWSBPTL1	7.14425	16.33601	0.43733	0.66211	0.05	0	-24.9709	39.2594
GWSBPTL3 TWSBPTL1	1.58561	16.33601	0.09706	0.92273	0.05	0	-30.5296	33.70076
GWSBPTL3 BWSBPTL2	30.41759	16.33601	1.862	0.06334	0.05	0	-1.69756	62.53275
GWSBPTL3 BWSBPTL2	-13.9253	16.33601	-0.85243	0.39449	0.05	0	-46.0404	18.18989
GWSBPTL3 PWSBPTL2	-13.5852	16.33601	-0.83161	0.40612	0.05	0	-45.7004	18.52993
GWSBPTL3 TWSBPTL2	-10.2696	16.33601	-0.62865	0.52994	0.05	0	-42.3847	21.84557
BWSBPTL3 GWSBPTL1	96.64979	16.33601	5.91637	7.08E-09	0.05	1	64.53463	128.7649
BWSBPTL3 BWSBPTL1	47.7101	16.33601	2.92055	0.00369	0.05	1	15.59494	79.82525
BWSBPTL3 PWSBPTL1	50.4452	16.33601	3.08798	0.00216	0.05	1	18.33004	82.56036
BWSBPTL3 TWSBPTL1	44.88656	16.33601	2.74771	0.00627	0.05	1	12.7714	77.00172
BWSBPTL3 GWSBPTL2	73.71855	16.33601	4.51264	8.43E-06	0.05	1	41.60339	105.8337
BWSBPTL3 BWSBPTL2	29.37569	16.33601	1.79822	0.0729	0.05	0	-2.73947	61.49085
BWSBPTL3 PWSBPTL2	29.71573	16.33601	1.81903	0.06965	0.05	0	-2.39943	61.83089
BWSBPTL3 TWSBPTL2	33.03137	16.33601	2.022	0.04384	0.05	1	0.91621	65.14653
BWSBPTL3 GWSBPTL3	43.30096	16.33601	2.65065	0.00835	0.05	1	11.1858	75.41611
PWSBPTL3 GWSBPTL1	83.62232	16.33601	5.1189	4.78E-07	0.05	1	51.50717	115.7375
PWSBPTL3 BWSBPTL1	34.68264	16.33601	2.12308	0.03436	0.05	1	2.56748	66.79779
PWSBPTL3 PWSBPTL1	37.41774	16.33601	2.29051	0.02251	0.05	1	5.30258	69.5329
PWSBPTL3 TWSBPTL1	31.8591	16.33601	1.95024	0.05185	0.05	0	-0.25606	63.97426
PWSBPTL3 GWSBPTL2	60.69109	16.33601	3.71517	2.32E-04	0.05	1	28.57593	92.80625
PWSBPTL3 BWSBPTL2	16.34823	16.33601	1.00075	0.31755	0.05	0	-15.7669	48.46339
PWSBPTL3 PWSBPTL2	16.68827	16.33601	1.02156	0.3076	0.05	0	-15.4269	48.80343
PWSBPTL3 TWSBPTL2	20.00391	16.33601	1.22453	0.22147	0.05	0	-12.1113	52.11907
PWSBPTL3 GWSBPTL3	30.27349	16.33601	1.85318	0.06459	0.05	0	-1.84166	62.38865
PWSBPTL3 BWSBPTL3	-13.0275	16.33601	-0.79747	0.42565	0.05	0	-45.1426	19.0877
TWSBPTL3 GWSBPTL1	85.39133	16.33601	5.22719	2.78E-07	0.05	1	53.27618	117.5065
TWSBPTL3 BWSBPTL1	36.45164	16.33601	2.23137	0.02621	0.05	1	4.33649	68.5668
TWSBPTL3 PWSBPTL1	39.18675	16.33601	2.3988	0.01691	0.05	1	7.07159	71.30191
TWSBPTL3 TWSBPTL1	33.62811	16.33601	2.05853	0.04019	0.05	1	1.51295	65.74327
TWSBPTL3 GWSBPTL2	62.4601	16.33601	3.82346	1.53E-04	0.05	1	30.34494	94.57525

Continues

TWSBPTL3 BWSBPTL2	18.11724	16.33601	1.10904	0.26808	0.05	0	-13.9979	50.23239
TWSBPTL3 PWSBPTL2	18.45728	16.33601	1.12985	0.25922	0.05	0	-13.6579	50.57244
TWSBPTL3 TWSBPTL2	21.77292	16.33601	1.33282	0.18335	0.05	0	-10.3422	53.88808
TWSBPTL3 GWSBPTL3	32.0425	16.33601	1.96146	0.05052	0.05	0	-0.07265	64.15766
TWSBPTL3 BWSBPTL3	-11.2585	16.33601	-0.68918	0.49111	0.05	0	-43.3736	20.8567
TWSBPTL3 PWSBPTL3	1.76901	16.33601	0.10829	0.91382	0.05	0	-30.3462	33.88417
GWSBPTL4 GWSBPTL1	59.74412	16.33601	3.6572	2.89E-04	0.05	1	27.62896	91.85927
GWSBPTL4 BWSBPTL1	10.80443	16.33601	0.66139	0.50874	0.05	0	-21.3107	42.91959
GWSBPTL4 PWSBPTL1	13.53953	16.33601	0.82882	0.4077	0.05	0	-18.5756	45.65469
GWSBPTL4 TWSBPTL1	7.98089	16.33601	0.48855	0.62543	0.05	0	-24.1343	40.09605
GWSBPTL4 GWSBPTL2	36.81288	16.33601	2.25348	0.02477	0.05	1	4.69772	68.92804
GWSBPTL4 BWSBPTL2	-7.52998	16.33601	-0.46094	0.64509	0.05	0	-39.6451	24.58518
GWSBPTL4 PWSBPTL2	-7.18994	16.33601	-0.44013	0.66008	0.05	0	-39.3051	24.92522
GWSBPTL4 TWSBPTL2	-3.8743	16.33601	-0.23716	0.81265	0.05	0	-35.9895	28.24086
GWSBPTL4 GWSBPTL3	6.39529	16.33601	0.39148	0.69565	0.05	0	-25.7199	38.51044
GWSBPTL4 BWSBPTL3	-36.9057	16.33601	-2.25916	0.02441	0.05	1	-69.0208	-4.79051
GWSBPTL4 PWSBPTL3	-23.8782	16.33601	-1.46169	0.14461	0.05	0	-55.9934	8.23695
GWSBPTL4 TWSBPTL3	-25.6472	16.33601	-1.56998	0.11721	0.05	0	-57.7624	6.46794
BWSBPTL4 GWSBPTL1	132.0287	16.33601	8.08207	7.63E-15	0.05	1	99.91352	164.1438
BWSBPTL4 BWSBPTL1	83.08899	16.33601	5.08625	5.63E-07	0.05	1	50.97383	115.2042
BWSBPTL4 PWSBPTL1	85.82409	16.33601	5.25368	2.43E-07	0.05	1	53.70894	117.9393
BWSBPTL4 TWSBPTL1	80.26545	16.33601	4.91341	1.31E-06	0.05	1	48.1503	112.3806
BWSBPTL4 GWSBPTL2	109.0974	16.33601	6.67834	8.11E-11	0.05	1	76.98229	141.2126
BWSBPTL4 BWSBPTL2	64.75458	16.33601	3.96392	8.73E-05	0.05	1	32.63943	96.86974
BWSBPTL4 PWSBPTL2	65.09462	16.33601	3.98473	8.03E-05	0.05	1	32.97947	97.20978
BWSBPTL4 TWSBPTL2	68.41027	16.33601	4.1877	3.47E-05	0.05	1	36.29511	100.5254
BWSBPTL4 GWSBPTL3	78.67985	16.33601	4.81635	2.08E-06	0.05	1	46.56469	110.795
BWSBPTL4 BWSBPTL3	35.37889	16.33601	2.1657	0.03092	0.05	1	3.26374	67.49405
BWSBPTL4 PWSBPTL3	48.40635	16.33601	2.96317	0.00323	0.05	1	16.2912	80.52151
BWSBPTL4 TWSBPTL3	46.63735	16.33601	2.85488	0.00453	0.05	1	14.52219	78.7525
BWSBPTL4 GWSBPTL4	72.28456	16.33601	4.42486	1.25E-05	0.05	1	40.1694	104.3997
PWSBPTL4 GWSBPTL1	86.98495	16.33601	5.32474	1.69E-07	0.05	1	54.8698	119.1001
PWSBPTL4 BWSBPTL1	38.04527	16.33601	2.32892	0.02036	0.05	1	5.93011	70.16042
PWSBPTL4 PWSBPTL1	40.78037	16.33601	2.49635	0.01295	0.05	1	8.66521	72.89553
PWSBPTL4 TWSBPTL1	35.22173	16.33601	2.15608	0.03167	0.05	1	3.10657	67.33689
PWSBPTL4 GWSBPTL2	64.05372	16.33601	3.92101	1.04E-04	0.05	1	31.93856	96.16888
PWSBPTL4 BWSBPTL2	19.71086	16.33601	1.20659	0.2283	0.05	0	-12.4043	51.82602
PWSBPTL4 PWSBPTL2	20.0509	16.33601	1.22741	0.22039	0.05	0	-12.0643	52.16606
PWSBPTL4 TWSBPTL2	23.36654	16.33601	1.43037	0.15339	0.05	0	-8.74862	55.4817
PWSBPTL4 GWSBPTL3	33.63612	16.33601	2.05902	0.04014	0.05	1	1.52097	65.75128
PWSBPTL4 BWSBPTL3	-9.66483	16.33601	-0.59163	0.55443	0.05	0	-41.78	22.45033
PWSBPTL4 PWSBPTL3	3.36263	16.33601	0.20584	0.83702	0.05	0	-28.7525	35.47779
PWSBPTL4 TWSBPTL3	1.59362	16.33601	0.09755	0.92234	0.05	0	-30.5215	33.70878
PWSBPTL4 GWSBPTL4	27.24084	16.33601	1.66753	0.09619	0.05	0	-4.87432	59.35599
PWSBPTL4 BWSBPTL4	-45.0437	16.33601	-2.75733	0.00609	0.05	1	-77.1589	-12.9286
TWSBPTL4 GWSBPTL1	93.03295	16.33601	5.69496	2.39E-08	0.05	1	60.91779	125.1481
TWSBPTL4 BWSBPTL1	44.09326	16.33601	2.69915	0.00725	0.05	1	11.9781	76.20842
TWSBPTL4 PWSBPTL1	46.82836	16.33601	2.86657	0.00437	0.05	1	14.7132	78.94352
TWSBPTL4 TWSBPTL1	41.26972	16.33601	2.5263	0.01191	0.05	1	9.15456	73.38488
TWSBPTL4 GWSBPTL2	70.10171	16.33601	4.29124	2.23E-05	0.05	1	37.98655	102.2169
TWSBPTL4 BWSBPTL2	25.75885	16.33601	1.57681	0.11563	0.05	0	-6.35631	57.87401
TWSBPTL4 PWSBPTL2	26.09889	16.33601	1.59763	0.11092	0.05	0	-6.01627	58.21405
TWSBPTL4 TWSBPTL2	29.41453	16.33601	1.8006	0.07252	0.05	0	-2.70062	61.52969
TWSBPTL4 GWSBPTL3	39.68412	16.33601	2.42924	0.01557	0.05	1	7.56896	71.79927
TWSBPTL4 BWSBPTL3	-3.61684	16.33601	-0.2214	0.82489	0.05	0	-35.732	28.49832
TWSBPTL4 PWSBPTL3	9.41062	16.33601	0.57607	0.56489	0.05	0	-22.7045	41.52578
TWSBPTL4 TWSBPTL3	7.64161	16.33601	0.46778	0.6402	0.05	0	-24.4735	39.75677
TWSBPTL4 GWSBPTL4	33.28883	16.33601	2.03776	0.04223	0.05	1	1.17367	65.40399
TWSBPTL4 BWSBPTL4	-38.9957	16.33601	-2.3871	0.01745	0.05	1	-71.1109	-6.88058
TWSBPTL4 PWSBPTL4	6.04799	16.33601	0.37022	0.71141	0.05	0	-26.0672	38.16315